



**Silesian  
University  
of Technology**

**PhD Thesis**

**MSc Eng Natalia Wielgus**

**Analysis of material properties of industrial  
waste-based geopolymers for assessment of their  
usability in construction**

**Doctoral dissertation submitted in the course of proceedings for the granting  
of the PhD degree in the discipline of civil engineering, geodesy, and transport**

Supervisors:

Prof. Jan Kubica, PhD, DSc. Eng  
Dr Marcin Górski, PhD Eng., SUT Prof.

Department of Structural Engineering  
Faculty of Civil Engineering

Gliwice, June 2023

# CONTENT

<b>Preface</b> .....	<b>4</b>
<b>Acknowledgement</b> .....	<b>4</b>
<b>CHAPTER 1 (INTRODUCTION)</b> .....	<b>6</b>
1.1 <i>Background and motivation</i> .....	6
1.2 <i>Problem definition</i> .....	7
1.3 <i>Hypotheses and limitations</i> .....	8
1.4 <i>Aim of the Thesis</i> .....	9
1.5 <i>Organization of the Thesis</i> .....	10
<b>CHAPTER 2 (STATE-OF-THE-ART)</b> .....	<b>12</b>
2.1 <i>Geopolymer – the basic characteristics</i> .....	12
2.1.1 <i>Chemical structure of geopolymers</i> .....	12
2.1.2 <i>Geopolymer composition</i> .....	14
2.1.3 <i>Different approaches to the geopolymer composition</i> .....	16
2.2 <i>Historical background</i> .....	18
2.3 <i>The current investigations on geopolymers</i> .....	21
2.4 <i>Application of geopolymers</i> .....	25
2.5 <i>Cathode ray tube glass</i> .....	27
2.5.1 <i>Description of the material</i> .....	27
2.5.2 <i>Application of CRT glass in concrete</i> .....	29
2.5.3 <i>Ability of geopolymers for immobilization of heavy metals</i> .....	32
2.5.4 <i>Application of CRT glass in geopolymers</i> .....	33
2.6 <i>State-of-the-art critical analysis and summary</i> .....	39
<b>CHAPTER 3 (PRELIMINARY RESEARCH)</b> .....	<b>42</b>
3.1 <i>The scope and test program</i> .....	42
3.2 <i>Materials</i> .....	44
3.3 <i>Research methods</i> .....	46
3.4 <i>Presentation of results</i> .....	48
3.5 <i>Study on CRT glass</i> .....	48
3.6 <i>Mechanical behavior of geopolymer with CRT glass and geopolymer with sand</i> .....	50
3.7 <i>Determination of the influence of CRT glass content on mechanical behavior</i> .....	53
3.7.1 <i>Preparation of samples</i> .....	53
3.7.2 <i>Results</i> .....	56
3.7.3 <i>Analysis</i> .....	59
3.8 <i>Determination of the influence of curing temperature on mechanical behavior</i> .....	61
3.8.1 <i>Preparation of samples</i> .....	61
3.8.2 <i>Results</i> .....	65
3.8.3 <i>Analysis</i> .....	67
3.9 <i>Determination of the temperature and strength changes over time</i> .....	71

3.9.1 Preparation of samples .....	71
3.9.2 Results.....	73
3.9.3 Analysis .....	76
<b>CHAPTER 4 (MAIN RESEARCH).....</b>	<b>83</b>
4.1 <i>Determination of the influence of curing temperature and curing time on mechanical behavior</i> .....	83
4.1.1 Preparation of samples .....	83
4.1.2 Results.....	86
4.1.3 Analysis .....	88
4.2 <i>Determination of the influence of sodium hydroxide concentration on mechanical behavior</i> .....	92
4.2.1 Preparation of samples .....	92
4.2.2 Results.....	93
4.2.3 Analysis .....	94
4.3 <i>Determination of the influence of CRT glass particle size on mechanical behavior</i> .....	96
4.3.1 Preparation of samples .....	96
4.3.2 Results.....	97
4.3.3 Analysis .....	99
4.4 <i>Determination of the change of mechanical behavior over time</i> .....	101
4.4.1 Preparation of samples .....	101
4.4.2 Results.....	101
4.4.3 Analysis .....	106
<b>CHAPTER 5 (COMPLEMENTARY RESEARCH).....</b>	<b>110</b>
5.1 <i>Porosity of geopolymer</i> .....	110
5.1.1 Preparation of samples .....	110
5.1.2 Results and analysis .....	111
5.2 <i>Physicochemical characteristics</i> .....	112
5.2.1 Description of the test .....	112
5.2.2 Atomic absorption spectrometry (AAS) results and analysis.....	113
<b>CHAPTER 6 (DISCUSSION).....</b>	<b>115</b>
6.1 <i>Determination of the influence of the CRT glass content on mechanical behavior – discussion</i> .....	115
6.2 <i>Determination of the influence of curing temperature on mechanical behavior – discussion</i> .....	116
6.3 <i>Determination of the temperature and strength changes over time – discussion</i> .....	117
6.4 <i>Determination of the influence of curing temperature and curing time on mechanical behavior – discussion</i> .....	119
6.5 <i>Determination of the influence of sodium hydroxide concentration on mechanical behavior – discussion</i> .....	120
6.6 <i>Determination of the influence of CRT glass particle size on mechanical behavior – discussion</i> .....	121
6.7 <i>Determination of the change of mechanical behavior over time – discussion</i> .....	121
6.8 <i>Determination of the porosity – discussion</i> .....	122
6.9 <i>Physicochemical characteristics – discussion</i> .....	123
<b>CHAPTER 7 (SUMMARY AND CONCLUSIONS) .....</b>	<b>125</b>
<b>CHAPTER 8 (DIRECTIONS FOR FURTHER RESEARCH) .....</b>	<b>128</b>

<b>Abstract .....</b>	<b>129</b>
<b>List of symbols.....</b>	<b>130</b>
<b>List of abbreviations.....</b>	<b>132</b>
<b>References .....</b>	<b>133</b>
<b>List of Figures .....</b>	<b>154</b>
<b>List of Tables .....</b>	<b>157</b>
<b>SUMMARY .....</b>	<b>158</b>

## Preface

The following Thesis has been prepared at the Silesian University of Technology, at the Department of Structural Engineering, Faculty of Civil Engineering.

The majority of investigations have been carried out at the Silesian University of Technology, in the Laboratory of Faculty of Civil Engineering (the flexural and compressive strength tests, part of sieve tests and the density measurements), in the Laboratory of the Faculty of Mechanical Engineering (the determination of porosity), in the Institute of Physics, Centre for Science and Education (some microscope photographs) and in the Laboratory of Faculty of Energy and Environmental Engineering (a physicochemical analysis done with the use of an atomic absorption spectrometry).

Metakaolin and CRT glass fine particles distribution were measured with the use of a laser particle analyzer at the Faculty of Engineering at the University in Porto.

## Acknowledgement

The following Thesis is the fruit of countless hours of my work in the laboratory and even more in the front of a computer screen. Despite the fact that I devoted lot of time and effort during the process of studying, working and writing, I would not be able to complete my task alone. That is why, at the very beginning of this Thesis, I would like to express my deepest gratitude to all who contributed in the process of creating this publication on different stages.

In the first place, I would like to express my sincere appreciation to my supervisors – Professor Jan Kubica and Professor Marcin Górski. I am grateful for your assistance, inspiration, guidance, all help and support I received from you through the whole process of PhD studies. Thank you for ability to evolve from the unexperienced student into the young researcher.

I would like to thank all my colleagues from the Department of Structural Engineering for advices, help and their kind words. Separate thanks for Tomek Hahn, Karol Konopka and Grzegorz Cygan for their help in laboratory.

I am immensely grateful to Prof. Jacek Gołaszewski for the possibility of using a special equipment in the laboratory. I am additionally grateful for kind words and advices.

I would like to thank the all those, who enable me to extend my research. I would like to express my gratitude here, especially to: Professor Marcin Adamiak, Professor Krzysztof Pikoń, Doctor Fatima Pawełczyk and Doctor Anna Woźniak.

I would not be able to proceed any tests without a materials obtained from donors. Here, I would like to express my gratefulness to TAURON Polska Energia SA and to Thormann Recycling Sp z o.o. for providing materials which stated the base of my investigations. The investigations would not be possible without a financial support as well. I thankfully acknowledge the financial support from the Silesian University of Technology with statutory funds from Department of Structural Engineering within grants agreements BKM-504/RB6/2017, BKM-547/RB6/2018 and BKM-587/RB6/2019. I am grateful also to the

international project REMINE-MSCA-RISE H2020 for funding my two internships at University of Beira Interior and Beira Serra in Covilha, Portugal and to the project POWER.03.03.00-IP.08-00-P13/18 implemented under Measure: 3.3 Internationalization of Polish higher education for funding my internship at the Universidade do Porto in Porto, Portugal.

My experience in the field of alkali activated materials would be much poorer without possibility of attendance in a foreign internships. I am deeply indebted to Prof. Joao Castro Gomes for inviting me to University of Beira Interior, for his hospitality, all advices, help and introduction to a “geopolymer world”. I am also grateful to the University of Beira Interior for the possibility of using the laboratory equipment. Simultaneously, I thank all colleagues from the UBI, especially Pedro Humbert for help and friendship. Writing about the University in Covilha, I cannot left Jorge Serra off. Jorge, you showed me how to prepare geopolymers, you taught me not to be afraid of experimenting and discovering. You also taught me to treat work in the lab as a fun. Thank you.

My thanks also go to Prof. Sara Rios and the Faculty of Engineering at University in Porto for an invitation and collaboration. Thank you Professor, for warm hospitality, kindness, all advices and help. I would also like to thank Claver Giovanni for his patience, companionship and share of the knowledge.

I would like to thank all my family (especially my parents – Hanna and Grzegorz) for immeasurable love and support. Even when you do not understand all my problems you are always standing by my side and I am aware of that.

I would also like to extend my special thanks to my husband – Michał. Thank you for your patience, help, all good advices, wiping my tears and simply being for me when I need you. Separate thanks for your practical help during the measurement of a temperature inside geopolymers – I would not be able to write this chapter of the Thesis without you. And special thanks to Szymek, my little and the greatest adventure. You taught me how to live and how to be present in every second of my life.

Friendship is one of the most beautiful things in the live. I could not have done this Thesis without all my friends. Playing board games, dancing, climbing, going to the mountain trips, working together, laughing, talking or just sitting in silence in good companionship – it all helped me to find the powers for the further work.

# CHAPTER 1 (INTRODUCTION)

## *1.1 Background and motivation*

Geopolymers are materials which are considered to be an environmentally friendly alternative for ordinary concrete in the building industry. They are usually compared to concrete since the mechanical properties and the behavior of these two kinds of materials are similar. The basic difference between geopolymers and concrete is their composition. Simplifying, concrete is basically made of water, cement, sand and coarse aggregate. Geopolymers in turn, are prepared with use of aluminosilicate material called a precursor (for instance metakaolin, fly ash, slag etc) and liquid activator (usually sodium silicate or sodium hydroxide or a mixture of both). Fine and coarse aggregate can also be added as fillers. After mixing the precursor with activators, the geopolymerization reaction starts. The duration of geopolymerization process depends on a variety of factors which are described in more detail in a further part of this Thesis. From a top-level perspective, in many cases one can expect high strength of geopolymer after 24 hours of curing time – this is one of the advantages of this material over the ordinary concrete. What is more, geopolymer shows some superior characteristics as: good flexural strength, high temperature resistance and chemical resistance. Finally, the environmental benefits cannot be overestimated.

Nowadays, environmental problems become a global and urgent concern. One of the most important issues is the amount of CO<sub>2</sub> emissions. According to the Emissions Gap Report 2020 (published by UNEP - United Nations Environment Programme), the global greenhouse gases emission reached 59,1 (range ± 5,9) gigatons of CO<sub>2</sub> equivalent in 2019 [1]. The newest Emission Gap Report 2022 [2], gives the preliminary estimation of CO<sub>2</sub> emission for 2021: 52,8 gigatons of CO<sub>2</sub> equivalent. This data does not include the land use, land-use change and forestry which is available only up to 2020, which means that total global greenhouse gases emission for 2021 is likely to exceed that of 2019 (the prediction is given in the Report [2]). According to [1], the industrial processes from mineral products and other chemical reactions are responsible for the 9% of total greenhouse gases emissions. The Emission Gap Report 2022 contains the subsection describing the steps needed in the industry field to achieve the Paris Agreement [3] - a “legally binding international treaty on climate change” [4], that starts with these words: “Reduce demand for and decrease carbon intensity of global cement and steel production” [2]. Cement production is a non-negligible component of the total CO<sub>2</sub> gases emission. The annual global cement production has been exceeding 4 billion tons since 2013 and reached 4,1 billion tons in 2020 [5]. Without any significant efforts to reduce the global demand for cement, the moderate grow of the production of this basic building material is predicted by 2030 [6]. During cement manufacturing, CO<sub>2</sub> gases are emitted as a result of two main processes. The first one is production of clinker, during which the heated carbonates (mainly CaCO<sub>3</sub>, present in a limestone) are decomposed into CO<sub>2</sub> and oxides. The second process involves fuel combustion needed for burning the raw materials in a kiln at temperatures ranging up to 1450°C. According to calculations, cement production currently accounts for approximately 8% of overall global carbon dioxide emissions [7], [8].

The issue of limiting the carbon dioxide emissions connected to the production of concrete is currently being addressed by various means [6], [9]–[14]. Using alternatives to concrete in new investments is one of them [15]. Geopolymer as a material with similar properties to concrete is one of the most promising solutions to that challenge. A lot of attention was put on the topic of environmental benefits coming from application of geopolymer instead of concrete. There is no consensus among scientists as to the extent to which this lowers the carbon footprint. The process of estimating it is complex, since there are many aspects and variables in place, including: which exact types (both of concrete and geopolymer) are being compared, which aspects of production of these materials are being considered, in which country the calculation has been done (which affects the availability of the necessary materials, that might either be readily available waste, or an imported resource) and many others. All these factors result in the quoted figures ranging from about 9% (research done in Melbourne [16]) to over 80% (summary of several existing studies made by Australian experts in field of inorganic polymers [16], [17]). Despite the high dispersion of results, most of scientists agree that replacing concrete with geopolymer reduces the emission of greenhouse gases.

Another concern related to concrete manufacturing is its high demand for water. According to the reports, in 2012 (when the annual production of cement was equal to 3,8 Gt), over 2 Gt of water were consumed in the overall process of concrete production [18]. The amount of consumed water raised along with the rise of cement production from 3,8 Gt up to 4,1 Gt in 2020 [5]. Due to the projections, the amount of produced concrete will increase in the following 30 years causing the serious problems with water supply especially in some regions where water is becoming a more and more scarce resource [18]. Concrete manufacturers report that the amount of water used in 2022 ranged from 304 to 402 liters per ton of cement material [19], [20]. The production of geopolymer is considered to be much less water consuming than the manufacturing of concrete. According to some calculations, comparing materials of similar workability, geopolymer allows for saving almost 30% of water even when the water reducing admixtures to concrete are used [21].

The next environmental and economic benefit of using geopolymers is the possibility of waste recycling (mainly industrial and mining, but the other types of waste, such as sewage sludge ash can be used as well [22], [23]). The role of main ingredient – the precursor, may be played by different types of waste: even those considered hazardous [24]. Fly ash, blast-furnace slag, metakaolin, waste glass and a variety of mine tailings are only the most popular examples [25]–[27]. The innovation of scientists in that field is almost unlimited. The topic of raw materials used for production of geopolymers is detailed in subsection “2.1.2 Geopolymer composition”. Concluding, geopolymers allow to make use of redundant waste (sometimes with the additional advantage of immobilization of toxic materials) and thereby to limit the exploitation of raw natural materials.

## *1.2 Problem definition*

Geopolymers can be a solution to extensive CO<sub>2</sub> production, raw material exploitation and the problem of waste (including a number of production and combustion’s by-products). However, the role of an aggregate is still most commonly played by natural materials such as:

sand [28], [29] limestone [30], granite [28], [30] or basaltic pumice as a lightweight aggregate [31]. There are several studies on possible usage of unconventional aggregates such as crushed, waste PET bottles [32], biomass produced during palm oil biomass combustion [33], steel furnace slag [34] or concrete and fired clay from construction and demolition waste [35] but they are an exception rather than a rule. It means, that searching for a potential aggregate that is not a raw material but a by-product is still an essential issue.

Using waste as a precursor is the most popular approach in geopolymers but there is also the possibility of recycling it as an aggregate – this topic is explored in this Thesis. The main goal of this Thesis was to determine if it is possible to use crushed discarded Cathode Ray Tube (CRT) glass as an aggregate in metakolin-based geopolymer matrix. The research starts from deriving the optimal mixture containing CRT glass and then focuses on mechanical properties of the new type of geopolymer and on factors influencing them. Study on geopolymer with CRT glass allows not only developing the knowledge about new environmentally friendly material but also allows recycling waste which is considered to be hazardous. The incisive description of characteristic and properties of CRT glass is presented in subsection “2.5 Cathode ray tube glass”. Author decided to use metakaolin as a precursor to limit the additional variability coming from heterogenous nature of by-product materials such as fly ash or blast-furnace slag. The idea to use CRT glass as an aggregate in geopolymer was an answer to the crucial needs of one of most significant CRT-related enterprise in Europe. Concluding, all works were done within the trial of solution of existing problem with recycling of CRT glass. The material was utilized almost in the same form in which it was obtained to minimize all additional activities which can considerably raise the cost of production on a large scale. CRT glass was obtained in already crushed form. The only additional activity was elimination of grains bigger than 4mm (which did not exceed 1% of the total mass) to adjust the aggregate to the size of samples.

According to the literature review, the topic of utilization of CRT glass inside geopolymer matrix is not popular. Moreover, most of existing works is devoted to the possibility of addition of powdered CRT glass in form of partial replacement of a precursor not in form of an aggregate. Therefore, the current work can possibly add the contribution to the subject of recycling of CRT glass inside geopolymer in form of an aggregate. Moreover, the solution presented within Thesis supplements list of possible alternative and environmental-friendly aggregates which can be used in geopolymer.

Author believes that geopolymers are interesting and future-promising material which is worth noting and may be a solution for many existing problems, while also hoping that this Thesis will be a valuable addition to the ever-growing research body on this promising and important subject.

### *1.3 Hypotheses and limitations*

Previous paragraphs presented the general description of the considered topic, the motivation for raising the subject within Thesis and the main problem definition. The current paragraph highlights all research hypothesis.

The following research hypotheses and related limitations were defined:

- **Hypothesis 1:** CRT glass can be recycled in metakaolin based geopolymer as an aggregate without any special pretreatments.  
Limitation: The research is limited to one type of metakaolin and crushed discarded CRT glass delivered by one supplier.
- **Hypothesis 2:** Metakaolin based geopolymer with aggregate in form of CRT glass can be considered as a potential building material with regard to flexural and compressive strength.  
Limitation: Flexural and compressive strength have been tested after 1, 3, 7, 14 and 28 days in the case of two chosen mixtures (metakaolin to CRT glass mass ratios 1:3 and 1:1). Flexural and compressive strength have been tested after 1, 3, 5, 7, 14, 28, 56 and 112 days in the case of one chosen mixture (of metakaolin to CRT glass mass ratio equal to 1:1). Three point flexural strength test and uniaxial compressive strength test were performed on prism samples of dimensions 40 x 40 x 160 mm according to standard PN-EN 196-1.
- **Hypothesis 3:** Metakaolin based geopolymer with CRT glass can be cured at different temperatures without crucial impact on flexural and compressive strength.  
Limitation: Research is limited to four mixtures of metakaolin to CRT mass ratio 1:3, 1:2, 1:1, 3:2. Samples were cured at 20°C or for the first 24 hours at the elevated temperature 40°C or 60°C. Strength characterization is limited to three-point flexural strength test and uniaxial compressive strength test.
- **Hypothesis 4:** Recycling CRT glass inside metakaolin base geopolymer limits the threat of environment contamination with heavy metals.  
Limitation: Research is limited to atomic absorption spectrometry performed on mixture of metakaolin to CRT mass ratio 1:1 and cured all the time at the room temperature. The number of following elements in the leachates were determined: Fe, Mn, Cu, Ni, Cr, Co, Zn, Pb, Cd.

#### *1.4 Aim of the Thesis*

The main purpose of the following Thesis was to determine and describe the potential application of metakaolin-based geopolymer with aggregate in form of crushed discarded CRT glass as an alternative building material, thereby suggesting the new possibility for recycling CRT glass. The realization of the main goal required confrontation with several minor objectives:

- The meticulous summary of the existing scientific literature devoted to different aspects of geopolymers and CRT glass with the particular attention paid to examples of utilization of CRT glass inside geopolymer matrix.
- Determination of an optimal mixture with metakaolin to CRT glass mass ratio as the main varying factor on the basis of flexural and compressive strength tests.

- Description of the influence of different curing conditions, NaOH concentration and CRT glass granulation on mechanical behavior of geopolymer made out of chosen mixtures.
- Evaluation of flexural and compressive strength changes of geopolymer made of one chosen mixture in time.
- Determination of temperature and mass changes inside metakaolin-based geopolymer with CRT glass during the curing process.
- Determination of porosity of metakaolin-based geopolymer with CRT glass.
- Assessment of the environmental threat of pure CRT glass and CRT glass incorporated into the metakaolin-based matrix on the base of physicochemical analysis of aqueous extracts.
- The discussion and comparison of all obtained results with data described in scientific literature.
- Formulation of conclusions and summary of performed tests and obtained results.
- Indication of future goals and directions for further research.

### *1.5 Organization of the Thesis*

- **Chapter 1** includes the introduction to the topic presented within Thesis, describes the main problem, defines the main aim and several sub-goals and as well, provides hypotheses of this Thesis and their possible limitations.
- **Chapter 2** provides theoretical research on the existing knowledge about issues risen within this Thesis with the main division on subjects devoted to geopolymers and to CRT glass. The subsection describing geopolymer includes: the historical background of the invention and development of geopolymers concluded with the overview of the newest research projects all over the world, examples of variable possible applications, description of chemical basis, description of mechanism of toxic metals' immobilization and possible compositions of mixtures. The subsection devoted to CRT glass includes: the overall description of CRT glass with respect to the possible ways of utilization and safe disposal and the examples of application of CRT glass in concrete. Both parts are combined finally with the in-depth presentation of already described examples of application of CRT glass in geopolymers.

- **Chapter 3** presents initial laboratory researches performed on metakaolin-based geopolymer with aggregate in form of CRT glass. The chapter starts with the description of all used materials, then presents the influence of metakaolin to CRT glass mass ratio and the influence of curing temperature on mechanical behavior. Chapter contains as well the determination of temperature changes inside curing geopolymer. Chapter concludes with determination of optimal mixture.
- **Chapter 4** delivers the main part of the research – the influence of the following factors on the mechanical behavior of geopolymer made of one chosen mixture: the curing time and temperature, NaOH concentration and CRT glass particle size. Chapter concludes with optimisation of chosen factors concerning the chosen mixture. describes chosen properties of tested material and compares the obtained results with the similar data already described in the scientific literature.
- **Chapter 5** contains the complementary research including determination of porosity and physicochemical characteristics of geopolymer.
- **Chapter 6** presents discussion of all achieved results together with comparison of the achieved results with the similar data already described in the scientific literature.
- **Chapter 7** summarizes the Thesis, shows the final conclusions and conclusions referring to the initial hypotheses.
- **Chapter 8** indicates the main future goals and directions for the further research.

## CHAPTER 2 (STATE-OF-THE-ART)

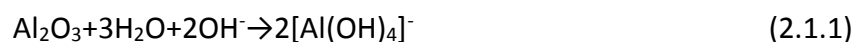
### 2.1 Geopolymer – the basic characteristics

#### 2.1.1 Chemical structure of geopolymers

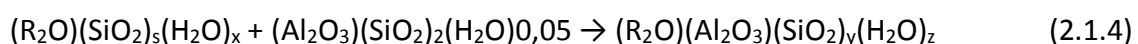
Geopolymers have been known and studied for nearly a century but the exact geopolymerization process and all factors which influence it are still not very well understood [36]. MacKenzie defines geopolymers as inorganic materials: having a three-dimensional structure build of tetrahedral Al-O and Si-O units which are charge-balanced by alkali ions; containing mainly alumina and silica; synthesized at room temperature by condensation of aluminosilicates at high pH; remaining stable and hard even when exposed to temperatures higher than 1000°C; being X-ray amorphous at each stage of life-cycle [37]. The geopolymerization process or its phases can be examined with use of few different methods such as: X-ray powder diffraction (XRD); energy-dispersive X-ray diffractometry (EDXRD); environmental scanning electron microscopy (ESEM); nuclear magnetic resonance (NMR); isothermal and non-isothermal differential scanning calorimetry (DSC) [36]. Each method has advantages and disadvantages. Some of above-mentioned methods are useful only for examination of the part of geopolymerization process.

Yao et al. [36] divides the whole geopolymerization process into three stages: deconstruction, polymerization and stabilization, although, he indicates that stages can occur at the same time and it is difficult to separate them clearly. De Silva et al. [38] offers more detailed description of the mentioned three stages. During the first stage the Si and Al particles are dissolute in the alkali solution. Then, the dissolved species are subjected to hydrolysis, transportation and orientation. At the end, the polycondensation occurs and, as an effect, the three-dimensional silico-aluminate networks are formed. Hou et al. [39] presents the geopolymerization reaction in slightly different way. In the first step the aluminate and silicate monomers are dissolute and released by alkali from the aluminosilicate source (called usually the raw material). In the second step, the oligomers are formatted on the surface of the solid particles through the cross-link of aluminate and silicate monomers. In the third step, a three-dimensional aluminosilicate network is formatted during the process of polycondensation [39].

Dissolution, hydrolysis and condensation processes which take place in metakaolin-based geopolymers can be formulated as following (formulas 2.1.1-2.1.3) [38]:



Whereas, Rahier et al. [40], on the basis of the reaction stoichiometry studies, gives the following equation for the geopolymerization when the metakaolin is the raw material (formula 2.1.4):



where  $R = \text{Na}$  or  $\text{K}$ ,  $s = \text{SiO}_2/\text{R}_2\text{O}$ ,  $x$  is the amount of water in the silicate solution,  $y = \text{SiO}_{2,\text{total}}/\text{Al}_2\text{O}_3$ ,  $z$  is the amount of bound water in the aluminosilicate [40].

Joseph Davidovits [41] divides the final possible products of geopolymerization into three groups: poly(sialate), poly(sialate-siloxo) and poly(sialate-disiloxo). Davidovits indicates especially the term “poly(sialate)” (where “sialate” stands for silicon-oxo-aluminate) as proper for chemical designation of the geopolymers which are based on silico-aluminates. He described the empirical formula for poly(sialates) as (formula 2.1.5):



where “M” is a cation; “n” indicates the degree of polycondensation and “z” is equal to 1, 2 or 3 [41].

Poly(sialate) polymer structures form in mixtures where Si/Al ratio is close to the value 1,0. In that case, the polycondensation occurs between silicate and aluminate species. The poly(sialate-siloxo) and poly(sialate-disiloxo), occurs when Si/Al ratio increases to the value 2,0 and 3,0 respectively and the silicate species start to condense among themselves and build oligomeric silicates [38], [42]. Geopolymers of highly aluminous compositions (when Si/Al < 1) have other properties than these one of higher Si/Al ratio including: early setting at ambient temperature; low strength; relevant amounts of crystalline phases (a normal geopolymer is characterized by rather amorphous structure); octahedral sites (in opposition to tetrahedral sites of a normal geopolymer); an existence of Si-rich and Al-rich phases [42].

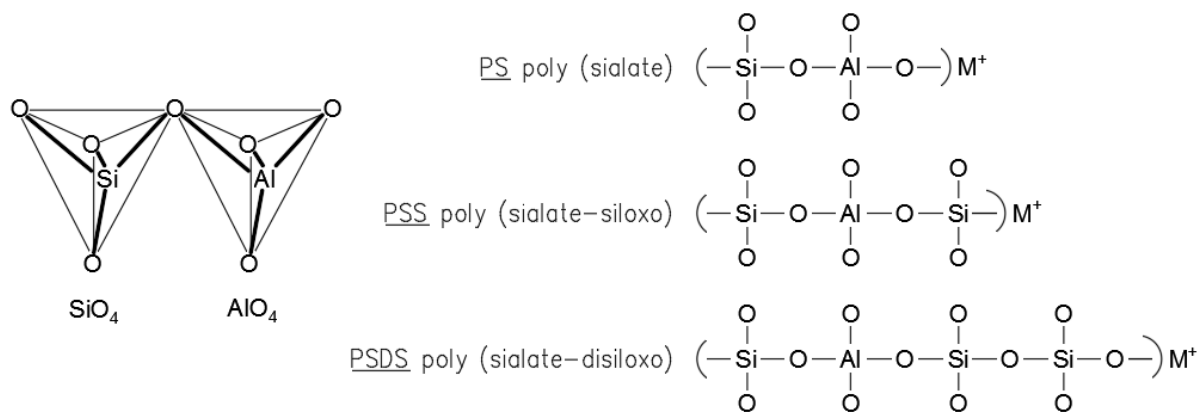


Fig. 2.1.1: The representation of possible tetrahedral sialate units [37], [41].

According to Davidovits [41], the geopolymer network is built of tetrahedral  $\text{AlO}_4$  and  $\text{SiO}_4$  units which are alternately linked by sharing the oxygens and randomly distributed within polymeric chains. The negative charge is balanced by the hydrated positive alkali metal ions (i.e.,  $\text{K}^+$ ,  $\text{Ca}^{++}$  or  $\text{Na}^+$ ) existing in the framework cavities. Poly(sialates) can be both chain and ring polymers where  $\text{Si}^{4+}$  and  $\text{Al}^{3+}$  are in IV-fold coordination with oxygen [37], [41].

Yao et al. [36] presents the analyse of the geopolymerization process performed with the use of air isothermal calorimeter, XRD and MAS NMR technology. The analyse was made

on metakaolin-based geopolymer activated with NaOH or KOH and sodium or potassium silicate solution. Scientists registered three exothermic peaks. The first peak occurred immediately after mixing of metakaolin with activator and was caused by the instant and intensive absorption of the alkali solution on the metakaolin particles surface. During the same exothermic peak, the metakaolin particles are dissolute, their Si-O and Al-O bond are broken. After completion of the initial reactions, the first exothermic peak decreases rapidly. The next step of the geopolymerization process connected with the second (smaller this time) exothermic peak is the final breaking down of metakaolin particles. In the same time, the oligomers and alumina/silica-hydroxy species (such as  $\text{Al}(\text{OH})_4^-$ ;  $\text{OSi}(\text{OH})_3^-$ ;  $(\text{OH})_3\text{-Si-O-Al}(\text{OH})_3$ ) are created. When the quantity of new products is high enough, they are polymerizing into gels what is connected with the third (and the last one) exothermic peak. The last stage is the transformation and reorganization of the small gels into the larger networks. In that moment (after about 75 hours) the geopolymerization process is at the thermally steady stage. The duration of the geopolymerization process depends among the other on the type and concentration of activator, on the type and particles diameter of the raw material and the reaction conditions [36].

The concentration of the activator (mainly of the NaOH solution) influences the geopolymerization process. When the concentration is higher, the reaction heat evolution at the first stage of the process is greater. However, the reaction rate at the second stage is the highest for the optimum concentration of activator. If concentration of  $\text{Na}^+$  ions is too high, the polymerization process (which occurs in the second stage of the whole process) may not be completed. Although, too much water can also be inappropriate since it decreases the destruction ability of activator during the first stage. The higher liquid to solid ratio elongates the geopolymerization [36].

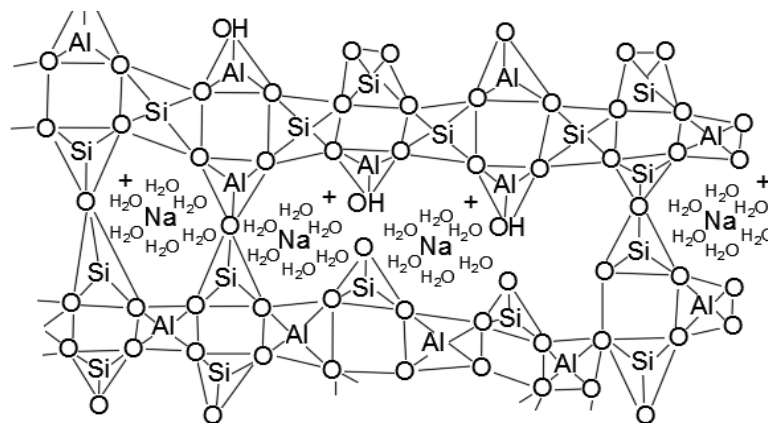


Fig. 2.1.2: Schematic structure of sodium poly-siloxo silate geopolymer [37].

### 2.1.2 Geopolymer composition

Geopolymers give much freedom to compose many different mixtures varying with raw materials, alkali activators and chemical ratios of basic elements. Literature presents numerous possibilities especially in the field of raw materials. Portuguese scientists discovered the superior characteristics of geopolymer based on tungsten mine waste mud taken from Panasqueira mine which is located in central Portugal [30]. Polish scientists successfully

designed geopolymer mixture based on volcanic tuff from small Polish village Filipowice [43]. Many of works were devoted to geopolymers based on a red mud as an addition to other raw materials such as: metakaolin [44], blast-furnace slag [45], soda lime glass [46] or fly ash [47]. Waste glass powder is also quite popular raw material – as the only precursor [48], [49] or as an addition to the other raw material, for example to metakaolin [50]. Some scientists are mixing several different raw materials containing also the unusual ones. Emdadi et al. [51] performed tests on geopolymer samples containing metakaolin, slag, rice husk and palm oil fuel ash in different proportions. Blast furnace slag can be mixed also with sugarcane bagasse ash [52] while coal fly ash has been already replaced with eggshell powder [53] or biomass ash coming from: combustion of switch grass, wheat straw, rice hull, cotton gin, corn cob and stalk alfalfa stem [54]. Many investigations are devoted to the possible utilization of different mine tailings in geopolymers: iron ore tailings [55], raw or mechanical activated vanadium tailings [56], phosphate tailings (from flotation and washing of phosphate ore) [57] or tin mine tailings [58]. Horpibulsuk et al. [59] describes preparation of masonry units containing water treatment sludge and fly ash. Merabtene et al. [60] presents geopolymer based on natural kaolin and sludge from hydraulic dam located in Algeria. Lin et al. [61] shows the replacement of metakaolin with silicon carbide sludge. Nevertheless, regardless of the quantity of possible solutions, the most popular raw materials are metakaolin, fly ash and blast furnace slag.

Metakaolin is produced by the calcination of kaolinite clays at high temperatures (ranging from 500 to 800°C). The temperature of calcination has to be high enough to remove the most of the water from the structure of the clay however, too high temperature could result in formation of a mullite. The temperature of calcination influences as well the reactivity of metakaolin during the alkaline activation. The source of kaolin can state both the natural deposits or different by-products such as mine tailings or industrial waste. The origin of kaolinite influences the purity, particle size and crystallinity of the final product. Due to the varying parameters of metakaolin in dependence on its origin, the formulation of one optimal composition for metakaolin-based geopolymers is complicated [62], [63].

Fly ash states one of the solid by-products of the coal burning process in coal-fired power plants. Fly ash is captured by special particle filtration equipment while escaping the boiler together with flue gases, before reaching chimneys. The composition of fly ash varies in dependence on the source of a coal. Generally, the following oxides: SiO<sub>2</sub>, Al<sub>2</sub>O<sub>3</sub>, CaO and Fe<sub>2</sub>O<sub>3</sub> are predominant ingredients of fly ash. Fly ash can be classified in dependence on calcium oxide content on Class C fly ash (high CaO content >20%, mainly from burning the lignite coal sources) and class F fly ash (low CaO content <10%, mainly from burning bituminous coal or anthracite) [64]. Recently, scientists started to put more attention of possible utilization of fluidized bed combustion fly ash in geopolymers as well. This type of fly ash is produced as an effect of coal combustion at relatively low temperatures (~800-900°C) what effects in a limited release of SO<sub>2</sub> and NO<sub>x</sub> gases during the process [65].

Ground granulated blast furnace slag (GGBFS) states a by-product during the pig iron production at temperatures ranging from 1300 to 1600°C in a large blast furnace. During the process of melting of the iron, slag is floating on the surface because of the low density, and therefore can be easily separated from the molten iron. After removing from the rest of molten iron, blast furnace slag is cooled and granulated. The characteristics of the slag depend on the type of raw materials used during the melting process: iron ore, flux (mainly dolomite

or limestone), as well as on the fuel and the whole process of production. Usually, GGBFS is composed mainly of CaO, SiO<sub>2</sub>, Al<sub>2</sub>O<sub>3</sub> and MgO [66]. In production of geopolymers, GGBFS can be used as the only raw material [67], [68] or together with the other raw material such as: metakaolin [69], fly ash [29] or red mud [45].

Scientists are much more conservative when it comes for the choice of the activator. The group of the most commonly used activators includes alkali hydroxides, specifically sodium and potassium hydroxides. Both of them can be dissolved in water up to high concentrations reaching 20 mol/l at the relatively low temperature (25°C). Potassium hydroxide is obtained via the process of the electrolysis of KCl solutions while sodium hydroxide is mainly produced during the process of the chlor-alkali, along with the Cl<sub>2</sub>. Both mentioned hydroxides are predominantly used in geopolymers in form of water solutions. Equally popular activators to alkali hydroxides are alkali silicates, especially sodium silicate and more rarely the potassium silicate, being a product of calcination and then the dissolution in water of carbonate salts and silica [62]. The novel studies derives that sodium silicate can be as well obtained from rice husk ash what is more sustainable way of activator development [70]. The other potential but extremely rarely applied activators are alkali carbonates and alkali sulphates [62]. The application of the mixture of sodium hydroxide and sodium silicate is definitely predominant in the scientific literature [39], [71]–[77], much less popular is the mixture of potassium hydroxide and sodium silicate [69], [72], [76]. The other possible solutions include among the others: potassium silicate and sodium or potassium hydroxide [78], sodium hydroxide with addition of silica fume [79], [80], potassium hydroxide with addition of silica [80], potassium silicate and potassium hydroxide [81], potassium silicate [82], sodium hydroxide [77], sodium silicate [83], potassium silicate with the fused silica powder [84], calcium hydroxide with sodium silicate and sodium carbonate [68].

### 2.1.3 Different approaches to the geopolymer composition

Most of the scientists design geopolymer mixture regarding to the chemical ratio of ingredients: raw material (or materials) and activator. A significant number of papers derives that the proper Si/Al combined with optimal Na/Al ratio is the most significant factor to ensure high strength [42], [77], [85]–[90]. However, some sources investigate varying Si/Al ratio only (while the Na/Al is constant) [72], [79], [86], [91] or varying Na/Al ratio only (while the Si/Al is constant) [38], [39], [74]. Generally, concluding several scientific investigations on the optimal chemical ratios, the good mechanical performance of the geopolymer can be expected for Si/Al ratio ranging from 1,75 to 2,2 [72], [77], [85]–[90], [92], [93], while the recommended Na/Al ratio is between 0,9 and 1,2 [38], [39], [74], [85]–[90]. However, some publications give recommendations which lie outside the given range of Si/Al and Na/Al ratio. Rowles et al. [87] observed that the highest compressive strength can be expected for Si/Al ~2,5 and Na/Al ~1,25, while for high compressive strength Si/Al can range from 1,75 to 2,75 for Na/Al ratio 1,0-1,5. By contrast, Riahi et al. [86] reports high compressive strength for lower ratios: Si/Al from 1,45 to 1,85 and Na/Al ranging from about 0,85 to 1,05. According to observations, too low Si/Al ratio may lead to less dense structure with unreacted parts and big structural pores. With the increase of Si/Al ratio, the geopolymer becomes denser and more compact and homogenous. Too high Si/Al ratio in turn, can cause shrinkage and internal cracking due

to the excessive removal of structural water [86]. Fletcher et al. [42] in turn, examined geopolymers containing Si/Al ratio ranging from 0,25 to as much as 150 and reports the highest compressive strength for Si/Al ratio 8. Many scientists indicate the water content as the crucial factor for good mechanical performance as well. Water content is usually given as the  $H_2O/Na_2O$  ratio. According to the results,  $H_2O/Na_2O$  ratio should range between 10 and 11 [86], [88], [89], [91], [94]. Especially higher  $H_2O/Na_2O$  ratio could result in significant drop of strength. Riahi et al. [86] reports that for  $H_2O/Na_2O$  ratio equal to 12, compressive strength about 55-60 MPa can be expected, while raising  $H_2O/Na_2O$  ratio to 14 causes a decrease of compressive strength to about 20 MPa. Some scientists indicate the role of the initial water expressed in mass percentage or water solid/ratio on the mechanical performance of geopolymer. Pouhet et al. [95] presents an investigation of the influence of the initial amount of water embodied in the geopolymer mixture on the mechanical behavior of a hardened material. It was observed that both flexural and compressive strength is decreasing with the increase of water content. The highest strength was observed for water mass content 27%. What is more, the total volume of the pores inside the structure is proportional to the amount of water which was initially introduced. By extension, both porosity and pores diameter are greater in samples containing more water. According to the scientists, more than 90% of water inside the geopolymer matrix is "free water" which does not contribute to the final strength and stiffness. Lizcano et al. [80] in turn, examined the influence of the initial water content measured as the ratio of  $H_2O$  to  $SiO_2+Al_2O_3$  on the density of geopolymer. The density decreased with the increase of initial water content both in Na-activated and K-activated geopolymers.

Showing the molar ratios between particular chemical compounds (mostly Si/Al; Na/Al and  $H_2O/Na_2O$ ) seems to be the most general and the most exact way of the description of the geopolymer mixture. However, many scientists choose the other way to characterize the composition of their material. Several papers present tables with the quantity (mass) of each ingredient (metakaolin or the other raw material, sodium silicate, sodium hydroxide, sand etc.) [36], [73], [96]–[99]. Other papers focus only on the mass ratios of the ingredients (in most cases raw material to activators ratio or sodium silicate to sodium hydroxide ratio) [100]–[105]. Some papers characterize particular mixtures by defining specifically the sodium silicate to sodium hydroxide ratio [106], [107]. Pelisser et al. [107] presents reports that  $Na_2OSiO_2/NaOH$  equal to 2,2 and 1,6 results in high compressive strength while  $Na_2OSiO_2/NaOH$  equal to 1,0 gives much smaller strength. Samples of the smallest sodium silicate to sodium hydroxide ratio had also the lowest hardness. Some scientists indicate precisely concentration of sodium hydroxide solution as the variable in their mixtures [98], [106], [108]–[110].

As shown above, there is variety of different approaches to the issue of geopolymer composition designing. There are some prevailing trends, but there are as well many not non-standard approaches. Generally, because of the variety of the possible compositions of geopolymer, the strict guidelines for its designing do not exist. Especially, the initial chemical ratios of basic elements (Si/Al and Na/Al) can change when in the mixture there are more than one source of  $SiO_2$  and  $Al_2O_3$  [38].

## 2.2 Historical background

Geopolymers are sometimes called „a new building material” or „a new alternative for the concrete”. Actually, in the last decades, the interest in this material has grown, and simultaneously, the number of scientific experiments has grown as well. Although, the history of geopolymers is much longer and richer than it could be initially assumed. It cannot be unquestionably stated when and where the history of geopolymers starts. According to the controversial theory established by famous French scientist Joseph Davidovits, one of the first evidences of the intentional use of geopolymers are pyramids [111]. Davidovits’ theory has both enthusiasts and detractors. Detailed scientific analysis of pyramid stone samples showed that it is hard to unequivocally uphold or refute the controversial theory [112].



Fig.2.2.1: Joseph Davidovits during the exploration of pyramids in Egypt [113], [114].

There are some evidences of a connection between geopolymers and ancient Roman mortars, the great durability of which concerned scientists [115]. Professor Roman Malinowski, with co-workers, started in the early 1960s an investigation which has shown that remain parts of Roman structures are made of fine calcite microcrystals [116]. Years later, Joseph Davidovits found connections of ancient mortars with geopolymers [115]. Studies on the ancient beginnings of geopolymers are still carried on. The recent studies concerns the monuments in the South American Andes [117], in Bolivia and the Indian Temple sculptures [118]. All ideas presented above are theories and there are no unquestionable proves of their full correctness. Thus, the formally registered history of geopolymers begins in more modern times.

The first proprietor of the patent involving the production of alkali-activated cement was a German chemist and engineer Hans Kuhl [62], [119]. The patent describing material based on vitreous slag and alkali sulphate/carbonate can be treated as the first publication concerning geopolymers [120]. The author of the next registered investigations (reactivity of slags with use of caustic potash and soda solution) was Chassevent in 1937 [121].

Research concerning alkali-activated slag-based binders was further extended by Belgian scientist Arthur Oscar Purdon whose paper [122] become the first detailed publication about alkali-activated materials. On the basis of experience gathered during an extended research process, Purdon patented the new material called Purdocement which was brought on the market after World War II by the company “Le Purdociment”. Purdocement, containing

about 90% of blast furnace slag with a small addition of Portland cement or lime optionally, was used in the 1950s during the production of residential flats, tunnels, school, factories and pavilions [62], [120] [123].



Fig.2.2.2: Structures in Brussels made partly of Purdocement [123].



Fig.2.2.3: a) 24-storey building made of alkali activated slag-based material in Lipetsk (Russia, 1994), b) Residential building build with alkali hydroxide-activated slag-based precast elements in Mariupol (Ukraine, 1960) [62].

Meanwhile, the Trief cement composed of 1,5% NaCl, 1,5% NaOH, and 97% blast furnace slag has been developed in the United States. Trief cement was used on a large scale by U.S. Army Engineer Waterways Experiment Station in the 1950s [124].

Simultaneously, alkali-activation has been investigated by Professor Victor Glukhovskiy in the former Soviet Union. Glukhovskiy focused on low basic calcium aluminosilicate clays and slags activated by alkali metal solutions, named his new material “soil silicates” and described it precisely in the book “Gruntosilikaty” [125], [62], [120]. The main continuator of his works since the 1980s was Pavel Krivenko who divided the binding systems into two categories and classified alkali-activated cements into five main categories: geocements, fly ash alkaline, slag-alkaline cements, alkaline aluminate cements and alkaline-Portland cements [126]. The ‘soil

silicates' found an application in pavements, pipes, sinks, trenches, stabilization of hazardous waste and in structural and masonry blocks [121], [62].

The next great researcher, who is claimed to be the father of term "geopolymer" is French material scientist Joseph Davidovits. The research efforts of Davidovits and his co-workers began in 1972 at the Cordi-Geopolymere laboratory [127]. The first significant achievement was the discovery of geopolymeric liquid binder based on metakaolin in 1975 [128]. The next breakthrough came when scientists realized that geopolymer cured in elevated temperatures can obtain high early-strength. Material developed by Davidovits was for the first time applied in fire-resistant panels as a coating for a wooden core [129].

In the early 1980s started the cooperation between Davidovits and American Lone Star Industries. The work was focused on binders combining the geopolymeric and hydraulic cement chemistries [129]. The Pyrament Blended Cement (consisting in 80% of Portland cement and in 20% of geopolymeric materials) was the effect of long-lasting works [130], [131]. Pyrament combined the rapidly gained high early strength with low producing costs and found an application in repairing industrial pavements, highway roads and the runways. The popularity of geopolymers in America continued. In the early 1990s, the Federal Aviation Administration has begun the searches for the new type of fire resistant and environmentally friendly aircraft cabin materials. The carbon fiber reinforced potassium aluminosilicate resin geopolymer composites characterized by required fire endurance and high flexural strength occurred to be a perfect solution [132], [129].

The research conducted at the early 1980s showed that geopolymer is acid-resistant and can be used for utilization of hazardous waste [129]. The first tests for encapsulation of heavy metal waste within the geopolymer matrix were performed in 1987, in Canada. Similar trials were carried in Europe within the project GEOCISTEM. The safe utilization of uranium mine tailings by manufacturing low-cost geopolymeric cements was the main double goal of the project, which was culminated with success [133].

In the 1990s geopolymer has debuted in automotive branch. During the season 1994 and 1995 in the Grand Prix of Formula 1, the Benetton team used in their car thermal shield containing parts made of GEOPOLYMER Composite [127].

There are also not negligible Polish emphases in the geopolymer's history. In 1986 two scientists Małolepszy and Petri presented results of their work on slag alkaline binders of the high strength and the work on the activation of synthetic melilite slags [134], [135]. Professor Małolepszy with Professor Nocuń-Wczelik conducted microcalorimetric tests on the alkaline binders based on slags [136]. In the late 80-s two Polish scientists: Jan Deja and Jan Małolepszy investigated the chemical resistance of alkali-activated slag mortars and pastes in chloride solutions [137]. Scientists raised several times the subject of immobilization of the heavy metals inside the structure of the slag-based alkali-activated mortars [138], [139]. They described as well different possible ways for the application of that materials i.e. in the anti-filtration screens [140]. Later, works has been continued by the other renowned scientists.

With each passing year, geopolymer has been gaining more and more attention of scientists all over the world. In 1990s over 100 active research centers have been working on the development of this branch of science [62]. The rate of growth of this sector did not slow down as evidenced by the massive number of the current researches.

### *2.3 The current investigations on geopolymers*

The popularity of geopolymer was growing over time. The history of geopolymer is long and abundant but there is still a lot to be found and discovered in that field of science. Today, research centers all over the world are increasing the knowledge about geopolymer.

Certainly, the person of John Provis cannot be omitted on the list of the scientists most influencing modern geopolymer's science. His book *Alkali Activated Materials* [62] written together with Jannie van Deventer, become for many scientists a guidebook in the geopolymer's (or rather in this case "alkali-activated material's") world. John Provis undertook the study on kinetics of geopolymerisation [141] and validated the mathematical model of chemical reaction kinetics [142]. His current works are focused on the recycling of iron silicate as a precursor [143]. He works as well on the microstructure of alkali-activated mortar and chloride penetration [144]. Brunel University is another center in the United Kingdom which pays attention to the geopolymer issue. Researchers introduced new, pre-dry-mixing method [145] and investigated addition of PCM vacuum-impregnated, thermal energy storing aggregates to the geopolymer based on aluminosilicate rich mud and milled waste glass powder [146].

Lot of vibrant scientific centers working on geopolymers are located in Portugal. Works are carried at University of Beira Interior, University of Minho, Castelo Branco Polytechnic, University of Porto, University of Aveiro and in others research centers. In Portugal, a distinctive direction of tests is geopolymeric binder based on powdered waste from underground tungsten mine located in Panasqueira, in the central part of Portugal [147]. The majority of works is led by Professor Joao Castro-Gomes, Professor Fernando Pacheco-Torgal and Professor Said Jalali. The most recent works concerns, among the others: mechanical and rheological characteristics of mixtures with different activator/precursor ratio [148]; the influence of ground granulated blast furnace slag addition on microstructural properties of hardened material [149]; production of low thermal conductivity foams with use of aluminium powder as a foaming agent [150] and the influence of precursor particle sizes on different mechanical parameters of the foams [151]. One of the most recent lines of research at the University of Beira Interior is the investigation of CO<sub>2</sub> cured binders. The new, ecological binder of good mechanical parameters can be obtained by treating the steel slag with carbon dioxide. The eCO<sub>2</sub>blocks has been already awarded in national and international competitions [152].

Works are as well carried out in Spain, among the others at the University of Granada, University of Sevilla and University of Jaen. The exemplary current work is innovative casting of glass with the use of geopolymers [153]. The attention is being put on ecological ingredients such as hemp fiber-reinforced geopolymer [154] or application of an olive pomace fly ash in the role of alkaline source [155].

One of the biggest names connected with geopolymer in Australia is Jan Stephanus Jakob van Deventer – a professor at the University of Melbourne. He described precisely the reaction mechanisms which accompany the process of transformation of waste materials into the geopolymer gel [72], [156], [157]. He investigated as well the immobilization of hazardous heavy metals inside the geopolymer structure [158]. In his later works, van Deventer paid particular attention to the issue of commercialization of geopolymer cement [159].

The next country which pays an attention to the geopolymer development is China. The current works includes improvement of properties of metakaolin based geopolymer by addition of the rice husk ash [160] or plant fibers [104]. A separate study concerns preparation of decorative, indoor coating [161]. Chinese scientists investigate now the application of geopolymers in 3D printing process [162]. Properties of geopolymer for 3D printing can be enhanced by addition of graphene oxide [163], [164] or steel micro cable reinforcement [165].

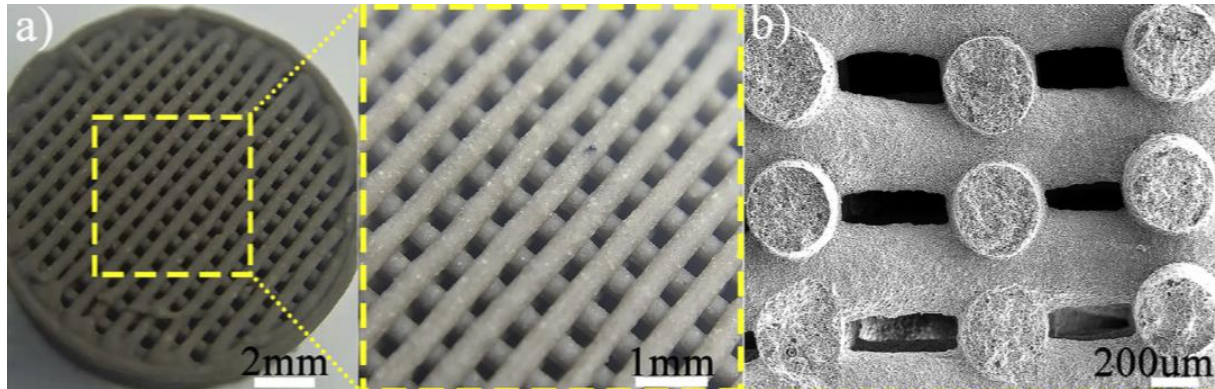


Fig.2.3.1: 3D printed, metakaolin-based geopolymer cellular structure [164].

Works on geopolymers are conducted also in several scientific centers in France. Joseph Davidovits (working currently at Geopolymer Institute in France) proposed recently a technique for testing metakaolin for geopolymer purposes based on the exothermal exothermicity of metakaolin with alkali silicates [166]. Professor Davidovits leads currently as well the project concerning ferro-silico-aluminate geopolymers [167].

Scientists from University of Arlington in United States described the synthesis and characterization of transition-metal free geopolymers containing synthetic aluminosilicate and potassium silicate [168]. Another scientific team derived the dependence between porosity (nanoporosity and microporosity) of metakaolin-based geopolymer composites and chemistry, reinforcement and strength [169].

Many works are conducted currently in Poland. Professor Janusz Mikuła from Cracow University of Technology works on the new kind of geopolymer based on tuff (volcanic rock) coming from Polish village – Filipowice [43]. The part of works concerning the production of zeolites and geopolymers based on volcanic tuff were patented [170], [171]. The first works of Professor Mikuła focused on fly ash-based geopolymers [172] and different possibilities of reinforcement such as distributed steel fibers, wood flour [173] or natural fibers [174]. Studies involve as well the comparison of the influence of casting and 3D printing methods on mechanical properties [175]. One of the most current works presents the non-contact method of large geopolymer surface analysis with the use of bidirectional reflectance distribution function, ellipsometry and spectrophotometry [176]. The current projects covers also investigation on mechanical properties and rheology of geopolymer based on fly coming from the Polish power plant in Połaniec [29], [177]. Professor Izabela Hager with other researchers determined composition of geopolymer achieving compressive strength even up to 67 MPa [29]. The tests involve the performance of fly ash-based geopolymers (including determination of penetration of chloride ions) activated with solutions of different origin [178], [179]. The optimization of geopolymer mixture composition for 3D printing has been as

well the subject of the recent research [180]. At the beginning of XXI century, the large research project on application of geopolymer slurries during the geoengineering works in the injection method has started at AGH University of Science and Technology [181], [182]. One of the more current projects covers a trial to reconstruct the geopolymer matrix with use of combination of small oligomers building blocks and clusters what can help in prediction of many material properties [183]. Another work focuses on the determination of strength and thermal conduction coefficient of slag-based geopolymer with addition of aluminium powder [184].

Professor Lech Czarnecki, from the Warsaw University of Technology, has been working for years on the polymer-concrete composites. The works focused among the others on the thorough studies on the existing knowledge about polymer-concrete composites [185], [186], on the application of polymers in repairing of concrete structures [187] and on understanding of the nature of the chemical interaction between cement and polymer [188].

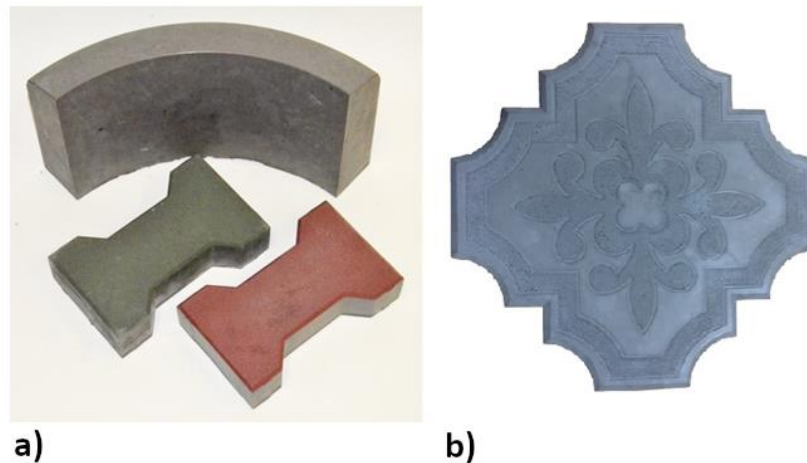


Fig.2.3.2: Examples of products made of geopolymer based on tuff: a) cobblestones, b) decorative plate [189].

Silesian University of Technology is involved in works on geopolymers as well. In 1976, Professor Tadeusz Hop published his book on concrete modified with polymers [190]. Although, this topic is not strictly connected with geopolymers, it shows a trend in searching for alternative solutions and enhancements in building material science and can be treated as a precursor for geopolymers in the Department of Structural Engineering. Researches concerning the application of polymers in civil engineering were continued by Professor Jan Kubica, who, in 2006, presented work on the strengthening of cracked masonry with polymeric resin [191]. The same origin of the relationship between the Silesian University of Technology and geopolymers dates to 2010 when Marcin Górski began work on the University of Beira Interior and started the cooperation with Professor Joao Castro-Gomes. The first works were made by the research team C-Made and then continued within the Master Thesis of Flavio Lacao [192], PhD Thesis of Domingos Coxo and Master Thesis of Natalia Paszek [193], all supervised by Marcin Górski. In the meantime one of the first scientific papers concerning geopolymers and numerical analysis of geopolymer-based elements were published [194]–[196]. Most of the recently performed tests was done within the international project REMINE.

Marcin Górski was one of the initiators and the main Polish coordinator of this project. Preliminary works concerned the mechanical properties of geopolymers based on the suspension obtained from the Polish fossil-fuel power station [197], [198]. Researchers worked also on conventional fly ash, metakaolin with the addition of CRT glass and on the fluidized bed combustion fly ash [199]–[202]. Some of the works involved the addition of granulated cork [195], polypropylene fibers [203], carbon fibers laminates [204] or graphene oxide [205]. The most current works involve the reinforcement of fly ash-based foamed geopolymer with fiberglass mesh [206]. Professor Łaźniewska-Piekarczyk recently has started an innovative research on the recycling of mineral wool coming from the demolition of old buildings in geopolymers [207].

Aside from a multiplicity of theoretical works, geopolymer has already been introduced into the industry and is currently used all over the world. Zeobond is well-known Australian company producing its own geopolymer – E-Crete™, consisting of a blend of ground blast furnace slag and fly ash [159]. Another company, Wagners, developed Earth Friendly Concrete (EFC). The greatest achievement of this company and simultaneously the largest commercial application of geopolymer in the latest time is Brisbane West Wellcamp Airport [208].

The MIDAR Technology, which can be used for the encapsulation of waste and in the production of construction products and ceramics, has been invented by Lucideon company [209]. A ready for use, geopolymeric binder system – BanahCEM (invented by Banah company), can be used in precast units, concrete elements manufacturers, insulation materials, marine constructions etc. [210]. Geopolymer found also an application in fire rated façade materials. Nu-core® A2 Fireproof Geopolymer Aluminum Composites are the new proposition on the interiors and exteriors precast composite panels market [211]. The RENCA company delivers a variety of ready to be used products such as sprayed fire-resistant foam or 3D ink [212]. Milliken® was one of the companies which introduced geopolymers to the market in the United States. GeoSpray® geopolymer mortar is a trenchless technology for rehabilitation and repair of storm and sewer water infrastructure. GeoRoc® is a rapidly hardening fiber-reinforced mortar which can be used for the weathering protection as well as surface reinforcement of rocks, soils and coal strata. GeoStrong® can be applied for both vertical and horizontal concrete surfaces which need to be strengthened [213]. Geopolymer Solutions® from Texas offers geopolymer material called Cold Fusion Concrete (CFC)® which is based on fly ash, slag and other kinds of waste. According to the producer, CFC can be used as alternative to conventional concrete in most of applications with special emphasis to superior chemical and corrosion resistance [214]. Kiran was developed with the help of Geopolymer Institute (France) by Kiran Global Chem Limited, India. A company offers the Geocement, Geobinder and Geocrete containing different by-products: fly ash, activated clay, rice husk ash or blast furnace slag [215]. The main goal of the Alsitech company is to refine, promulgate and implement to the industry the tuff-based geopolymer invented in Cracow University of Technology. Material can be used for production of cobblestones, decorative elements, insulation materials and precast building elements [216].

Geopolymer is a subject of investigations all over the world and on each continent (except from Antarctica). It is impossible to list each country not to mention each scientific

center which is handling the issue of geopolymer. Each year many new papers are written, many conferences are organized and many new projects are begun. The world is looking now for environmentally friendly solutions and geopolymer seems to be one of them.

## 2.4 Application of geopolymers

Geopolymers can find application in many branches of technology and science. Geopolymer as a material for constructional purposes has been already used in building industry. In 1950s in Belgium dozens of structures were made of Purdocement [123]. Later, in the 1990s blast furnace slag-based geopolymer multistory, residential buildings were built in Russia, Ukraine and China [62]. Elements performed by Zeobond with the use of their own geopolymer – E-Crete™ are examples of more recent geopolymer structures [159]. The list of achievements includes freeway expansion works, bridge construction, footpaths, in-situ retaining walls, precast panels and others. The next impressive example of geopolymer application is the Brisbane West Wellcamp Airport. High flexural strength, good workability and low shrinkage allowed to use geopolymer for production of pavements, entry bridge, culverts, curbs, road barriers, sewer tanks, footings, piles and the tunnel slab in terminal building etc. [208].

Aside from the already existing geopolymer structures, there are many examples of theoretical works concerning structural application of this material: containers for water storage, water channels, water filtration systems, culverts and even precast head walls or tunnel segments in back shunt tunnels [217], [218], [219].

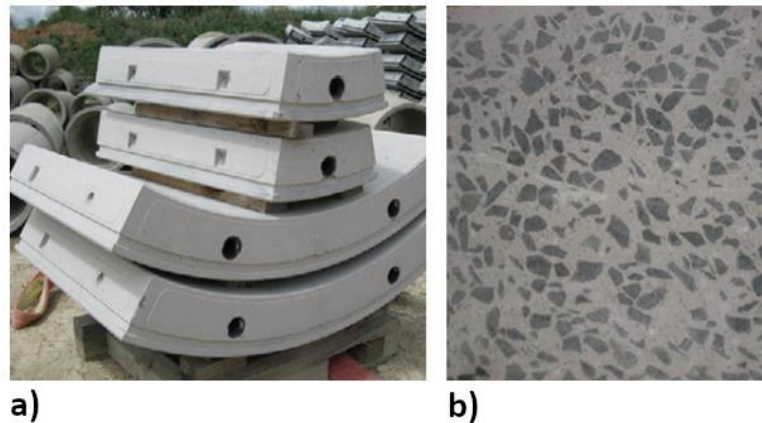


Fig.2.4.1: a) Prototype fibre reinforced geopolymer tunnel segments, b) cross-section of a segment [219].

Suksiripattanapong et al. [220] and Horpibulsuk et al. [59] proposed using fly ash mixed with water treatment sludge for a production of geopolymer masonry units of good compressive strength and better durability and longer service life than clay-cement masonry units. Hoy et al. 2016 [221] describes the possibility of using compacted recycled asphalt pavement stabilized with fly ash geopolymer as a pavement base coarse material. Geopolymer mixtures can be used also for stabilization of pavement sub-base [222]. Another possible application is a production of durable roofing tiles [62], [223]. Researches from United

Kingdom and Malaysia within a project LowCoPreCon are designing domestic buildings made of geopolymer based on waste and by-products available in Malaysia [224]. Gu et al. [225] presents application of soft magnetic geopolymer as an induction heating of pavement at the airports to allow ice or snow melting.

Excellent anticorrosion property of geopolymers was an inspiration for scientists to consider this material as a protection for reinforced concrete against corrosion [226], [227] [228]. An optimal setting time, good geopolymer to cement bond strength, low permeability, quick compression strength development and very good anticorrosion are properties propitious for the coating work at the seaside. Additionally, the aluminosilicate geopolymerization products, state stable when immersed in sea water or exposed in air, what gives concrete a chemical protection [226], [227], [229].

The excellent bond strength between the geopolymer and the concrete allows using geopolymers as a material for infrastructure rehabilitation. Geopolymer achieves high bond strength very early and is relatively cheap in comparison to materials commercially used for infrastructure rehabilitation. Because of great anticorrosion properties, geopolymers can be used also for trenchless rehabilitation of sewage pipelines [230]. Balaguru [231] reports research on geopolymer protective coating of transportation infrastructures which can be applied using squeeze, brush or sprayer and are compatible with different surfaces (concrete, steel and timber). What is more, smooth and glassy surface enable easy graffiti removal.



Fig.2.4.2: Sewage pipeline during and after rehabilitation [230].

Researches reveal that geopolymer can be used as well as a fire protection for concrete structures. Sakkas et al. [232] presents subjecting the concrete block covered with 5cm thick geopolymer to the dangerous fire scenario. The geopolymer covering layer was not affected by any visible signs of damage indicating its potential application in passive fire protection for underground structures. What is more, the great adhesion to the metal substrates proves its usability as fire protection coating for steel structures [233].

Good flexural strength, fire endurance and non-combustibility are also main reasons why geopolymer is considered for aircraft applications. The geopolymer honeycomb and foam (reinforced with carbon fibers) applied in sandwich structure has been tested as the main construction of emergency exit door. Geopolymer composite has shown excellent heat and flame resistance and low material and manufacturing costs [234].

A wide range of research was dedicated to the geopolymers ability of stabilization of mine tailings and immobilization of toxic and hazardous elements within the three dimensional framework of geopolymeric matrix [41]. Mine tailings usually contains heavy metals and toxic substances, which, disposed in tailing ponds can state an environmental threat [235]. According to Jaarsveld et al. [156] it is possible to product strong and low permeable geopolymer consisting in 65-70% of tailings for capping mine tailings. Rao et al. [235] presents the oil sand tailings consolidation using the geopolymerization process. Boca Santa et al. [236] describes an immobilization of heavy metals (Pb, Cu, Zn, As, Sn) from industrial waste of printed circuit board within fly ash-based geopolymer matrix.

Three-dimensional (3D) printing states another potential application for geopolymers. According to researches, geopolymer can be used in both powder-based [237] and extrusion-based [238] 3D printing technique. According to results, geopolymer is able to replace commercially used materials showing even greater compressive strength and can be considered for 3D printed structural elements.

Koster et al. [239] shows a novel application for geopolymers in self-healing concrete, where the special type of bacterial spores is introduced to the concrete mixture. When hardened concrete cracks and water enters the structure, the bacteria germinate and plug the cracks with the calcium carbonate. Geopolymer cover can protect bacteria during the concrete mixing process. It opens only during the concrete cracking (due to the strong bond between geopolymer and concrete matrixes) releasing encapsulated bacteria. The other innovative application of geopolymer as a bioactive material used for bone repair is described in MacKenzie et al. [240].

Geopolymer can be used in artistic branches as well. Clausi et al. [94] have explored the application of metakaolin-based geopolymer in Cultural Heritage as a mortar used for restoration. Tested geopolymer is reported to be durable, to have versatile range of physical properties which can be adjusted to the original material and to be similar to the natural stone what is evidence of the aesthetic compatibility.

Considering future initiatives, geopolymer is taken into account as the possible building material for the lunar structures [241], [242].

## *2.5 Cathode ray tube glass*

### **2.5.1 Description of the material**

The Cathode Ray Tube (CRT) is a crucial part in most of computer monitors and television sets produced for decades. Simply put, CRT can be described as a specialized vacuum tube which is emitting images at the moment when an electron beam meets a phosphorescent surface [243]. Two basic types of CRTs can be distinguished: black and white (called also as monochrome) and color. CRT represents about two thirds of computer or television monitor weights and is built in almost 85% out of glass which is called the CRT glass [244]. CRT glass can be divided into three main parts: panel (screen) barium-strontium glass (~65 wt%), funnel lead silicate glass (~30 wt%) and neck lead silicate glass (~5 wt%) (see Fig. 2.5.1) [245], [246]. Screen glass is free of lead (or contains trace amounts of lead) but contains small amounts of barium and strontium. By contrast, funnel and cone glass can

contain 22-28% and about 25% of lead respectively [247]. In the color CRTs the frit glass is also present. Frit glass is a thin layer between the panel and cone of high lead content (~85 wt%). Additionally, the panel part is covered with a thin fluorescent layer which is rich in yttrium, zinc sulphides, europium and cadmium sulphides [248]. There is non-negligible difference in Pb content between color and monochrome CRTs, to the disadvantage of the color ones. The variation is caused by the presence of the frit part in color CRT and the higher content of Pb in the funnel glass [249]. Generally, a typical computer CRT contains up to ~1 kg of lead while a typical TV CRT may even contain over 3,5 kg of lead [249]. Heavy metals (mainly Pb, Sr and Ba) are components of CRT glass which most draw the attention. Nevertheless, CRT glass is mainly built of SiO<sub>2</sub>. The rest of the main compounds present in each part of CRT glass although in different quantity is as follow: Na<sub>2</sub>O, Al<sub>2</sub>O<sub>3</sub> and K<sub>2</sub>O. The exact composition of CRT glass varies among the others in dependence of the type (monochrome or color), manufacturer and year of the production [248].

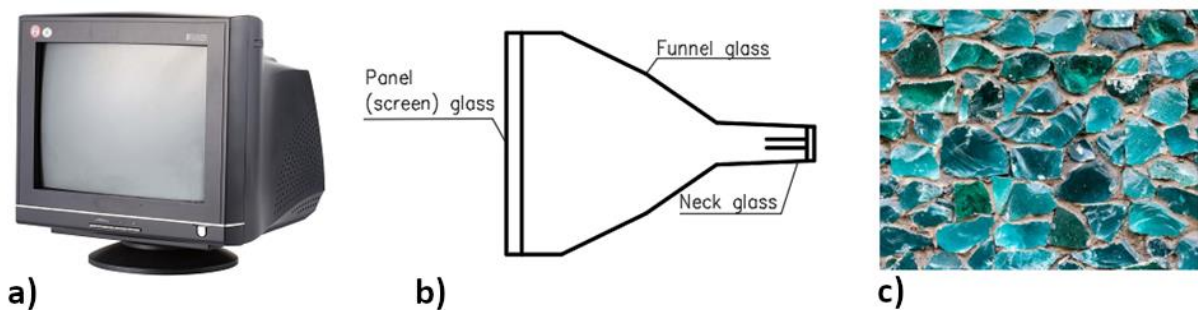


Fig.2.5.1: a) The old television set containing cathode ray tube (CRT) [250], b) schematic view of CRT components [245], c) CRT glass [251].

The high lead content which can cause serious environmental effects is the main problem connected with the CRT glass storage and recycling. The potential leaching of lead from CRT glass storage on landfills poses a serious environmental threat [252]. The importance of the problem had an effect on several legal acts. Restrictions concerning collecting, utilizing, recycling and recovery of electronic waste in a way which will ensure the safety of human and animal lives and health and environmental safety are depicted among the others in European Directive WEEE [253], [254]. Because of its toxicity, the recycling of the CRT glass is much more complicated and demands more attention than the recycling of ordinary glass. Possible ways for CRT glass reuse can be classified into two main groups: closed-loop recycling and open-loop recycling [245]. Closed-loop recycling is simply manufacturing of new CRT glass from an old and discarded one. After being disassembled, cleaned and subjected to other pre-treatments if needed, old CRT glass is mixed with fresh material to produce new CRT glass. Such practice is well known all over the world. Recycling of CRT glass in closed-loop allows to save energy and materials and decrease the contamination level in comparison to the production of CRT glass from raw materials. The most significant disadvantage of this method is a decline of CRT glass production in few last years which will be probably limited even more strictly in the future. Liquid crystal displays (LCDs), light-emitting diodes (LED) and plasma display panels (PDP) are technologies which almost entirely displaced CRTs [245], [247]. Such tendency gives rise to the bigger interest of the industry and scientists in the open-loop recycling. In this

method, the old material is used for the production of many different products or materials [245]. The general idea of closed and open-loop recycling is presented in Figure 2.5.2.

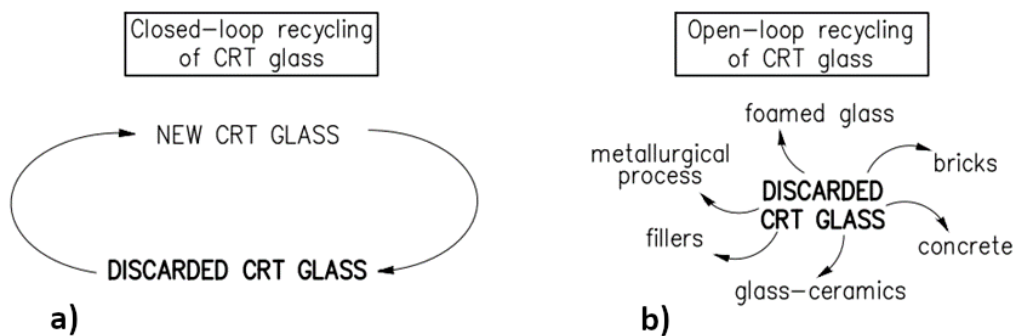


Fig.2.5.2: Possible ways of CRT glass recycling a) in open-loop, b) in closed-loop.

Scientists developed a variety of application paths for discarded CRT glass. It can be used in the production of glass-ceramics [244], [255], [256]; foamed glass (for example for insulation purposes) [257]–[259]; glass foams with use of eggshells as a non-typical calcium carbonate-based foaming agent [260]; in ceramic tiles production (as a replacement for a frit in transparent glazes) [261]; in manufacturing of roof tiles and clay bricks [262]; for a production of glass fibers to be used as a filler in polypropylene materials [263]; in microwave applications (in foamed form – as an electromagnetic absorbent used in building industry) [264]; application in metallurgical processes as fluxing material (in lead and copper smelting process) [265] and even as a lead adsorbent in aqueous systems [266]. Some methods allow using CRT glass without any special treatment (still with the high lead content). Other methods, however, require partial or complete lead removal. Several methods for lead removal from the glass matrix were developed. Self-propagating high-temperature synthesis (SHS) allows for stabilization of heavy metals (including lead) in CRT glass [267]. The other method is a subcritical hydrothermal treatment which causes the conversion of glass into chemically active layered silicate compound. In the next step, the lead is removed by immersion in the dilute nitric acid [268]. Yuan et al. [269] proposed the mechanical activation by ball milling what caused physicochemical changes such as chemical breakage of the glass matrix. Mechanical activation facilitated the further dissolution of material and thus, the lead removal. Another idea is the removal of lead with the use of chlorination-volatilization process [270].

### 2.5.2 Application of CRT glass in concrete

The possibility of recycling of CRT glass in concrete is the separate, much-discussed topic. Since this method of glass reuse is closest to the topic raised in this Thesis, the more careful attention will be paid to the description of investigations done previously in this field of science. Scientific papers cover examples of application of various fractions of CRT glass inside concrete [271]–[273]. One of the biggest problems connected with the introduction of this hazardous waste into the concrete is heavy metals leaching. It was reported that the concentration of heavy metals (especially lead) in the leachates from concrete with CRT glass

could not fulfil the required limits [274]. The several trials of application of CRT glass into the cement mortar or concrete are presented below.

Hui et al. [275] presents studies on the replacement of fine aggregate (the natural river sand) with CRT glass in OPC concrete with the addition of ground granulated blast-furnace slag and fly ash. Mortar with CRT glass achieved higher early and long-term strength than the mortar with river sand. The difference after 28 days reached almost 65%. Flexural strength and static elasticity modulus of mortar with CRT glass were also higher than with river sand, although, this time the differences were small. Authors suggest that the significant increase of compressive strength can be caused by the fact that more CRT glass is used for replacement of the sand what improves the packing of aggregate particles. Mortar with CRT glass had larger alkali-silica reaction expansion and was affected by bigger drying shrinkage (measured as the length change) than mortar with the sand. No lead leaching was measured.

The improvement of flexural and compressive strength of cement mortar (both short-term and long-term) after addition of crushed CRT glass instead of natural sand was observed also by Walczak et al. [276]. The compressive strength increases of about 16% and flexural – of about 14%. Authors suggest that CRT glass is more reactive than sand what helps obtaining higher strength. What is more, the high silica content in the mortar allows for the reaction with the calcium hydroxide (generated during the hydration process) and for the production of a C-S-H gel (calcium silicate hydrate gel) which has an impact on the strength. The same authors participated in successful experiment on the application of CRT glass as an additive in autoclaved aerated concrete [277]. The addition of CRT glass had no negative effect on the strength nor on the quality of the hydration products.

The small increase in compressive strength of cement mortar with 10% and 20% of CRT glass instead of sand was noticed by Jura et al. [278]. Although, CRT glass replacing sand in 30% caused small decrease of compressive strength. No evident influence of CRT glass content on frost resistance was observed. No negative effects of CRT glass on strength of cement mortar was described by the same authors in [279]. Similar dependence (the increase of strength for small percentage replacement of natural aggregate with CRT glass) was mentioned also in [280]. The improvement of high temperature resistance with the increase of CRT content is the separate conclusion of this paper.

Romero et al. [273] reports, that compressive strength of concrete containing 10%, 20% and 30% of CRT glass increases in comparison to concrete containing natural limestone aggregate. Scientists also report that workability is affected negatively by addition of CRT glass. The lead leaching can be limited by introducing cross-linked biopolymer into the matrix. The enhancement of concrete with CRT glass thank to biopolymer was also described in [281].

The opposite results present Ling et al. [282] who investigated a recycling of high density CRT glass as a fine heavyweight aggregate in barite concrete. Scientists replaced natural granite and barite aggregates with treated (without lead) and untreated (with lead content) CRT glass. It was noticed that the bigger replacement of natural aggregate with CRT glass, the bigger density of concrete samples. Moreover, samples with untreated CRT glass had higher density than that with treated CRT, probably because of the lead content. Scientists found out that splitting tensile strength is falling monotonically with the increase of CRT content (untreated CRT glass has more negative influence on the strength). CRT replacement has also negative influence on compressive strength but in that case, differences were much

less significant (not exceeding 20%). Authors suggest that the decrease of the strength could be caused by smoother and plainer surface of CRT glass particles than of natural aggregate. No strict, monotonic dependence between CRT content and elastic modulus was found. The growth of CRT content decreases the resistance to carbonation of the concrete but reduces the drying shrinkage. The drying shrinkage is reduced because the glass addition decreased the total water content. The leaching test indicated that it is possible to use treated CRT glass up to 100% but not treated CRT glass can be used only to 25% as replacement of natural aggregate in heavyweight concrete.

The same scientists repeated the trial of application of CRT glass this time as an aggregate in X-ray radiation-resistant cement mortar [283]. The behavior of the mortar with CRT glass was compared to the behavior of the mortar with natural river sand. Once again, the decrease of the strength with the increase of glass content was registered. However, the strength of material with CRT glass was good enough to qualify such mortar for structural purposes. The tests have shown that the addition of CRT glass (both treated and untreated) enhances the radiation-shielding properties of the mortar and allows to use this material in CT-scanner and X-ray diagnostic rooms. The other idea of Tung-Chai Ling and Chi-Sun Poon was to add crushed CRT glass as an aggregate (both fine and coarse one) into dry-mixed concrete paving blocks [284]. The replacement of natural aggregate with CRT glass decreased water absorption. As in the previous tests of these authors, the density growth while the dry shrinkage and compressive strength decreased (till the acceptable level) with the increase of CRT content. Lead leaching showed that the maximum content of CRT glass replacing the fine aggregate in the material could be equal to 25%. Much less lead was leached from samples containing bigger particles of CRT glass. The expansion due to alkali-silica reaction enlarged with the increase of glass content. The authors concluded that CRT glass is an appropriate material for aggregate in concrete paving blocks.

The decline in the strength with the increase of the replacement rate of natural sand with CRT glass was also described in [285] and [271]. The addition of CRT glass leads to the reduction of storage modulus (stiffness) of mortar. No strict, monotonic influence on the consistency of the fresh mortar nor on its loss tangent was observed [285]. The presence of CRT glass can enhance the long-term resistance to chloride ion penetration. The elastic modulus decreased with the increase of CRT glass content [271]. Liu et al. 2020 [272] reports that the increase of CRT glass content results in a decrease of both short-term and long-term flexural and compressive strength of ultra-high performance concrete. The flowability of the fresh mixture as well as the porosity of the hardened material increases with the increase of CRT glass content. The lead leaching grows monotonically along with the increase of CRT glass content although, even for the replacement rate 100%, the leached lead concentration is still below the allowed limit.

Studies done by Song et al. [286] confirms most of described above characteristics of concrete with CRT glass: the increase in density, a decrease of water absorption, elastic modulus and strength. This paper adds a new behavior: damping ratio, which is not impacted significantly by addition of CRT glass. The influence of CRT grains size was also investigated. Concrete containing smaller CRT grains obtained higher strength and higher modulus of elasticity than concrete with CRT particles of a bigger size. By contrast, Witkowski et al. [287] noticed the increase of water absorption of concrete with incorporated CRT glass into the

composition. Scientists also observed the decrease of both flexural and compressive strength of concrete with glass.

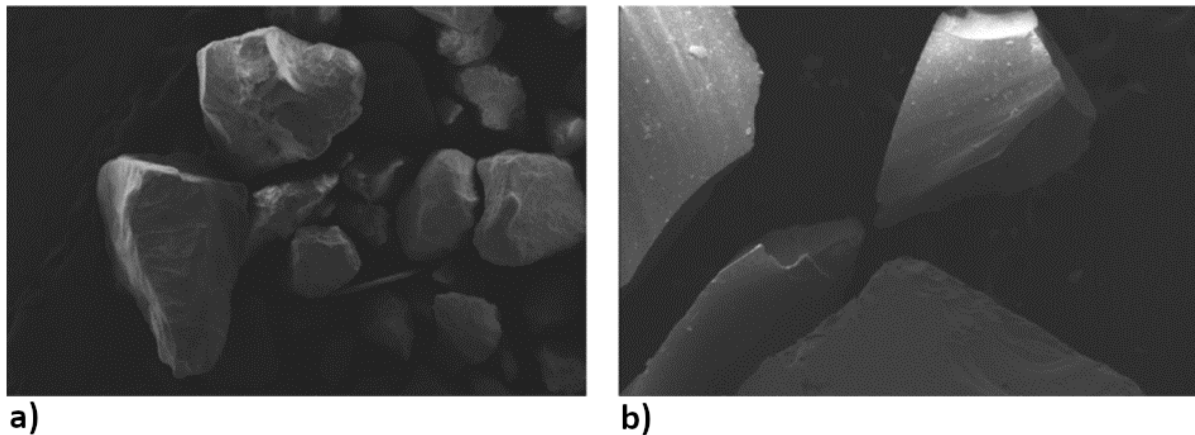


Fig.2.5.3: a) Natural sand grains versus, b) CRT glass particles [285].

Pauzi et al. [288] investigated the behavior of concrete with spherical and crushed CRT glass as a replacement of the natural coarse aggregate. Samples with CRT glass (both spherical and crushed) achieved significantly smaller compressive and splitting tensile and flexural strength after 7, 28 and 56 days than samples with natural aggregate. Samples with CRT grains of a spherical shape obtained slightly higher compressive strength but smaller splitting tensile and flexural strength than these with crushed CRT glass. Authors concluded that the smooth surface of CRT glass weakens the bond between cement paste and aggregate what causes the decrease in strength. The study has shown that concrete with CRT glass replacing 100% of natural aggregate fulfil the lead leaching standards for CRT glass grains higher than 4,75mm.

Despite conducting laboratory tests, many scientists focused on the theoretical aspect of application of CRT glass in building materials and on the State of Art [245], [246], [289]–[291] as well.

### 2.5.3 Ability of geopolymers for immobilization of heavy metals

Geopolymers are claimed to have abilities to immobilize toxic elemental waste within their matrix. Hazardous elements (such as heavy metals) after introducing into the mixture, are locked inside the rigid network of the geopolymer matrix [41]. Heavy metal ions are adsorbed onto geopolymer structure due to the bond, which is formed between the aluminosilicate matrix and toxic waste particles on the base of the surface reactivity [292], [293]. The new phase is formatted after reaction of the insoluble Cu, Pb or other compounds with species dissolved from Al source, rich in Si and Al [294]. The efficiency of the immobilization of heavy ions can be affected by such factors as: type of cation present in alkaline solution, the concentration of alkaline solution, curing time, pH level etc. The leaching test is the most efficient way to asses if the immobilization process was successful. The high content of heavy metals in leachates can be caused by disruption or degradation of the geopolymer matrix or the release of toxic particles from the intact matrix (a process which can be compared to the ion exchange) [292]. The issue of immobilization of toxic waste inside geopolymers is broadly described by different scientists.

Boca Santa et al. [236] introduced a waste solution (containing among the others such metals as Pb, Cr, Cu, Fe, Sn, As, Ni) into the bottom ash-based geopolymer matrix activated with sodium hydroxide or potassium hydroxide mixed with sodium silicate. Test results indicated that heavy metals were successfully immobilized in the geopolymer structure however, in different proportions. Leaching and solubility tests indicated that all heavy metals were immobilized physically and chemically in about 97%. Most of metals were immobilized in almost 99,99%.

The water introduced into the mixture in the form of waste solution which can interfere with the geopolymer matrix and affect its characteristics negatively states the disadvantage of this method. Somna et al. [295] presents the immobilization of heavy metals (Ni, Cd and Zn) in fly ash-based geopolymer. Authors observed that incorporation of heavy metals has an adverse effect on compressive strength, but they conclude that fly ash-based geopolymer can be used for immobilization of heavy metals.

The high immobilization of heavy metals (Zn, Pb, Cd and Cr) inside alkali-activated cementitious slag materials were observed by Professor Małolepszy and Professor Deja [138], [139]. Authors explain that the structure and properties of alkali-activated slag hydration products (i.e., the high gel pores content) are crucial for the immobilization abilities.

Palomo et al. [296] investigated the introducing of chromium and lead into the fly ash-based geopolymer matrix. Chromium is not immobilized effectively, and it is disturbing the fly ash activation and hardening process. Leaching test showed that lead had been successfully solidified and stabilized in the structure. Zhang et al. [158] also reports problems with immobilization of the chromium element. Heavy metals were introduced to fly ash-based geopolymer matrix in the form of nitrate and chromate salts. Contaminant ions were dispersed throughout the matrix what did not change the geopolymer structure significantly. Toxic waste if added in small amounts, do not decrease relevantly compressive strength and may even enhance it. Lead and cadmium were successfully stabilized inside the material. Ji et al. [297] presents the immobilization of heavy metals (Cd, Pb and Zn) in metakaolin-based geopolymer in which part of raw material was replaced with aluminium or iron-based drinking water treatment residuals. Scientists added 1, 2 or 4% of heavy metal to the mixture. The compressive strength decreases with the increase of toxic ions content. The immobilization rate ranged from 97,8% (4% of Zn) to 99,7% (1% of Cd). The efficiency of lead stabilization was not lower than 98,3%. According to Phair et al. [294] the efficiency of Pb immobilization depends on the type of activator and overall extractable alkali cation concentration of Al source. NaOH was the best from activators used during the research (the concentration of lead in leachates from samples activated with NaOH fulfilled requirements). The immobilization of Cu was much less effective. Authors suggest that the toxic waste pre-treatment (with the Al source) before introduction to the mixture would increase the efficiency of its immobilization.

#### 2.5.4 Application of CRT glass in geopolymers

All scientific works listed above treat about possible immobilization of toxic waste inside the geopolymeric matrix. That allows assuming that the utilization of CRT glass (which is toxic and contains heavy metals) inside the geopolymer matrix is possible. Nonetheless,

introduction of toxic metal ions to the structure varies from the introduction of CRT glass. The different attempts of adding of CRT glass into the geopolymer and the effect on the mechanical behavior of the final product are presented below.

Moncea et al. [298] conducted studies at the possible immobilization of Pb from discarded, waste, powdered CRT glass from television sets and computer screens inside the geopolymer matrix. The mixture contained type F fly ash, sand, sodium hydroxide and sodium silicate. The amount of CRT glass was dosed in such amount to bring 2% to 10% of Pb to the mixture (13% - 69% of CRT glass to the mass of the fly ash). The CRT glass contained 15,5% of Pb. Samples were subjected to the thermal treatment at 60°C by the first 24 hours. For the next 27 days, samples were cured at the room temperature. The immobilization ratio was assessed according to the leaching test (due to the standard NEN 7345 [299]). The acidified and distilled water was used as the leaching agent. Tests have shown that the highest amount of the lead is leached from the matrix during the first 6 hours. At 64 days, the Pb<sup>2+</sup> concentration in acidified water and distilled water was equal to 8 and 5,45 mg/m<sup>2</sup> consecutively. These values are below the maximum allowed limit (100 mg/m<sup>2</sup>) given by Dutch Building Material Decree [300]. The final pH of distilled water was equal to 10 while of acidified water – 11. The small amount of CRT glass powder did not influence the compressive strength significantly. The increase of CRT glass content affected negatively the early compressive strength of geopolymer but enhanced the long-term compressive strength. As the continuation of the previous work, the behavior of slag-based geopolymer was investigated by the same group of scientists [301]. Authors observed that the hydration process is not affected when the small amount of Pb (0,18%) is incorporated in the matrix. Higher content of Pb (10%) slows down the hydration.

Gao et al. [302] presents application of CRT glass as fine aggregate in fly ash and ground granulated blast furnace slag-based geopolymer. Scientists proved that geopolymer incorporating CRT glass shows much smaller alkali silica reaction expansion and are able to better maintain high compressive strength than Portland cement concrete with CRT glass. Geopolymer containing CRT glass showed enhanced shielding performance. Incorporation of CRT inside geopolymer matrix decreased Pb leaching in comparison to pure CRT glass as well as to concrete with CRT glass.

Catauro et al. [303] presents the attempt of the utilization of milled CRT glass coming from TV and personal computer kinescopes (in particular funnel glass VFNL, reach in PbO – 18% and glass named VBa, reach in BaO – 10%) in metakaolin-based geopolymer. The mixtures contained 60 wt % of metakaolin and 40 wt % of CRT glass and were activated with sodium silicate and sodium hydroxide solutions. Geopolymers were cured at the room temperature. The leaching test was conducted according to the European standard EN 12457 [304]. Due to the test described in [303], the CRT glass does not show high reactivity in the geopolymer structure but as well does not interrupt the geopolymerization process. The addition of CRT glass increases the Si content and Si/Al ratio what, in effect leads to the lower release of the Al from the geopolymer. The amount of all leached metals (except of Pb and Sb) was beyond the allowable limits. The compressive strength was not investigated.

Ogundiran et al. [105] presents the recycling of powdered CRT glass inside metakaolin clay-based geopolymer activated by sodium hydroxide and sodium silicate mixture. CRT glass was added as a replacement of metakaolin clay in proportions 0% - 20%. CRT glass contained

24,1% of PbO by mass. Samples were cured at the room temperature. The leaching test was carried out according to the toxicity characteristic leaching procedure (TCLP) [305]. The concentration of extractable Pb particles in geopolymers is much lower than in non-stabilized starting materials. The amount of Pb particles ranged from 0,27 to 4,28 mg/l. The maximum mass content of CRT glass in the geopolymer, which allows fulfilling the leaching standards is 15%. Samples with CRT glass were less water absorbent and had higher density. Tests have shown that the compressive strength increases with the increase of CRT glass content. The growth of compressive strength of geopolymer with 20% of CRT glass in comparison to the geopolymer without CRT glass ranged between 19% and 30% in dependence on the curing period length.

Authors indicate three main possible reasons for higher strength of geopolymer with CRT glass:

1. Increased amount of SiO<sub>2</sub> content what resulted in more Si-O-Si bonds which are reported to be stronger than Al-O-Al bonds.
2. Higher water demand of mixtures without CRT glass what resulted in more rapid hardening and lower time for development of rigid, strong structure.
3. The presence of Pb in the structure.

Ogundele et al. [306] reports a partial replacement of calcined clay with powdered CRT glass (0%, 25%, 50% and 75% by mass). The used CRT glass contained 2,93% of Pb. Samples were cured at ambient temperature. According to the results, the compressive strength decreases while the drying shrinkage and water absorption increase along with the increase of CRT glass content. The compressive strength of samples containing 50% of CRT glass was equal to 13,44 MPa.

Long et al. [307] investigated the behavior of ground granulated blast furnace slag-based geopolymer with powdered CRT glass as a partial replacement (0%, 10%, 30%, 50% and 70% by mass) of the raw material. The mixture contained slag, powdered CRT glass (of high PbO content – 24,52% by mass), sand, sodium silicate and sodium hydroxide. The leaching test (done according to the TCLP) has shown that when the CRT glass content is below 50%, the lead leaching fits in the required limits. The concentration of Pb present in alkali activated slag mortar ranged from 6,04 to 42,31 mg/l in dependence on CRT glass content. After stabilization of the mixture, the extraction values dropped beneath the 1 mg/l in case of geopolymers containing 10-30% of CRT glass. Leachate from material containing 50% and 70% of CRT glass contained respectively 1,78 and 8,83 mg/l of Pb. What is more, CRT glass has no significant negative effect on the strength of the final product. Scientists observed, that both flexural and compressive strength decreases with the increase of CRT glass content. Although, when the CRT glass content does not exceed 50%, the long-term flexural strength decreases by about 12% while compressive strength decreases by approximately 8%. For 70% of CRT glass content, the drop in strength is much higher – over 35% both in the case of flexural and compressive strength. The structure of the geopolymer was not changed, and no additional geopolymerization products are produced. This test has shown that CRT with the lead content can be efficiently and safely immobilized in the geopolymer structure. Tests conducted by Long et al. [307] have been continued but this time CRT glass was applied in the form of a fine aggregate as a partial replacement of sand (sand to CRT glass mass ratio was equal to 1:1)

[308]. Ground granulated blast furnace slag replaced with a fly ash in 0, 30, 50, 70 and 100% was used as the precursor. Geopolymer was cured at the ambient temperature. All samples containing CRT glass and sand achieved smaller compressive strength than samples with sand only. The decrease of strength ranged between 15% and 18% with the exception of geopolymer based on fly ash only, where after the addition of CRT glass compressive strength decreased by over 72%. Generally, the compressive strength of samples with sand ranged from 9,0 to 23,6 MPa and samples with sand and CRT glass from 2,5 MPa to 19,4 MPa in dependence on slag to fly ash ratio. According to scientists, the Pb leached from the hardened material fulfils the required limits in geopolymer containing 0, 30 and 50% of fly ash. The PbO does not affect the crystalline phase nor the aluminosilicate structure of the matrix but retards the hydration process. The continuation of an investigation is described in recently published paper [309]. CRT glass and sand have been used as fine aggregates in mass ratio 1:1. Fly ash and slag, in mass ratio 1:1, have been used in the role of raw materials. Silica modulus ( $\text{SiO}_2$  to  $\text{Na}_2\text{O}$  ratio) and alkali dosage ( $\text{Na}_2\text{O}$  to binder ratio) were the varying factors. According to results, compressive strength increases significantly along with the increase of silica modulus from 0 to 1,5. The optimum alkali dosage was specified between 6% and 8%. The maximum compressive strength achieved during test exceeded 72 MPa. That result is significantly higher than in previously reported tests [307], [308]. An increase of silica modulus improves compressive strength, interfacial transition zone between CRT glass particles and geopolymer, limits the Pb leaching, increases the chemical solidification of Pb and decreases the total porosity. Authors emphasize, that Pb ions are both physically encapsulated and chemically solidified inside geopolymer matrix. All tested samples fulfilled limits for Pb leaching what means that CRT glass can be successfully recycled within proposed geopolymer mixture.

Carrillo et al. (2021) [310] presents the research on the influence of addition of CRT glass particles (of size 0,010 mm to 1,100 mm) to metakaolin-based geopolymer in ratio 5, 10 and 20% by weight. Samples were cured at 65°C for the first 20 h, then at the room temperature. According to the results, encapsulation of CRT within metakolin-based matrix reduces significantly concentration of toxic metals (lead and barium) in leachates. In case of the not solidified CRT glass powder, the concentrations of Pb are equal to  $32,4 \pm 2.74$  mg/l and exceed limit value 16 times or 6,5 times in dependence on the considered standard. Scientists proved that the amount of Pb in leachate can be reduced to 1,48 mg/l for geopolymer with CRT glass content 5% and 10% or to 2,43 mg/l for CRT glass content 20% by weight. Scientists indicate that the reduction of Na<sup>+</sup> ions and application of less alkaline medium provide higher immobilization rate since the surface of the CRT glass is dissolved more easily (mainly Si and Al elements) and reacts with the rest of geopolymer matrix. Consequently, toxic metals are encapsulated within the new phase (called by scientists an albite) which enable better anchoring of CRT glass particles to the matrix (see Fig. 2.5.4). In geopolymer mixtures with higher NaOH amount, the polymerization takes place faster hampering the immobilization of toxic ion metals.

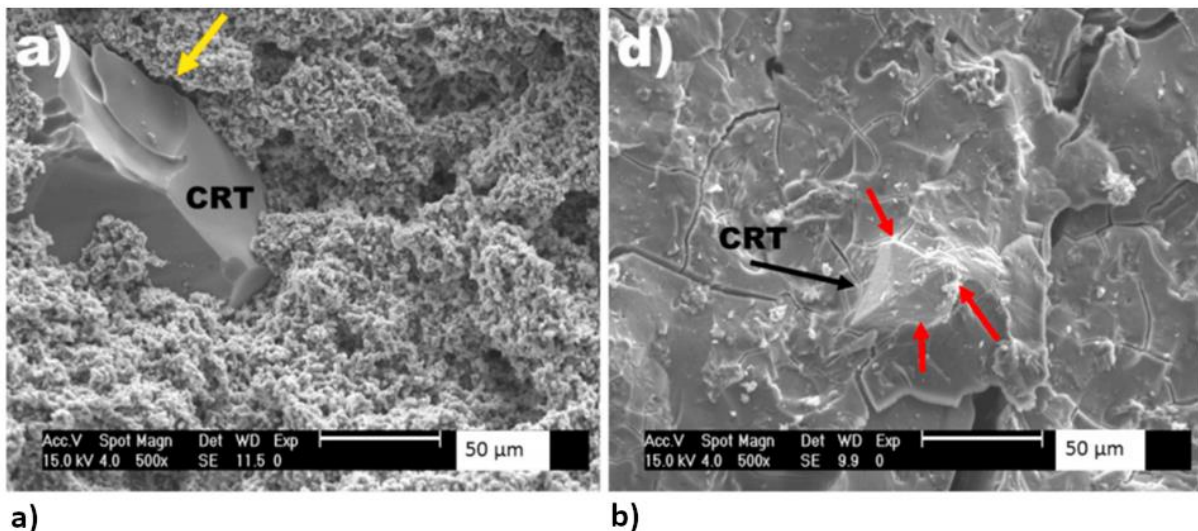


Fig.2.5.4: SEM micrographs of metakaolin based geopolymer with CRT glass with the molar elements ratios: a) Na/Si=0,74, b) Na/Si=0,51 [310].

Recycling of hazardous high leaded CRT glass was risen with the European programme HORIZON 2020 as well. The main goal was to design and produce high performance geopolymer blocks containing discarded CRT glass. The first step was to precipitate CRT glass out of the lead using the novel hydrochemistry method. The retrieved lead could be sold, and the unleaded CRT glass was to be used in the production of VirtuCrete new kind of geopolymer concrete. The project lasted from July 2015 till the end of December 2015 and was coordinated by the Virtus Projects Limited in the United Kingdom. Unfortunately, the author could not find any further details of the project (concerning methodology or used materials) evidence of the success nor the evidence of the failure [311].

The preparation of radiation-proof geopolymer with use of powdered CRT glass was patented recently by Chinese scientists [312]. Authors indicate the silicon and aluminium rich ingredients as the possible raw materials (i.e., silicon rich aluminium ash, ground granulated blast furnace slag or metakaolin) and the mixture of sodium silicate and sodium hydroxide as activators. The presence of CRT glass (particularly the heavy metals incorporated inside as galena, barium, lead and strontium) enhances the radiation ray absorbance ability of the geopolymer. The geopolymer should be cured at the temperature ranging from 30°C to 50°C by 24 to 48 h. According to the inventors, the addition of calcined dolomite reduces the lead leaching effect. The final product can achieve approximately 31-62 MPa compressive strength. Authors mention several possible ways of application of their invention: construction radiation shield body, nuclear reactor housing, nuclear waste curing treatment.

Badanoiu et al. [313] investigated the possibility of preparing the geopolymer based only on crushed CRT glass (without any other raw materials) and compared its properties with geopolymers based on fly ash replaced with powdered CRT glass. The mixture was activated with NaOH or KOH solutions. Scientists observed that samples containing only CRT glass obtained significantly higher compressive strength than samples with CRT glass and fly ash and with the fly ash only. However, generally, the results of compressive strength were not very high. Within mixtures activated with NaOH solution, the highest strengths (about 16 MPa and 22 MPa) were obtained by samples cured for 90 days, containing liquid to solid ratio

0,4 and 0,5 respectively. Samples cured at the room temperature achieved generally smaller short-term and higher long-term compressive strength than samples cured for the first 4 days at 60°C. Geopolymer activated with KOH solution had higher strength (over 25 MPa after few days of curing) than geopolymer activated with NaOH, but its strength had shown a worrying tendency to fall down in time. Authors observed that geopolymer based on CRT glass has better workability than the one containing fly ash probably because of the higher water absorption of fly ash grains. Samples with CRT glass loose more mass and more strength after immersion in the demineralized water than samples with fly ash addition.

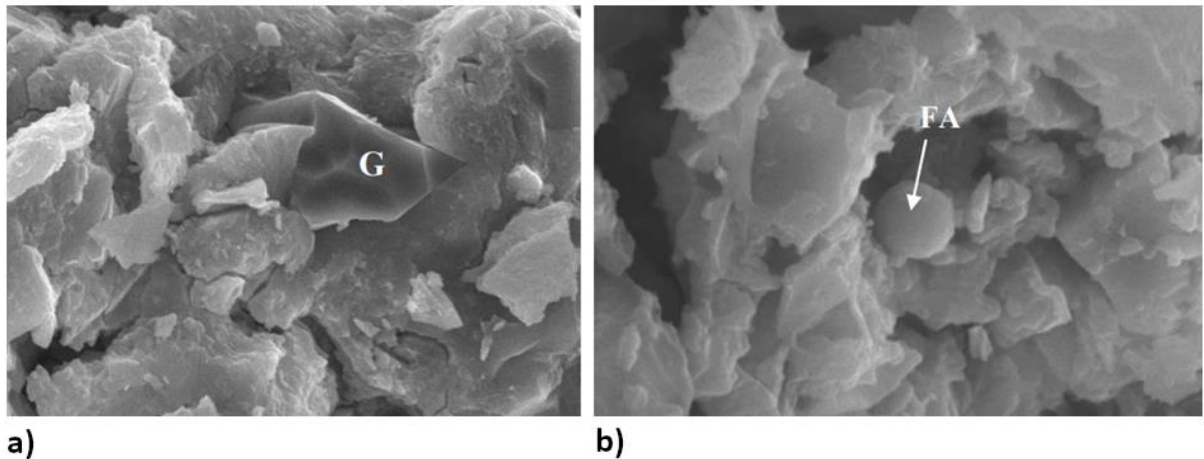


Fig.2.5.5: SEM micrographs of geopolymer containing a) CRT glass (G - glass particle) b) fly ash (FA – fly ash particle) [313].

The utilization of CRT glass in geopolymer was one of raised subjects in Master Thesis of Tomas Opletal, from Czech Republic [314]. He used crushed CRT glass from the cone and screen parts (high Pb content). Particles smaller than 63  $\mu\text{m}$  were treated as the raw material. The rest of grains (from 63  $\mu\text{m}$  to 5,6 mm) were added as a fine aggregate. The mixture was prepared from metakaolin or blast-furnace slag (being the by-product of the steel production), CRT glass, sodium silicate and sodium hydroxide. Compressive strength test was conducted on samples of approximate dimensions 20x20x100 mm (not all samples had regular shape) cured at the ambient temperature for 28 days. Samples were prepared from 37 different mixtures. Most of the specimens obtained relatively high compressive strengths. The compressive strength of geopolymer based on metakaolin ranged from 34,2 to 111,6 MPa while geopolymer based on the slag – from 11,2 to 119,2 MPa. Two best results of compressive strength were obtained by geopolymer of compositions: 1) CRT grains of dimension 2 – 4 mm, raw material to activator ratio – 10:9, metakaolin to CRT ratio – 1:3, 2) CRT grains 2 – 4 mm, raw material to activator ratio – 5:4, slag to CRT ratio – 1:3. The leaching test was conducted on several samples of the best compressive strength. None of the tested geopolymers could be qualified as the first-class due to the standard 294/2005 Sb [315] (material which can be stored on a landfill site without any special treatments). Only 2 within nine tested samples of different compositions could be qualified as the waste of the second class (material which can be stored only on special landfill sites for hazardous waste). The work also presents the research on the interface between CRT glass particles and geopolymer matrix done with the use of EDX-SEM and EDX. The reaction between the surface of some of

the glass grains and geopolymer matrix was observed. The Author explains that the sharp edge of the crushed glass can react with alkali solution. The Author observed also some microcracks inside the geopolymeric matrix, which can be explained by shrinkage occurring in the matrix with the excess of water during the hardening process. In some mixtures, cracks could be caused by the wrong proportion of CRT glass to the rest of the ingredients.



Fig.2.5.6: a) reaction on the surface between CRT particle and metakaolin, b) microcracks caused probably by improper amount of liquid, c) microcracks caused probably by too much CRT glass inside matrix [314].

## 2.6 State-of-the-art critical analysis and summary

Chapter begins with the general description of the geopolymer from the chemical point of view. The first subsection contains the definition, description, analysis and division into the stages of the geopolymerization process as well as the chemical structure of geopolymers. The second subsection shows the variety of possible compositions focusing on raw materials and activators. Among the many innovative ideas concerning waste which can be used as the raw material, there are three the most commonly used: fly ash, metakaolin and slag. The best-known activators, in turn, are sodium or potassium hydroxide and sodium silicate.

Then follows the description of many different approaches to the geopolymerization process design where the chemical ratios optimisation (mostly Si/Al and Na/Al) seems to be the most frequently chosen approach. The next subsection describes the history of geopolymer, beginning from the questionable but intriguing idea about ancient buildings and then focusing on the reliable facts from the modern times. The history is supplemented with the current investigations conducted all over the world together with the practical and theoretical applications of geopolymers in many different branches with the special emphasize on the civil engineering branch. The most popular ways of application of geopolymer are: as a building material for structural elements, in fire and chemical protection for concrete or steel elements, in thermal insulation.

The next part concerns CRT glass – its origin, composition (with the special regard to heavy metals content), recycling methods and possible applications. The unquestionably the most efficient way of recycling is so called open loop, where CRT glass is used for production of new materials or elements. The utilization of CRT glass in concrete industry is extensively explored way of recycling. There is lot of works devoted to the application of crushed CRT glass as a total or partial replacement of sand in concrete mixtures. However, even in case of concrete which is much deeper investigated than geopolymer, the observations on the impact

of CRT glass on the characteristics and behavior of the material are inconclusive. Part of the publications reports the increase of strength after application of CRT glass while many other scientists observed a negative impact of CRT glass on mechanical behavior. The issue of lead leaching is inconclusive as well. There are both sources claiming that concrete with CRT glass fulfils the regulatory limits for toxic metals leaching and investigations invalidating this theory.

The last parts contain study of heavy metals immobilization inside the geopolymer matrix and the careful analysis of existing researches on the utilization of CRT glass in geopolymer. Since the so far conducted investigations on utilization of CRT glass in geopolymer are the most crucial with respect to the topic of this Thesis, the extended summary of that subsection is enclosed below.

The amount of works devoted to the utilization of CRT glass in geopolymer is limited. Moreover, the scope of existing investigations is limited as well. The following limitations within the works describing the utilization of CRT glass in geopolymer have been listed:

- The majority of existing works concerns the application of CRT glass in powdered form as a replacement or partial replacement of the raw material [105], [298], [301], [303], [306], [307], [312], [313] while there is less publications describing geopolymer with CRT glass in form of an aggregate [302], [308]–[310], [314].
- The majority of tests has been done on only one mixture, mostly on samples cured in one specific conditions.
- The majority of tests concerns only one type of strength test, mostly compressive strength test without flexural strength test [105], [298], [306], [309], [313], [314] or lead leaching only without the description of mechanical performance [303], [310].
- There is lack of the extended laboratory tests exploring various aspects of one chosen material, such as: different combinations of mixtures, curing regimes, the influence of curing time, influence of the concentration of activator or size of an aggregate, and description of different characteristic – both flexural and compressive strength, density, porosity and toxic metals leaching.

Among the cited investigations concerning the addition of bigger than powdered fractions of CRT glass into the geopolymer mixture, there are still some deficiencies:

- Carrillo et al. [310] does not present mechanical parameters of the material at all.
- Opletal [314] describes an explorative studies on metakaolin-based geopolymer with CRT glass in form of an aggregate but there is lack of test on the flexural strength or stress-strain relationship. Additionally, compressive strength tests have been performed on samples of irregular shape what can affect results. There is also lack of the description of the influence of time or temperature of curing on mechanical performance as well.
- Long et al. [308] investigates the incorporation of CRT glass in form of an aggregate but only into the fly ash and slag-based geopolymers. Besides, the maximal presented sand replacement ratio was equal to 1:1 by mass. The compressive strength only was determined. There are as well deficiencies in the influence of various factors on the mechanical behavior of the material.

- Long et al. [309] presents tests done on fly ash and slag-based geopolymer containing sand to CRT glass in one ratio (1:1), cured in one specific conditions (28 days in room temperature). The flexural strength was not checked during the investigation.
- Gao et al. [293] introduces tests on geopolymer based on fly ash and slag with CRT glass as fine aggregate. Only one geopolymer mixture containing CRT glass was tested. One curing regime has been used. Only compressive strength was investigated. The research was focused mainly on alkali silica reaction expansion.

Concluding, CRT glass is dangerous waste which has to be utilized in the safe way. Geopolymers, with their ability to immobilize toxic metals give the innovative and environmentally friendly opportunity for recycling of CRT glass. There are studies indicating that incorporation of CRT glass in the geopolymer matrix is a promising way of utilization of that type of waste. However, the lack of an extensive studies of one chosen type of geopolymer limits the chances of the successful application of such solution in practice. In light of described deficiencies, an Author of this Thesis decided to closely investigate metakaolin-based geopolymer incorporating crushed discarded CRT glass in form of an aggregate.

One of the main goals of the following Thesis was to assess if the specific type of CRT glass achieved from the local landfill can be used in metakaolin-based geopolymer as an aggregate. The research program focuses on the determination of an optimal mixture composition and the description of the influence of the following factors on the mechanical behavior of the geopolymer: curing temperature, curing conditions and time, concentration of the activator and size of the used CRT glass. The research includes a description of several characteristics of the material: flexural and compressive strength, temperature inside material during hardening, porosity, density and toxic metals leaching. An Author believes that the in-depth studies will allow to accelerate the process of application of the geopolymer with CRT glass in form of an aggregate as a potential structural material in practice. Moreover, an Author has faith that this Thesis will be a valuable extension of the existing knowledge on geopolymer incorporating CRT glass.

## CHAPTER 3 (PRELIMINARY RESEARCH)

### *3.1 The scope and test program*

To facilitate the reading of the research part of this Thesis, the graphical scheme of the research part is included below. The scheme details three main parts: preliminary research, main research and complementary research. Each part is associated with the particular color: violet, green and red respectively. Further, in this Thesis, each page is signed at the top with the particular color as well to facilitate quick recognition which part of the research is currently being described.

The scheme presents all subsections of the main research chapters as well. In the preliminary research, where the main goal was to find an optimal mixture, there are given short notes describing how many mixtures or curing conditions were taken at the beginning of the test and how many of them were qualified for the further tests.

## SCHEME OF THE RESEARCH PART

### 3 Preliminary research (main goal: determination of one optimal mixture)

- 3.1 The scope and test program
- 3.2 Materials
- 3.3 Research methods
- 3.4 Presentation of results
- 3.5 Study on CRT glass
- 3.6 Mechanical behaviour of geopolymer with CRT glass and geopolymer with sand

3.7 Determination of the influence of CRT glass content on mechanical behaviour

- Performed on 8 mixtures
- **4 mixtures selected for further tests**



3.8 Determination of the influence of curing temperature on mechanical behaviour

- Performed on 4 mixtures and 4 curing temperatures
- **1 curing temperature and 2 mixtures selected for further tests**



3.9 Determination of the temperature and strength changes over time

- Performed on 2 mixtures
- **1 mixture selected for the main research**

### 4 Main research (main goal: optimisation of one selected mixture)

- 4.1 Determination of the influence of curing temperature and curing time on mechanical behaviour
- 4.2 Determination of the influence of sodium hydroxide concentration on mechanical behaviour
- 4.3 Determination of the influence of CRT glass particle size on mechanical behaviour
- 4.4 Determination of the change of mechanical behaviour over time

### 5 Complementary research (main goal: diagnostic of the chosen physical characteristics)

- 5.1 Porosity
- 5.2 Physicochemical characteristics

### 3.2 Materials

Geopolymer mixtures contained following materials: metakaolin (precursor), crushed CRT glass (aggregate), sodium silicate and sodium hydroxide (activators). No extra water (except of this one present in solutions) was added to mixtures. The exact data concerning each ingredient of mixtures is given below.

Metakaolin was used as the only precursor in all mixtures. Metakaolin MK-40 was supplied by Astra Technologia Betonu® company. Material was not subjected to any additional treatment after receiving from the manufacturer. The exact chemical composition is presented in Table 3.2.1.

Table 3.2.1: Chemical composition of metakaolin<sup>1</sup>.

	SiO <sub>2</sub>	Al <sub>2</sub> O <sub>3</sub>	K <sub>2</sub> O	TiO <sub>2</sub>	Fe <sub>2</sub> O <sub>3</sub>	CaO	MgO	H <sub>2</sub> O	Na <sub>2</sub> O	P <sub>2</sub> O <sub>5</sub>	Cl	S
[%]	53,12	42,24	0,73	0,64	0,45	0,44	0,26	0,22	0,09	0,03	0,02	0,01

<sup>1</sup>Data obtained from producer – Astra Technologia Betonu®



Fig.3.2.1: a) Metakaolin, b) CRT glass.

Crushed Cathode Ray Tube (CRT) glass was used as an aggregate. CRT glass used during the works came from old discarded television sets and computer screens. Chemical composition of CRT glass is presented in Table 3.2.2. Material was delivered by Thornmann Recycling LTD. It has been already crushed and stored at the landfill. Three batches of CRT glass taken from different locations of the storage scarp were obtained in different time periods. Sample representing each batch was subjected to sieve test. One of the main goals of the work was to check if it is possible to use waste glass in almost the same form as it was obtained from a deliverer to limit works connected with the recycling process since each additional work activates consumption of time and costs. The biggest particles of glass fit in range 4-8 mm although, the large majority of particles ranged from a dust fraction (> 0 mm) to 4 mm. Fragments of CRT glass bigger than 4 mm were weed out since majority of tests was

performed on relatively small prismatic samples of dimensions 40x40x160 mm. The cumulative distribution of CRT glass particles being the average from the results of each batch of glass is presented in Figure 3.2.2. The sieve test has been done by the Author in Laboratory of Civil Engineering (Silesian University of Technology). Figure 3.2.3, in turn, presents the exact cumulative distribution of the finest parts of CRT glass (those which passed the sieve of size 0,125 mm) together with the metakaolin particles. The measurement was done with the use of the laser particle analyzer by Professor Sara Rios at Faculty of Civil Engineering, University of Porto.

Table 3.2.2: Chemical composition of CRT glass<sup>1</sup>, [%].

SiO <sub>2</sub>	Na <sub>2</sub> O	CaO	BaO	K <sub>2</sub> O	MgO	PbO	SrO	Al <sub>2</sub> O <sub>3</sub>	SO <sub>3</sub>	Fe <sub>2</sub> O <sub>3</sub>	ZrO <sub>2</sub>	TiO <sub>2</sub>	ZnO	As <sub>2</sub> O <sub>3</sub>
76,10	6,25	5,24	2,62	2,36	1,64	1,61	1,42	1,37	0,55	0,38	0,28	0,12	0,05	0,01

<sup>1</sup>Chemical composition was determined by the XRF analysis by EkotechLAB®

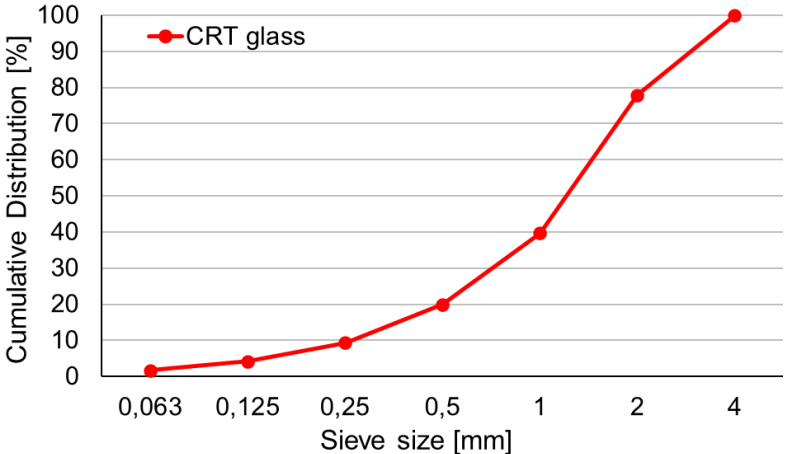


Fig.3.2.2: The particle size distribution of CRT glass (done by the Author in Laboratory of Civil Engineering, Silesian University of Technology).

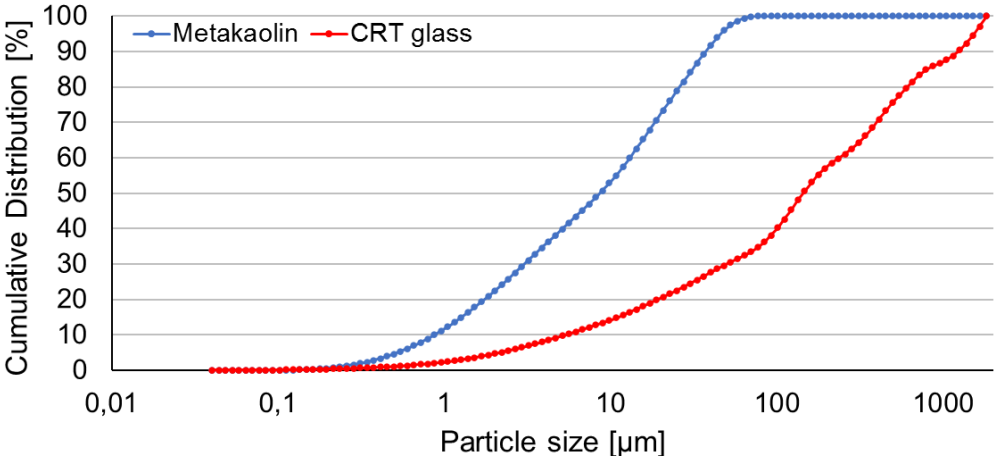


Fig.3.2.3: The particle size distribution of metakaolin and fine particles of CRT glass (done by Professor Sara Rios at Faculty of Civil Engineering, University of Porto).

Sodium silicate was supplied by Zakłady Chemiczne “Rudniki” S.A. company in form of water solution ready for use (type 145). According to the producer, the sodium silicate

solution had a molar ratio of  $\text{SiO}_2/\text{Na}_2\text{O}$  between 2,4 and 2,6. The minimum content of oxides ( $\text{SiO}_2$  and  $\text{Na}_2\text{O}$ ) in the sodium hydroxide solution was equal to 39%. The density at  $20^\circ\text{C}$  was between 1,45 and 1,48  $\text{g}/\text{cm}^3$ .

Sodium hydroxide was supplied by Chempur<sup>®</sup> company in form of white pellets. Sodium hydroxide characterized with molar mass equal to 40  $\text{g}/\text{mol}$  and purity not less than 98% (the exact purity varied in dependence on manufacturing lot but each time it was considered in calculations during preparation of the solution). Sodium hydroxide was used in form of solution prepared minimum 24 hours before the preparation of samples. The sodium hydroxide pellets were dissolved in demineralized water in proper amount to obtain solution with demanded concentration (in most cases the concentration was equal to 10  $\text{mol}/\text{L}$ ).

### 3.3 Research methods

Mechanical mixing of precursor (metakaolin) with the aggregate (crushed CRT glass) was the first step of samples preparation in case of all mixtures. In the next step, activators (sodium hydroxide and sodium silicate) were mixed together with use of magnetic stirrer for 5 minutes. Then, activators were poured into the vessel containing dry ingredients and mixed with mechanical mixer. The homogenous geopolymer mixture was placed in moulds. The curing process was various thus it is presented in the description of each test. All samples were measured with a caliper and weighted just before strength test. The density of samples (if not stated otherwise in the description of the particular test) was obtained by dividing mass of sample by its volume. The strength tests were performed on samples of shape of small beams of approximate dimensions  $40 \times 40 \times 160$  mm, according to EN 196-1:2016 regulations [316]. Standards for cement testing were applied since there are no valid documents concerning geopolymers testing. It is widely practiced among scientists to employ standards established for typical cement mortars also for geopolymer testing [30], [39], [92], [96], [103], [174]. The schematic view of the geopolymer beam and of sample during the flexural strength test is presented in Figure 3.3.1. All deviations in dimensions were taken into account in calculations of both compressive and flexural strength.

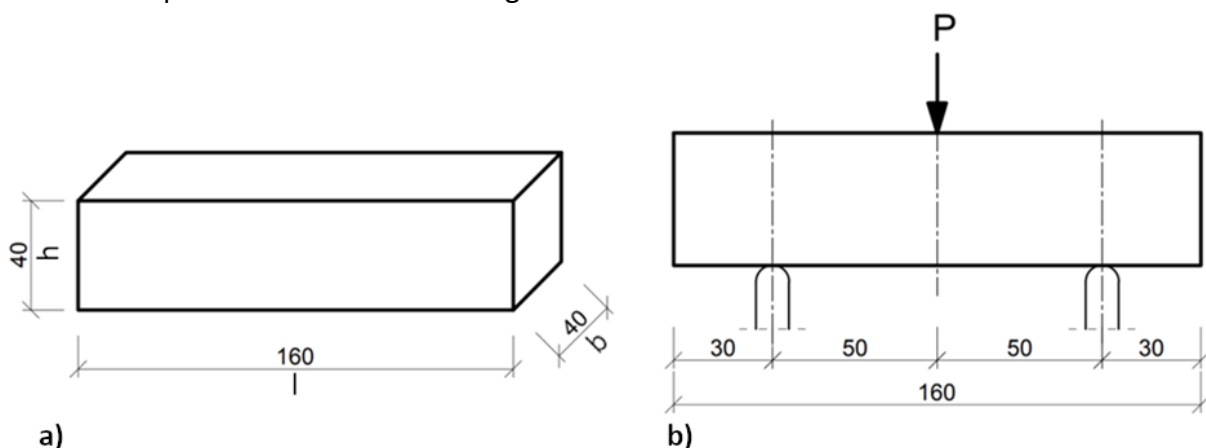


Fig.3.3.1: Schematic view of the prismatic sample (all dimensions in mm) a) overall dimensions, b) sample during the flexural strength test.

The strength test machine Controls® Model 65-L27C12 Serial nr 12020060 was used during strength tests (Figure 3.3.2). The beams were subjected firstly to the flexural strength test (three-points-bending test). The geopolymer beam was loaded with velocity equal to 50000 N/s. Flexural strength was determined according to the following formula 3.3.1:

$$f_x = \frac{P * l_1}{4} * \frac{6}{b * h^2} \quad (3.3.1)$$

where:

$f_x$  – flexural strength [Pa]

$P$  – maximal compressive force at the state of sample failure [N]

$l_1$  – distance between supports [m]

$b$  – width of the sample [m]

$h$  – height of the sample [m]

Halves of samples obtained after flexural strength test were subjected to compressive strength test and loaded with velocity equal to 2400 N/s. Samples were subjected to the compression through two metal plates (the upper and bottom one) of dimensions 40x40 mm, presented in Figure 3.3.3. All tests (if not stated otherwise in the description of a particular test) have been done by the Author in Laboratory of Civil Engineering (Silesian University of Technology).



Fig.3.3.2: Strength tests machine Controls® Model 65-L27C12 Serial nr 12020060, during the compressive strength test.

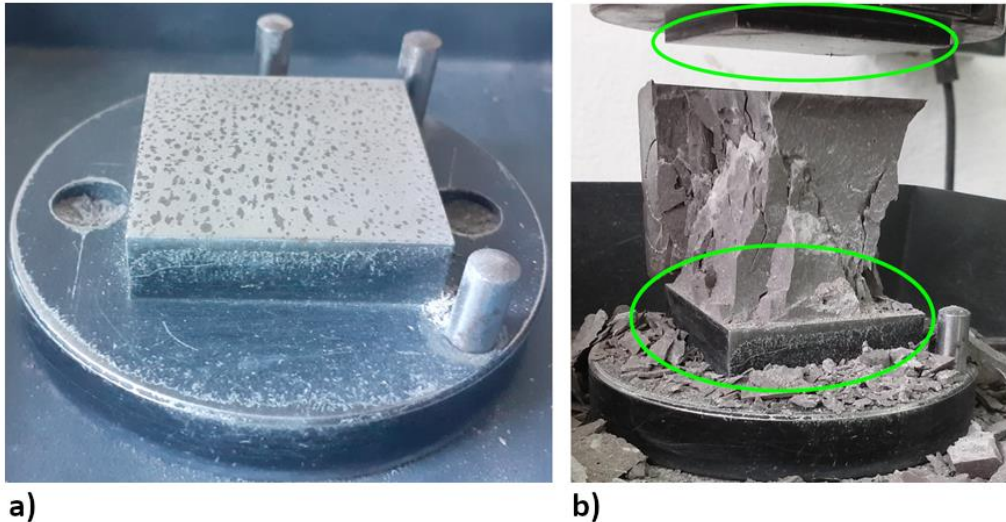


Fig.3.3.3: Metal plates of dimensions 40x40 mm in compressive strength test machine, a) the bottom plate, b) geopolymer sample after compressive strength test, the bottom and upper plates are marked with the use of green circle.

### 3.4 Presentation of results

All values achieved during the mechanical tests are included in tables in the subsections “Results” in the description of each following test. The standard deviations and coefficients of variation calculated for the achieved results are given in the separate tables in the same subsection. The graphical presentation of results and calculated densities are presented in the subsection “Analysis”. Results achieved during tests and rejected during the statistical analysis were not included in determination of standard deviations, coefficients of variation and graphs.

The majority of results achieved during the laboratory tests is presented in the form of the bar graphs where each bar represents the average value of compressive or flexural strength. Values given above bars are the average of results from each series. The black segment on the top of each bar represents respectively: the smallest result from particular series (the bottom part of the black segment) and the highest result (the upper part).

### 3.5 Study on CRT glass

Test were done on CRT glass obtained in different time period, coming from different locations of the same storage scarp and therefore having slightly different granulation of particles. In the view of the above, the short test checking the convergence of results has been done before continuation of works on CRT glass from the next batch. Two tests were repeated using geopolymer with CRT glass from different batches. Table X1 shows results of flexural and compressive strength performed on samples containing CRT glass from three different batches (CRT glass 1, 2 and 3) cured at different conditions. The first series was cured all the time at the room temperature (~20°C) and unmolded after 7 days of curing. For the whole curing time, samples were placed in moulds and covered (protected against drying). The second series was cured for the first 24 hours at elevated temperature of 40°C and humidity

equal to 40%, then unmolded and kept at the room temperature (~20°C, without any cover), for the rest of the curing period. Strength tests were performed after 7 days. In the case of geopolymer made of CRT glass from batches no 1 and no 2, three samples were subjected to flexural strength test and six samples were subjected to compressive strength test. In the case of geopolymer made of CRT glass from batch no 3, four samples were subjected to flexural strength test and eight to compressive strength test. Table 3.5.1 contains all flexural and compressive strength results, Table 3.5.2 contains standard deviations and coefficients of variation.

Table 3.5.1: Flexural ( $f_x$ ) and compressive ( $f_c$ ) strength results.

Mixture	Curing temperature		No. 1	No. 2	No. 3	No. 4
CRT glass 1	20°C	$f_x$ [MPa]	5,61	4,13	4,61	-
		$f_c$ [MPa]	41,92	50,96	42,45	-
			57,04	54,66	52,41	-
	40°C	$f_x$ [MPa]	4,82	6,30	5,92	-
		$f_c$ [MPa]	<del>56,90*</del>	50,18	52,27	-
			51,49	50,42	51,19	-
CRT glass 2	20°C	$f_x$ [MPa]	4,42	4,90	4,05	-
		$f_c$ [MPa]	55,42	52,27	55,40	-
			52,86	53,99	57,38	-
	40°C	$f_x$ [MPa]	5,55	6,25	6,56	-
		$f_c$ [MPa]	51,63	56,24	53,52	-
			57,24	52,32	53,16	-
CRT glass 3	20°C	$f_x$ [MPa]	3,51	3,94	4,93	6,30
		$f_c$ [MPa]	51,60	53,21	53,53	51,58
			54,44	52,90	55,07	<del>41,05*</del>

\* Result was rejected on the basis of statistical method - elimination of one extreme value.

Table 3.5.2: Standard deviation and coefficient of variation of flexural and compressive strength results.

Standard deviation [-] (CoV [%])	CRT glass 1		CRT glass 2		CRT glass 3
	20°C	40°C	20°C	40°C	20°C
Flexural strength	0,75 (15,8%)	0,77 (13,5%)	0,42 (9,5%)	0,52 (8,5%)	1,24 (26,5%)
Compressive strength	6,33 (12,7%)	0,84 (1,6%)	1,89 (3,5%)	2,23 (4,1%)	1,32 (2,5%)

The average values of flexural and compressive strength of geopolymer with CRT glass taken from different batches are presented in Figure 3.5.1.

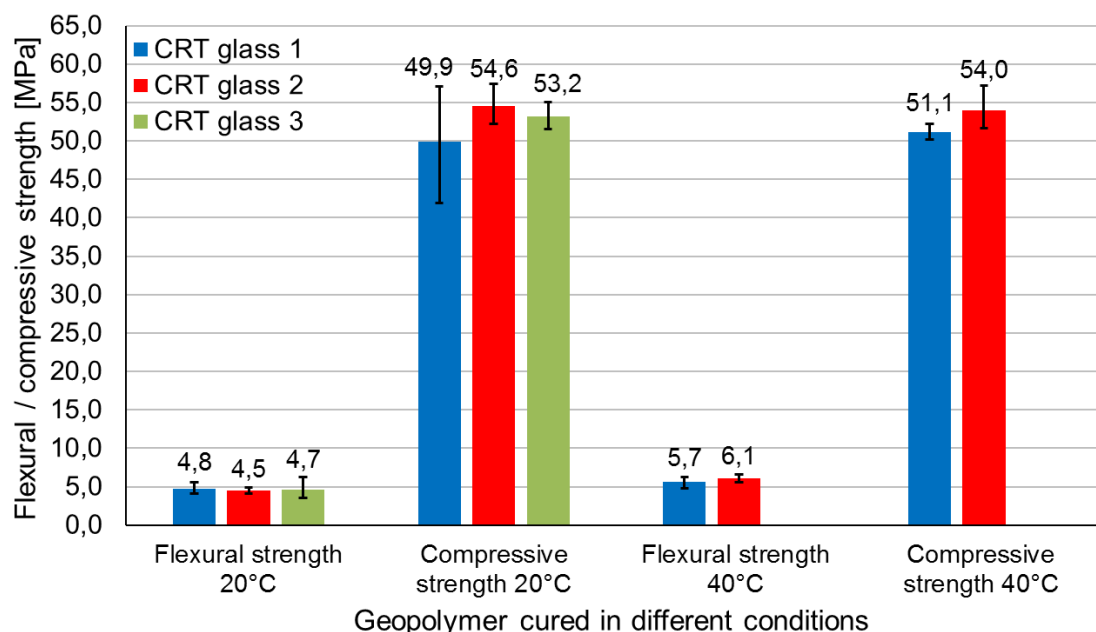


Fig.3.5.1: Seventh day flexural and compressive strength of geopolymer containing CRT glass from three different batches, cured at 20°C or at 40°C.

The divergences between results obtained by geopolymer containing CRT glass from different batches (CRT glass 1, 2 and 3) were relatively small. Respectively to the graph, the maximal divergence in the average flexural strength was equal to 7,0%, and in compressive strength – 9,4%. On the base of presented test it was assumed that results in the further parts of this Thesis obtained by geopolymers containing glass from different batches can be compared with each other.

### 3.6 Mechanical behavior of geopolymer with CRT glass and geopolymer with sand

The main goal of the test was to compare the flexural and compressive strength of metakaolin-based geopolymer with two different types of aggregate – CRT glass and standardized natural sand. Sand is usually used as fine aggregate in geopolymer mixtures [39], [73], [83], [97], [308], [317]–[321] and therefore, during the preliminary investigation, the Author decided to assess if there is a significant difference in mechanical behavior between samples prepared with the use of sand and CRT glass. Standardized sand (with accordance to standard EN 196-1:2016 [316]) was delivered by the Polish company Kwarcmix®. Samples contained aggregate to metakaolin in mass ratio 1:1, were activated with sodium silicate and sodium hydroxide of concentration 10 mol/L, were cured at room temperature and demoulded after 7 days of curing. The aggregate type was the only varying factor. The composition of the mixtures is given in Table 3.6.1 below.

Table 3.6.1: Mixture composition.

Mixture		Metakaolin	CRT glass	Sand	Sodium silicate	Sodium hydroxide
<b>CRT glass</b>	[kg/m <sup>3</sup> ]	898	898	0	449	225
<b>Sand</b>	[kg/m <sup>3</sup> ]	898	0	898	449	225

No external difference between samples containing CRT glass and sand was noticed (Figure 3.6.1). There was no difference in color of surface between samples with CRT glass and sand. The brighter surface of samples containing sand is connected in that case with different color of background what influenced the internal settings in the camera.

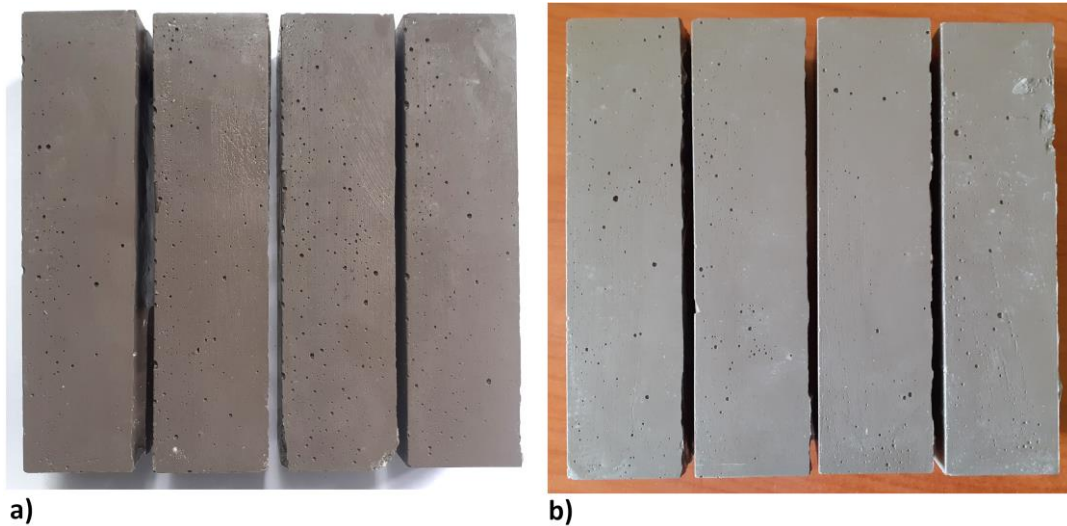


Fig.3.6.1: a) Samples with CRT glass aggregate, b) samples with sand aggregate.

Table 3.6.2 contains all results of flexural and compressive strength tests. In case of samples containing CRT glass, the average values from 5 tests carried out at different time are given. In turn, in the case of geopolymer with sand, five samples were prepared and subjected to the strength test.

Table 3.6.2: Flexural ( $f_x$ ) and compressive ( $f_c$ ) strength results.

Sample		No. 1	No. 2	No. 3	No. 4	No. 5
<b>CRT glass</b>	$f_x$ [MPa]	6,0	4,6	4,7	4,5	4,6
	$f_c$ [MPa]	56,0	52,2	53,2	54,6	59,6
<b>Sand</b>	$f_x$ [MPa]	6,27	7,36	6,70	6,49	6,43
	$f_c$ [MPa]	46,44	54,66	55,86	58,13	58,06
		65,25	55,76	54,53	52,56	56,89

Figure 3.6.2 presents comparison of cross sections of samples containing CRT glass and sand. In the Figure 3.6.2 a) there are visible CRT grains, while in Figure 3.6.2 b), there are visible sand grains. The number of visible, in macroscopic way, air pores are similar in both cross-sections.

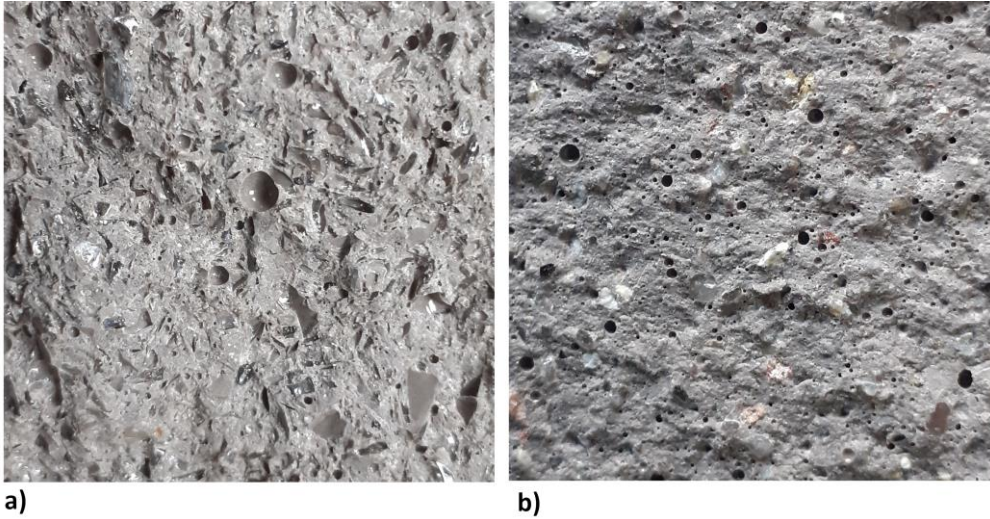


Fig.3.6.2: Cross section of sample containing a) CRT glass, b) sand.

Figure 3.6.3 presents flexural and compressive strength obtained by geopolymer containing CRT glass or sand.

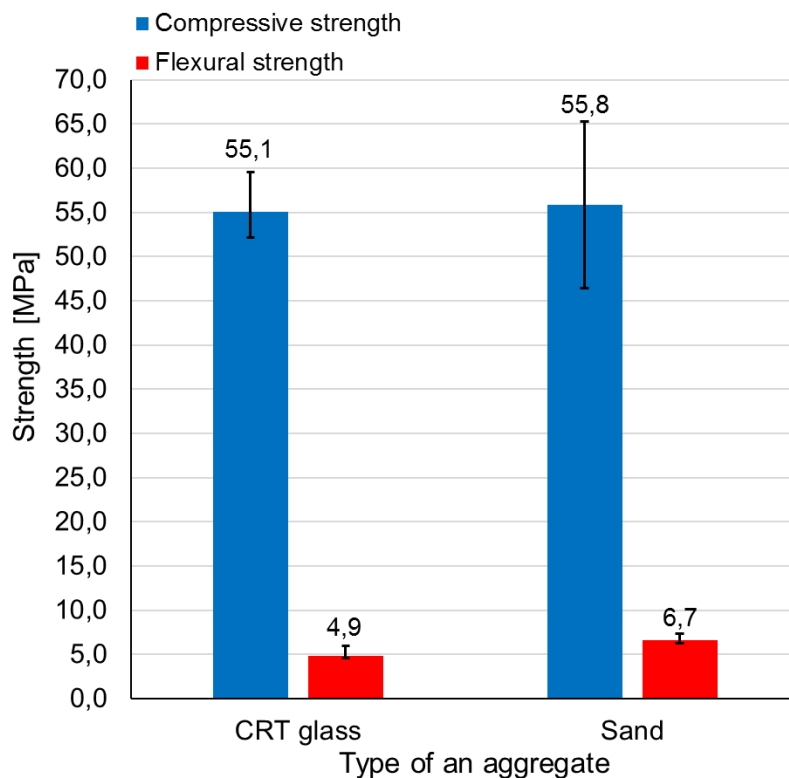


Fig.3.6.3: Flexural and compressive strength of samples containing CRT glass or sand cured for 7 days.

Samples containing CRT glass achieved 27% smaller flexural strength than samples with sand aggregate. Compressive strength of both types of geopolymer was almost the same. Table 3.6.3 contains the average density of samples containing CRT glass or sand aggregate. According to the result, geopolymer with CRT glass aggregate is slightly (less than 1,5%) heavier than geopolymer with sand aggregate.

Table 3.6.3: Average density of geopolymer containing CRT glass or sand.

	<b>CRT glass</b>	<b>Sand</b>
Density [kg/m <sup>3</sup> ]	2050	2020

Compressive strength results obtained within this Thesis are divergent with results presented in the literature concerning replacement of sand with CRT glass in geopolymer or concrete. According to the average values from this Thesis, the compressive strength of geopolymer with CRT glass is almost equal to compressive strength of samples with sand while the literature reports the significant decrease [283], [285], [286], [308], [322], [323] or considerable increase [275], [276], [324] of compressive strength along with the replacement of sand with CRT glass. The smaller value of flexural strength of geopolymer with CRT glass is convergent with some studies although differences between strength reported by other scientists are considerably higher [283] or lower [285], [286] than the one obtained within this Thesis. Scientists who compared density of geopolymer with different kind of aggregate report higher density when CRT glass is used. The same observation was made by the Author although the difference noticed within this Thesis (1,5%) is much smaller than difference reported in other publications (8-14%) [283], [324].

Concluding, according to the results presented in this Thesis, the replacement of sand with CRT glass does not lead to the decrease of compressive strength. Flexural strength was decreased but its value is still high. Geopolymer with CRT glass has good mechanical characteristics even in comparison to the geopolymer containing sand.

### *3.7 Determination of the influence of CRT glass content on mechanical behavior*

#### **3.7.1 Preparation of samples**

This part of the research was devoted to determination of the influence of content of aggregate (crushed CRT glass) on flexural and compressive strength of metakaolin-based geopolymer. At the beginning of tests author tried to prepare samples using only CRT glass to check if the amount of powder size particles is enough to react with activators. All trials were unsuccessful – the samples did not show any signs of hardening within 7 days.

Eight mixtures with different aggregate to precursor mass ratio were designed. All mixtures were prepared according to the procedure described in subsection “3.3 Research Methods”. The amount of activator was dosed so that to maintain approximately similar metakaolin to activator mass ratio. Some mixtures were more water demanded what implied adding an extra amount of activator during the mixing what caused inaccuracy in keeping metakaolin to activator ratio stable in all cases. The exact composition of each of preliminary mixtures is given in Table 3.7.1. Table contains the amount of each ingredient (in [kg/m<sup>3</sup>]) and the percentage contribution of each ingredient. The abbreviation M/G X/Y was used for mixture containing X mass percentage content of metakaolin (M) and Y mass percentage content of CRT glass (G), where 100% is the overall mass of metakaolin and CRT glass in one mixture. As an example, the mixture M/G 33/67 contains 33% of the metakaolin and 67% of CRT glass by mass. The solution of the sodium hydroxide with concentration of 10 mol/L was

used. Sodium silicate to sodium hydroxide ratio was equal to 2,0 and was kept constant in all mixtures.

Table 3.7.1: Mixtures compositions.

Mixture		Metakaolin	CRT glass	Sodium silicate	Sodium hydroxide	Si/Al [-]	Na/Al [-]	H <sub>2</sub> O/Na <sub>2</sub> O [-]	Water content wt [%]
<b>M/G 25/75</b>	[kg/m <sup>3</sup> ] [%]	524 20,4	1572 61,3	314 12,2	157 6,1	1,40	0,55	14,56	31
<b>M/G 33/67</b>	[kg/m <sup>3</sup> ] [%]	657 25,9	1335 52,6	365 14,4	182 7,2	1,37	0,51	14,55	30
<b>M/G 40/60</b>	[kg/m <sup>3</sup> ] [%]	755 30,1	1133 45,1	417 16,6	208 8,3	1,37	0,50	14,55	30
<b>M/G 50/50</b>	[kg/m <sup>3</sup> ] [%]	898 36,4	898 36,4	449 18,2	225 9,1	1,34	0,46	14,54	28
<b>M/G 60/40</b>	[kg/m <sup>3</sup> ] [%]	995 40,8	663 27,2	521 21,4	260 10,7	1,36	0,48	14,55	29
<b>M/G 67/33</b>	[kg/m <sup>3</sup> ] [%]	1037 43,6	510 21,5	553 23,3	276 11,6	1,36	0,49	14,55	29
<b>M/G 75/25</b>	[kg/m <sup>3</sup> ] [%]	1078 46,5	359 15,5	586 25,3	293 12,6	1,37	0,48	14,44	29
<b>M/G 100/0</b>	[kg/m <sup>3</sup> ] [%]	1083 51,7	0 0	675 32,2	337 16,1	1,41	0,57	14,56	32

It was observed that workability of mixture decreases with the increase of CRT glass content. Three samples were made of each mixture. The moulds were covered to prevent moisture escape and placed in the climatic chamber at the temperature 60°C and humidity 40% for the initial 24 hours of curing. After this time, hardened samples were unmolded, weighed and kept at the room temperature in the laboratory for the next 6 days. Strength tests were performed after 7 days since casting. The Author decided to cure samples at the beginning of the preliminary research at 60°C for several reasons. Curing at 60°C for the first 24 hours or shorter is commonly chosen conditions by the other scientists [75], [80], [93], [325] [317]. Many scientists report that curing at elevated temperature enhances strength [28], [326]–[329]. Additionally, there is significant amount of researches which prove that the increase of the curing temperature to 60°C gives the best results of strength or that the profit in further increase of the temperature is relatively low [101], [102], [326], [327], [330]. Besides, the previous works of the Author were carried on geopolymers cured at 60°C for the first 24 hours [199], [331]–[333]. Beginning of works on metakaolin-based geopolymer with CRT glass cured in the same conditions allowed for comparison of results. Samples were kept in elevated temperature for 24 hours because it is reported that the most rapid increase of strength of samples cured at 60°C is up to 24 hours of curing [28].

The humidity equal to 40% was chosen because during the investigations done previously by the Author ([199], [331]–[333]), samples were kept in the climatic chamber at

the same humidity and none of them were affected by any cracks or extensive shrinkage. Therefore, it was decided to keep geopolymer samples investigated in the following research also in humidity 40%.

The Author decided to test samples after 7 days of curing since many previously conducted works proves that at this time geopolymer achieves a significant percentage of final strength. Rovnanik [334] observed that samples cured at 60°C achieved the highest compressive strength after 7 days of curing. Ekaputri et al. [101] reports 85% of final strength after 7 days and the most rapid increase of strength during the first 7 days of curing. Long et al. [307] reports that after 7 days geopolymer achieves 70-80% and 65-75% of final flexural and compressive strength respectively. Moncea et al. [335] describes 90-100% or 80-83% of 90<sup>th</sup> days compressive strength and 95-100% or 95-115% of 28<sup>th</sup> day compressive strength. Ogundiran et al. [105] observed that 70-80% of 28<sup>th</sup> day strength is achieved after 7 days of curing.

After 7 days samples were measured, weighed (see Figure 3.7.1) and subjected to flexural and compressive strength tests according to the procedure described in subsection “3.3 Research Methods”. Three beams from each mixture were subjected to the flexural strength test, then, six halves were subjected to the compressive strength test. Figure 3.7.2 presents samples during the flexural and compressive strength tests.

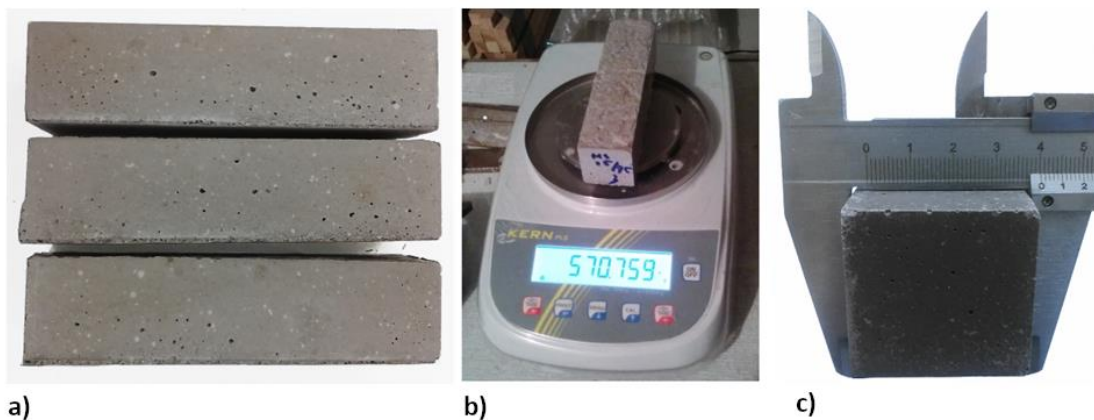


Fig.3.7.1: a) Metakaolin-based geopolymer samples with CRT glass, b) weighing of sample, c) measuring of sample's cross-section dimensions.

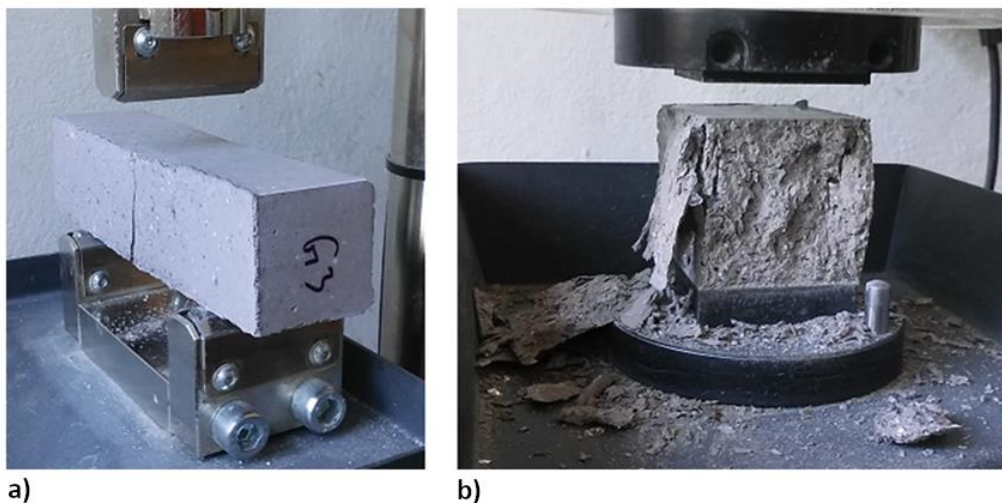


Fig.3.7.2: Sample from series M/G 50/50, after a) flexural strength test b) compressive strength test.

### 3.7.2 Results

All results achieved during the flexural and compressive strength tests are presented in Table 3.7.2.

Table 3.7.2: Flexural ( $f_x$ ) and compressive ( $f_c$ ) strength results.

Mixture		No. 1	No. 2	No. 3	No. 4	No. 5	No. 6	$f_x/f_c$
<b>M/G 25/75</b>	$f_x$ [MPa]	5,20	5,17	4,59	-	-	-	0,106
	$f_c$ [MPa]	48,65	50,86	46,65	49,94	42,70	44,35	
<b>M/G 33/67</b>	$f_x$ [MPa]	4,32	4,88	4,62	-	-	-	0,096
	$f_c$ [MPa]	44,73	51,14	47,18	49,54	48,58	47,36	
<b>M/G 40/60</b>	$f_x$ [MPa]	6,31	5,67	5,25	-	-	-	0,123
	$f_c$ [MPa]	51,65	48,88	40,98	46,25	44,48	48,50	
<b>M/G 50/50</b>	$f_x$ [MPa]	6,63	5,93	5,98	-	-	-	0,123
	$f_c$ [MPa]	53,93	54,13	52,01	48,92	49,12	42,69	
<b>M/G 60/40</b>	$f_x$ [MPa]	5,99	5,96	5,31	-	-	-	0,118
	$f_c$ [MPa]	50,10	51,20	46,54	46,17	50,56	47,24	
<b>M/G 67/33</b>	$f_x$ [MPa]	4,33	3,34	3,03	-	-	-	0,072
	$f_c$ [MPa]	50,68	48,20	47,74	<del>24,65</del> *	49,67	52,72	
<b>M/G 75/25</b>	$f_x$ [MPa]	5,84	5,48	4,76	-	-	-	0,129
	$f_c$ [MPa]	41,77	35,09	45,90	37,44	49,04	40,65	
<b>M/G 100/0</b>	$f_x$ [MPa]	5,60	4,87	6,50	-	-	-	0,118
	$f_c$ [MPa]	37,43	46,69	50,12	48,69	55,34	48,80	

\*Result was rejected on the basis of statistical method - elimination of one extreme value.

Generally, the differences between results (both flexural and compressive strength) obtained by samples containing different CRT glass content were small. No strict dependence between CRT glass content and mechanical behavior was noticed at this stage. All flexural and compressive strength results were relatively high.

Table 3.7.3 contains standard deviations and coefficients of variation of flexural and compressive strength results presented in Table 3.7.2. There is not monotonic dependence between CRT glass content and stability of results. Results of samples containing 75% and 100% of metakaolin are characterized by higher coefficient of variation than other samples.

Table 3.7.3: Standard deviation and coefficient of variation (CoV) of flexural and compressive strength results.

Standard deviation [-] (CoV [%])	M/G 27/75	M/G 33/67	M/G 40/60	M/G 50/50	M/G 60/40	M/G 67/33	M/G 75/25	M/G 100/0
Flexural strength	0,34 (6,9)	0,28 (6,1)	0,53 (9,3)	0,39 (6,3)	0,39 (6,7)	0,68 (19,0)	0,55 (10,3)	0,82 (14,5)
Compressive strength	3,21 (6,8)	2,20 (4,6)	3,75 (8,0)	4,29 (8,5)	2,23 (4,6)	2,01 (4,0)	5,19 (12,5)	5,88 (12,3)

Samples containing more metakaolin (and consequently less CRT glass) were destroyed more abruptly both during the flexural and compressive strength test. During flexural strength test, the halves of beams containing the metakaolin only (series M/G 100/0), were abruptly falling apart in the moment of failure with a resonant tone. Along with the increasing content of CRT glass, the destruction moment was appearing less rapidly. Samples containing less metakaolin and more CRT glass were only cracked after flexural strength test. In several cases, samples had to be additionally broken to obtain separate halves before compressive strength test. The comparison of two different samples only after flexural strength tests is presented in Figure 3.7.3.

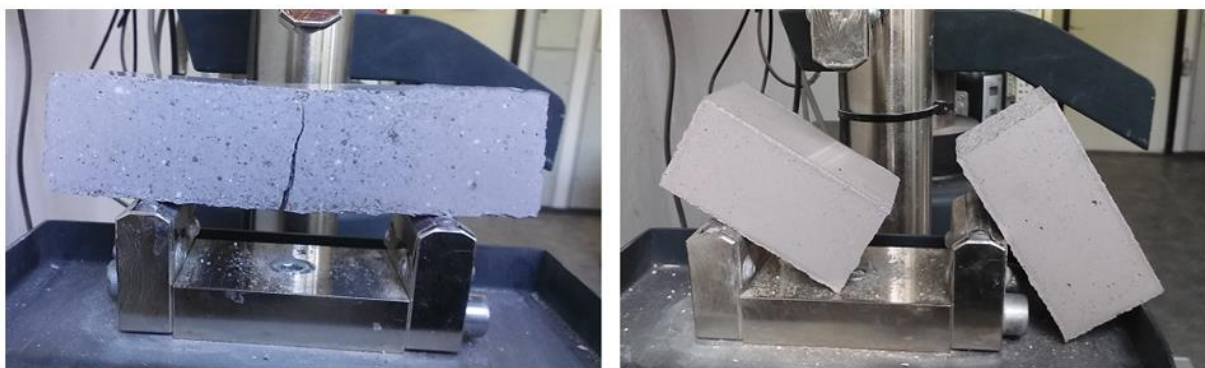


Fig.3.7.3: a) Sample with high CRT glass content (from series M/G 40/60), b) sample with low CRT glass content (from series M/G 75/25).

Similar dependence between CRT glass content and the character of destruction was visible during compressive strength test. In case of samples containing metakaolin only, during the moment of failure, the large pieces of material were being flaked off with the resonant

sound. The material was brittle. The small fragment of sample in the shape of double cone remained on the plate of the machine after the moment of failure (Figure 3.7.4 a). In case of samples containing CRT glass, the parts of samples were not being flaked off during the test or were flaked off less abruptly. In the majority of tests, the whole sample was still withing the steel plates after the moment of failure (Figure 3.7.4 b and c).

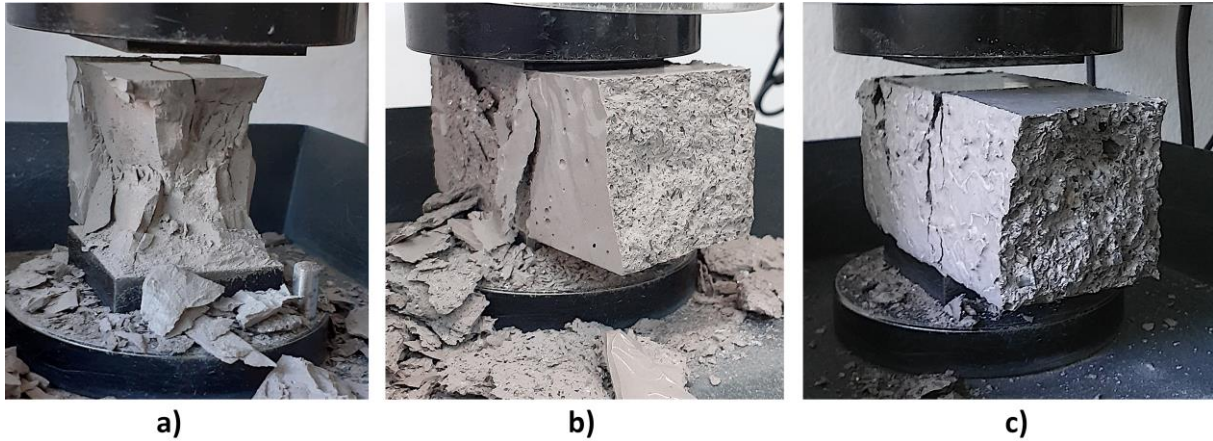


Fig.3.7.4: Sample after compressive strength test a) sample without CRT glass (only metakaolin), b) sample from series M/G 50/50 (metakaolin to CRT glass mass ratio equal to 1:1), c) sample from series M/G 25/75 (metakaolin to CRT glass mass ratio equal to 1:3).

Figure 3.7.5 presents the cross section through the broken sample without CRT glass (M/G 100/0) and containing 50% of CRT glass (M/G 50/50). The surface of broken samples containing metakolin only was smooth, although the small voids of air could be visible. The surface of sample containing CRT glass was rough, the evenly distributed glass particles were visible with the unaided eye.

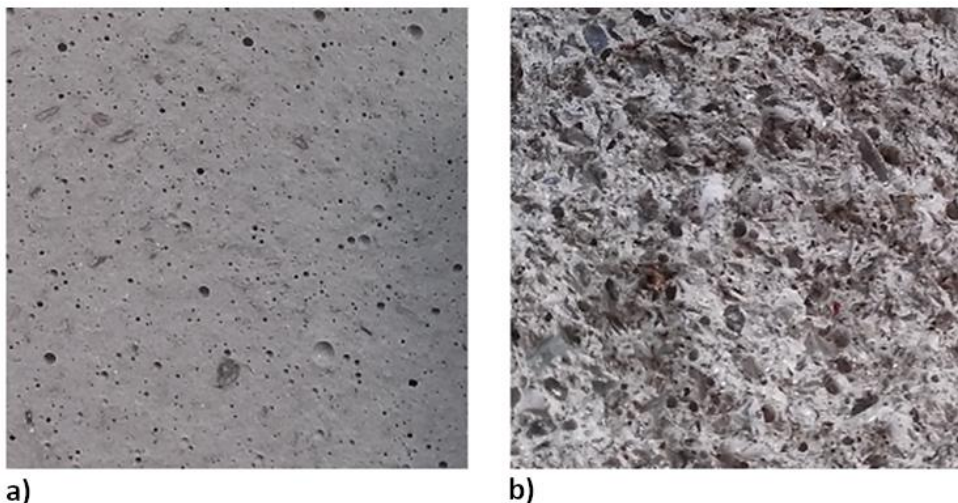


Fig.3.7.5: The surface of a broken sample a) without CRT glass (series M/G 100/0), b) with CRT glass (series M/G 40/60).

### 3.7.3 Analysis

The results of the preliminary tests are presented in Figure 3.7.6. Each bar represents average value of compressive or flexural strength obtained by samples from particular mixture.

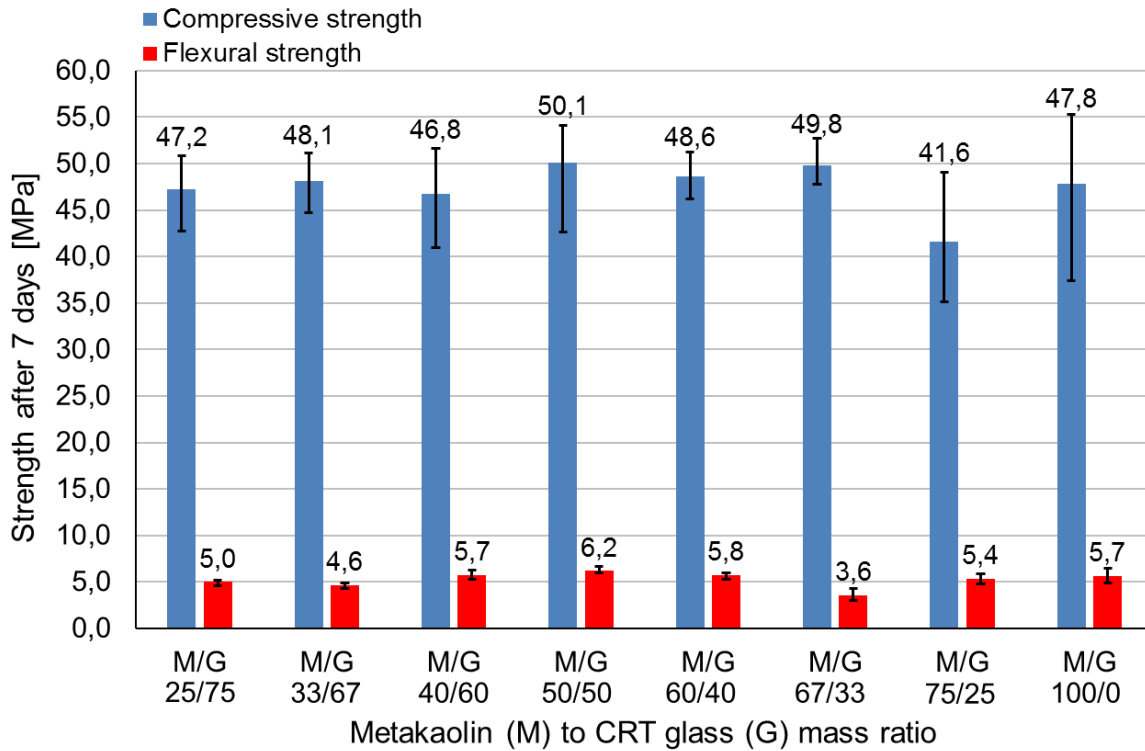


Fig.3.7.6: Seventh days compressive and flexural strength of geopolymer made of mixtures containing different metakaolin to CRT glass mass ratio.

No significant dependence between CRT glass content and strength was observed. The average values of the flexural strength ranged from 3,6 MPa (series M/G 67/33) to 6,2 MPa (series M/G 50/50) while average values of compressive strength ranged from 41,6 MPa (series M/G 75/25) to 50,1 MPa (series M/G 50/50). Generally, samples from all series achieved high compressive strength and good flexural strength. The highest strength (both flexural and compressive) obtained samples from mixture M/G 50/50 (containing 50% of CRT glass). Based on coefficient of variations calculated for obtained results it was observed, that the smallest stability of flexural strength results had samples made of mixtures M/G 67/33 and M/G 100/0 while in case of compressive strength the biggest variability had samples made of mixture M/G 75/25 and M/G 100/0. No correlation between stability of flexural strength results and stability of compressive strength results was observed. Neither, no strict dependence between CRT glass content and stability of results was noticed.

Figure 3.7.7 presents the graphical interpretation of  $f_x/f_c$  ratio for samples made from each mixture.

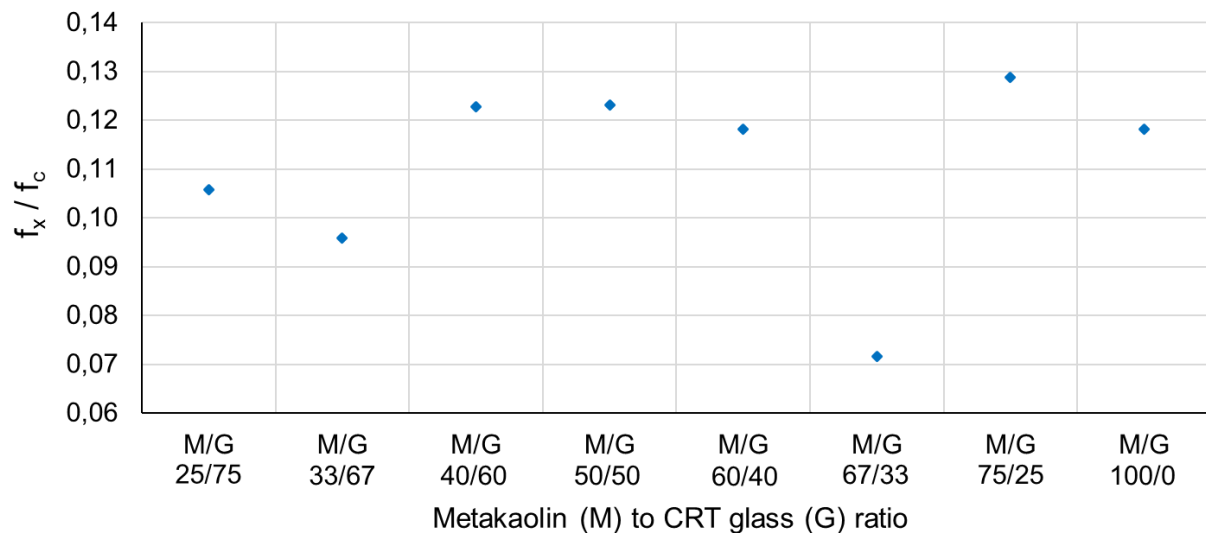


Fig.3.7.7: The  $f_x/f_c$  ratio of geopolymer with different CRT glass content.

The  $f_x/f_c$  ratio varied from about 0,07 to 0,13 but the majority of values fluctuated around 0,12. No clear dependence between CRT glass content and  $f_x/f_c$  ratio was noticed. Geopolymer made of mixture M/G 67/33 was characterized by significantly lower value of  $f_x/f_c$  ratio than others. Samples made of mixture M/G 67/33 achieved the lowest flexural strength and approximately the same compressive strength in comparison to other samples, what decreased the  $f_x/f_c$  ratio.

In publication published by Long et al. [307] there is similarly no correlation between increasing CRT glass content and  $f_x/f_c$  ratio of geopolymer. The  $f_x/f_c$  ratio is approximately constant and oscillates around 0,25 which is significantly higher value than in this Thesis. In the scientific literature, there are several examples of introducing CRT glass into the concrete mixture. Song et al. [286] reports that an increase of CRT glass content does not influence this  $f_x/f_c$  ratio of hardened concrete which fluctuates around the value 0,12 (similarly like in the Thesis). No monotonic influence of rising CRT glass content on  $f_x/f_c$  ratio of cement mortar has been noticed by Liu et al. [285] as well, but, here  $f_x/f_c$  values are higher and range from 0,19 to 0,20. Ling et al. [283] used acid treated and untreated CRT glass as a sand replacement in cement mortar. According to results, no correlation between untreated CRT glass content and  $f_x/f_c$  ratio has been found. The majority of values oscillated around 0,16 which is slightly higher result than in this Thesis. In the case of treated CRT glass,  $f_x/f_c$  ratio decreased along with increase of CRT glass content from 0,16 to 0,13. This magnitude is more similar to values obtained within Thesis.

Each sample was weighed twice – after demolding (24 hours since casting) and before testing. Additionally, before testing each sample was measured. The density of geopolymer was determined by division of sample's weight by its volume. Table 3.7.4 contains the average density from each series of samples and the average mass loss (expressed in %) which was determined by the subtraction of mass of each sample after demolding and before the test. The mass loss describes changes inside geopolymer only during the curing process at the room temperature (outside the climatic chamber).

The density of geopolymer is decreasing with the decrease of CRT glass content what is natural since the bulk density of CRT glass is higher than the bulk density of metakaolin.

Comparing conterminous values in Table 3.7.4, the biggest difference in average density ( $190 \text{ kg/m}^3$ ) was observed between samples containing 25% of CRT glass (M/G 75/25) and samples containing no CRT glass (M/G 100/0). Despite the high density of CRT glass, the big difference in density of samples without CRT glass and the rest of samples is probably caused by the fact that this series had biggest water content (32%). The water is evaporating during the curing process what is shown also by the biggest mass loss.

Table 3.7.4: Average density and mass loss of geopolymer samples made of each mixture.

	<b>M/G 25/75</b>	<b>M/G 33/67</b>	<b>M/G 40/60</b>	<b>M/G 50/50</b>	<b>M/G 60/40</b>	<b>M/G 67/33</b>	<b>M/G 75/25</b>	<b>M/G 100/0</b>
Density [ $\text{kg/m}^3$ ]	2090	1960	1940	1920	1770	1720	1690	1500
Mass loss [%]	5,6	6,5	4,8	5,8	6,5	10,3	7,1	12,5

Described test has not shown monotonic dependence between CRT glass content and mechanical behavior but samples made of some mixtures had better mechanical characteristics than the other ones. Author decided to continue works on material showing the best mechanical performance as well as on the material containing the most of CRT glass since the utilization of that waste is the main goal of this Thesis. Four mixtures were chosen for further test: M/G 25/75; M/G 33/67; M/G 50/50 and M/G 60/40. Two first mixtures were chosen because of good strength results combined with high content of CRT glass which utilization is the main goal of the works presented in Thesis. Samples made of mixture M/G 50/50 had the highest flexural and compressive strength. Samples made of mixture M/G 60/40 obtained high and stable results.

### ***3.8 Determination of the influence of curing temperature on mechanical behavior***

#### **3.8.1 Preparation of samples**

In the second phase of the research, the influence of the curing temperature on the mechanical behavior was examined on samples made of four previously chosen mixtures: M/G 25/75; M/G 33/67; M/G 50/50 and M/G 60/40. The goal of the test was to determine the influence of curing temperature on mechanical behavior and to choose the optimal curing temperature for further tests. The exact composition of the mixtures is given in Table 3.7.1 (subsection “3.7.1 Preparation of samples”). The simplified version of the composition is given in Table 3.8.1 below.

Table 3.8.1: Mixtures compositions.

Mixture		Metakaolin	CRT glass	Sodium silicate	Sodium hydroxide
<b>M/G 25/75</b>	[ $\text{kg/m}^3$ ]	524	1572	314	157
<b>M/G 33/67</b>	[ $\text{kg/m}^3$ ]	657	1335	365	182
<b>M/G 50/50</b>	[ $\text{kg/m}^3$ ]	898	898	449	225
<b>M/G 60/40</b>	[ $\text{kg/m}^3$ ]	995	663	521	260

Three prismatic samples were made of each mixture. All moulds were covered. Samples were cured in four different conditions. Two batches were cured all the time at the room temperature ( $\sim 20^{\circ}\text{C}$ ) but the first was demoulded after 24 hours and the second one was kept in moulds until the strength tests (for 7 days). Third batch was cured for the first 24 hours in climatic chamber at temperature  $40^{\circ}\text{C}$  and humidity 40%. Forth batch was cured for the first 24 hours in climatic chamber at temperature  $60^{\circ}\text{C}$  and humidity 40%. After 24 hours samples from batch three and four were unmolded and kept at room temperature for the next 6 days.

The Author decided to choose curing temperatures equal to 20, 40 and  $60^{\circ}\text{C}$  since assorting the curing temperatures every  $20^{\circ}\text{C}$  is widely used among the scientists [75], [101], [102], [110], [327], [334]. The  $60^{\circ}\text{C}$  was established as the highest curing temperature since, according to reports included in the literature, the further increase of the curing temperature leads to the decrease of the strength of the hardened material [75], [102], [326], [327], [336]. According to some sources, the increase of the curing temperature above the  $60^{\circ}\text{C}$  leads to small (less than 10%) [28], [334] or negligible (1-2%) [101] increase of strength. The  $20^{\circ}\text{C}$  (ambient temperature) was chosen as the lowest curing temperature since it is economically efficient to cure samples at the laboratory conditions. Moreover, it is reported that geopolymer cured at lower temperature needs special treatment, gains the strength slowly and cannot be unmolded earlier than after 7 days [334].

Process of curing of samples inside climatic chamber is presented in Figure 3.8.1. Three beams from each mixture were subjected to flexural strength test, then, six halves were subjected to the compressive strength test.

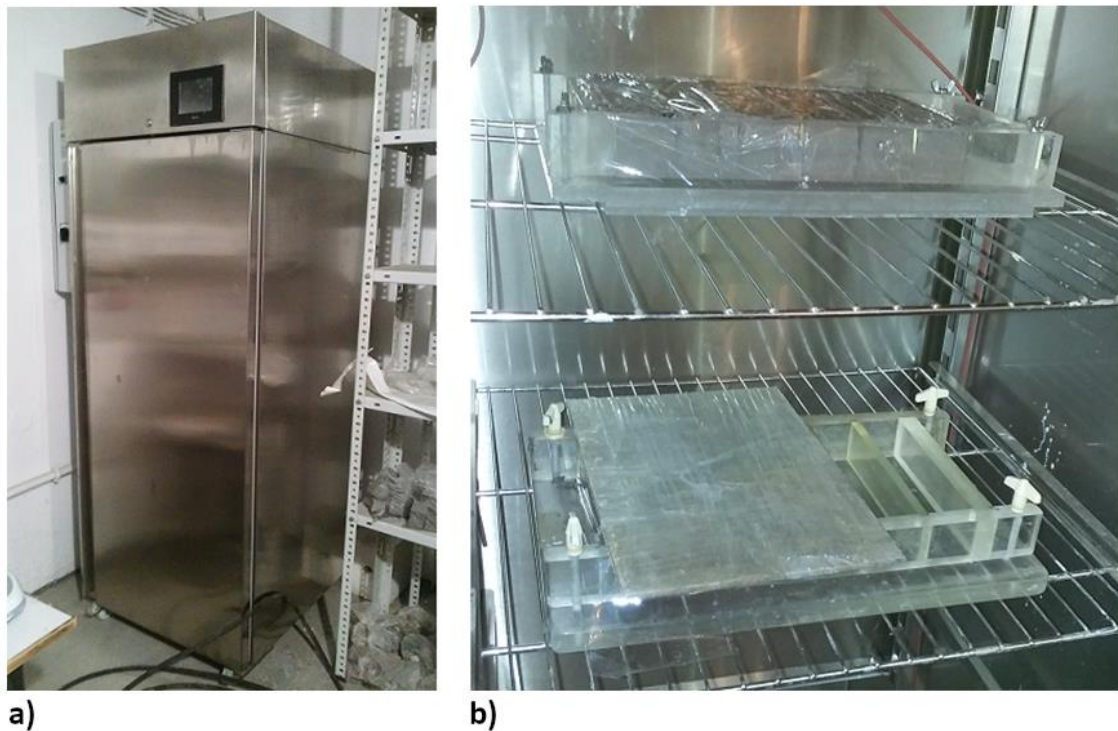


Fig.3.8.1: a) Climatic chamber, b) samples cured inside the climatic chamber.

Only after unmolding, geopolymer had dark grey color which turned into the light gray with the time. The difference in color of the surface is presented in Figure 3.8.2.

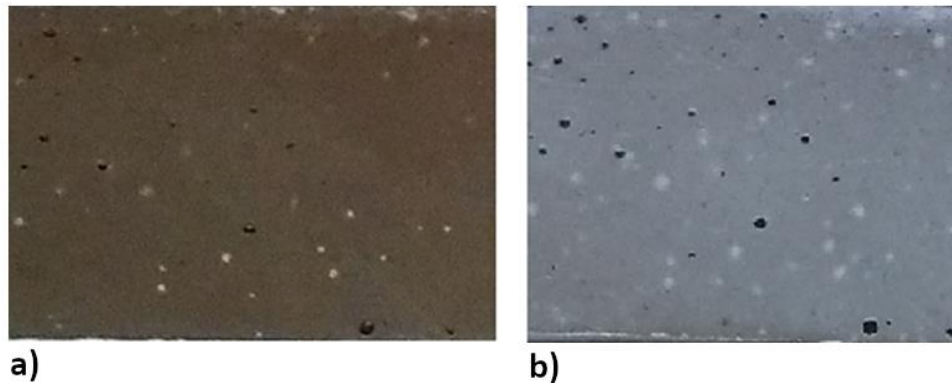


Fig.3.8.2: Comparison of differences in color of the surface of the same sample a) only after unmolding, b) after 7 days of curing.

Samples cured at elevated temperatures for the first 24 hours and samples cured at the room temperature and unmolded just before the tests were not affected by any cracks. The surface was plain and covered only with some air cavities (see Figure 3.8.3 and Figure 3.8.4 b). However, samples cured at the room temperature and demoulded after 24 hours were affected by visible cracks after 7 days (see Figure 3.8.4 a) and Figure 3.8.5). Small, shallow cracks started appearing within an hour after unmolding. After 7 days all surfaces which had a contact with the air were cracked (see Figure 3.8.5). The only uncracked surface was the bottom of the prisms. The network of cracks was relatively shallow. No visible cracks inside broken beams were observed. The possible reason of registered situation was an extensive shrinkage of samples which were unmolded too early. The water in geopolymer material is essential to achieve the proper workability of the mixture and to enable the destruction of solid particles but is not incorporated directly in the final hardened geopolymer gel. As a result, there is an excess of unbound water [81], [337]. The rapid contact with the air can cause the evaporation of the moisture at least from the external surfaces of the geopolymer prisms. Because of the extensive shrinkage, the network of cracks appeared on surfaces which had the contact with the air. Creation of cracks is explained by high capillary pressures which take place between dry and wet areas inside the network of micropores. The shrinkage can be controlled by proper curing conditions and/or adjusting Na/Al and Si/Al ratio. Na/Al ratio is crucial if shrinkage is affected by loss of  $\text{Na}^+$  spheres of hydration. Si/Al ratio in turn, can be crucial for the relative number of  $\text{AlO}_4^-$  sites inside the structure [81]. The investigation of the shrinkage affecting the geopolymer is out of the scope of this Thesis. That topic will be explored in the future.

To withdraw the problem of drying and cracking, lot of scientists report keeping geopolymer samples inside moulds until the testing when the curing takes place at the room temperature [74], [89], [101], [327]. Alternatively, samples can be unmolded and kept in hermetic conditions for example in sealed plastic bags [90] or in high humidity (>95%) [39].

Surface of samples cured at 20°C and demoulded after 7 days was darker than surface of samples demolded after 24 hours, especially than surface of samples cured at elevated temperature for the first 24 hours (compare Figure 3.8.4 b) and Figure 3.8.3 a) and b) ).

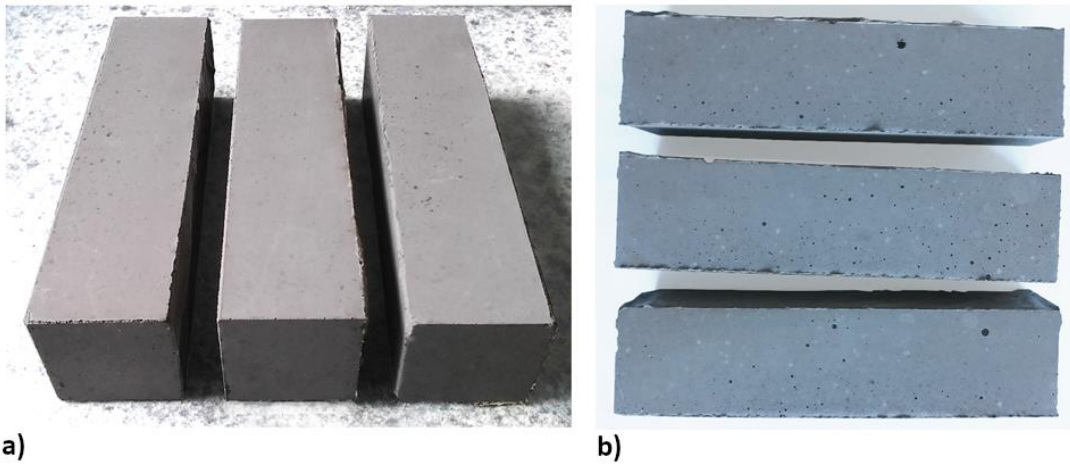


Fig.3.8.3: Uncracked side surface of samples cured at a) 60°C (M/G 50/50) and b) 40°C (M/G 60/40). Photos made after 7 days of curing. There was no significant difference in color between samples. The difference visible in photos is caused by the difference in lighting.

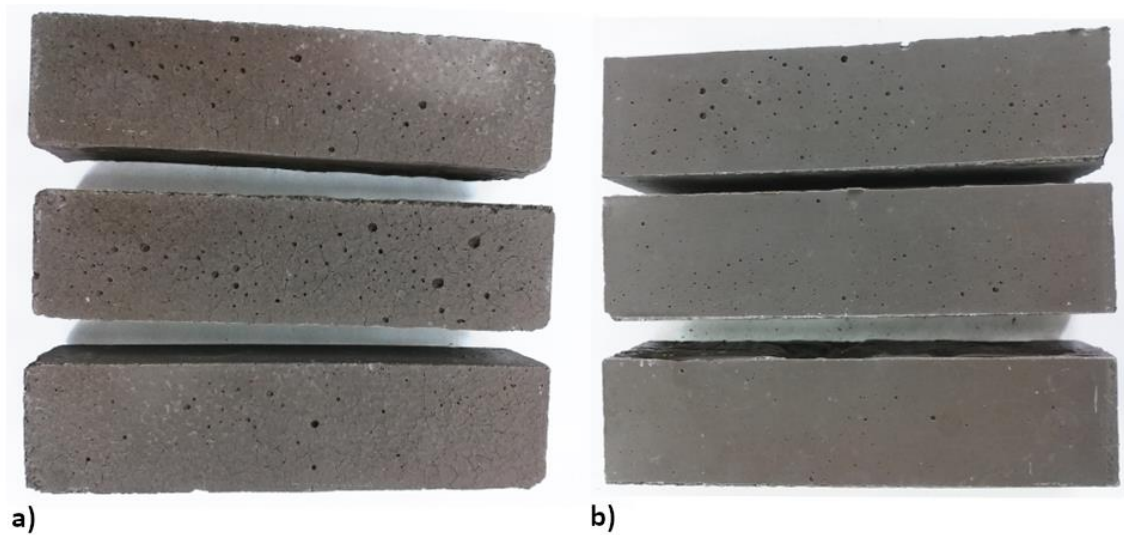


Fig.3.8.4: a) Cracked side surface of samples cured at 20°C and demoulded after 24 hours (M/G 50/50) b) uncracked side surface of samples cured at 20°C and demoulded after 7 days (M/G 60/40). Photos made after 7 days of curing.



Fig.3.8.5: Samples cured at 20°C and demoulded after 24 hours (M/G 60/40): a) upper surface, b) side surface, c) bottom surface. Photos made after 7 days of curing.

### 3.8.2 Results

Table 3.8.2 contains the results achieved during the flexural and compressive strength tests.

Table 3.8.2: Flexural ( $f_x$ ) and compressive ( $f_c$ ) strength results.

Mixture			No. 1	No. 2	No. 3	No. 4	No. 5	No. 6	$f_x/f_c$
<b>M/G 25/75</b>	20°C (2)	$f_x$ [MPa]	3,12	3,31	3,66	-	-	-	0,062
		$f_c$ [MPa]	51,96	49,94	56,07	54,63	56,05	55,08	
	40°C	$f_x$ [MPa]	4,22	4,27	4,37	-	-	-	0,083
		$f_c$ [MPa]	50,55	52,00	49,75	54,91	50,70	52,51	
	60°C	$f_x$ [MPa]	5,20	5,17	4,59	-	-	-	0,106
		$f_c$ [MPa]	48,65	50,86	46,65	49,94	42,70	44,35	
<b>M/G 33/67</b>	20°C (1)	$f_x$ [MPa]	2,59	3,13	2,36	-	-	-	0,085
		$f_c$ [MPa]	27,64	31,40	31,10	30,53	36,65	33,58	
	20°C (2)	$f_x$ [MPa]	4,64	5,58	5,13	-	-	-	0,107
		$f_c$ [MPa]	44,75	44,97	44,10	42,83	52,38	58,09	
	40°C	$f_x$ [MPa]	5,32	5,40	5,39	-	-	-	0,122
		$f_c$ [MPa]	43,34	40,41	45,73	47,46	38,61	48,58	
	60°C	$f_x$ [MPa]	4,32	4,88	4,62	-	-	-	0,096
		$f_c$ [MPa]	44,73	51,14	47,18	49,54	48,58	47,36	
<b>M/G 50/50</b>	20°C (1)	$f_x$ [MPa]	2,82	2,07	3,95	-	-	-	0,070
		$f_c$ [MPa]	39,99	43,47	45,75	37,34	48,86	37,46	
	20°C (2)	$f_x$ [MPa]	5,61	4,13	4,61	-	-	-	0,096
		$f_c$ [MPa]	41,92	57,04	50,96	54,66	42,45	52,41	
	40°C	$f_x$ [MPa]	4,82	6,30	5,92	-	-	-	0,111
		$f_c$ [MPa]	<del>56,99*</del>	51,49	50,18	50,42	52,27	51,19	
	60°C	$f_x$ [MPa]	6,63	5,93	5,98	-	-	-	0,123
		$f_c$ [MPa]	53,93	54,13	52,01	48,92	49,12	42,69	
<b>M/G 60/40</b>	20°C (1)	$f_x$ [MPa]	2,51	3,21	2,80	-	-	-	0,075
		$f_c$ [MPa]	39,15	39,41	36,38	34,94	42,08	36,15	
	20°C (2)	$f_x$ [MPa]	4,19	3,82	3,29	-	-	-	0,077
		$f_c$ [MPa]	39,57	50,38	51,46	55,86	45,43	49,96	
	40°C	$f_x$ [MPa]	4,91	4,88	50,6	-	-	-	0,112
		$f_c$ [MPa]	45,50	43,00	38,51	43,10	47,07	48,96	
	60°C	$f_x$ [MPa]	5,99	5,96	5,31	-	-	-	0,118
		$f_c$ [MPa]	50,10	51,20	46,54	46,17	50,56	47,24	

\* Result was rejected on the basis of statistical method - elimination of one extreme value.

Symbols used in the Table 3.8.2 indicates respectively: 20°C (1) – geopolymer cured at the room temperature and unmolded after 24 hours; 20°C (2) geopolymer cured at the room

temperature and unmolded after 7 days; 40°C – geopolymer cured at 40°C for the first 24 hours then unmolded and cured at the room temperature; 60°C – geopolymer cured at 60°C for the first 24 hours then unmolded and cured at the room temperature.

Samples from series 20°C (1) were repetitively characterized by significantly lower flexural and compressive strength than the rest of samples. Samples cured at elevated temperatures obtained rather high strength results.

Standard deviations and coefficients of variation of flexural and compressive strength results which were presented in Table 3.8.3 are shown in Table 3.8.3. Flexural strength results of samples cured at 20°C and demoulded after 24 hours had the highest coefficient of variation. In turn, among the compressive strength results, the least stable values were achieved by samples cured at 20°C and demoulded after 7 days. Samples cured at elevated temperatures have shown generally more stable results than samples cured at ambient temperature. This dependence is probably caused by the fact that after 7 days the chemical process inside samples cured at ambient temperature is not fully finished and the strength is less developed than in samples cured at elevated temperatures which gains strength more rapidly [327], [334], [338].

Table 3.8.3: Standard deviation and coefficient of variation of flexural and compressive strength results.

	Standard deviation [-] (CoV [%])	20°C (1)	20°C (2)	40°C	60°C
<b>Flexural strength</b>	<b>M/G 25/75</b>	-	0,27 (8,1)	0,08 (1,8)	0,34 (6,9)
	<b>M/G 33/67</b>	0,40 (14,7)	0,47 (9,2)	0,05 (0,9)	0,28 (6,1)
	<b>M/G 50/50</b>	0,95 (32,1)	0,75 (15,8)	0,77 (13,5)	0,39 (6,3)
	<b>M/G 60/40</b>	0,35 (12,3)	0,45 (11,9)	0,10 (2,0)	0,38 (6,7)
<b>Compressive strength</b>	<b>M/G 25/75</b>	-	2,48 (4,6)	1,85 (3,6)	3,21 (6,8)
	<b>M/G 33/67</b>	3,04 (9,6)	6,04 (12,6)	3,96 (9,0)	2,20 (4,6)
	<b>M/G 50/50</b>	4,68 (11,1)	6,33 (12,7)	0,84 (1,6)	4,29 (8,5)
	<b>M/G 60/40</b>	2,66 (7,0)	5,61 (11,5)	3,67 (8,3)	2,23 (4,6)

Samples cured at 20°C and demoulded after 7 days of curing (series 20°C (2)) were characterized with less brittle way of failure (see Figure 3.8.6 a)) than samples cured at elevated temperature for the first 24 hours (Figure 3.8.6 b)). The crack appearing after flexural strength test was wider and more visible in samples cured at elevated temperature. No

significant difference was noticed between the failure of samples cured at 40°C and 60°C for the first 24 hours.

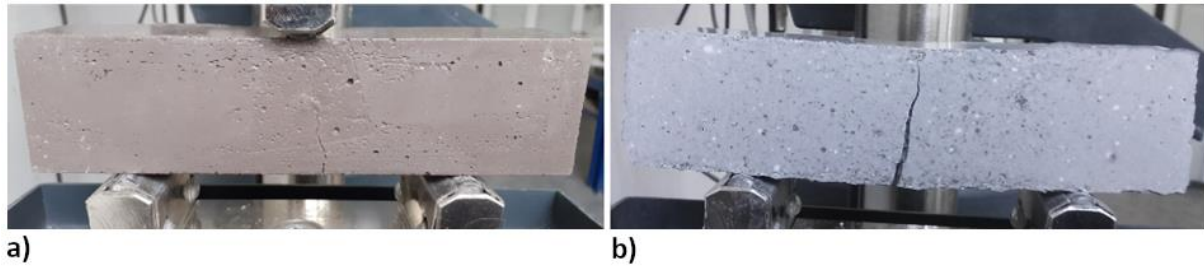


Fig.3.8.6: The beam after flexural strength test. Samples containing metakaolin to glass in mass ratio (M/G 50/50): a) series 20°C (2), b) series 60°C. There is visible the difference in color between picture a) and b). The color of samples cured at 20°C was darker than of samples cured at 60°C.

### 3.8.3 Analysis

Results of the second part of the preliminary tests are presented in Figure 3.8.7 and Figure 3.8.8. Each bar represents average value of compressive or flexural strength obtained by samples from particular mixture and subjected to different curing conditions.

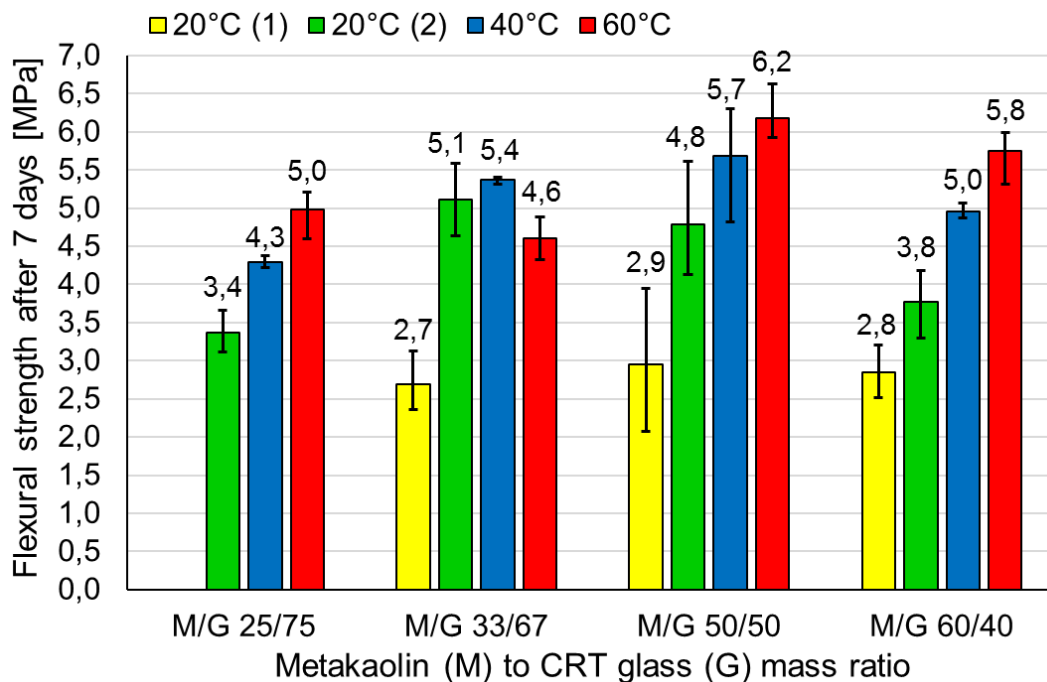


Fig.3.8.7: Seventh days flexural strength of geopolymer made of mixtures containing different metakaolin to CRT glass mass ratio and cured in different conditions.

According to the results, flexural strength increases with the increase of curing temperature (the increase is monotonic and linear excluding samples cured at 20°C and demoulded after 24 hours which obtained unequivocally the lowest strength, significantly lower than the other samples). These samples had network of cracks on their surface. The only exception are samples made of mixture M/G 33/67 cured at 60°C which obtained smaller

results than samples cured at 20°C (2) and 40°C. The highest value of flexural strength (6,2 MPa) obtained geopolymer made of mixture M/G 50/50 cured at 60°C. Generally, samples made of this mixture achieved the highest values of flexural strength in comparison to samples made of other mixtures and cured at the same conditions. The only exception was samples from series M/G 50/50 cured at 20°C (2) which had smaller strength than specimens made of mixture M/G 33/67 cured at the same conditions.

Generally, the least stable (characterized by the highest coefficient of variation) were results of geopolymer cured at 20°C and demoulded after 24 hours. It can be explained by cracks which affected samples at different levels. No other direct dependence between the curing regime and stability of flexural strength results has been noticed.

Figure 3.8.8 presents results of compressive strength of geopolymer samples cured at different conditions.

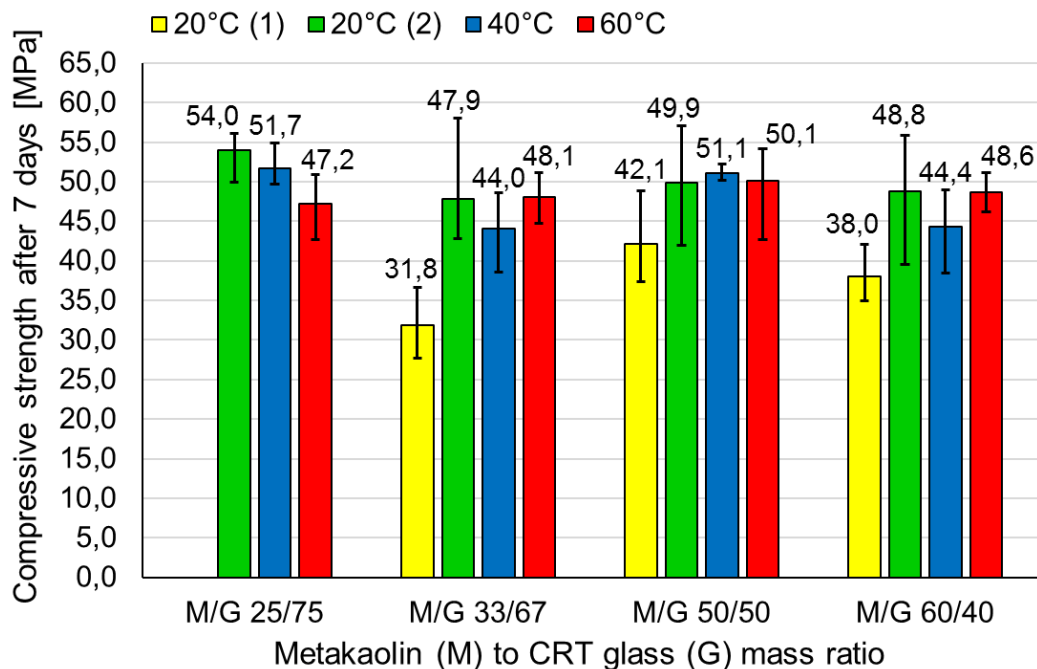


Fig.3.8.8: Seventh days compressive strength of geopolymer made of mixtures containing different metakaolin to CRT glass mass ratio and cured in different conditions.

Geopolymer cured at the room temperature and demoulded after 24 hours (20°C (1)) obtained considerably the lowest compressive strength and is excluded from most of the further comparisons. The dependences between curing temperature and compressive strength are less direct than in case of flexural strength. Compressive strength of samples made of mixture M/G 25/75 decreases with the increase of the curing temperature. Samples made of mixture M/G 33/67 and cured at 20°C (2) had higher strength than samples cured at 40°C but slightly lower than those one cured at 60°C. In case of geopolymer M/G 50/50 all achieved compressive strengths were very close to each other save for the results obtained from samples cured at 20°C (1). The highest and most stable values of compressive strength in the case of this mixture were obtained by samples cured at 40°C. Geopolymer prepared from the last mixture M/G 60/40 exhibited the highest strength while cured at 20°C (2) and

lowest while cured at 40°C (excluding samples cured at the room temperature and demoulded after 24 hours). Generally, all results of compressive strength are more or less similar to each other. Compressive strengths of samples made of mixtures M/G 33/67 and M/G 60/40 and cured at 40°C constitute a major deviation from the rest of results. The best compressive strength (54,0 MPa) was obtained by geopolymer M/G 25/75 cured at 20°C (2). Surprisingly, samples from series 20°C (1) obtained relatively high compressive strength what can be a sign that shrinkage and cracks affected mostly the surface rather than the interior of prisms.

The lowest coefficient of variation characterizes samples made of mixtures M/G 25/75 and M/G 50/50 cured at 40°C. The least stable results were shown generally by samples from series 20°C (2).

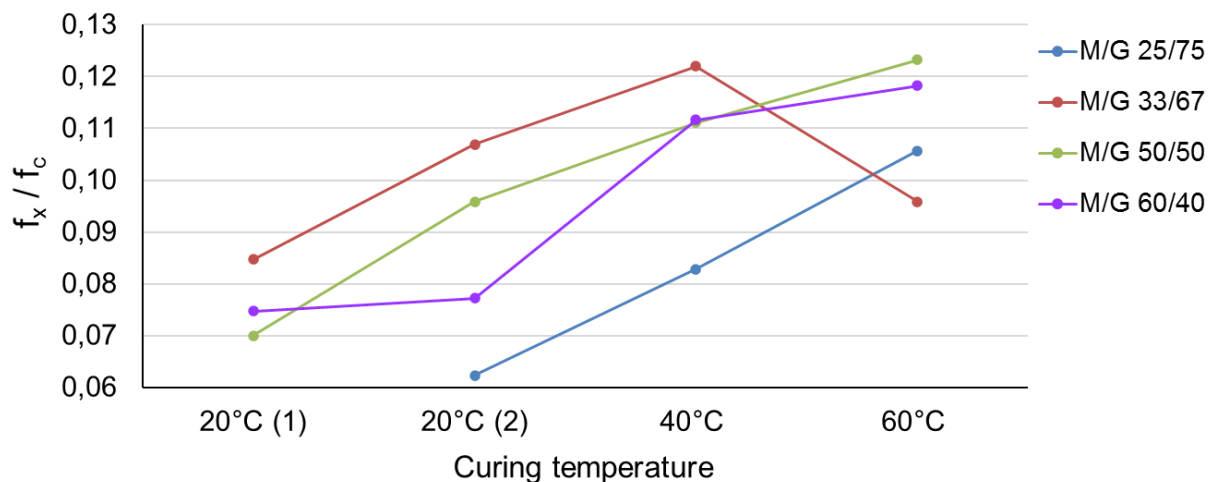


Fig.3.8.9: The  $f_x/f_c$  ratio of geopolymer of different CRT glass content and cured in different temperatures.

According to the graph presented in Figure 3.8.9,  $f_x/f_c$  ratio increases along with the increase of curing temperature. The only exception was  $f_x/f_c$  ratio of geopolymer made of mixture M/G 33/67 where value obtained after curing at 60°C was smaller than after curing at 20°C and 40°C. Samples made of mixture M/G 33/67 were the only one not showing the monotonic increase of flexural strength along with the increase of curing temperature. Flexural strength achieved by samples M/G 33/67 cured at 60°C was smaller than of samples cured at 20°C and 40°C. The possible reason could be improper compaction of those samples. Similarly, as in subsection 3.7.3, no monotonic dependence between CRT glass content and  $f_x/f_c$  ratio was observed.

An increase of tensile to compressive strength ratio along with the increase of curing temperature has been noted by Ekaputri et al. [101]. The reported  $f_x/f_c$  ratio is much lower than in this Thesis and ranges from 0,014 to 0,058 in dependence on the exact composition of the mixture. According to data published by Rovnanik [334], temperature of curing did not influence significantly the  $f_x/f_c$  ratio which fluctuates for all specimens around 0,18 and surpasses values achieved within this Thesis.

All samples (with those one cured at 20°C and demoulded after 7 days being the only exception) were weighed only after demolding and just before test to obtain mass loss during

the curing period at the room temperature. Densities of all geopolymers and their mass losses are presented in Table 3.8.4.

Table 3.8.4: Average density and mass loss of geopolymer samples made of different mixtures and cured at different conditions.

Density[kg/m <sup>3</sup> ] Mass loss [%]	20°C (1)	20°C (2)	40°C	60°C
<b>M/G 25/75</b>	-	2240 -	2110 3,7	2090 5,6
<b>M/G 33/67</b>	2100 4,0	2160 -	1980 5,9	1960 6,5
<b>M/G 50/50</b>	1910 5,5	2040 -	1890 6,8	1920 5,8
<b>M/G 60/40</b>	1870 6,2	1940 -	1790 8,9	1770 6,5

For prisms cured at the same temperature, the density is increasing with the increase of CRT glass content. Then, comparing geopolymers containing the same amount of CRT glass, considerably higher density had those one cured at 20°C (2) than geopolymers cured at 40°C or 60°C. By contrast, difference between density of samples cured at 40°C and 60°C is much lower (equal to 20 kg/m<sup>3</sup> for samples made of all mixtures save for mixture M/G 50/50). In case of samples made of mixture M/G 50/50 the density of geopolymer cured at 60°C is even higher than density of geopolymer cured at 40°C. Series cured at 20°C (2) are much heavier than cured at 20°C (1). Generally, for geopolymer prepared from all mixtures, the greatest density have those cured at the room temperature and unmolded after 7 days (20°C (2)) since they had no contact with the air before weighing. For geopolymer cured at 20°C (1) and 40°C, specimens containing more metakaolin were affected by higher mass loss. In samples made of mixtures M/G 25/75 and M/G 33/67, the mass loss is increasing with the increase of curing temperature. By contrast, in prisms made of mixtures M/G 50/50 and M/G 60/40 the mass loss is lower when curing at 60°C than at 40°C. Even then, series M/G 60/40 cured at 60°C are lighter than cured at 40°C. Described relations can indicate that the part of important changes inside geopolymer affecting also its density take place during the first 24 hours of curing (during this time the mass loss was not measured).

Two mixtures M/G 25/75 and M/G 50/50 were chosen for further tests. Samples made of mixture M/G 50/50 obtained very high flexural and compressive strength. Samples made of mixture M/G 25/75 obtained very high compressive strength and good flexural strength. Moreover, mixture M/G 25/75 had the highest CRT glass content. One curing condition was chosen for further tests: curing for the first 24 hours at elevated temperature 40°C and then at the room temperature. The following curing condition was chosen because of higher

flexural strength of results obtained by geopolymer cured in that way and because of high and more stable results of compressive strength.

### 3.9 Determination of the temperature and strength changes over time

#### 3.9.1 Preparation of samples

The main goal of the test was to describe the changes of the temperature inside the geopolymer sample over time and to determine the influence of the age of geopolymer samples on mechanical behavior (flexural and compressive strength and density). Research has been done on samples made of mixtures M/G 25/75 and M/G 50/50 cured for the first 24 hours at 40°C. The composition of mixtures is presented in Table 3.9.1.

Table 3.9.1: Mixtures compositions.

Mixture		Metakaolin	CRT glass	Sodium silicate	Sodium hydroxide
<b>M/G 25/75</b>	[kg/m <sup>3</sup> ]	524	1572	314	157
<b>M/G 50/50</b>	[kg/m <sup>3</sup> ]	898	898	449	225

Moulds filled with the mixtures were covered and put into the climatic chamber at temperature 40°C and humidity 40% for the first 24 hours. Then, samples were unmolded and kept at the room temperature for the rest of the curing period. Specimens were subjected to flexural and compressive strength tests after 1, 3, 7, 14 and 28 days. Three beams from each mixture were subjected to every flexural strength test, then, six halves were subjected to each compressive strength test.

Besides, the accurate measurement of the mass and dimension changes withing time was carried out on samples cured for 7 days (see Figure 3.9.1) to determine the dependence between curing time and mass loss and to observe if dimensions are changing in visible way. Every day each sample was measured with caliper with accuracy 0,02mm in eleven places (height in three places, width in three places and length in two places) and weighed. The main goal was to register the mass loss each following day of curing and the evident change of dimensions. No change in dimensions was registered what indicated that no evident shrinkage (which could be measured with a caliper of accuracy 0,02mm) took place. No tendency to expansion was observed as well.

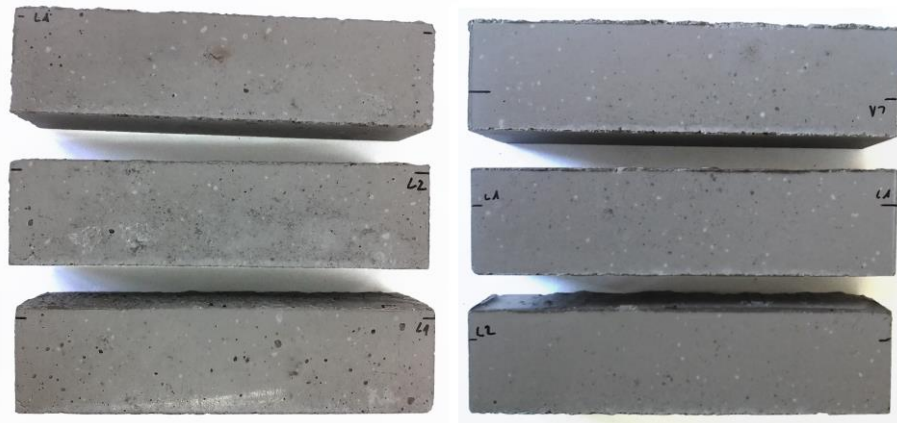


Fig.3.9.1: Samples prepared for measurement with use of a caliper.

The temperature measurement inside prismatic samples of dimensions 40x40x160 mm has been done with use of DS thermometers which were attached to the inside walls of moulds with use of a tape. Thermometers were stabilized in the middle of the height and width on both ends of each sample subjected to the test (see Figure 3.9.2). Figure 3.9.3 presents form with attached thermometers filled with fresh geopolymer mixture and form inside the climatic chamber. Temperature was registered in two samples made of each mixture. Summarizing, the measurement for geopolymer made of particular mixture and cured at particular conditions has been done with 4 thermometers. Thermometers were connected with electronic data processing apparatus with use of thin wires (see Figure 3.9.4). All steel parts of thermometers and wires were protected against fresh mixture. Temperature was measured since placing the mixture inside the moulds, through all time when samples were inside climatic chamber, till a few days after removing samples from the moulds. Simultaneously, the temperature inside climatic chamber was registered.

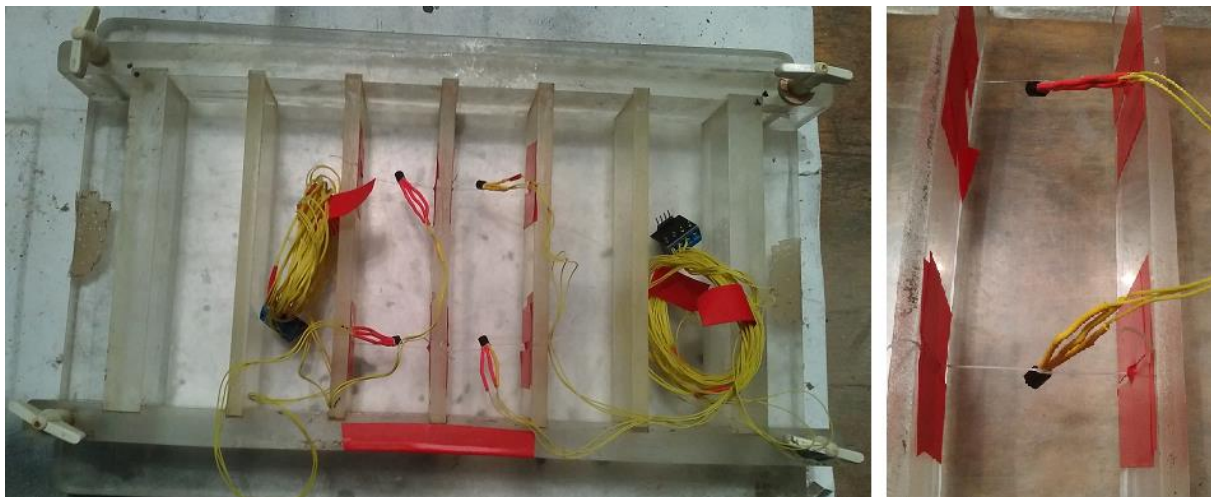


Fig.3.9.2: Thermometers attached inside the forms.

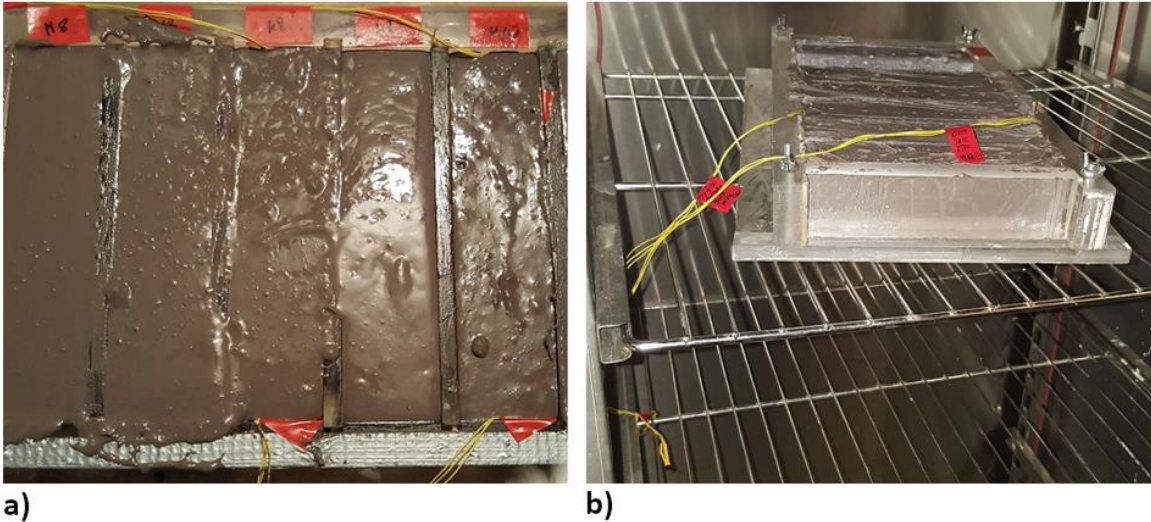


Fig.3.9.3: a) Form filled with mixture, b) form inside climatic chamber.

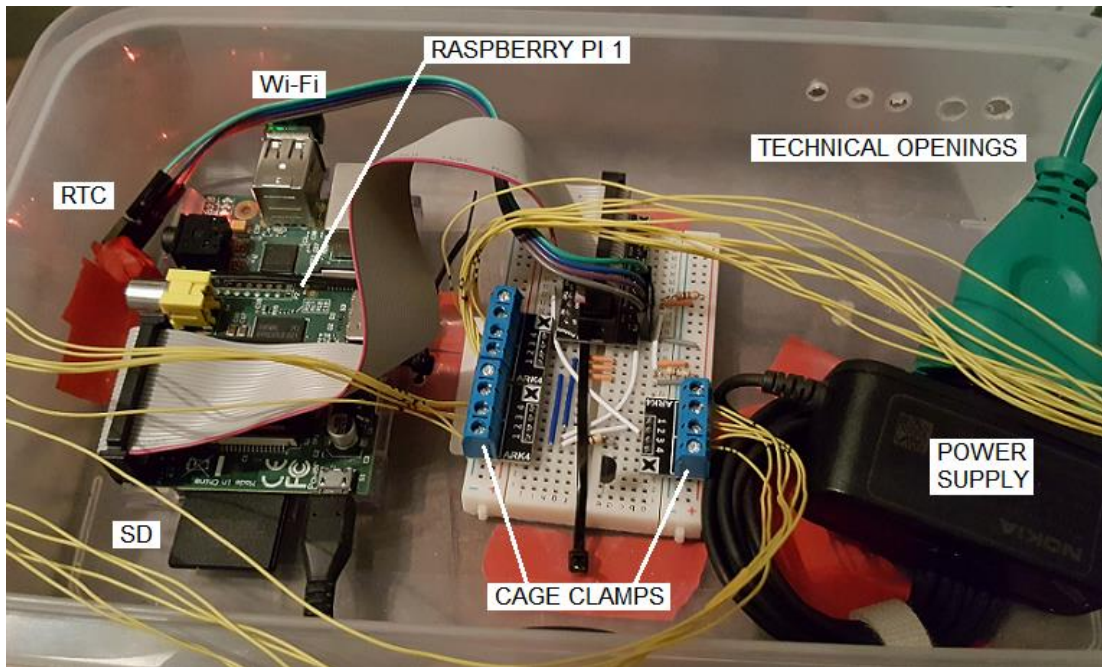


Fig.3.9.4: The electronic device for registering of temperature measurement.

### 3.9.2 Results

Table 3.9.2 includes all flexural and compressive strength tests results. Flexural strength results seemed not to be dependent on curing time. Samples from series M/G 50/50 achieved rather higher strength values than samples from series M/G 25/75. All results (of both flexural and compressive strength) were high.

Table 3.9.3 includes standard deviations and coefficients of variation of results presented in Table 3.9.2. The smallest standard deviation (and coefficient of variation) characterizes flexural strength results obtained by geopolymer containing 50% of CRT glass and cured for 28 days. Excluding series cured for 1 day and 28 days, samples containing 75% of CRT glass had more stable results than samples with 50% of CRT glass. No direct dependence between curing period and stability of results was observed. No dependence

between curing time and stability of compressive strength results was observed. The stability of compressive strength results of samples made of mixture M/G 25/75 and M/G 50/50 were approximately similar. The most stable results were shown by samples made of mixture M/G 25/75 and cured for 28 days.

Table 3.9.2: Flexural ( $f_x$ ) and compressive ( $f_c$ ) strength results.

Mixture			No. 1	No. 2	No. 3	No. 4	No. 5	No. 6	$f_x/f_c$
<b>M/G 25/75</b>	1 day	$f_x$ [MPa]	4,75	4,79	4,00	-	-	-	0,096
		$f_c$ [MPa]	50,51	46,92	44,23	48,68	49,13	41,38	
	3 days	$f_x$ [MPa]	4,93	4,45	4,63	-	-	-	0,093
		$f_c$ [MPa]	45,48	47,51	51,68	52,05	49,84	55,28	
	7 days	$f_x$ [MPa]	4,22	4,27	4,37	-	-	-	0,083
		$f_c$ [MPa]	50,55	52,00	49,75	54,91	50,70	52,51	
	14 days	$f_x$ [MPa]	4,61	4,73	5,45	-	-	-	0,101
		$f_c$ [MPa]	48,50	54,08	44,95	50,02	44,32	51,65	
	28 days	$f_x$ [MPa]	3,99	3,85	4,80	-	-	-	0,097
		$f_c$ [MPa]	<del>31,76</del> *	42,82	42,04	44,17	42,78	44,44	
<b>M/G 50/50</b>	1 day	$f_x$ [MPa]	5,13	5,29	4,76	-	-	-	0,109
		$f_c$ [MPa]	42,44	43,51	51,63	44,54	49,13	46,56	
	3 days	$f_x$ [MPa]	5,91	4,50	4,99	-	-	-	0,106
		$f_c$ [MPa]	46,16	49,19	46,15	47,51	49,31	52,48	
	7 days	$f_x$ [MPa]	5,55	6,25	6,56	-	-	-	0,113
		$f_c$ [MPa]	51,63	57,24	56,24	52,32	53,52	53,16	
	14 days	$f_x$ [MPa]	5,63	6,45	7,20	-	-	-	0,111
		$f_c$ [MPa]	61,19	59,46	51,80	56,33	58,76	59,79	
	28 days	$f_x$ [MPa]	5,96	5,93	5,91	-	-	-	0,100
		$f_c$ [MPa]	66,03	54,26	55,84	60,20	58,02	61,34	

\*Result was rejected on the basis of statistical method - elimination of one extreme value.

Table 3.9.3: Standard deviation and coefficient of variation of flexural and compressive strength results.

	Standard deviation [-] (CoV [%])	1 day	3 days	7 days	14 days	28 days
<b>Flexural strength</b>	<b>M/G 25/75</b>	0,45 (9,9)	0,24 (5,2)	0,08 (1,8)	0,46 (9,3)	0,51 (12,1)
	<b>M/G 50/50</b>	0,27 (5,3)	0,72 (14,0)	0,52 (8,5)	0,78 (12,2)	0,03 (0,4)
<b>Compressive strength</b>	<b>M/G 25/75</b>	3,43 (7,3)	3,49 (6,9)	1,85 (3,6)	3,80 (7,8)	1,01 (2,3)
	<b>M/G 50/50</b>	3,53 (7,6)	2,40 (5,0)	2,23 (4,1)	3,38 (5,8)	4,23 (7,1)

The brittleness of samples increased along with the increase of the age of tested sample. In samples cured for 1 day, during the flexural strength test only small crack appeared after breaking. Samples cured for 28 days were destroyed with a resonant tone, two halves of the beam have been falling apart.

Figure 3.9.5 presents the visual difference between the interior of geopolymer made of mixture M/G 25/75 (containing 75% of CRT glass) and made of mixture M/G 50/50 (containing 50% of CRT glass). The increased amount of CRT glass has been clearly visible in the cross section of broken sample.

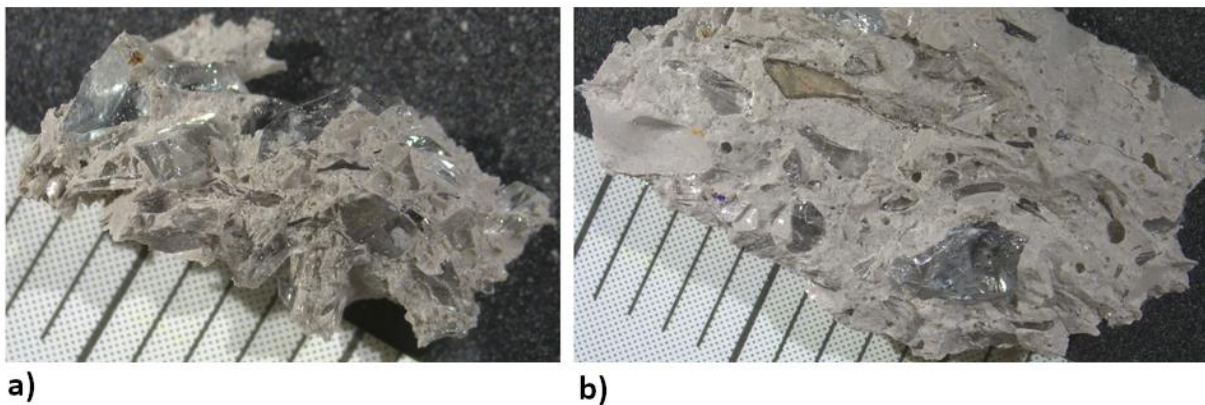


Fig.3.9.3: Broken surface of sample containing a) 75% of CRT glass b) 50% of CRT glass (photographs were taken by dr Fatima Pawełczyk in Institute of Physics, Centre for Science and Education, Silesian University of Technology).

Mixture M/G 27/75 had much worse workability than mixture M/G 50/50. What is more, the high content of CRT glass hindered compaction of mixture inside moulds. As an effect, not all samples were compacted enough what caused creation of some cavities inside hardened material. Cavities were visible after broking prisms during the flexural strength test. Some exemplary cavities are shown in Figure 3.9.6. Cavities were marked with use of the green circle.



Fig.3.9.4: Cavities in geopolymer containing 75% of CRT glass. The biggest cavities were marked with the green circle.

Table 3.9.4 contains results of measurements of mass taken on each day since demolding which has been done on samples tested after 7 days of curing. Samples from series

M/G 25/75 were heavier than samples from series M/G 50/50. Samples made of both mixtures were generally losing weight along with the curing time.

Table 3.9.4: Mass of each sample tested after 7 days on each following day of curing.

Mass [g]	1 <sup>st</sup> day	2 <sup>nd</sup> day	3 <sup>rd</sup> day	4 <sup>th</sup> day	5 <sup>th</sup> day	6 <sup>th</sup> day	7 <sup>th</sup> day
<b>M/G 25/75</b>	594	589	583	580	577	574	573
	612	606	599	596	593	591	589
	603	596	588	586	584	581	579
<b>M/G 50/50</b>	538	530	522	515	510	507	505
	529	522	515	510	506	504	502
	552	544	537	532	528	525	523

### 3.9.3 Analysis

Figure 3.9.7 shows changes of the temperature inside geopolymer made of mixtures M/G 25/75 and M/G 50/50 during the first 10 hours of curing. Figure 3.9.8 shows changes of the temperature inside geopolymer during the first 30 hours of curing. The whole measurement is presented in two Figures 3.9.7 and 3.9.8 to show clearly both the details which took place at the beginning of curing and the overall view on the behavior of the temperature inside samples. The graph presented in Figure 3.9.8 is cut after 30 hours of curing since no further changes of temperature took place inside samples. Several stages can be distinct in the temperature graph: 1) the rapid increase at the very beginning, only after placing the mixture in moulds, 2) the slight drop within minutes after placing, 3) the steady increase since placement of moulds in climatic chamber, 4) the gradual drop after achieving the maximum point within an hours since casting, 5) stabilization on the level of the temperature inside the climatic chamber approximately after 18-20 hours since casting, 6) the significant and rapid decline between 24 and 26 hours since casting (the decline started at the moment when samples were taken off from the climatic chamber), 7) the stagnation at the level of the room temperature after 26-30 hours since casting.

Figure 3.9.7 shows temperature changes inside geopolymer since the moment of placing the mixture in the forms. At a very beginning of measurement, the temperature increased sharply. After 1,5 minute it reached averagely 27,23°C in mixture M/G 50/50 and 26,81°C in mixture M/G 25/75. After 10,5 or 12 minutes since the beginning of measurement (respectively inside mixture M/G 50/50 and M/G 25/75), temperature declined to 26,67°C in mixture M/G 50/50 and to 26,14°C in mixture M/G 25/75. All given values of temperature and time are the average from four measurements. The temperature remained stable by 6,5 minutes and after that period, started increasing steadily. In case of samples made of mixture M/G 50/50 the maximum temperature (47,06°C) was reached after 342 minutes of curing (almost 6 hours) while samples made of the mixture M/G 25/75 needed 386 minutes (about 6,5 hours) to gain its maximum value (43,80°C).

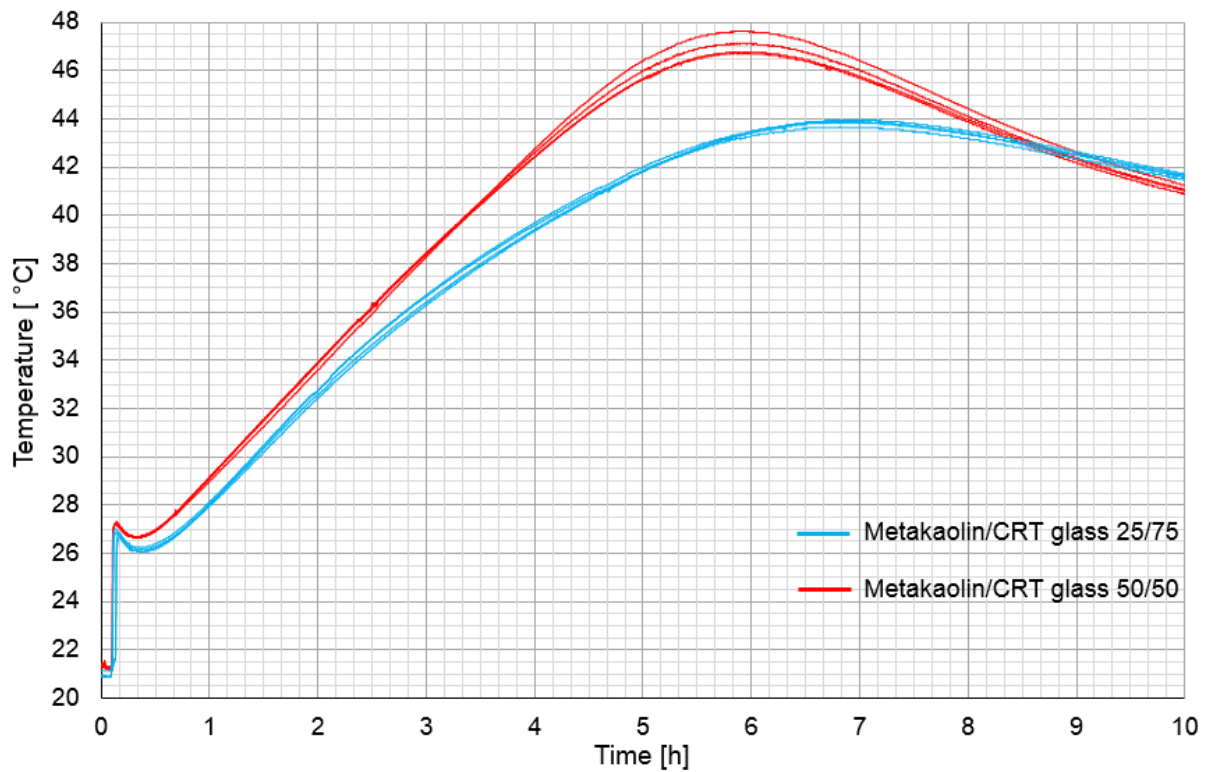


Fig.3.9.5: The temperature changes during the first 10 hours of curing.

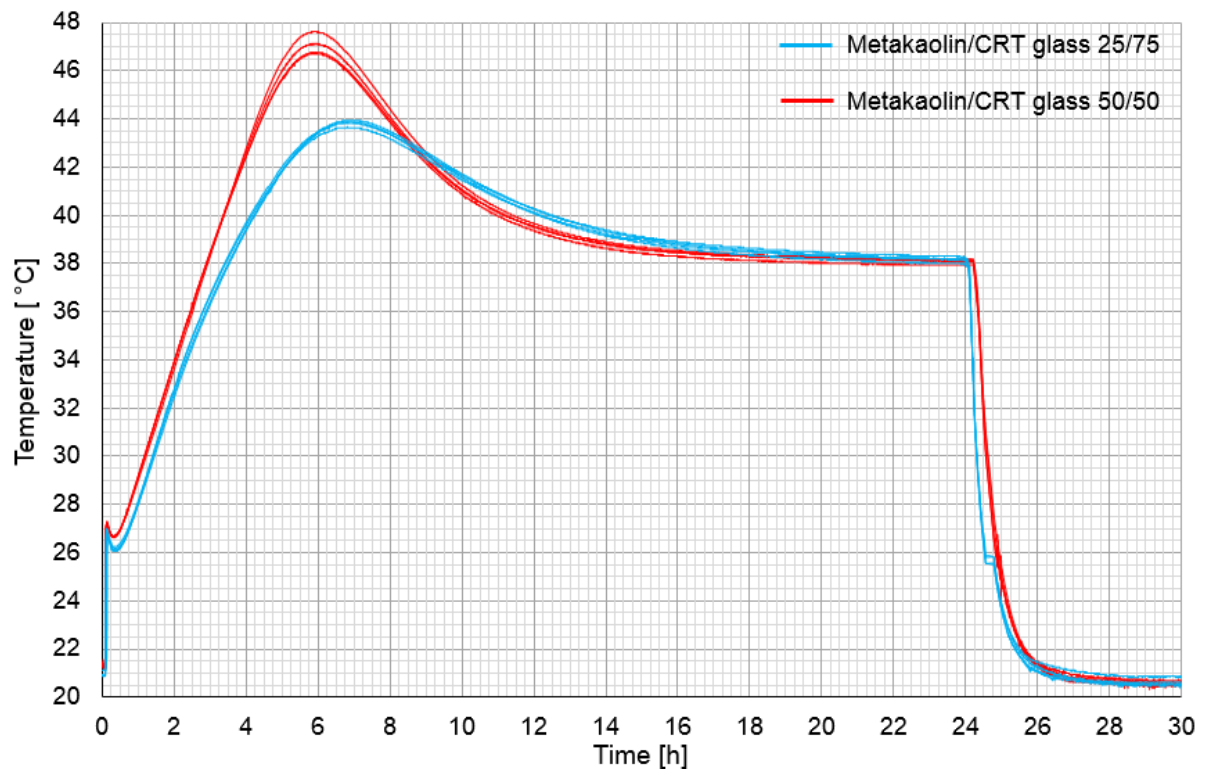


Fig.3.9.6: The temperature changes during the first 30 hours of curing.

After reaching the top value, the temperature in both geopolymers went down steadily and stagnated at 38°C (in about 19<sup>th</sup> hour of curing). After 24 hours of curing, specimens were taken off the climatic chamber and unmolded. That moment is visible in the graph in the form

of a sudden and significant reduction of the temperature. After about 1,5 hours since demolding, temperature started leveling off. The room temperature (~20,5°C) inside geopolymers made of both mixtures was achieved after 28-30 hours since casting.

In general, the temperature gained higher values inside geopolymer samples containing 50% of CRT glass. What is more, excluding the first growth and the last decrease which took place simultaneously, the temperature was rising and falling down more quickly in specimens prepared of mixture M/G 50/50. Changes in geopolymer containing 75% of CRT glass were occurring more gradually.

Based on the descriptions in the literature, Author concluded that the two peaks in the temperature diagram (Figure 3.9.8) are caused respectively with dissolving of metakaolin particles and formation of geopolymeric gel [36], [166], [339]–[342]. The lack of the visible three peaks described in the some sources [36], [339], [340] is probably caused by different measurement method (thermometers instead of isothermal calorimetry) and the fact that measurement was started after placing of mixture in molds. The maximal temperatures inside the material during the curing process are relatively low what is a positive sign while considering using geopolymer for preparing of large structure elements. However, the temperature will probably increase with the increase of element volume what demand an extensive study in the future.

Results of the strength tests are presented in Figure 3.9.9 and Figure 3.9.10. Each bar represents average value of compressive or flexural strength obtained by samples from particular mixture cured for different time (1, 3, 7, 14 or 28 days).

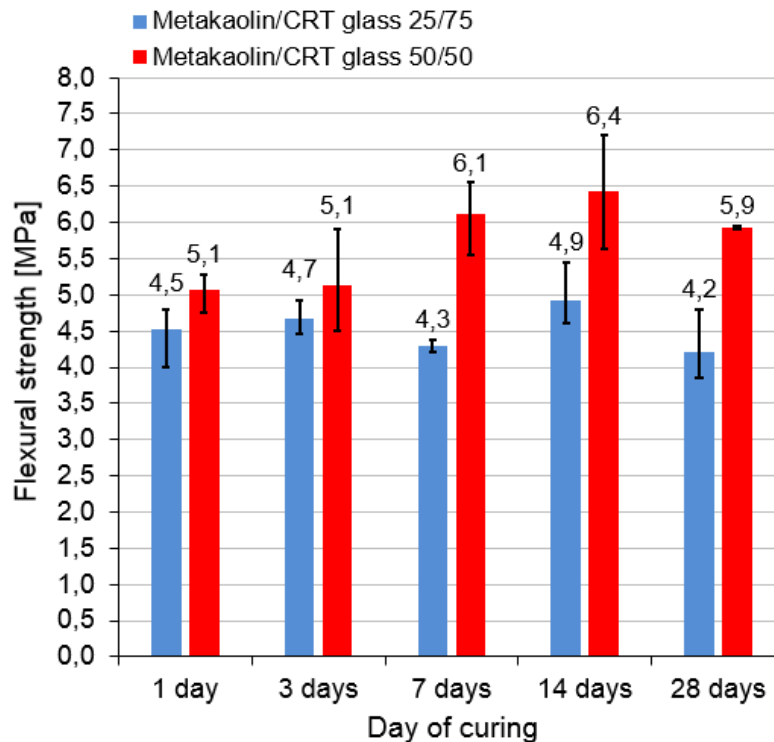


Fig.3.9.7: Flexural strength of geopolymer made of mixtures containing different metakaolin to CRT glass mass ratio and cured for different time.

Geopolymer made of mixture M/G 50/50 regardless the period of curing, had higher flexural strength results than the one prepared on the base of mixture M/G 25/75. The difference in early-strength was relatively small but increased with time. The average flexural strength of geopolymer containing 50% of CRT glass was growing with time (except for series tested after 28 days which was a slightly smaller than after 7 and 14 days). The behavior of geopolymer containing 75% of CRT glass was less predictable. The differences in strength were changing not monotonically in time (every other measurement of strength was smaller than the previous one). Samples made of mixture M/G 25/75 obtained their almost final flexural strength only after 24 hours of curing while strength of samples made of the mixture M/G 50/50 was high after 1 day but was still increasing in time. Such situation could be caused by the fact that geopolymer M/G 25/75 contained less metakolin so that the chemical reactions could be finished earlier than in geopolymer containing more metakolin.

Figure 3.9.10 presents compressive strength results obtained after 1, 3, 7, 14 and 28 days of curing.

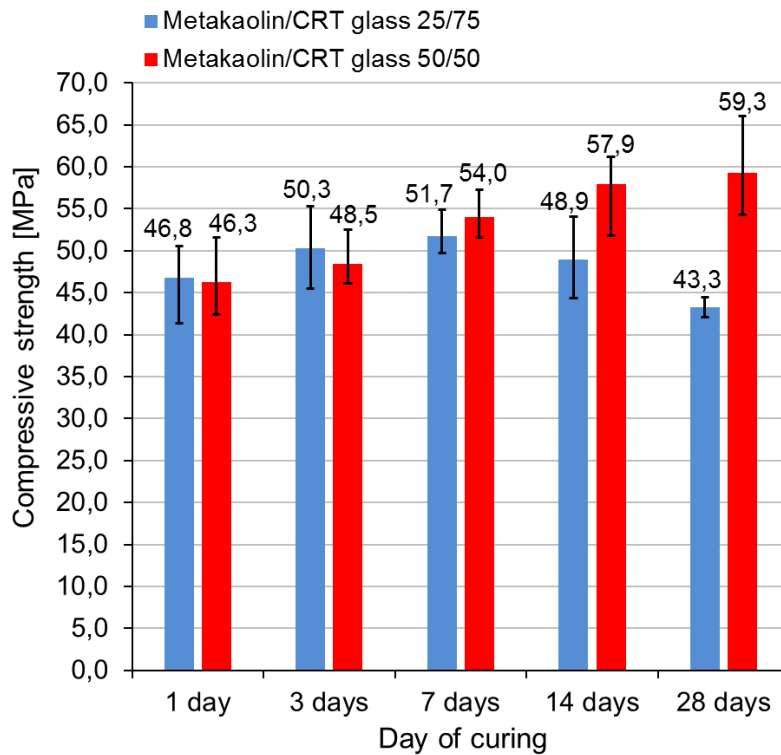


Fig.3.9.8: Compressive strength of geopolymer made of mixtures containing different metakaolin to CRT glass mass ratio and cured for different time.

The early-compressive strength (after 1 and 3 days) of geopolymer containing 50% of CRT glass is smaller than strength of geopolymer containing 75% of CRT glass. However, after 7 days of curing, the inter-relation between geopolymers of different aggregate content was diverted. On the 7<sup>th</sup> day of curing, samples made of mixture M/G 50/50 achieved higher strength than those made of mixture M/G 25/75 and the difference was further enlarging in time. The higher early strength of geopolymer containing 75% of CRT glass can be cause by the fact that the smaller content of metakaolin can shorten the geopolymerization processes inside the material. Compressive strength of specimens prepared with mixture M/G 50/50 is monotonically growing with time reaching the maximum value (59,3 MPa) after 28 days, while

the strength of specimens made of mixture M/G 25/75 starts to decline since the 7 days of curing. After 28 days, the average compressive strength of geopolymer with 75% of CRT glass is 7,5% smaller than one day compressive strength.

Figure 3.9.11 shows the  $f_x/f_c$  ratio change over time.

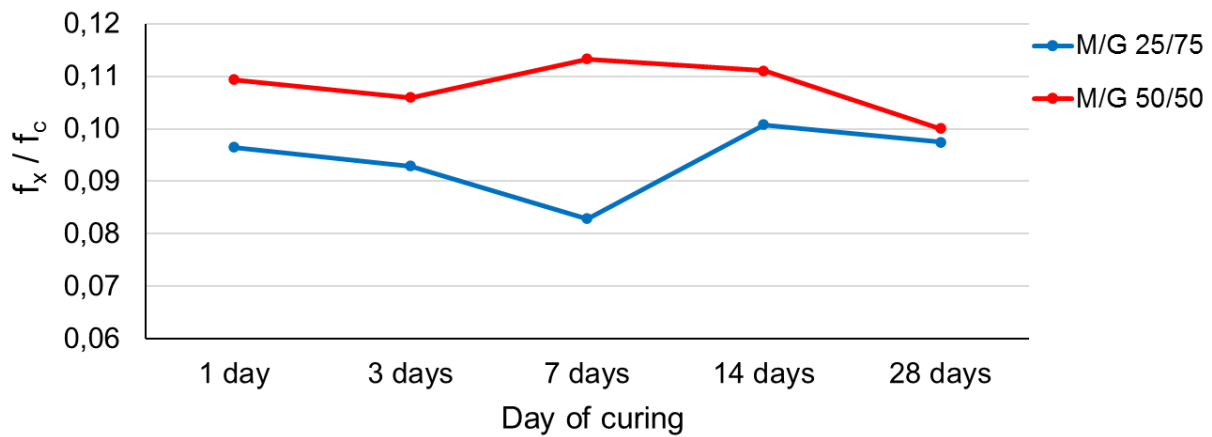


Fig.3.9.9: The change of  $f_x/f_c$  ratio of geopolymer with different CRT glass content over time.

The change of  $f_x/f_c$  ratio over time was more significant in case of geopolymer containing 75% of CRT glass than in case of geopolymer with 50% of CRT glass. In case of geopolymer made of both mixtures,  $f_x/f_c$  ratio dropped on the 3<sup>rd</sup> day of curing. Then, on the 7<sup>th</sup> day, the further decrease and the lowest value was noted in the case of M/G 25/75, while, oppositely, for M/G 50/50,  $f_x/f_c$  ratio increased gaining the highest value. For M/G 50/50  $f_x/f_c$  ratio started decreasing after 7<sup>th</sup> of curing. By contrast, for geopolymer M/G 25/75, after the 7<sup>th</sup> day of curing,  $f_x/f_c$  ratio firstly increased and then decreased on 28<sup>th</sup> day. Independently on the curing age, the  $f_x/f_c$  ratio for M/G 25/75 mixture was all the time smaller than for M/G 50/50.

By contrast to observations made within this Thesis, Rovnanik [334] reports the constant decrease of  $f_x/f_c$  ratio of geopolymer cured at 40°C in time. Long et al. [307] made strength tests only after 7 and 28 days but independently on CRT glass content,  $f_x/f_c$  ratio after 28 days was always lower than after 7 days.

Each sample was measured and weighed only after demolding and before the test. Table 3.9.5 contains average densities of geopolymer on the following days of curing and values of mass loss during the period of curing.

Table 3.9.5: Average density and mass loss of geopolymer samples made of different mixtures and cured for different time periods.

Density[kg/m <sup>3</sup> ] Mass loss [%]	1 day	3 days	7 days	14 days	28 days
<b>M/G 25/75</b>	2200 -	2130 3,2	2110 3,7	2090 5,1	2070 6,2
<b>M/G 50/50</b>	1970 -	1930 3,0	1920 5,4	1900 7,5	1870 9,2

Independently on the period of curing, samples prepared with mixture M/G 25/75 had higher density than samples made of mixture M/G 50/50. In case of geopolymer made of both mixtures, the density was declining with time. The most rapid drop in density was observed between the first and third day. The mass loss increases with the decrease of density. Except for the value registered on the third day, geopolymer containing 50% of CRT glass was affected by higher mass loss than geopolymer with 75% of CRT glass.

Figure 3.9.12 shows the mass loss of each sample made both of mixture M/G 25/75 and M/G 50/50 every following day of curing. The value 100% indicates the weight after 24 hours of curing in climatic chamber at 40°C (only after unmolding). For the rest of time, prisms were kept at the room temperature in the laboratory.

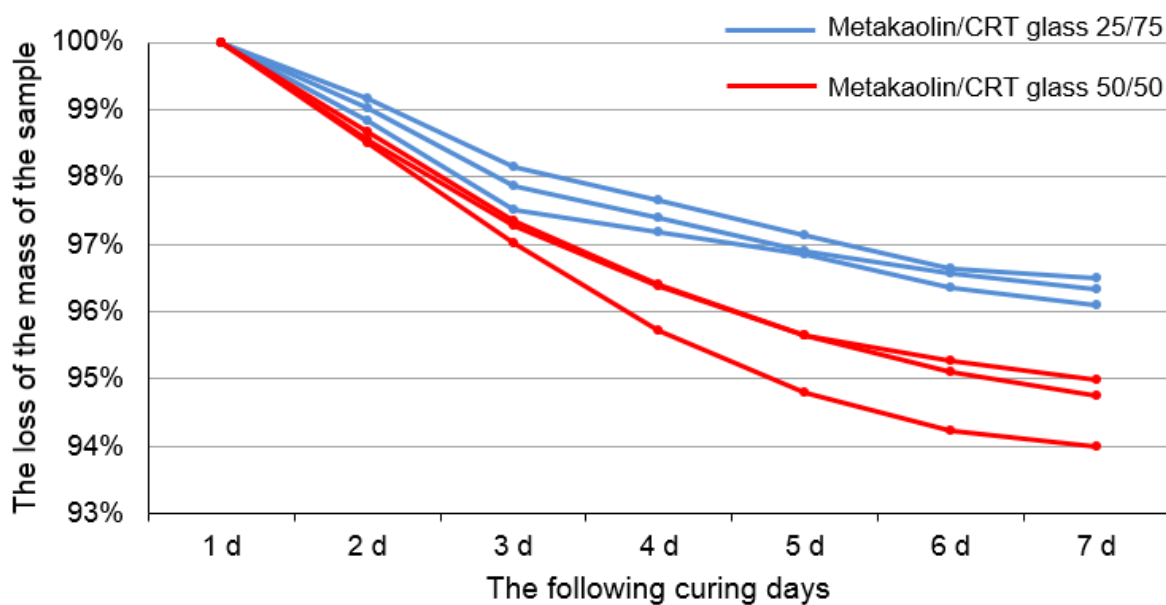


Fig.3.9.10: The loss of the mass of the samples during the following curing days.

The mass loss of geopolymer containing 75% of CRT glass is evidently smaller than mass loss of geopolymer with 50% of CRT glass. This phenomenon is probably caused by the fact, that mixture M/G 50/50 contained overall more liquid (activators) than mixture M/G 25/75 since the number of activators was dosed depending on the metakaolin mass content. Besides, mixture M/G 50/50 includes more precursor which reacts during the geopolymerization process. During the first 3 days there is a significant drop in a mass loss. Then, the reduce in mass become steadier especially in case of geopolymer made of mixture M/G 25/75. The average mass loss during the 7 days of curing at the room temperature was about 3,7% in case of geopolymer containing 75% of CRT glass and about 5,4% in case of geopolymer containing 50% of CRT glass.

Table 3.9.6 shows the average values of density of samples made of both mixtures for the following curing days. The same samples were weighed every day. The following values of density varies from those one given in Table 3.9.5 since the continues measurement had to be done on different series of samples. The divergence between corresponding values from Table 3.9.5 and Table 3.9.6 did not exceed 3% and can be caused by different level of

compaction. The same dependences in both Tables can be noticed such as that on each day of curing, geopolymer containing 75% of CRT glass has higher density than geopolymer with 50% of CRT glass.

Table 3.9.6: Average density of geopolymer in the following curing days.

Density [kg/m <sup>3</sup> ]	1 day	2 days	3 days	4 days	5 days	6 days	7 days
<b>M/G 25/75</b>	2170	2140	2120	2110	2100	2090	2080
<b>M/G 50/50</b>	2030	2010	1980	1960	1940	1930	1920

Basing on the test of the influence of curing time on mechanical behavior of geopolymer samples made of two mixtures M/G 25/75 and M/G 50/50, the mixture M/G 50/50 has been chosen for the further investigations – for the main research. Samples from series M/G 25/75 achieved considerably lower flexural strength results and, since 7<sup>th</sup> day of curing, lower compressive strength values as well, than samples from series M/G 50/50. Moreover, samples from series M/G 25/75 have shown alarming tendency of the loss of compressive strength in time. Compressive strength decreased by over 16% between 7<sup>th</sup> and 28<sup>th</sup> day of curing. The decrease of compressive strength in time, lower flexural strength, high density and poor workability leading to the cavities in the hardened samples from series M/G 25/75 were the main reasons an Author decided to continue works only on samples made of mixture M/G 50/50.



# CHAPTER 4 (MAIN RESEARCH)

## 4.1 Determination of the influence of curing temperature and curing time on mechanical behavior

### 4.1.1 Preparation of samples

This part of the research has been done on one chosen mixture: M/G 50/50. The main goal was to establish the change of mechanical behavior (flexural and compressive strength and density) of samples cured at room temperature (~20°C) and at 40°C over time. Results presented in the previous subsection 3.9.2 achieved by samples made of mixture M/G 50/50 and cured at 40°C were compared with new results obtained by samples cured at the room temperature. The composition of the chosen mixture is presented in Table 4.1.1 below.

Table 4.1.1: Mixture composition.

Mixture		Metakaolin	CRT glass	Sodium silicate	Sodium hydroxide
<b>M/G 50/50</b>	[kg/m <sup>3</sup> ]	898	898	449	225

Mixture was placed in the prismatic moulds. Samples were cured at two different conditions: 1) all the time at the room temperature with unmolding just before test, 2) for the first 24 hours in climatic chamber at 40°C and then (after unmolding) at the room temperature. Strength tests were performed after 1, 3, 7, 14 and 28 days of curing. In case of samples cured all the time at the room temperature, the additional test after 5 days was performed, since differences in strength in that time interval were significant. The quantity of samples subjected to strength tests after each period of curing varied in dependence of curing regime: 1) regarding geopolymer cured all the time at 20°C – 6 samples were subjected to flexural strength test and 12 to compressive strength test, 2) regarding geopolymer cured for the first 24 hours at 40°C – 3 samples were subjected to flexural strength test and 6 to compressive strength test.

Figure 4.1.1 presents samples cured at different temperatures and different time just before the strength test. Samples cured at 40°C were brighter than samples cured at 20°C independently on the time of curing. As in the case of series of samples 20°C (1) (described in section “3.8 Determination of the influence of curing temperature on mechanical behavior”), samples tested after 1 day (and in relation to this unmolded after 24 hours) were affected by cracks. After several minutes, the surface of samples cured only for 1 day started covering with network of shallow and barely visible cracks (see Figure 4.1.2). While, at the very beginning, just after unmolding, there was no visible difference between samples cured for 1 day and for 28 days with unmolding after 28 days (see comparison in the Figure 4.1.3). One sample from the series demoulded after 24 hours was left in the laboratory for further observations. After 28 days of curing (including the first 24 hours in the mold), the sample was entirely covered with cracks (see Figure 4.1.4). Figure 4.1.5 shows the comparison of the condition of the upper surface of discussed sample after about an hour after demolding and



after 28 days of curing. The appearance of cracks was probably caused by the rapid and excessive shrinkage which took place after contact of not fully hardened samples with the air. The shrinkage started several minutes after demolding (as shown in Figure 4.1.2) and intensified in time (Figures 4.1.4 and 4.1.5). Cracks appearing on the 1 day samples are the evidence that the chemical process inside geopolymer was not fully completed after that time. This theory is confirmed by significantly lower strength achieved by samples after 1 day of curing (flexural and compressive strength results are given in Table 4.1.2 below). The problem of the shrinkage affecting too early demoulded samples has been described more precisely in section “3.8 Determination of the influence of curing temperature on mechanical behavior”.

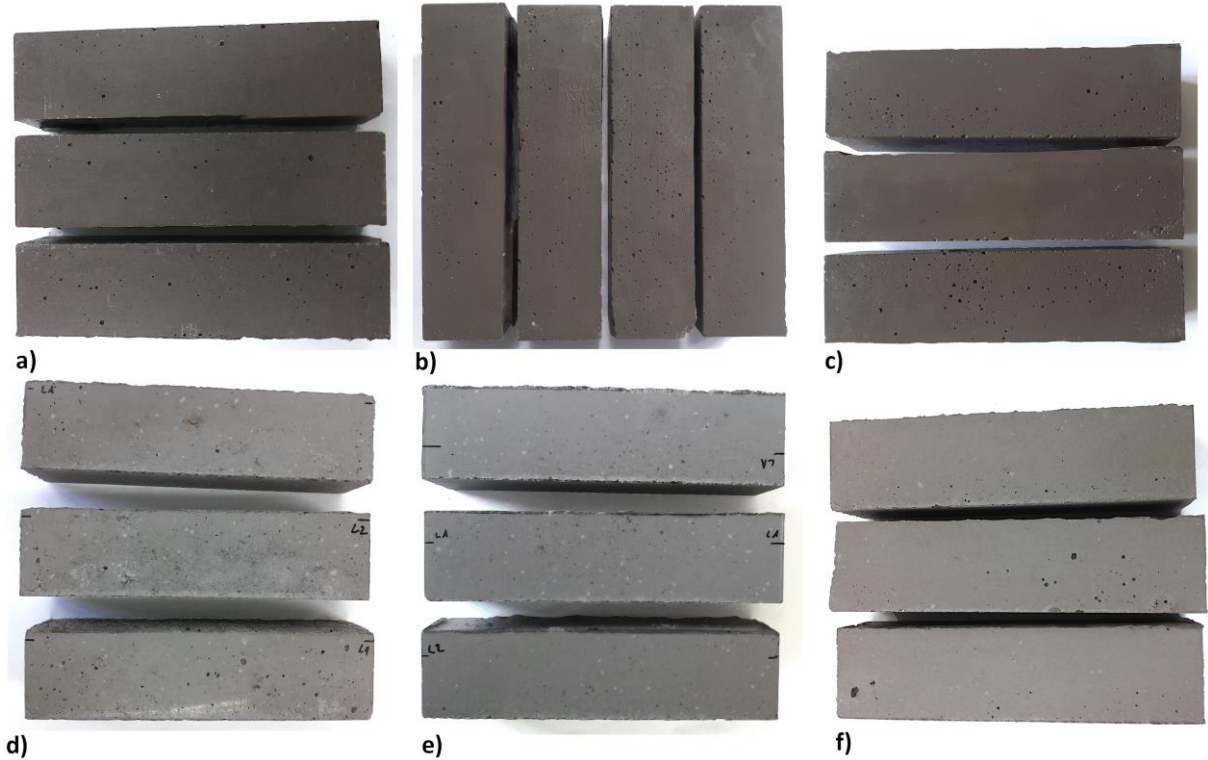


Fig.4.1.1: Samples cured at different temperatures and cured for different time period: a) 20°C, 3 days, b) 20°C, 7 days, c) 20°C, 28 days, d) 40°C, 3 days, e) 40°C, 7 days, f) 40°C, 28 days. The color of samples cured at 20°C (a), b), and c)) was significantly darker than color of samples cured at 40°C (d), e) and f)).

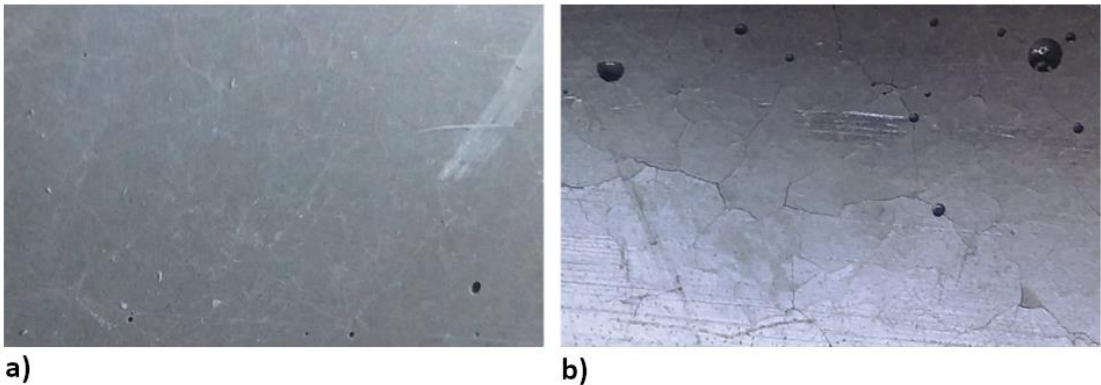


Fig.4.1.2: The surface of samples cured at 20°C and demoulded after 1 day, a) just after demolding, b) 1 hour after demolding.

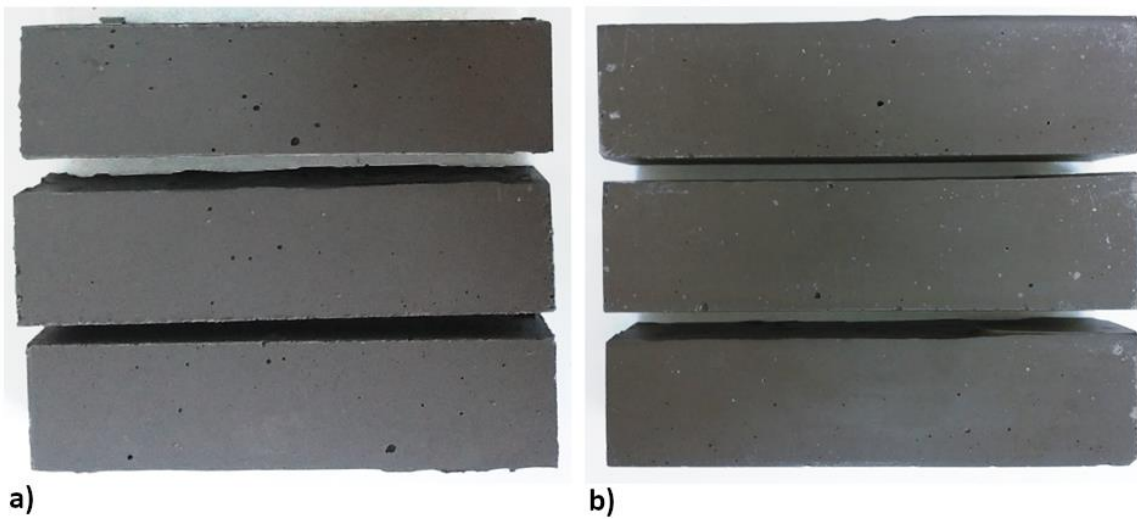


Fig.4.1.3: a) Samples cured at 20°C for 1 day (picture taken only after demolding), b) Samples cured at 20°C for 28 days (picture taken only after demolding). There was no significant difference in color between samples.



Fig.4.1.2: Sample cured at 20°C and demoulded after 24 hours. Picture taken after 27 days of further curing at the room temperature in the laboratory.

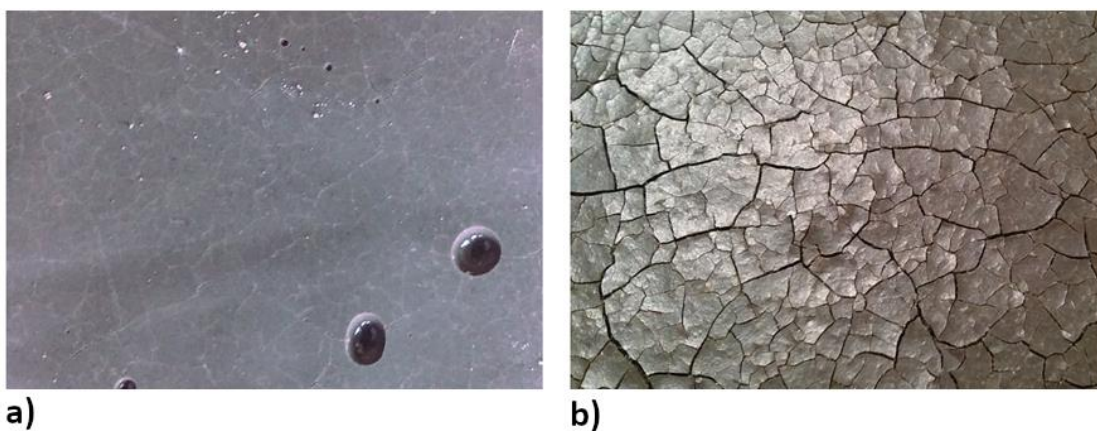


Fig.4.1.3: The upper surface of sample cured at 20°C and demoulded after 24 hours a) picture taken after unmolding (after 24 hours of curing) b) picture taken after 27 days of further curing at the room temperature in the laboratory.

#### 4.1.2 Results

Table 4.1.2 contains all results achieved during the flexural and compressive strength tests.

Table 4.1.2: Flexural ( $f_x$ ) and compressive ( $f_c$ ) strength results.

Mixture			No. 1	No. 2	No. 3	No. 4	No. 5	No. 6	$f_x/f_c$	
20°C	1 day	$f_x$ [MPa]	<del>1,26</del> *	1,09	1,13	1,16	1,14	1,15	0,131	
		$f_c$ [MPa]	7,64	8,87	8,14	8,26	9,13	9,26		
	3 days	$f_x$ [MPa]	2,42	2,94	2,48	2,52	2,88	3,32	0,072	
		$f_c$ [MPa]	36,16	36,59	35,29	36,95	40,63	42,17		
	5 days	$f_x$ [MPa]	2,84	3,48	3,25	4,17	3,99	3,64	0,076	
		$f_c$ [MPa]	48,54	48,81	45,26	49,06	<del>34,62</del> *	43,13		
	7 days	$f_x$ [MPa]	5,61	4,13	4,61	4,42	4,90	4,05	0,088	
		$f_c$ [MPa]	41,92	50,96	42,45	55,42	52,27	55,40		
	14 days	$f_x$ [MPa]	4,91	4,93	<del>5,42</del> *	4,94	5,11	4,89	0,081	
		$f_c$ [MPa]	60,87	60,53	60,57	61,32	<del>64,48</del> *	62,49		
	28 days	$f_x$ [MPa]	5,57	5,09	5,21	4,83	4,97	5,14	0,076	
		$f_c$ [MPa]	67,26	70,17	66,70	67,31	67,74	66,62		
	40°C	1 day	$f_x$ [MPa]	5,13	5,29	4,76	-	-	-	0,109
			$f_c$ [MPa]	42,44	43,51	51,63	44,54	49,13	46,56	
3 days		$f_x$ [MPa]	5,91	4,50	4,99	-	-	-	0,106	
		$f_c$ [MPa]	46,16	49,19	46,15	47,51	49,31	52,48		
7 days		$f_x$ [MPa]	5,55	6,25	6,56	-	-	-	0,113	
		$f_c$ [MPa]	51,63	57,24	56,24	52,32	53,52	53,16		
14 days		$f_x$ [MPa]	5,63	6,45	7,20	-	-	-	0,111	
		$f_c$ [MPa]	61,19	59,46	51,80	56,33	58,76	59,79		
28 days		$f_x$ [MPa]	5,96	5,93	5,91	-	-	-	0,100	
		$f_c$ [MPa]	66,03	54,26	55,84	60,20	58,02	61,34		

\*Result was rejected on the basis of statistical method - elimination of one extreme value.

Samples cured all the time at 20°C were characterized by low early strength (especially after 1 day of curing). Samples cured at 40°C achieved high flexural and compressive strength both after 1 day and 28 days of curing. The highest compressive strength showed samples cured at 20°C for 28 days.

Table 4.1.3 shows standard deviations and coefficients of variation of flexural and compressive strength results presented above, in Table 4.1.2. With the exception of results obtained after 7 and 28 days, samples cured all the time at the room temperature achieved more stable (characterized with smaller coefficient of variation) values of flexural strength. No monotonic correlation between period of curing and variation of results was observed. No strict dependence between conditions of curing and variation of compressive strength results was observed. Samples cured at 20°C achieved significantly more stable values after 14 and 28 days of curing than after shorter curing period.

Table 4.1.3: Standard deviation and coefficient of variation of flexural and compressive strength results.

	Standard deviation [-] (CoV [%])	1 day	3 days	5 days	7 days	14 days	28 days
Flexural strength	Cured at 20°C	0,03 (2,3)	0,35 (12,6)	0,49 (13,6)	0,57 (12,4)	0,09 (1,8)	0,25 (4,9)
	Cured at 40°C	0,27 (5,3)	0,72 (14,0)	-	0,52 (8,5)	0,78 (12,2)	0,03 (0,4)
Compressive strength	Cured at 20°C	0,59 (6,8)	2,74 (7,2)	3,19 (6,8)	5,07 (9,7)	0,90 (1,5)	1,56 (2,3)
	Cured at 40°C	3,53 (7,6)	2,40 (5,0)	-	2,23 (4,1)	3,38 (5,8)	4,23 (7,1)

The brittleness of samples was increasing along with the increase of curing time. Figure 4.1.6 presents the appearance of samples after flexural strength test. It was noticed that the crack was wider in samples cured for a longer time.

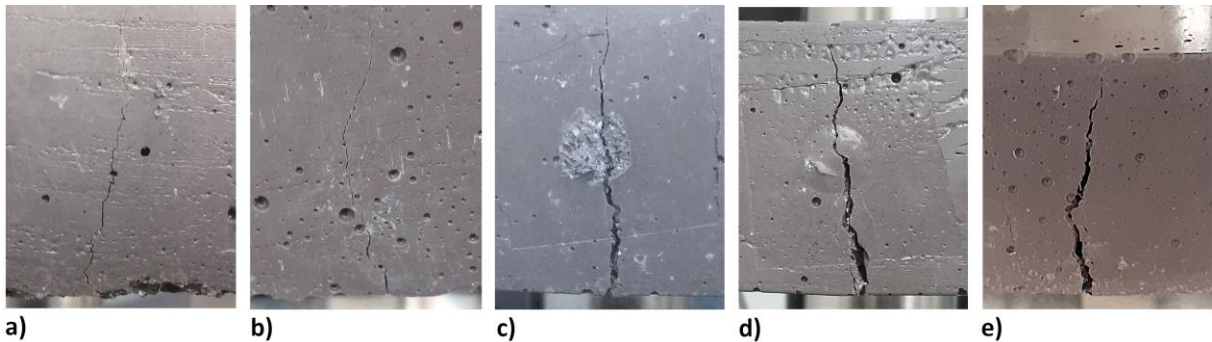


Fig.4.1.4: Crack formed in the middle of the beam span (below the concentrated force) after flexural strength test. Sample cured for: a) 1 day, b) 3 days, c) 7 days, d) 14 days, e) 28 days. There was no significant difference in color between samples. The difference visible in pictures has been caused by the difference in lighting.

### 4.1.3 Analysis

Results of this part of the research are presented in Figure 4.1.7 and Figure 4.1.8. Each bar represents average value of compressive or flexural strength obtained by samples from mixture M/G 50/50 cured at different conditions and tested after 1, 3, 7, 14 or 28 days (samples cured all the time at the room temperature were additionally tested after 5 days).

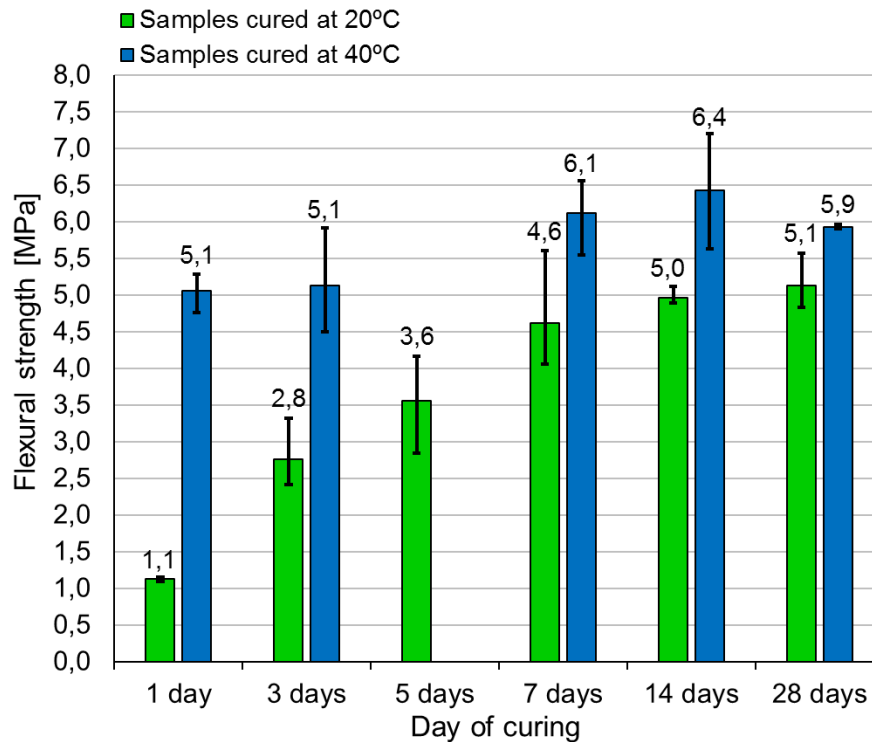


Fig.4.1.5: Change of the flexural strength of geopolymer made of mixture M/G 50/50 and cured at different temperatures over time.

The flexural strength of geopolymer cured all the time at the room temperature increases monotonically over time. Early strength of material cured at 20°C was very low. The biggest and more rapid increment was observed between the first and the seventh day of curing. Flexural strength on the third day more than doubled one-day flexural strength. The further increase (between third and seventh day) become slower and almost linear. After 7 days of curing the increase of flexural strength stabilized. The difference in strength between samples tested after 14 and 28 days was negligible.

Geopolymer cured for the first 24 hours at elevated temperature 40°C gains the flexural strength quicker than geopolymer cured all the time at the room temperature. Only after one day of curing geopolymer achieves flexural strength close to the final one. There is no difference between average flexural strength on the first and on the third day. Then, strength increases slightly. Long term flexural strength (measured after 28 days) was a little bit smaller than strength after 7 and 14 days. In contrast, results obtained after 28 days were more stable than all other values of flexural strength. Independently on time of curing, the flexural strength of geopolymer cured at 40°C was higher than strength of geopolymer cured all the time at 20°C although, the difference was decreasing in time.



Figure 4.1.8 presents results of compressive strength tested after different periods of time.

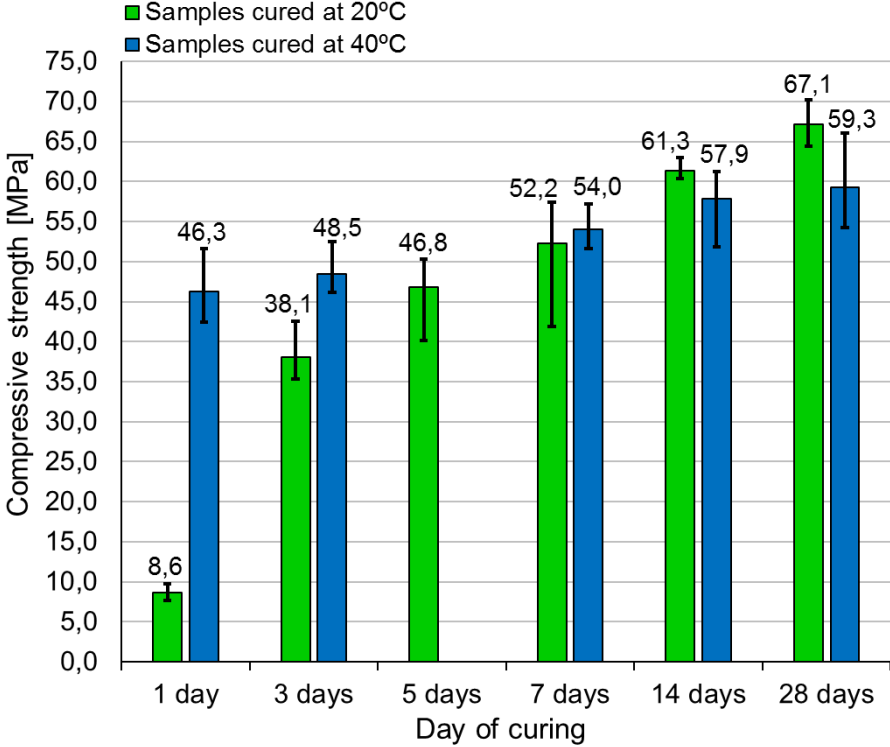


Fig.4.1.6: Change of the compressive strength of geopolymer made of mixture M/G 50/50 and cured at different temperatures over time.

As in the case of flexural strength, the compressive strength of samples cured all the time at 20°C increases monotonically in time. The early compressive strength is low (8,6 MPa). Once again, the biggest growth was observed between first and third day of curing. The compressive strength increased almost 4,5 times in that period. The further increase is gradual and almost linear. Also, as in the case of flexural strength, geopolymer cured at 40°C gains compressive strength much more quickly than geopolymer cured at the room temperature. Only after one day of curing geopolymer achieves high compressive strength (46,3 MPa). The increase of compressive strength is monotonic. Until the 14 day the increase is significant. The difference in compressive strength between 14 and 28 day is negligible.

Until the seventh day of curing, the compressive strength of geopolymer cured at 40°C is higher than of geopolymer cured at 20°C. At the beginning the divergence is high (almost 440% after 1 day of curing) but it is disappearing in time. Since fourteenth day, the strength of geopolymer cured at 20°C surpass the strength of geopolymer cured at 40°C (by 5,9% after 14 days and 13,2% after 28 days of curing).

The change of  $f_x/f_c$  ratio of geopolymer cured at the room temperature and the elevated temperature over time, has been presented in Figure 4.1.9.

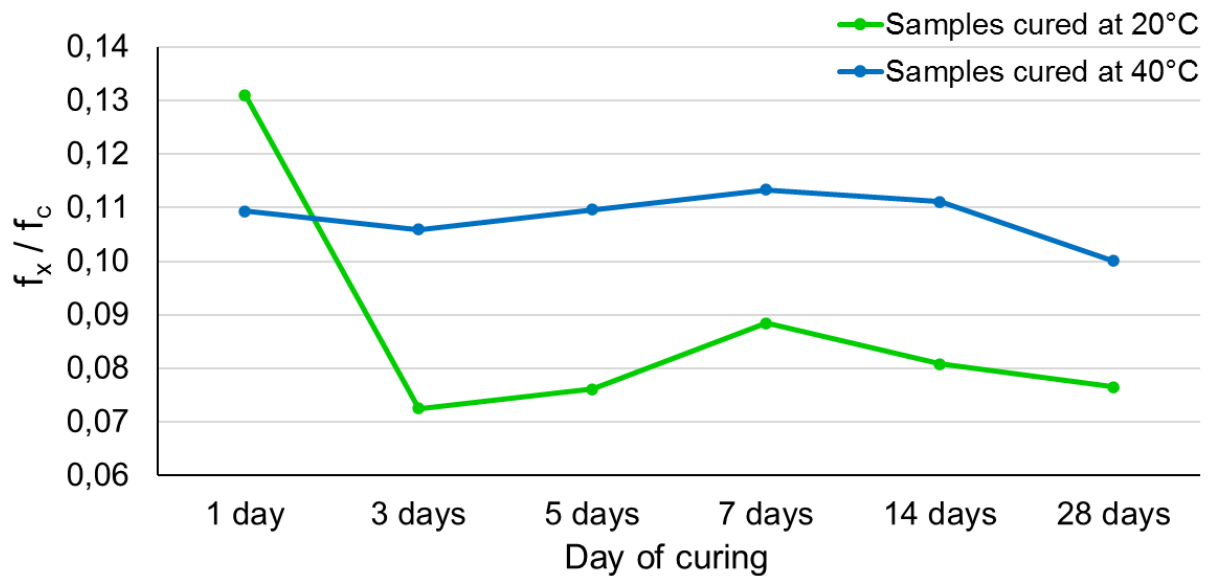


Fig.4.1.7: Change of the  $f_x/f_c$  ratio of geopolymer made of mixture M/G 50/50 and cured at different temperatures over time.

The general pattern of  $f_x/f_c$  change over time is the same for geopolymer cured at 20°C and 40°C, however, the amplitudes are much bigger in case of geopolymer cured at the room temperature. In case of geopolymer cured at both conditions,  $f_x/f_c$  ratio at 3<sup>rd</sup> day is lower than at the 1<sup>st</sup> day of curing. Then,  $f_x/f_c$  ratio increases monotonically reaching the peak value at 7<sup>th</sup> day and then decreases again. The highest value of  $f_x/f_c$  ratio was observed at 1<sup>st</sup> day in case of geopolymer cured at 20°C and at 7<sup>th</sup> day for geopolymer cured at 40°C. The lowest value of  $f_x/f_c$  ratio was obtained after 3 days of curing by geopolymer cured at 20°C. The same mixture cured at 40°C achieved minimum  $f_x/f_c$  ratio after 28 days. Except of 1<sup>st</sup> day, during the whole curing period, geopolymer cured at 40°C was characterized by higher  $f_x/f_c$  ratio than the one cured at 20°C.

Rovnanik [334] reports the constant decrease of  $f_x/f_c$  ratio of geopolymer cured at 40°C for the following curing days. The maximum  $f_x/f_c$  ratio in the first day of curing was equal to 0,22. The smallest, at 28<sup>th</sup> day of curing – 0,18. By contrast, in case of geopolymer cured at 20°C,  $f_x/f_c$  ratio decreased between 1<sup>st</sup> and 3<sup>rd</sup> day and then raised on the 7<sup>th</sup> day and decreased again at 28<sup>th</sup> day which is similar behavior to those one showed by geopolymer in this Thesis. The maximum  $f_x/f_c$  ratio was 0,23 and the smallest – 0,19. All values of  $f_x/f_c$  ratio were higher than in this Thesis.

Table 4.1.4 includes the average density of samples cured in different conditions, in the following curing days.

Table 4.1.4: Average density of geopolymer made of mixture M/G 50/50 in the following curing days.

Density [kg/m <sup>3</sup> ]	1 day	3 days	5 days	7 days	14 days	28 days
<b>Cured at 20°C</b>	2060	2080	2070	2060	2080	2090
<b>Cured at 40°C</b>	1970	1930	-	1920	1900	1870



Density of geopolymer cured at 40°C decreases in time. The biggest drop in density was registered between the first and third day of curing. In case of geopolymer cured all the time at the room temperature, there is no dependence between density and period of curing. All values are close to each other (small differences can be caused for example by different level of compaction). Observations connected with geopolymer cured at 20°C and unmolded just before strength test indicate that the significant loss of density take place during curing without form, cover or any other protection. Samples cured all the time at the room temperature were protected by form and cover until the test day and as a result had no access to air while samples cured at 40°C were unmolded after 24 hours of curing. Although, the considerable difference in one-day density between geopolymer cured at 20°C and at 40°C indicates that significant loss of density may be also caused by higher curing temperature even though, the samples were covered during this time. Generally, independently on the period of curing, samples cured at lower temperature had greater density than samples cured at elevated temperature.

Generally, a significant number of researches reports that strength of geopolymer cured at elevated temperature is much higher than of geopolymer cured at the room temperature during the first days, but then the difference is vanishing and even the dependence can change [47], [327], [334], [338], [343]. The fact that curing at elevated temperature increases significantly strength of geopolymer in the first days may be crucial for some applications where the rapid gain of strength and quick demolding is required. However, both the observations made by an Author and by other scientists indicates, that the difference in strength between geopolymer cured at the ambient temperature and at elevated temperature is vanishing in time. Moreover, some studies [334], [338] (including observations made within this Thesis) report that strength of geopolymer cured at ambient temperature surpasses strength of geopolymer cured at elevated temperature after long time of curing (14-28 days). Additionally, curing at ambient temperatures is more ecological, easier and cheaper than curing at elevated temperature, although, the need of keeping material in moulds for longer period is the negative aspect of that method of curing. After considering all in favor and against, Author decided to choose curing at ambient temperature as an optimal for further tests. The better compressive strength after 14 and 28 days of curing, the facility of this solution together with the ecological and economical aspects were the main reasons why Author decided to continue tests on samples cured all the time at the ambient temperature.

## 4.2 Determination of the influence of sodium hydroxide concentration on mechanical behavior

### 4.2.1 Preparation of samples

The main goal of the test was to determine the influence of the concentration of sodium hydroxide on flexural strength, compressive strength and density of the geopolymer. Samples were made of mixture M/G 50/50, cured at the room temperature and demoulded after 7 days of curing. The only factor distinguishing the following mixtures was concentration of sodium hydroxide which ranged from 6 mol/L to 12 mol/L. The sodium hydroxide of appropriate concentration was prepared minimum 24 hours before preparation of the samples. During preparation of the samples it was observed that workability of a mixture decreases slightly with the increase of NaOH concentration.

Four prismatic samples were made of each mixture. No external visual difference between samples activated with NaOH of different concentration was noticed (compare Figure 4.2.1). Four samples from each series were subjected to flexural strength test. Eight halves of prismatic samples were subjected to compressive strength test.

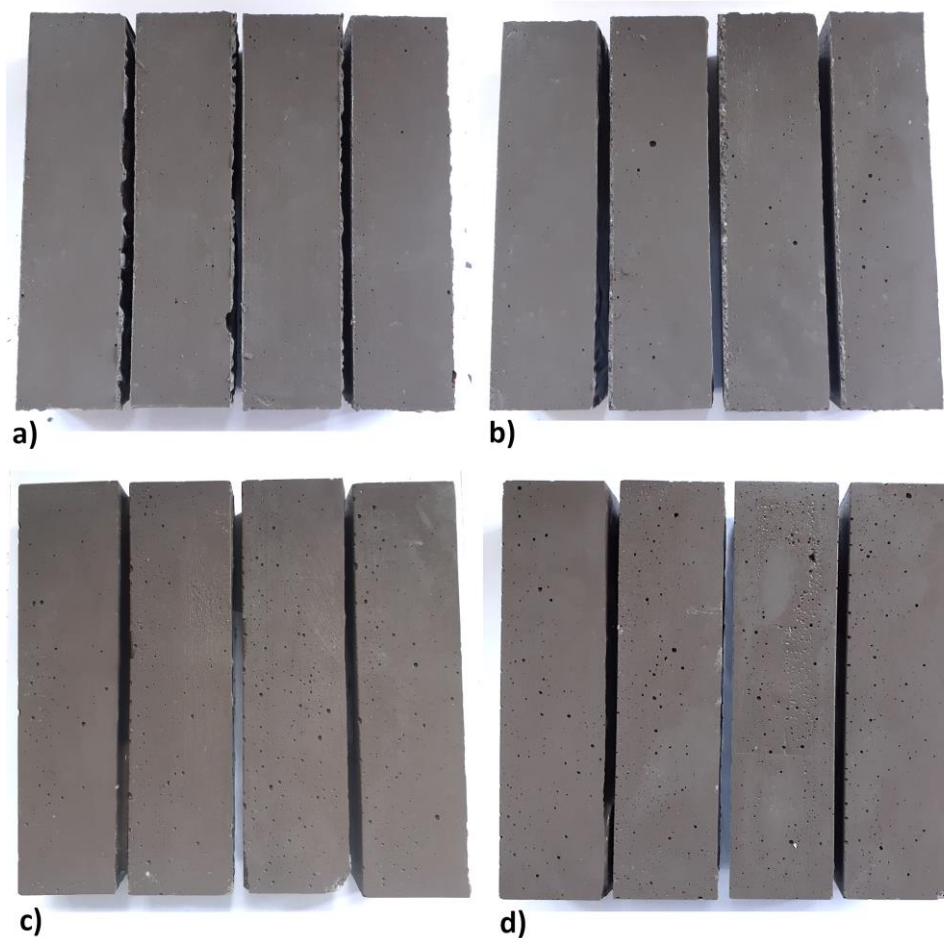


Fig.4.2.1: Beams before strength tests. Series containing NaOH of concentration a) 6 mol/L, b) 8 mol/L, c) 10 mol/L, d) 12 mol/L.

#### 4.2.2 Results

Table 4.2.1 presents the flexural and compressive strength tests results.

Table 4.2.1: Flexural and compressive strength results.

Mixture		No. 1	No. 2	No. 3	No. 4	$f_x/f_c$
<b>NaOH 6M</b>	$f_x$ [MPa]	4,32	4,06	4,56	4,88	0,126
	$f_c$ [MPa]	35,51	35,50	35,94	34,12	
		35,54	33,62	37,66	34,48	
<b>NaOH 8M</b>	$f_x$ [MPa]	5,96	5,84	5,63	5,63	0,146
	$f_c$ [MPa]	38,95	37,88	32,79	42,21	
		44,15	35,50	36,63	48,42	
<b>NaOH 10M</b>	$f_x$ [MPa]	6,63	5,96	5,67	5,56	0,106
	$f_c$ [MPa]	57,14	55,30	55,92	53,66	
		58,04	58,12	53,96	55,87	
<b>NaOH 12M</b>	$f_x$ [MPa]	5,53	4,98	4,78	5,03	0,089
	$f_c$ [MPa]	60,34	55,21	54,65	55,86	
		60,49	56,32	56,48	56,93	

Samples activated with sodium hydroxide of concentration 6 mol/L showed lower flexural and compressive strength than the rest of samples. Samples activated with sodium hydroxide of concentration 10 and 12 mol/L achieved considerably higher compressive strength than samples containing 8 and 10 mol/L NaOH.

Standard deviations and coefficients of variation of values from Table 4.2.1 are given in Table 4.2.2. For all series of results (except of compressive strength of samples activated with 8 mol/L NaOH), coefficient of standard deviation is below 10%. No monotonic dependence between NaOH molarity and stability of results was registered.

Table 4.2.2: Standard deviation and coefficient of variation of compressive strength results.

Standard deviation [-] (CoV [%])	<b>NaOH 6M</b>	<b>NaOH 8M</b>	<b>NaOH 10M</b>	<b>NaOH 12M</b>
<b>Flexural strength</b>	0,35 (7,8)	0,16 (2,8)	0,48 (8,1)	0,32 (6,3)
<b>Compressive strength</b>	1,26 (3,6)	5,08 (12,8)	1,69 (3,0)	2,21 (3,9)

Samples activated with sodium hydroxide of concentration 6 mol/L were characterized with less brittle failure than the rest of samples. The crack in broken sample containing NaOH of concentration 6 mol/L was much smaller than crack appearing in samples containing activators of higher concentration (Figure 4.2.2). Much smaller difference in the model of failure between samples containing NaOH of concentrations 8, 10 and 12 mol/L was noticed.



Photography of sample activated with 12 mol/L, cracked after flexural strength test was not clear and therefore it was not included in Figure 4.2.2.

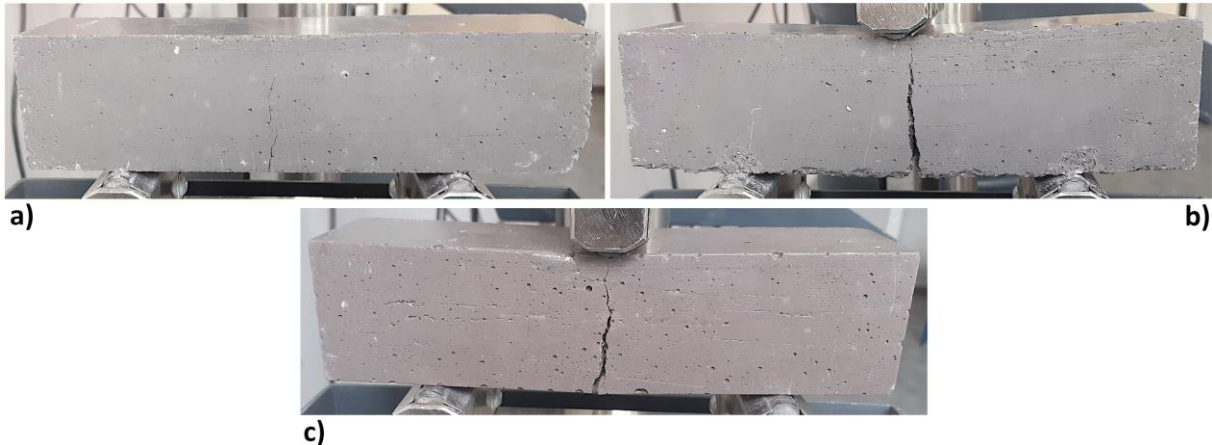


Fig.4.2.2: Beams cracked after flexural strength test. Sample containing NaOH of concentration a) 6 mol/L, b) 8 mol/L, c) 10 mol/L.

### 4.2.3 Analysis

Figure 4.2.3 presents flexural and compressive strength obtained by geopolymers of activated with sodium hydroxide of different concentration.

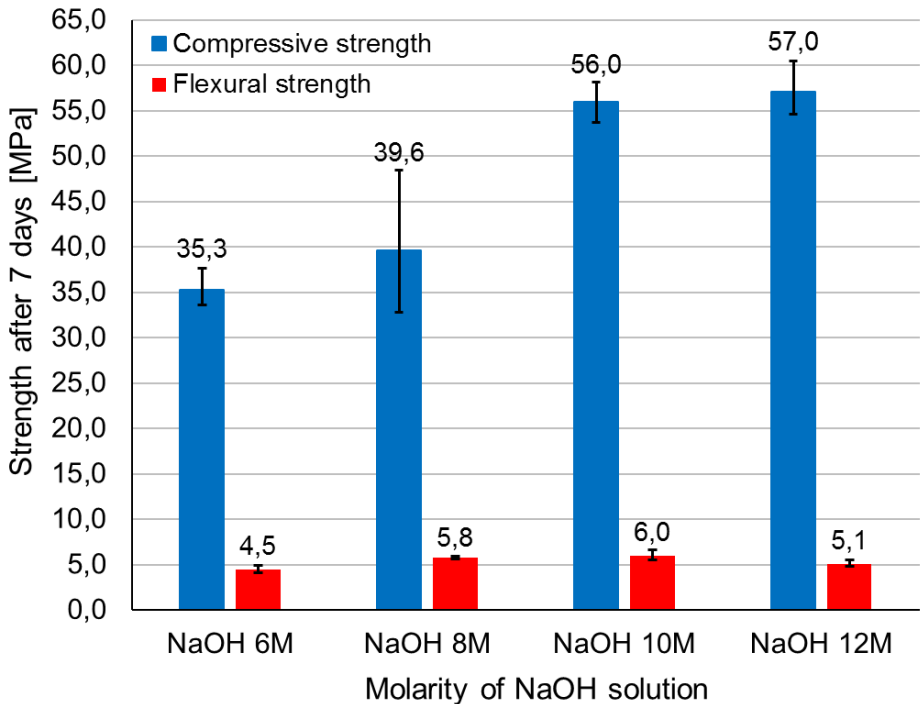


Fig.4.2.3: Seventh days compressive and flexural strength of geopolymer made of mixtures activated with NaOH of different concentration.

According to results presented in Figure 4.2.3, compressive strength increases monotonically with the increase of sodium hydroxide molarity. The greatest growth of compressive strength (over 41 %) was registered between samples activated with 8 mol/L and

10 mol/L NaOH. The further rise of the strength is almost negligible. Flexural strength also increases with the increase of NaOH concentration but only within values 6 mol/L and 10 mol/L. The sudden drop of strength of samples activated with 12 mol/L NaOH was observed. In the case of flexural strength, the biggest increase (over 28%) was observed between samples activated with 6 mol/L and 8 mol/L NaOH.

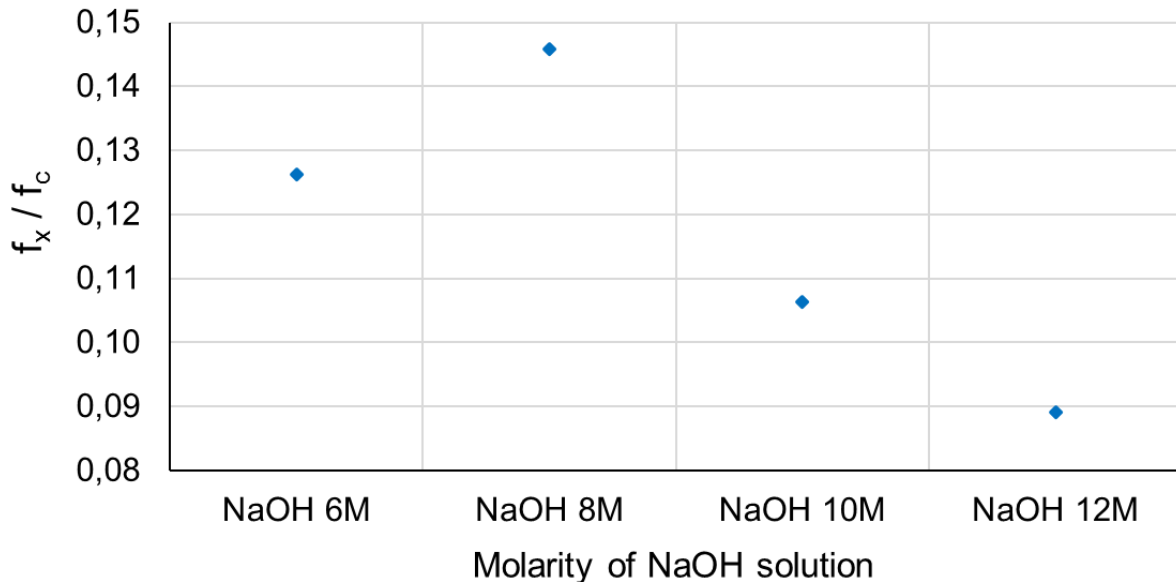


Fig.4.2.4: The  $f_x/f_c$  ratio of geopolymer of different NaOH concentration.

According to the graph shown in Figure 4.2.4, the  $f_x/f_c$  decreases along with the increase of activator concentration with exception of the lowest NaOH concentration. Geopolymer with NaOH of 8M was characterized by the highest value of  $f_x/f_c$  ratio. The difference between  $f_x/f_c$  ratio of geopolymer with NaOH 8M and 10M was significantly higher than between NaOH 6M and 8M or between NaOH 10M and 12M.

Wang et al. [108] does not report the monotonic dependence between NaOH concentration and  $f_x/f_c$  ratio. The lowest value of  $f_x/f_c$  ( $\sim 0,40$ ) was obtained by geopolymer containing NaOH of concentration 4M, while the highest value ( $\sim 0,94$ ) by samples with 8M NaOH. The  $f_x/f_c$  ratio increases along with the increase of NaOH from 4M to 8M and then decrease for 10 and 12M. Such behavior is convergent with the one presented in Figure 4.2.4. However, all values of  $f_x/f_c$  are much higher than reported in this Thesis.

Table 4.2.3 contains density of geopolymer activated with NaOH of different concentration. Generally, density increases along with the increase of NaOH concentration within 6-10 mol/L, although, the differences are small. Samples containing NaOH of concentration 12 mol/L have shown slightly smaller density than samples activated with 10 mol/L activator.

Table 4.2.3: Average density of geopolymer activated by NaOH of different concentrations.

	NaOH 6M	NaOH 8M	NaOH 10M	NaOH 12M
Density [ $\text{kg/m}^3$ ]	1990	2010	2030	2020

According to the results, it was decided that 10 mol/L is an optimal concentration for metakaolin-based geopolymer with addition of the CRT glass. The compressive strength of geopolymer activated with 10 mol/L NaOH is substantially greater than strength of samples containing activator of lower molarities. The flexural strength was the highest (6,0 MPa) within all series of samples. Besides, the further growth of the molarity of the activator does not make significant profits. From the economic and environmental point of view, the lowest concentration of sodium hydroxide the better. Although, the mechanical behavior must not be neglected during such consideration. It was decided that molarity 10 mol/L brings the biggest benefits in strength being still acceptable from the other perspectives. Therefore, the rest of tests has been carried on geopolymer activated with sodium hydroxide of concentration 10 mol/L.

### *4.3 Determination of the influence of CRT glass particle size on mechanical behavior*

#### **4.3.1 Preparation of samples**

The main goal of the test was to determine the influence of the CRT glass particle size on flexural strength, compressive strength and density of the geopolymer. Samples were made of mixture M/G 50/50, activated with sodium hydroxide of concentration 10 mol/L, cured at the room temperature and demoulded after 7 days of curing. The CRT glass size was the differentiating factor. Before preparation of all mixtures, CRT glass was divided with the use of sieves onto two batches. The first one contained fractions < 0,5 mm while the second one contained fractions ranging from 0,5 mm to 4 mm. Compressive and flexural strength of samples containing CRT glass of size < 0,5 mm and 0,5 – 4 mm were compared with results obtained by samples from the previous tests, characterized by the same composition and curing regime but containing CRT glass of size < 4 mm. Three various CRT glass fractions used in the test are presented in Figure 4.3.1.



Fig.4.3.1: CRT glass of grain fraction a) < 0,5 mm, b) < 4 mm, c) 0,5 – 4 mm.

Four prismatic beams from each series were subjected to flexural strength test. Eight samples were subjected then to compressive strength test. No evident external visual

difference visible with the naked eye was noticed between samples containing CRT glass of different particle size (Figure 4.3.2).

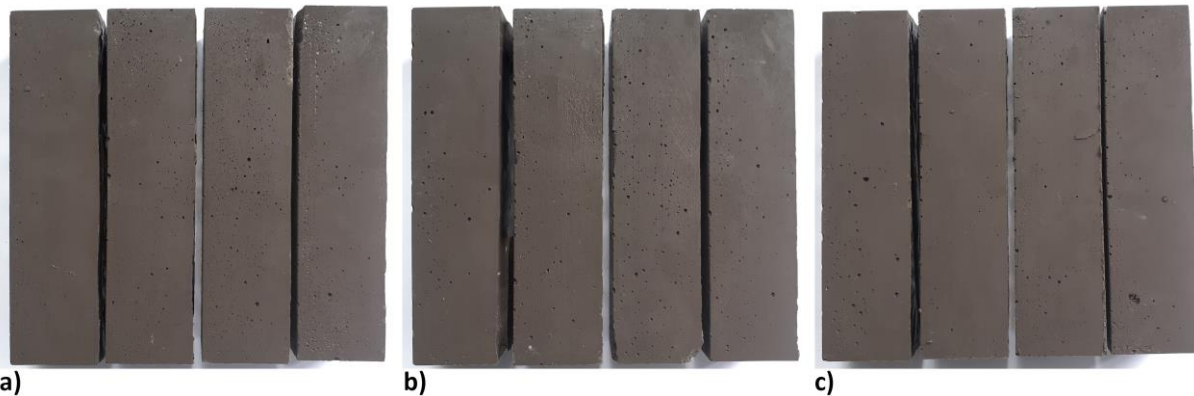


Fig.4.3.2: Samples containing CRT glass of grain fraction a) < 0,5 mm, b) < 4 mm, c) 0,5 – 4 mm.

#### 4.3.2 Results

Results achieved during the flexural and compressive strength tests are shown in Table 4.3.1. All samples achieved approximately similar flexural and compressive strength results. It is worth emphasizing that all results obtained during that test were relatively high.

Table 4.3.1: Flexural and compressive strength results

Mixture		No. 1	No. 2	No. 3	No. 4	$f_x/f_c$
<b>&lt; 0,5 mm</b>	$f_x$ [MPa]	5,79	<del>4,41</del> *	5,57	5,59	0,105
	$f_c$ [MPa]	56,14	53,62	53,08	53,78	
		54,11	54,22	52,13	53,43	
<b>&lt; 4 mm</b>	$f_x$ [MPa]	6,63	5,96	5,67	5,56	0,106
	$f_c$ [MPa]	57,14	55,30	55,92	53,66	
		58,04	58,12	53,96	55,87	
<b>0,5-4 mm</b>	$f_x$ [MPa]	6,07	4,49	4,42	5,22	0,091
	$f_c$ [MPa]	<del>61,01</del> *	56,79	54,48	54,03	
		57,50	55,18	55,14	56,95	

\*Result was rejected on the basis of statistical method - elimination of one extreme value.

Table 4.3.2 contains standard deviations and coefficients of variation of flexural and compressive strength results presented in Table 4.3.1. Samples with aggregate of size < 0,5 mm obtained more stable flexural and compressive strength results than samples from two other series. Compressive strength results were generally more stable than flexural strength results. No other dependence between stability of results and CRT glass size were observed.

Table 4.3.2: Standard deviation and coefficient of variation of flexural and compressive strength results.

Standard deviation [-] (CoV [%])	< 0,5 mm	< 4 mm	0,5 – 4 mm
<b>Flexural strength</b>	0,12 (2,1)	0,48 (8,1)	0,77 (15,2)
<b>Compressive strength</b>	1,15 (2,1)	1,69 (3,0)	1,35 (2,4)

No significant difference in the failure mode of samples containing different fractions of CRT glass was observed. The crack appearing in the moment of failure during flexural strength test was slightly smaller in samples containing CRT glass particles of the largest size (0,5 – 4 mm) what is visible in Figure 4.3.3.

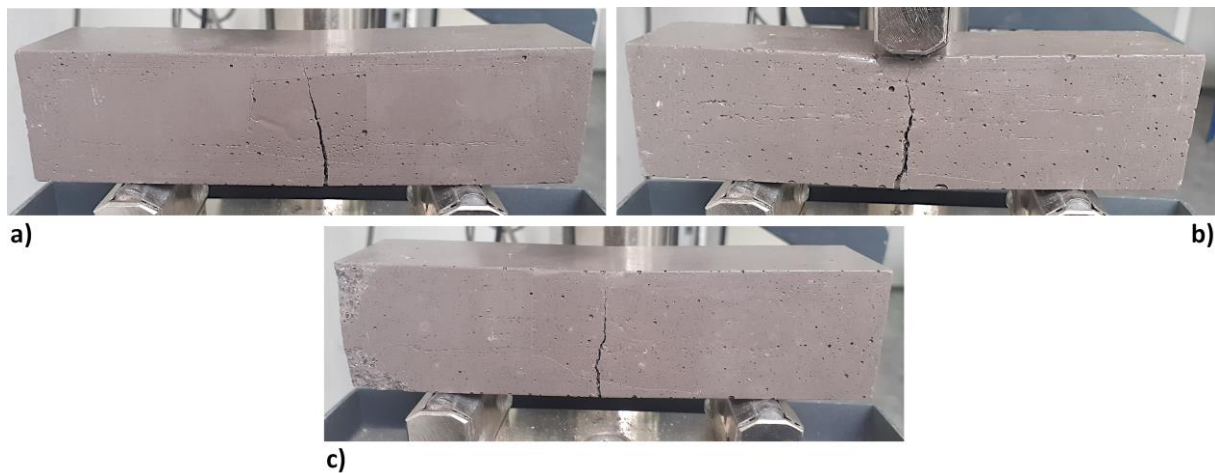


Fig.4.3.3: Beams cracked after flexural strength test. Sample containing CRT glass of fraction a) < 0,5 mm, b) < 4 mm, c) 0,5 – 4 mm.

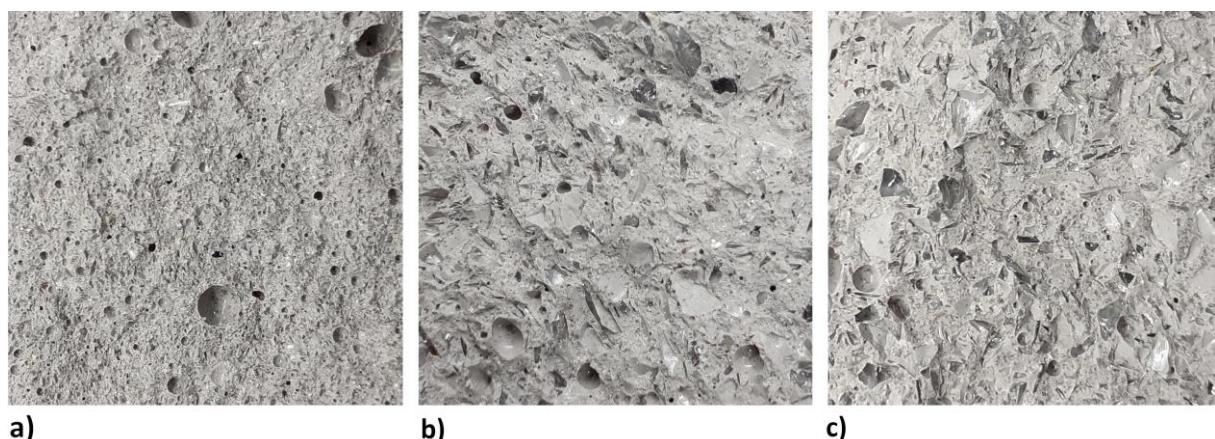


Fig.4.3.4: Cross-section of a broken sample containing CRT glass of size a) < 0,5 mm, b) < 4 mm, c) 0,5 – 4 mm. Picture taken 7 days after strength test.

Figure 4.3.4 presents the cross section of samples containing CRT glass of different size range. Photographs were taken 7 days after strength tests. The biggest visual difference can

be noticed between cross section of sample containing only the particles of size less than 0,5 mm (Figure 4.3.4 a)) and samples with bigger glass particles (Figures 4.3.4 b) and c)). In the case of samples containing CRT glass of range < 4 mm (Figure 4.3.4 b)) and 0,5-4 mm (Figure 4.3.4 c)), the glass particles are visible with the naked eye in contrary to section of samples containing glass particles smaller than 0,5 mm (Figure 4.3.4 a)). In turn, air cavities are much more visible in cross sections of samples containing glass particles of size smaller than 0,5 mm (Figure 4.3.4 a)).

Figure 4.3.5 as well presents the cross section of samples containing CRT glass of different size range. Photographs were taken just after flexural strength tests, so color of samples is much darker than in Figure 4.3.4, because of water which had no time to escape. What is more, the background for those photographs was brighter than in case of Figure 4.3.4, what resulted in deepened difference in color. Figure 4.3.5 much better than Figure 4.3.4 presents the difference between cross section of samples containing CRT glass of size < 4 mm and of samples containing glass particles of size 0,5 – 4 mm. The areas between big CRT glass particles in section of samples containing the whole range of glass particles (Figure 4.3.5 b)) is similar to section of samples containing only particles smaller than 0,5 mm (Figure 4.3.5 a)). By contrast, in samples containing CRT glass of size 0,5-4 mm (Figure 4.3.5 c)), area between big particles is plainer.

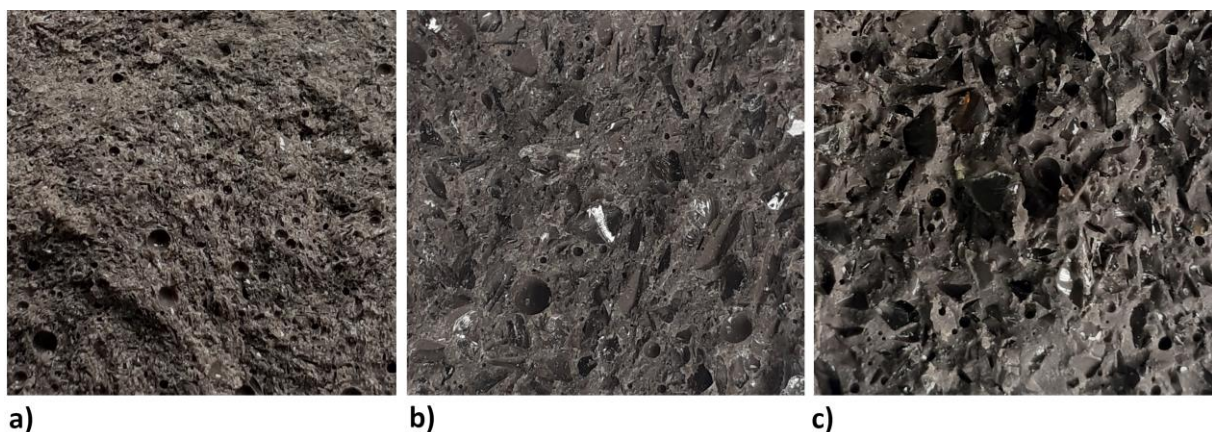


Fig.4.3.5: Cross-section of a broken sample containing CRT glass of size a) < 0,5 mm, b) < 4 mm, c) 0,5 – 4 mm. Picture taken immediately after flexural strength test.

#### 4.3.3 Analysis

Figure 4.3.6 presents flexural and compressive strength obtained by geopolymers containing CRT glass of different size. Samples containing smaller fractions of CRT glass (< 0,5 mm) than the other ones, achieved the lowest compressive strength. By contrast, samples containing CRT glass ranging from 0,5 to 4 mm achieved the lowest flexural strength. In general, differences between results from different series were rather small. The biggest difference between compressive strength results was equal to 4% while the biggest difference in flexural strength results was equal to 17,6%. It was concluded that particle size distribution of CRT glass has no significant influence on flexural and compressive strength. Figure 4.3.7 presents the  $f_x/f_c$  ratio for geopolymer containing CRT glass of different size.

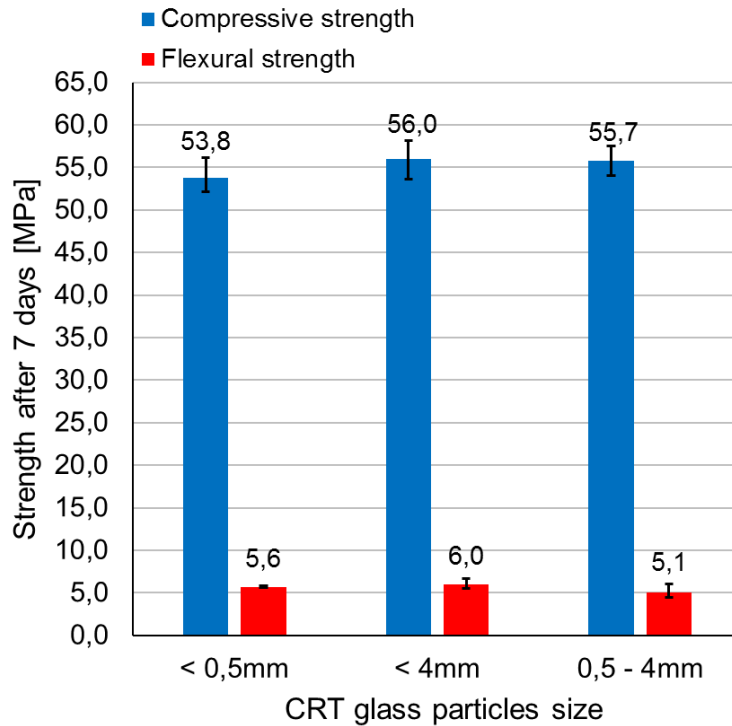


Fig.4.3.6: Seventh days compressive and flexural strength of geopolymer made of mixtures containing CRT glass of different particle's size.

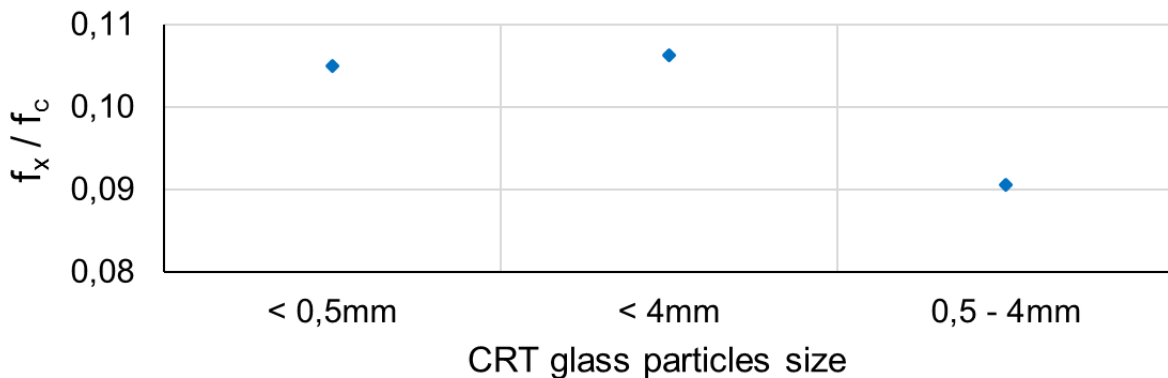


Fig.4.3.7: The  $f_x/f_c$  ratio of geopolymer made of mixtures containing CRT glass of different particle's size.

The highest  $f_x/f_c$  ratio value achieved geopolymer containing CRT glass particles of size < 4 mm while the lowest value has shown geopolymer containing only particles between 0,5 mm and 4 mm. Among two mixtures containing CRT glass segregated with the size (< 0,5 mm and 0,5-4 mm), the  $f_x/f_c$  ratio decreased along with the increase of aggregate size. The differences in the  $f_x/f_c$  ratios of geopolymer made of the following mixtures were small.

Adhikary et al. [344] reports a decrease of  $f_x/f_c$  ratio along with the decrease of glass particles in lightweight concrete. The maximum value of  $f_x/f_c$  ratio (0,31) was reached by samples containing glass particles of size 1-2 mm while the smallest ratio (0,20) by samples with particles of size 0,01-0,3 mm. Such dependence is not convergent with the one observed within this Thesis.

According to data presented in Table 4.3.3, density increases with a growth of CRT glass particles size. The smallest density had samples containing only CRT glass particles not greater than 0,5 mm while samples containing only glass particles of size above 0,5 mm occurred to have the highest density.

Table 4.3.3: Average density of geopolymer containing CRT glass of different size.

	< 0,5 mm	< 4 mm	0,5 – 4 mm
Density [kg/m <sup>3</sup> ]	1980	2030	2070

Considering results achieved during the test on the influence of CRT glass grading on mechanical behavior, it was decided, that the optimal CRT glass particle size range is < 4 mm. Samples containing the full range of CRT glass particles sizes obtained the highest compressive and flexural strength. Admittedly, the density of could be limited with the reduction of CRT glass particle size, but it implies not negligible reduction of strength. Moreover, application of full range of CRT glass particle size do not require any additional pretreatment of that material and, what is also important, gives possibility to recycle more waste. It gives economic and environmental benefits and limits an effort which has to be put into the preparation process. It was decided that CRT glass of size < 4 mm will be used in the future tests.

#### 4.4 Determination of the change of mechanical behavior over time

##### 4.4.1 Preparation of samples

The main goal of the test was to establish the long-term mechanical behavior of metakaolin-based geopolymer with CRT glass. Results previously presented in section “4.1 Determination of the influence of curing temperature and curing time on mechanical behavior” were completed with flexural and compressive strength tested after 56 and 112 days of curing. Test was conducted on samples made of the one chosen mixture M/G 50/50. Each series consisted of 6 prismatic samples of dimensions 40 x 40 x 160 mm. Geopolymer was cured all the time at the room temperature. Samples were demoulded just before the strength test except of those one tested after 56 and 112 days which were demoulded after 28 days and kept in the laboratory for the rest of time (until the testing). Six samples were subjected to flexural strength test, 12 samples were subjected to compressive strength test.

##### 4.4.2 Results

Table 4.4.1 presents the results achieved during the flexural and compressive strength tests. Samples cured for 1 day achieved considerably lower strength values than samples cured longer. The difference was the most visible in case of compressive strength. Long-term cured samples (28, 56 and 112 days) were generally characterized by very high compressive strength.

Table 4.4.1: Flexural ( $f_x$ ) and compressive ( $f_c$ ) strength results

Mixture		No. 1	No. 2	No. 3	No. 4	No. 5	No. 6	$f_x/f_c$
<b>1 day</b>	$f_x$ [MPa]	<del>1,26</del> *	1,09	1,13	1,16	1,14	1,15	0,131
	$f_c$ [MPa]	7,64	8,87	8,14	8,26	9,13	9,26	
<b>3 days</b>	$f_x$ [MPa]	2,42	2,94	2,48	2,52	2,88	3,32	0,072
	$f_c$ [MPa]	36,16	36,59	35,29	36,95	40,63	42,17	
<b>5 days</b>	$f_x$ [MPa]	2,84	3,48	3,25	4,17	3,99	3,64	0,076
	$f_c$ [MPa]	48,54	48,81	45,26	49,06	<del>34,62</del> *	43,13	
<b>7 days</b>	$f_x$ [MPa]	5,61	4,13	4,61	4,42	4,90	4,05	0,088
	$f_c$ [MPa]	41,92	50,96	42,45	55,42	52,27	55,40	
<b>14 days</b>	$f_x$ [MPa]	4,91	4,93	<del>5,42</del> *	4,94	5,11	4,89	0,081
	$f_c$ [MPa]	60,87	60,53	60,57	61,32	<del>64,48</del> *	62,49	
<b>28 days</b>	$f_x$ [MPa]	5,57	5,09	5,21	4,83	4,97	5,14	0,076
	$f_c$ [MPa]	67,26	70,17	66,70	67,31	67,74	66,62	
<b>56 days</b>	$f_x$ [MPa]	6,03	6,34	<del>6,73</del> *	6,17	6,13	6,14	0,086
	$f_c$ [MPa]	67,30	71,62	64,66	73,41	75,96	77,89	
<b>112 days</b>	$f_x$ [MPa]	5,96	6,54	6,48	6,46	7,18	7,15	0,094
	$f_c$ [MPa]	68,53	71,42	67,46	71,82	72,54	70,48	
		71,56	70,78	68,60	70,13	70,96	69,89	

\*Result was rejected on the basis of statistical method - elimination of one extreme value.

Table 4.4.2 includes standard deviations and coefficients of variation of values presented in Table 4.4.1. No strict dependence between stability of results and the curing time was registered (Table 4.4.2). Compressive strength results were generally more stable than flexural strength results. Only samples cured for 1 day and 56 days achieved compressive strength characterized by higher coefficient of variation than flexural strength. The value of coefficient of variation of both compressive and flexural strength results is not decreasing monotonically with time. The possible reason of the lack of dependence between curing time and stability of results can be the chemical deformation which takes place on the different stages of geopolymerization process. Li et al. [345] describes precisely the chemical deformation of metakaolin-based geopolymer activated with sodium silicate and sodium hydroxide solution and cured at ambient temperature. According to [345], geopolymer since casting undergoes three stages of chemical deformation followed by volume changes: initial

chemical shrinkage, chemical expansion and chemical shrinkage in the final stage. By contrast, the OPC concrete shows monotonic volume decrease and chemical shrinkage associated with cement hydration. The first chemical shrinkage of geopolymer occurs during first 8 hours when metakaolin particles are dissolute in activator. The following stage – the chemical expansion is caused by formation of zeolites and takes place between ~ 8 and 48 hours of curing. Monomers and small oligomers during polymerization turn into crystalline structures (like zeolites) in form of the frameworks containing small pores. The part of pores due to the small size cannot be occupied by guest molecules (even water) creating occluded volume and leading to the expansion of material. The expansion is followed by the chemical shrinkage during formation of space-filling geopolymer gel. The pores formed during this stage are capillary or gel pores which can be filled with water molecules. The occluded volume is negligible what results in higher density. The chemical shrinkage starts approximately after 48 hours and is constant (the experiment [345] was carried on for 14 days).

Table 4.4.2: Standard deviation [-] and coefficient of variation [%] of compressive and flexural strength results.

Standard deviation [-] (CoV [%])	1 day	3 days	5 days	7 days	14 days	28 days	56 days	112 days
<b>Flexural strength</b>	0,03 (2,3)	0,35 (12,6)	0,49 (13,6)	0,57 (12,4)	0,09 (1,8)	0,25 (4,9)	0,11 (1,8)	0,47 (7,0)
<b>Compressive strength</b>	0,59 (6,8)	2,74 (7,2)	3,19 (6,8)	5,07 (9,7)	0,90 (1,5)	1,56 (2,3)	5,11 (7,1)	1,51 (2,1)

The value of coefficient of variation of both compressive and flexural strength results is not decreasing monotonically with time. The possible reason of the lack of dependence between curing time and stability of results can be the chemical deformation which takes place on the different stages of geopolymerization process. Li et al. [345] describes precisely the chemical deformation of metakaolin-based geopolymer activated with sodium silicate and sodium hydroxide solution and cured at ambient temperature. According to [345], geopolymer since casting undergoes three stages of chemical deformation followed by volume changes: initial chemical shrinkage, chemical expansion and chemical shrinkage in the final stage. By contrast, the OPC concrete shows monotonic volume decrease and chemical shrinkage associated with cement hydration. The first chemical shrinkage of geopolymer occurs during first 8 hours when metakaolin particles are dissolute in activator. The following stage – the chemical expansion is caused by formation of zeolites and takes place between ~ 8 hours and 48 hours of curing. Monomers and small oligomers during polymerization turn into crystalline structures (like zeolites) in form of the frameworks containing small pores. The part of pores due to the small size cannot be occupied by guest molecules (even water) creating occluded volume and leading to the expansion of material. The expansion is followed by the chemical shrinkage during formation of space-filling geopolymer gel. The pores formed during this stage are capillary or gel pores which can be filled with water molecules. The occluded volume is negligible now what results in higher density. The chemical shrinkage



starts approximately after 48 hours and is constant (the experiment [345] was carried on for 14 days). Undergoing chemical deformations followed with changing volume can be possible reason for the varying coefficient of variation of results on different stages of curing. The research on the chemical changes of the material is out of the scope of this Thesis. This problem will be explored in the future.

The brittleness of samples increased along with the increase of curing time. The width of crack separating halves of samples after the failure during the flexural strength test was increasing with the increase of curing time. That dependence is shown in Figure 4.4.1.

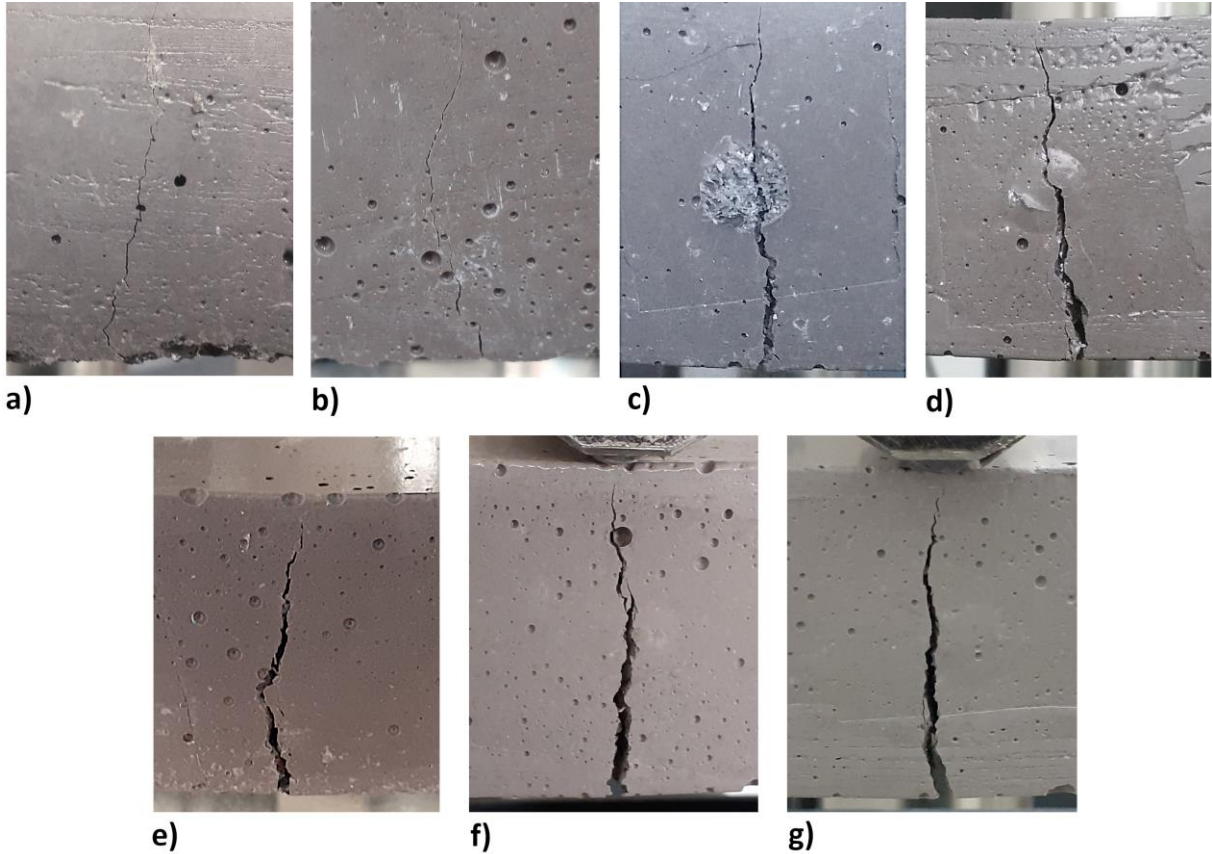


Fig.4.4.1: Crack appearing in the place of subjection of load after flexural strength test. Sample cured for: a) 1 day, b) 3 days, c) 7 days, d) 14 days, e) 28 days, f) 56 days, g) 112 days. There was no significant difference in color between samples presented in a), b), c), d) and e). The difference visible in photos is caused by the difference in lighting. Samples presented in f) and g) were visibly brighter.

The increasing width of the crack is not followed by the decreasing  $f_x/f_c$  ratio (Figure 4.4.5). Only the value of  $f_x/f_c$  ratio measured after 1 day is significantly higher than the values of  $f_x/f_c$  ratio measured in the following curing days. That indicates that the increase of the crack is caused by the increase the maximal force causing the destruction of sample rather than by the decrease of ductility of geopolymer.

Figure 4.4.2 shows the cross section of broken samples after compressive strength tests performed on beams made of mixture M/G 50/50. Photographs were taken two years

after casting of the samples. The particles of CRT glass of different sizes are visible in the cross-sections. Since the waste glass came from different parts of the cathode ray tube, its color was not unified. The majority of CRT glass particles was transparent (what is best visible in Figure 4.4.2 d) which presents relatively large and sparkling CRT glass particle). However, the part of CRT glass particles had different colors. The exemplary CRT glass of different color (reddish in that case) can be noticed in the upper side of Figure 4.4.2 b).

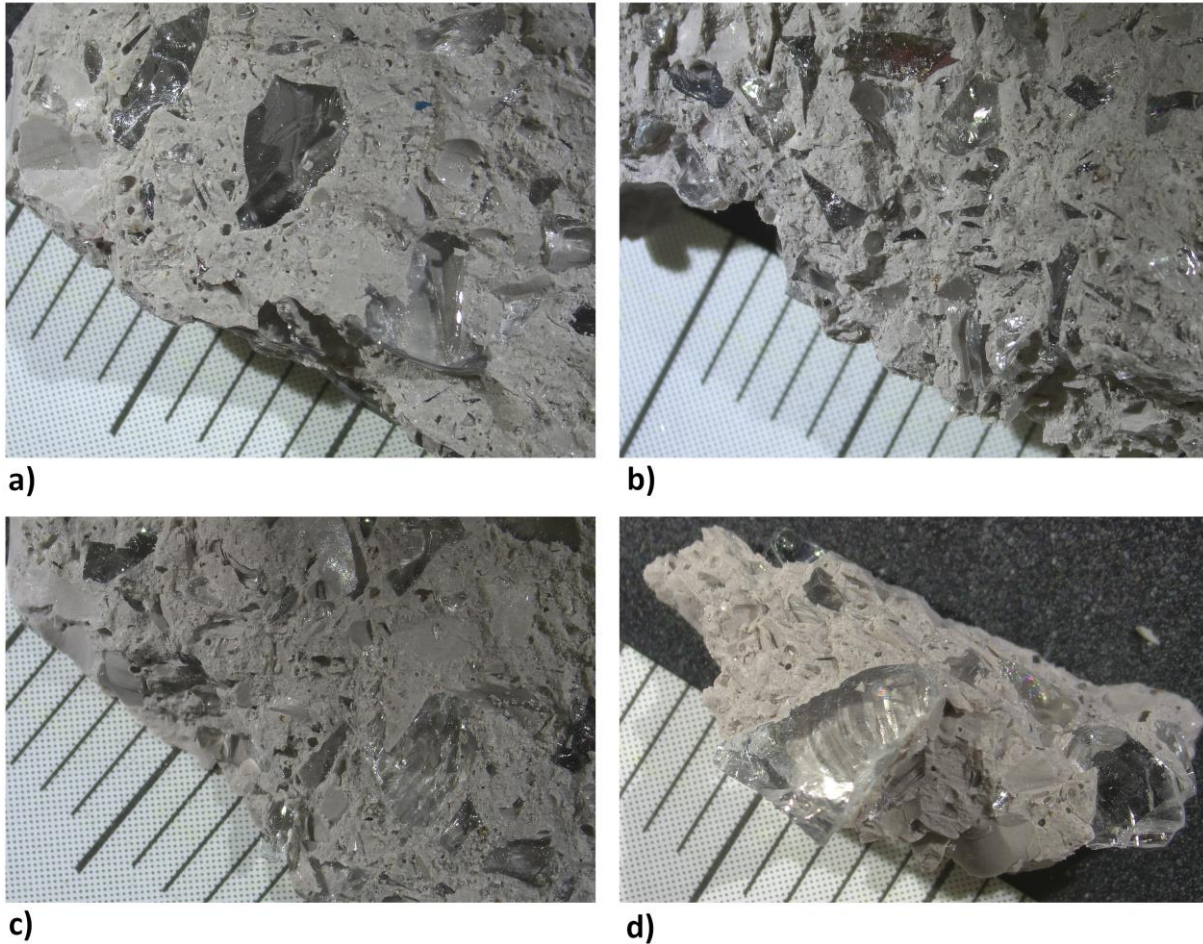


Fig.4.4.2: Broken surface of four samples made of mixture M/G 50/50 (containing 50% of CRT glass). (Photographs were taken by dr Fatima Pawełczyk in Institute of Physics, Centre for Science and Education, Silesian University of Technology).

To present more clearly the particular components visible on the surface of broken sample, one chosen cross-section has been presented in Figure 4.4.3. The exemplary components of the sample have been circled. CRT glass particles are edged with green circles. CRT glass particles visible in Figure 4.4.3, have different sizes and shapes. They stand the most visible part of cross-section, despite the grey-color metakaolin geopolymer matrix filling space between the glass. The orange circles show place of round air gaps of different sizes which are distributed randomly in the matrix. The blue circles round smooth places where CRT glass particle has been detached from the geopolymer matrix during strength test.



Fig.4.4.3: Broken surface of one chosen sample made of mixture M/G 50/50. (Photograph was taken by dr Fatima Pawełczyk in Institute of Physics, Centre for Science and Education, Silesian University of Technology).

#### 4.4.3 Analysis

Results are presented in Figure 4.4.4.

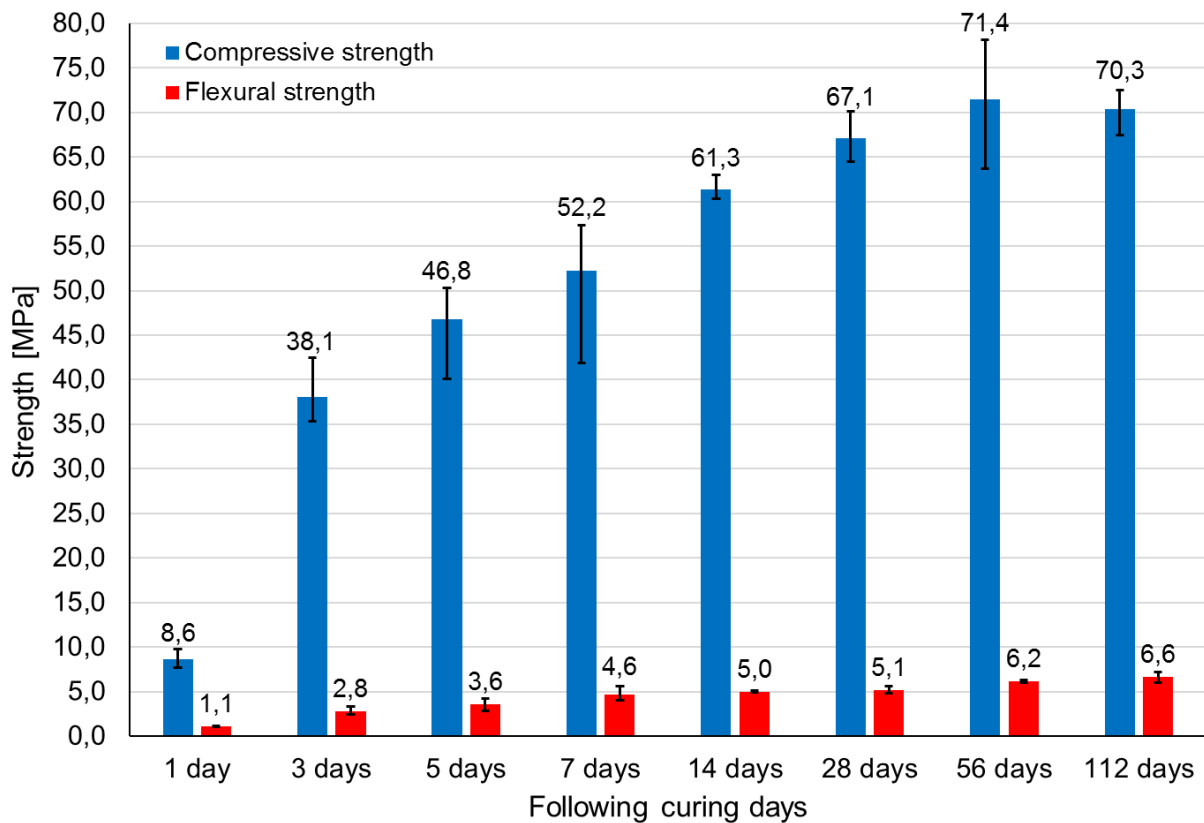


Fig.4.4.4: Change of the compressive and flexural strength of geopolymer made of mixture M/G 50/50 and cured at ambient temperature, over time.

According to diagram presented in Figure 4.4.4, both flexural and compressive strength increases in time. The only exception is compressive strength of samples cured for 112 days which is less than 2% smaller than compressive strength of samples cured for 56 days. Both in case of flexural and compressive strength, the biggest difference was observed between samples cured for 1 and 3 days. Flexural strength increased by 155% and compressive strength increased by 343% during this time. The increase of compressive strength was declining in time. In case of flexural strength, the dependence between the increase of strength and following curing days was not monotonic.

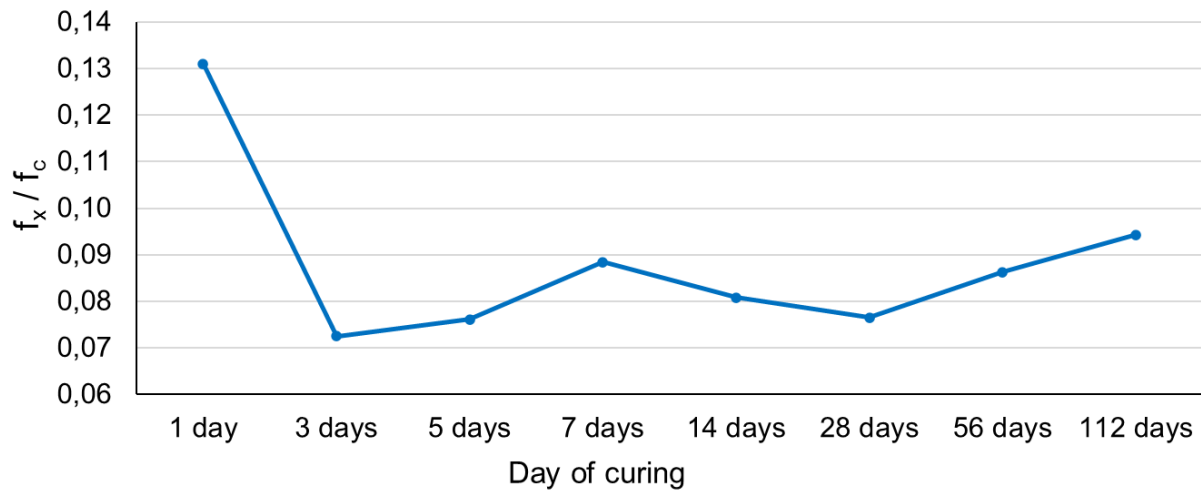


Fig.4.4.5: Change of the  $f_x/f_c$  ratio of geopolymer made of mixture M/G 50/50 and cured at ambient temperature, over time.

No monotonic dependence between geopolymer age and  $f_x/f_c$  ratio has been noticed (see Figure 4.4.5). The highest and lowest values were observed respectively after 1 day and 3 days of curing. The majority of  $f_x/f_c$  ratio values fluctuates between 0,07 and 0,09.

American Concrete Institute (ACI Code 318-19 [346]) describes the tensile strength of concrete in flexure as modulus of rupture and assess that its value is approximately equal to 10 - 15 % of the compressive strength ( $f_x/f_c$  ratio should be respectively equal in that case to 0,10 - 0,15). ACI Code 318-19 recommends calculating the estimated value of modulus of rupture of normal-weight concrete according to the following dependence:

$$f_r = 0,62\sqrt{f'_c} \quad (4.4.1)$$

Where:

$f_r$  – modulus of rupture of concrete, [MPa]

$f'_c$  – specified compressive strength of concrete, after 28 days of curing, [MPa]

Nath et al. [347] reports that flexural to compressive strength ratio of fly ash-based geopolymer with additions of Portland cement, slag or calcium hydroxide, cured at room temperature for 28 days ranges from 0,11 to 0,19. Mixtures contained both fine and coarse aggregate. Authors noted that values of flexural strength achieved during tests are higher than values predicted according to ACI Code 318-19 [346]. Scientists proposed their own equation

describing the dependence between flexural and compressive strength which fits the most accurately results obtained during tests:

$$f_{ct.f} = 0,93\sqrt{f_{cm}} \quad (4.4.2)$$

Where:

$f_{ct.f}$  – mean characteristic flexural strength of geopolymer, [MPa]

$f_{cm}$  – mean cylinder strength of geopolymer, [MPa]

Nath et al. [347] tested as well OPC concrete samples. The  $f_x/f_c$  ratio was equal to 0,09-0,10. Diaz-Loya et al. proposes the following dependence between flexural and compressive strength of fly ash-based geopolymer containing both fine and coarse aggregate:

$$f_r = 0,69\sqrt{f'_c} \quad (4.4.3)$$

Where:

$f_r$  – flexural strength of geopolymer, [MPa]

$f'_c$  – specified compressive strength of geopolymer after 3 days of curing, [MPa]

Zhang et al. [348] quotes a lot of flexural and compressive strength tests made on different geopolymer porous composites (with various raw materials, fillers and reinforcements). The majority of reported  $f_x/f_c$  ratios fits within one of two ranges: 0,07 to 0,16 and 0,25 to 0,32. Medri et al. [349] in turn, reports that geopolymer with an expanded vermiculite as an aggregate, has  $f_x/f_c$  ratio equal to 1,2 what is significantly higher value that quoted above. Bai et al. [350] reports that  $f_x/f_c$  ratio of highly porous geopolymers ranges from 0,09 to 0,55. However, the majority of values fits within the range 0,17 to 0,43. The  $f_x/f_c$  ratio of aerated concrete in turn, ranges from 0,22 to 0,27 [351].

Summarizing, the flexural strength of metakaolin-based geopolymer with CRT glass achieved in tests is the most convergent with the estimated value of the flexural strength calculated according to the formula given in ACI Code 318-19 [346] (Formula 4.4.1). The compliance of those two values is equal to 99%. In reference to the other scientific sources,  $f_x/f_c$  ratio calculated within this Thesis fits in the lower range of values for porous geopolymers given by Zhang et al. [348], but is below the range given for the other porous geopolymers and porous concrete [349], [350], [351]. It is also smaller than values declared by Nath et al. [347] for fly ash-based geopolymers.

Generally, the small  $f_x/f_c$  ratio of metakaolin-based geopolymer with CRT glass indicates that material is brittle. Materials characterized by low  $f_x/f_c$  ratio are less ductile and more vulnerable to the shrinkage than materials with high  $f_x/f_c$  ratio. The flexural strength on 28<sup>th</sup> day of curing is convergent with estimated flexural strength calculated according to ACI Code 318-19 [346] for concrete. The ACI Code 318-19 states that tensile strength of concrete in flexure is neglected during calculations of nominal flexural strength. Thus, metakaolin-based geopolymer with CRT glass, described within this Thesis, should be reinforced if applied in structural elements, especially, when applied in elements subjected to bending.

Table 4.4.3 presents the density of geopolymer in the following curing days. There is no significant difference between density of samples cured for 1, 3, 5, 7, 14 and 28 days. Samples cured for 14 and 28 days were characterized by slightly greater density (up to 1%) than samples cured for 1, 5 and 7 days. Then, a clear decline in density (by 12% and 10% in comparison to the rest of samples) for geopolymer cured for respectively 56 and 112 days was noticed. What should be emphasized, samples cured for 28 days and shorter were demoulded (and weighted) just before the test. In turn, samples cured for 56 and 112 days were demoulded after 28 days and then cured at the laboratory without any moulds or cover. Therefore, it can be concluded, that the drop of density takes place during the period when samples are demoulded. The most probable reason is that an excess of water is escaping the system when samples have contact with an air.

Table 4.4.3: Average density of geopolymer in the following curing days [kg/m<sup>3</sup>].

<b>1 day</b>	<b>3 days</b>	<b>5 days</b>	<b>7 days</b>	<b>14 days</b>	<b>28 days</b>	<b>56 days</b>	<b>112 days</b>
2060	2080	2070	2060	2080	2090	1820	1860

The investigation presented in the above subsection indicates that both flexural and compressive strength of geopolymer made on the chosen mixture is increasing in time. This is a promising finding which allows to assume that material with high probability has stable properties not changing in time. This conclusion should be confirmed in the future by mechanical strength tests carried out after longer period of time that 112 days.

## CHAPTER 5 (COMPLEMENTARY RESEARCH)

### 5.1 Porosity of geopolymer

#### 5.1.1 Preparation of samples

The main goal of this part was to determine the porosity of geopolymer. Investigation has been performed on two samples made of mixture M/G 50/50, cured more than 56 days at ambient temperature (the first 28 days in moulds, then demoulded). Test has been performed with the help of mgr inż. Anna Woźniak at Silesian University of Technology, Faculty of Mechanical Engineering, Department of Engineering Materials and Biomaterials. Determination of the density of geopolymer has been done according to the immersion method (based on Archimedes' principle). Test has been done with use of analytical balance (Radwag, AS 220.R2), accurate to 0,1 mg. Each sample was adequately prepared before the test. Firstly, samples were cleaned and then degreased in ultrasonic bath in acetone and deionized water (mass proportion 2:1) for 15 minutes. Then, the mass of samples was measured both in air and in deionized water. The measurement was repeated for three times in each sample what resulted in 6 outcomes. The density, apparent volume, apparent density, water absorption, open porosity and total porosity were calculated according to the formulas (5.1.1)-(5.1.6).

$$\rho_s = \frac{m_1}{m_1 - m_2} (\rho_w - \rho_a) + \rho_a \quad (5.1.1)$$

$$V_p = \frac{m_3 - m_2}{\rho_w} \quad (5.1.2)$$

$$\rho_p = \frac{m_1}{m_3 - m_2} \rho_w \quad (5.1.3)$$

$$WA = \frac{m_3 - m_1}{m_1} * 100 \quad (5.1.4)$$

$$P_o = \frac{m_3 - m_1}{m_3 - m_2} * 100 \quad (5.1.5)$$

$$P_t = \frac{\rho_s - \rho_p}{\rho_s} * 100 \quad (5.1.6)$$

where:

$\rho_s$  – density of sample [g/cm<sup>3</sup>]

$V_p$  – apparent volume [cm<sup>3</sup>]

$P_o$  – open porosity [%]

$\rho_p$  – apparent density of sample [g/cm<sup>3</sup>]

$WA$  – water absorption [%]

$P_t$  – total porosity [%]

- $m_1$  – mass of dry sample, measured in air [g]  
 $m_2$  – mass of saturated sample, measured in water [g]  
 $m_3$  – mass of saturated sample, measured in air [g]  
 $\rho_w$  – 0,998203 g/cm<sup>3</sup> - density of deionized water in temperature 20 ± 1°C  
 $\rho_a$  – 0,001205 g/cm<sup>3</sup> - density of air in temperature 20 ± 1°C

### 5.1.2 Results and analysis

Table 5.5.1 contains all results obtained during test. Table includes results of measurement of mass, performed on two samples and repeated three times. Table 5.5.1 includes as well the density, apparent density, apparent volume, water absorption, open porosity and total porosity.

Table 5.1.1: Results.

$m_1$ [g]	5,38	5,20	5,35	<del>7,26</del> *	5,37	5,47
$m_2$ [g]	2,83	2,66	2,86	<del>3,74</del> *	2,80	2,87
$m_3$ [g]	5,77	5,75	5,65	<del>7,60</del> *	5,87	5,93
$\rho_s$ [g/cm <sup>3</sup> ]	2,11	2,04	2,14	2,06	2,08	2,10
$V_p$ [cm <sup>3</sup> ]	2,94	3,09	2,80	<del>3,86</del> *	3,08	3,06
$\rho_p$ [g/cm <sup>3</sup> ]	1,83	1,68	1,91	1,88	1,74	1,78
WA [%]	7,11	10,54	5,59	4,68	9,44	8,38
$P_o$ [%]	13,06	17,75	10,73	8,82	16,47	15,00
$P_t$ [%]	13,10	17,80	10,78	8,88	16,51	15,05

\*Result was rejected on the basis of statistical method - elimination of one extreme value.

Table 5.5.2 contains average value, standard deviations and coefficients of variation of results presented in Table 5.5.1. The values of water absorption, open porosity and the total porosity are characterized by high coefficient of variation. It may lead to the conclusion that the compaction of the samples was not unified enough.

Table 5.1.2: Average values, standard deviations and coefficient of variation for each test result.

	Average	Standard deviation [-]	Coefficient of variation [%]
$m_1$ - Mass of dry sample [g]	5,36	0,10	1,8
$m_2$ - Mass of saturated sample, measured in water [g]	2,81	0,09	3,0
$m_3$ - Mass of saturated sample, measured in air [g]	5,80	0,11	1,9
$\rho_s$ – Density of sample (Archimedes) [g/cm <sup>3</sup> ]	2,09	0,04	1,7
$V_p$ - Apparent volume [cm <sup>3</sup> ]	3,00	0,13	4,3
$\rho_p$ – Apparent (bulk) density [g/cm <sup>3</sup> ]	1,80	0,09	4,8
WA - Water absorption [%]	7,63	2,25	29,5
$P_o$ - Open porosity [%]	13,64	3,43	25,1
$P_t$ - Total porosity [%]	13,69	3,43	25,0



Porosity of samples tested within this Thesis is lower than porosity reported by other scientists [50], [94], [101], [324], [352], [353]. Lower porosity of geopolymer described in Thesis can be treated as an advantage since pores (especially those one of bigger sizes) may lead to decline of strength [169]. By contrast, in case of density of metakaolin-based geopolymer, some scientists reported smaller values [352], [353] than the one in this Thesis but some of them reported higher values [50], [324]. There are also investigations indicating almost the same values of density [101].

## *5.2 Physicochemical characteristics*

### 5.2.1 Description of the test

The main goal of the test was to determine the physicochemical characteristics of the material with particular emphasis on the leaching of toxic metals from the matrix of hardened geopolymer. Test was conducted with the use of atomic absorption spectrometry (AAS). AAS is an innovative method requiring high-quality environment in order to avoid any possible errors of measurement and to ensure reliable and repeatable analysis. To fulfill test requirements all analytical works were carried out in the carefully prepared laboratory. The laboratory room was air conditioned what ensured stable and repeatable measurements. The three-stage filtration of the supply air allowed prevention of any impurity of samples. Works have been performed on two atomic absorption spectrometers made by Varian company.

Wet microwave digestion method was used to prepare samples for testing. Two kinds of material were subjected to AAS method: crushed CRT glass and metakaolin-based geopolymer containing CRT glass in form of an aggregate. Sample made from mixture M/G 50/50, cured at the room temperature for 28 days was chosen for the determination of properties of leachate from geopolymer containing CRT glass. The prismatic sample was broken before the test to simulate situation where geopolymer is placed in the ground and its surface can be destroyed for instance by cracking. The main goal of the investigation was to determine and then to compare properties of the leachate from the not-stabilized CRT glass and from the geopolymer containing CRT glass. The comparison would allow to assess if the addition of CRT glass to the geopolymer mixture is an effective way for immobilization of hazardous metals. The procedure for preparation and testing of CRT glass and geopolymer was the same although materials were tested separately. Each material was placed in the glass vessel filled with purified water. The mass ratio of tested material to water was 1:10. After 1 hour of resting, vessels were covered tightly and shaken for 4 hours in the shaking machine. Thereafter, vessels were resting in static conditions in the absence of light for 16 hours. After this time, vessels were shaken once more for the next 4 hours. Then, samples were put away for 2 hours to allow the sedimentation to proceed. Afterwards, the obtained extract was filtered through the filter paper and subjected to atomic absorption spectrometry. Different types of AAS were used for identification of metals in samples: flame, electrothermal, hydride and cold-vapor method. The Mohr method was used for designation of chlorides. The total hardness, total and mineral alkalinity and total and mineral acidity were designed using titration method. Calomel and glass electrodes were used for determination of pH.

Various methods of AAS were used for the analysis of a metal content: electrothermal AAS (spectrometer SpectrAA-880 Zeeman), the flame AAS (spectrometer SpectrAA-880) and the VGA-77 vapor generation accessory. Test and the interpretation of the results has been done with the help of: dr hab. inż. Krzysztof Loska, dr inż. Michał Koziół, dr inż. Marcin Landrat, dr inż. Waldemar Ścierański and prof. dr hab. inż. Krzysztof Pikoń at Silesian University of Technology, Faculty of Energy and Environmental Engineering.

## 5.2.2 Atomic absorption spectrometry (AAS) results and analysis

Results of physicochemical analysis are presented in Table 5.2.1. Table 5.2.1 contains both results of analysis of aqueous extract from not-stabilized crushed CRT glass and from geopolymer sample containing CRT glass.

Table 5.2.1: Physicochemical analysis of aqueous extracts from CRT glass and geopolymer containing CRT glass.

Designation	Unit	Aqueous extract from geopolymer	Aqueous extract from CRT glass	The limit values (according to [354])
pH	-	11,0	6,3	6,5-9
Total hardness	mval/dm <sup>3</sup>	0,08	0,82	-
Chloride	gCl/dm <sup>3</sup>	0,0138	0,0138	1
Total acidity	mval/dm <sup>3</sup>	0,0	0,8	-
Mineral acidity	mval/dm <sup>3</sup>	0,0	0,0	-
Total alkalinity	mval/dm <sup>3</sup>	6,0	0,0	-
Mineral alkalinity	mval/dm <sup>3</sup>	10,2	0,6	-
Fe	ppm	0,12	0,42	10
Mn	ppm	<0,015	<0,015	-
Cu	ppm	0,01	0,02	0,1
Ni	ppm	<0,02	<0,02	0,1
Cr	ppm	<0,03	<0,03	0,05
Co	ppm	<0,025	<0,025	0,1
Zn	ppm	0,03	0,31	2
Pb	ppm	0,12	1,66	0,5
Cd	ppm	<0,006	<0,006	0,07

According to the AAS results, extract from geopolymer has much higher alkalinity than extract from CRT glass and consequently, much higher pH as well. The chloride content and mineral acidity of both extracts are the same. Designation of metal content in leachate from both samples was the important part of the analysis. The content of following metals: Mn, Cu, Ni, Cr, Co and Cd in extract from CRT glass and geopolymer was very similar or exact. However, the content of elements: Fe, Zn, and Pb in extract from CRT glass was much higher than in extract from metakaolin-based geopolymer with CRT glass. Leachate from metakaolin-based geopolymer contains almost 14 times less Pb and 10 times less Zn than leachate from CRT glass. Obtained results were compared with Polish regulatory limits (harmonized with



regulations of European Union) determining permissible parameters of waste water introduced to the ground or to the water [354]. The concentration of following elements: Fe, Cu, Ni, Cr, Co, Zn and Cd, in leachates from both CRT glass and geopolymer containing CRT glass was below the maximal regulatory value. However, concentration of Pb in the leachate from pure CRT glass exceeded the maximum allowable value by over 230% while in the aqueous extract from geopolymer, the same element did not reach 25% of the limit value. Such results can lead to the conclusion that addition of CRT glass in form of an aggregate into the metakaolin-based geopolymer mixture allows for successful encapsulation of hazardous metals present in CRT glass inside the geopolymer matrix. According to the results compared with the existing Polish regulations, CRT glass incorporated in geopolymer is no longer harmful for environment in terms of toxic metals pollution. Admittedly, the pH value in case of both extracts does not fit the range of regulatory values. The pH of extract from pure CRT glass is slightly below the low limit value while the pH of extract from geopolymer exceed the maximum allowable value. That issue should be considered before application of described material in conditions where leachates could directly have contact with ground or water.

The number of papers devoted to addition of CRT glass to the geopolymer is limited but a lot of successful investigations were done on the capability of encapsulation of toxic elements inside geopolymers [138], [139], [294], [296], [297]. Results described in the above chapter are promising with regard to the safe incorporation of CRT glass inside metakaolin-based geopolymer matrix. The amounts of toxic metals (especially Pb and Zn) leached from hardened material fulfill the regulatory limits. Described investigation indicates that designed material has not only superior mechanical characteristics but is as well with high probability safe for environment. The extent studies shall be surely performed in that field to confirm that initial results.

## CHAPTER 6 (DISCUSSION)

The number of publications devoted to incorporation of CRT glass in geopolymer is limited while investigations of the CRT glass replacing aggregate are extremely rare. Therefore, in the discussion on the achieved results, there are evoked as well researches concerning powdered glass added to geopolymer, common glass included into geopolymer in form of an aggregate and rarely, concrete with CRT glass aggregate.

---

### *6.1 Determination of the influence of the CRT glass content on mechanical behavior – discussion*

According to [314], the increase of CRT glass aggregate content has an adversely impact on compressive strength. The compressive strength decreased by 11% when the metakaolin to CRT glass ratio changed from 1:3 to 1:7 and by 6% when metakolin to CRT glass ratio changed from 1:2 to 1:3. Within this Thesis, the change of CRT glass content from 1:2 to 1:3 caused also decrease of strength, however, the decrease was smaller (only 2%).

More publications raise the topic of addition of CRT glass into the geopolymer matrix but in form of a powder as a replacement of raw material, not an aggregate. Long et al. [307] registered that after 7 days, both flexural and compressive strength decrease gradually with the increase of CRT glass content. In case of both strengths the decrease is relatively small (2-7%) up to replacement equal to 50% while the significant drop (by 18%) was registered between samples containing 50% and 70% of CRT glass. According to [307], the decrease of strength is related to smaller pozzolanic activity of CRT glass in comparison to slag which results in slower geopolymerization, smaller amount of geopolymerization products and finally in reduction of strength. By contrast, Ogundiran et al. [105] observed the increase of compressive strength of metakaolin-based geopolymer along with the increase of powdered CRT glass content from 0% to 20%. Badanoiu et al. [313] noted that samples containing CRT glass only, obtained over two times higher compressive strength than samples with CRT glass and fly ash. Moncea et al. [335] reports that the compressive strength of slag-based geopolymer decreased along with the increase of CRT glass content. By contrast, in case of fly ash-based geopolymer, compressive strength firstly increased when CRT glass content increased from 0 to 11,4% and then decreased for 22,6% CRT glass content.

Some studies describe the utilization of common glass in geopolymer as a replacement of sand. Khan et al. [322] describes the monotonic, relatively small (up to 5%) decrease of compressive strength along with the increase of glass content. Gutierrez et al. [324] by contrast, reports that in metakaolin-based geopolymer, the replacement of sand with glass causes an increase of strength.

The topic of utilization of CRT glass was more often risen in the context of concrete as the replacement of natural aggregate. In this field of science, different opinions regarding the influence of CRT glass on mechanical behavior can be found as well. Romero et al. [273] reports the increase of compressive strength with the increase of CRT glass content from 0 to

20% and a small further decrease for 30% of CRT glass. Walczak et al. [276] observed that concrete samples incorporating 100% of CRT glass instead of sand achieved higher flexural and compressive strength than control samples containing sand. By contrast, [288], [288], [323], [355] report decreasing compressive strength of concrete with an increase of CRT glass content.

As presented above, opinions of scientists on the influence of CRT glass or common glass on mechanical behavior of geopolymer and concrete as well are divided. Some sources declare the decrease of strength [288], [307], [314], [322], [323], [355] while some of them observed increase of strength [105], [276], [313], [324] related to the increase of glass content. Some publications report in turn the lack of monotonic influence of glass content on mechanical behavior of tested material [273], [335]. The lack of unambiguous effect of glass content on strength is convergent with results presented within this Thesis. Studies which described the change of density, reports the increase of that parameter with the increase of glass content what is consistent with observations done by the Author [105], [324].

---

## *6.2 Determination of the influence of curing temperature on mechanical behavior – discussion*

The topic of the influence of curing temperature on the mechanical behavior of geopolymer has been extensively described in the literature. However, the observations made by different scientists are not always convergent. The most popular observation made by scientists is that the compressive strength increases along with the increase of curing temperature but only until the specific value of the temperature [75], [326], [327], [336], [356], [357]. Mo et al. [327] and Chen et al. [75] observed that the seven-day compressive strength increased monotonically along with the increase of curing temperature from 20°C to 60°C and then decreased along with the further increase of the temperature (up to 100°C). Gorhan et al. [102] shows results where within 4 mixtures only one series achieved greater compressive strength while cured at 80°C than at 60°C.

According to Mo et al. [327] Chen et al. [75], the low curing temperature retards the dissolution of metakaolin particles and slows down the production of geopolymer gel. The amount of precursor (mainly Al) dissolved during the amorphous phases, which has to polymerize with Si particles (coming mainly from activators), is not sufficient enough to build plenty of aluminosilicate gels. That reduces the compressive strength. Curing at the elevated temperature helps in dissolution of Al and Si elements from the amorphous phase in metakaolin and accelerates the rigid structure formation. In samples cured at high temperature, the amount of geopolymer gel is sufficient for tough bonding of the metakolin particles at the early stage of the process. What is more, the rise of curing temperature helps removing water from the system what causes more rapid formation of gel phase and increases strength. The influence of elevated curing temperature is more visible at the early-stages of geopolymerization process. In turn, too high curing temperature may lead to the situation when initial and final setting time are too short and the dissolved precursors are reacting too rapidly. Consequently, the part of metakaolin particles can be covered with gel before

dissolution what stops the process and prevent building the compact and strong structure. Moreover, high curing temperatures can lead to the rapid dehydration and shrinkage what results in microcracks.

In turn, Ekaputri et al. [101] reports the small (about ~1-2%) but monotonic increase of the compressive and tensile splitting strength along with the increase of the curing temperature even up to 80°C. A monotonic increase of strength with the increase of curing temperature was also reported by Alonso et al. [109] and Hardjito et al. [28]. According to Alvarez-Ayuso et al. [110], the compressive strength of fly-ash based geopolymer samples cured at 80°C is higher than compressive strength of samples cured at 40°C and 60°C (those values were close to each other).

By contrast, Rovnanik [334] indicates that compressive and flexural strength of metakaolin-based geopolymer increases along with the increase of curing temperature only on early stages of curing process (after one day). As early as after 3 days, the compressive strength of samples cured at 20°C was higher than of those cured at 60°C and 80°C. Author explains that the elevated curing temperature helps to gain high early strength but causes greater porosity of the structure and less effective compaction of samples, thus, affecting the quality and lowering long-term strength.

The results presented within this Thesis are the most convergent with observations presented by Ekaputri et al. [101] and Rovnanik [334]. Rovnanik reports that after 7 days, the highest compressive strength was obtained by samples cured at the very beginning at 40°C. Compressive strength of samples cured at 20°C were only 4% smaller. In this Thesis, two out of four series of samples achieved after 7 days the highest compressive strength while curing all the time at the room temperature. In one case the highest compressive strength was achieved by samples cured at the beginning at 40°C. The differences between the following results presented in this Thesis were very small what is, in turn, convergent with results presented by Ekaputri et al. On the other hand, Ekaputri et al. indicates the small increasing tendency of the compressive strength along with the curing temperature which was not registered in tests done within this Thesis. Ekaputri et al. observed that the flexural strength also increases with the increase of the curing temperature. Results presented within Thesis also shows increasing tendency of the flexural strength however with a bigger differences than noticed in [101]. The increase of flexural strength along with the increase of curing temperature was also reported by Alonso et al. [109].

The density of samples tested within this Thesis generally decreases with the increase of the curing temperature what is convergent with data presented in several papers [102], [334], [336].

---

### *6.3 Determination of the temperature and strength changes over time – discussion*

Davidovits et al. [166] presents the temperature changes inside metakaolin-based geopolymer cured at 85°C, 60°C and 40°C. Mixtures were based on metakolin only (no aggregate addition) and activated with NaOH of concentration 12 mol/L. The exothermic peak

(maximal temperature) inside samples was achieved quicker in those one cured at higher temperatures. In samples cured at 40°C, the maximum temperature (~70°C) was achieved after approximately 3,5 hours of curing. The maximum temperature was much higher than the one achieved within this Thesis (~47°C). An exothermic peak took place earlier than in this Thesis as well (~3,5 hour versus 6 or 7 hours in samples containing metakaolin to CRT glass in ratio 1:1 and 1:3 respectively). The higher maximum temperature developed in the material can be caused by the higher NaOH concentration [36], [339], [342] and the lack of aggregate (within this Thesis, the higher temperature was achieved in samples with smaller amount of aggregate as well). Davidovits et al. did not register on the graph the first exothermic peak and the small drop of temperature just after placing of mixture in moulds. Scientists explain, that the first exothermic peak took place in the bowl, while mixing. According to [166], the intensity and speed of the exothermic polycondensation depend on curing conditions (mainly temperature) and alkalinity of soluble materials. Yao et al. [36] describes the geopolymerization process carried out at ambient temperature by isothermal calorimetry. Scientists observed the first exothermic peak in the moment of mixing of metakaolin with activator. According to [36], the first peak is related to the breaking of Si-O and Al-O bonds on the surface of particles, during the dissolution of metakaolin particles in alkaline solution, which is an exothermic process. After the first peak, the reactions are slowing down, what results in the decline on the heat evolution graph. The second exothermic peak is related to the rapid breaking down of metakaolin particles. The further increase of the heat evolution takes place together with the polymerization of the deconstruction products into gels. Granizo et al. [339] presents the similar division into particular phases of deconstruction of metakaolin and building the hard matrix. Observations has been made on the basis of results of isothermal conduction calorimetry. The presence of three exothermic regions is confirmed by Kuenzel et al. [340] as well. According to [340], the differences in the rate of heat output can be caused by the source of the basic material (metakaolin). The presence of the last exothermic peak varied from ~20 hours to over 80 hours in dependence on the metakaolin type.

Zhang et al. [341] used isothermal conduction calorimetry to determine the geopolymerization kinetics of metakaolin-based geopolymer. Scientists indicate two exothermic peaks assigned to respectively: the dissolution of metakolin particles and the geopolymeric gel formation. In case of geopolymer cured at 40°C, the first peak took place after about 3-6 min (in dependence on alkali concentration) and the second one after 40 min – 1 h 40 min. Scientists observed as well, that the heat evolution rate is higher and peaks took place earlier along with the increase of curing temperature. According to Zhang et al., the lack of the third peak is caused by the type of activator (in NaOH activated systems, the third peak is related to the reorganization of gel during the NaOH activation of metakaolin). Buchwald et al. [342] also indicates two visible peaks in heat evolution diagram of ambient-cured geopolymer. The first – initial and sharp peak was caused by dissolution of solid particles. The second one (related to condensation process) took place 2 to over 14 hours after mixing in dependence on composition of geopolymer. The higher concentration of activator lead to quicker appearance of the second peak. The peak was higher as well.

The topic of the influence of time on mechanical behavior of geopolymer has been extensively explored and presented in the literature.

The tendency of the increase of strength along with the curing time (observed in the case of samples from series M/G 50/50) is convergent with observations presented in the series of publications [101], [105], [307], [322], [327], [357]. Besides, some of the papers confirm the most rapid increase of strength between 3<sup>rd</sup> and 7<sup>th</sup> day of curing [101], [327]. Khan et al. [322] observed that the growth rate is decreasing for the following curing days what is convergent with results presented in Thesis but only for samples containing 50% of CRT glass. By contrast, some scientists reports the lack of the dependence between day of curing and strength of tested geopolymer [335].

Moncea et al [335] observed the decrease of strength along with the increase of CRT glass content. Long et al. and Khan et al. [307], [322] report that samples containing 50% of glass achieves higher strength than samples containing around 70% of glass. In turn, Badanoiu et al. [313] observed the opposite tendency – the compressive strength of samples with 75% of CRT glass overpassed strength of samples with 50% of CRT glass. Additionally, the strength of samples with 50% of glass decreased in time while strength of samples with 75% of glass remained stable what is opposite to observations made within Thesis. The increase of strength along with the increase of CRT glass content is as well reported in [105]. Zhang et al. [357] reports that addition of 50% of powdered glass increases strength of geopolymer cured at elevated temperatures.

The increase of density of geopolymer along with the increase of CRT glass content observed in this Thesis as well found a confirmation in the literature [105].

Obtained results obtained are the most convergent with those one presented by Long et al. [307] and partially with Khan et al. [322]. However, there are significant differences between procedures described in each of cited publications and the test presented in this Thesis. Therefore, only the general comparisons can be made. The lack of more similar tests indicates that the topic risen within this Thesis is useful for the current knowledge about geopolymers.

---

#### *6.4 Determination of the influence of curing temperature and curing time on mechanical behavior – discussion*

According to tests described in Thesis, the compressive strength of samples cured at 40°C exceeds strength of samples cured at 20°C up to 14<sup>th</sup> day of curing, when the dependence is reversed. The flexural strength of samples cured at 20°C remains smaller through the whole curing time. The supremacy of compressive strength of geopolymer cured at elevated temperature at early age is confirmed by other studies [47], [101], [327], [334], [338], [343], [357]. According to part of sources, like in this Thesis, the is decreasing in time and then is reversed (around 28<sup>th</sup> day) [334], [338], [343]. In contrary to results achieved in Thesis, Rovnanik [334] found that the flexural strength of samples cured at 20°C exceeded strength of samples cured at 40°C after 7<sup>th</sup> day of curing.

Tests described in Thesis has shown that geopolymer cured at 40°C gains strength more rapidly during the first days of curing than geopolymer cured at the room temperature. That dependence was as well observed by other scientists [327], [334], [343]. According to [334], the high temperature of curing rises the degree of geopolymerization process what enlarges the amount of reaction products and leads to the faster development of strength. On the other hand, in the low temperatures, geopolymer builds its structure more slowly what effects in lower porosity, higher toughness and finally, enhances the quality.

The biggest increase of compressive strength of samples cured at 20°C was observed within this Thesis between 1<sup>st</sup> and 3<sup>rd</sup> day of curing. The same observation was noted in [327], [334]. In turn, [101], [343] reports the biggest increase of strength of samples cured at ambient temperature between 3<sup>rd</sup> and 7<sup>th</sup> day of curing, while Nasir et al. [338] between 7<sup>th</sup> and 28<sup>th</sup> day of curing. According to tests done in Thesis, samples cured at 40°C gained the most rapidly compressive strength between 3<sup>rd</sup> and 7<sup>th</sup> day what is confirmed by several other studies [101], [327], [338]. By contrast, Rovnanik [334] observed the biggest increase of strength of samples cured at 40°C between 1<sup>st</sup> and 3<sup>rd</sup> day while Dezfouli et al. between 7<sup>th</sup> and 28<sup>th</sup> day.

---

## *6.5 Determination of the influence of sodium hydroxide concentration on mechanical behavior – discussion*

Results obtained within this Thesis are convergent with the majority of tests presented in the literature where is generally proven that strength of geopolymer enlarges with the increase of sodium hydroxide concentration [28], [71], [98], [108], [110], [358]. However, the reported in the publication's growth is not linear and usually the highest concentration is not indicated as optimal. Some researchers observed the decrease of strength for high NaOH molarities however, this behavior concerns values higher than tested within Thesis (15 mol/L [71] and 16 mol/L [98]). The compressive strength results show the biggest convergence with those one presented by Wang et al. [108] since the greatest increase of strength took place for samples activated with 8 and 10 mol/L NaOH while differences between 6 and 8 mol/L as well as between 10 and 12 mol/L were relatively small. Flexural strength results are more difficult to compare since this type of strength is less frequently presented in the literature. The dependence between NaOH molarity ranging from 6 to 10 mol/L and flexural strength is similar to the one described in [108] since the strength increases along with the increase of NaOH concentration. However, Wang et al. observed the rapid increase of flexural strength for 12 mol/L NaOH while the Author noticed for this value the small decrease of the flexural strength. In this point the result is convergent with the work of Alonso et al. [109] who observed the gradual decrease of flexural strength for the NaOH concentrations exceeding 10 mol/L. The density of a geopolymer had a tendency to growth with the increase of NaOH molarity what is convergent with data found in the literature [28], [108], [358]. The loss of workability along with the increase of NaOH concentration is as well validated by results achieved by the other scientists [36], [71].

According to the literature, at the first stage of the geopolymerization process, the growing concentration of the activator leads to the increase in the rate of reaction heat

evolution. In geopolymers containing activator of high concentration, the peak of heat evolution rate takes place earlier and the peak is higher than in geopolymers activated with NaOH of lower concentration [36] [98]. The higher concentration of sodium hydroxide provides enhanced dissolution of metakaolin particulates and leads to the production of more reactive bond for monomer what increases inter-molecular bonding strength and, as an effect, leads to the creation of more compacted geopolymer with higher strength. However, too high concentration can be undesirable to polymerization due to the residual raw material particles present in the geopolymer matrix [36] [108], [358]. The enlarging amount of unreacted particles with the fact that high alkali concentration increases the setting rate and reduces the time for dissolution of metakolin particles [358]. The excessive increase of NaOH molarity may leads to the increase of pH of the mixture in the liquid phase which results in favoring anionic forms of silicate what delays the polymerization process (the polymerization takes place quicker when components are in the molecular forms). Moreover, the high concentration of activator increases as well the ion's species concentration implicitly reducing their mobility which leads to the delay of the formation of coagulated structures [109].

---

### *6.6 Determination of the influence of CRT glass particle size on mechanical behavior – discussion*

The number of publications describing the influence of glass particle size on the geopolymer strength is limited. The majority of papers found by the Author indicates the lack of the strict and clear dependence between the size of glass particles and mechanical behavior of geopolymer or concrete what is convergent with results achieved in this Thesis [314], [359], [360]. Opletal [314] reports two comparisons where once the compressive strength increased and once decreased along with the increase of micro fractions content. Zhang et al. [357] reports the decrease of strength along with the increase of glass particle size, however, only the micro fractions were used during the test. Zhang et al. [359] observed that the highest compressive strength was achieved by geopolymer samples containing glass of all sizes mixed together, what is convergent with results presented within this Thesis. In turn, the compressive strength of OPC concrete increased along with the increase of particle size. According to the results [359], the density was decreasing along with the increase of glass size what is divergent with results presented within this Thesis where samples geopolymer with higher CRT glass size was characterized by higher density. Yang et al. [360] reports that despite the differences in glass particle size, concrete blocks achieved almost the same compressive strength. The density of material increased along with the increase of glass size. The behavior of both measured characteristics is similar to the behavior presented within this Thesis.

---

### *6.7 Determination of the change of mechanical behavior over time – discussion*

The influence of curing time on mechanical behavior of geopolymer has been discussed in the previous subsections (6.3 and 6.4). Therefore, in the following Chapter, only the changes in strength after 28 days of curing are considered. Ekaputri et al. [101] reports that

compressive strength of metakaolin-based samples increases by 4% between 28<sup>th</sup> and 56<sup>th</sup> day of curing. Dezfouli et al. [343], shows the increase of compressive strength by 2% in ground glass fiber and fly ash-based geopolymer during the same time period. Those results are close to findings reported in this Thesis where compressive strength increased by 7% between 28<sup>th</sup> and 56<sup>th</sup> day of curing. Moncea et al. [335] reports the minor increase of strength (by ~1-4%) of slag-based geopolymer and more significant increase (by ~20-40%) of fly ash-based geopolymer between 28<sup>th</sup> and 90<sup>th</sup> day of curing. Khan et al. [322] observed the increase of compressive strength between 28<sup>th</sup> and 90<sup>th</sup> day ranging from 8% to 11%. Findings presented by Khan et al. and by Moncea et al. (only slag-based geopolymer with no CRT glass) are convergent with result from this Thesis where compressive strength increased by 5% in the same period.

---

## *6.8 Determination of the porosity – discussion*

Latella et al. [352] reports that open porosity and bulk density of metakaolin-based geopolymer with sand aggregate, cured for 24 hours at 60°C are equal to respectively 20% and 1,60 g/cm<sup>3</sup>. Samples were characterized with similar compressive strength to the one presented in this Thesis (70 MPa). Reported open porosity is higher than in Thesis (13,64%), while the density value is lower than the one determined in Thesis (1,80 g/cm<sup>3</sup>). Hao et al. [353] observed that bulk density decreases from 1,42 g/cm<sup>3</sup> to 1,35 g/cm<sup>3</sup> with the increase of glass powder from 0 to 40% (replacement of metakaolin by mass), while porosity increases from 42,31% to 45,84% along with the increase of glass content. Gutierrez et al. [324] tested metakaolin-based geopolymer with sand replaced partially by glass. According to [324], bulk density increases along with the increase of glass content from 2,30 g/cm<sup>3</sup> to 2,48 g/cm<sup>3</sup>. According to [324], both water absorption and total porosity decreased along with the increase of glass content. Samples containing crushed glass only (no sand) were characterized by water absorption and porosity equal to respectively 11,5% and 22,7%. Both values are higher than in this Thesis (7,63% and 13,69% respectively). El-Naggar et al. [50] reports that 28 days bulk density of metakaolin-based geopolymer with 7% of waste glass addition cured at ambient temperature is equal to ~1,93 g/cm<sup>3</sup> while porosity is equal to ~19%. Clausi et al. [94] tested metakaolin-based geopolymer with sand as fine aggregate. According to results, porosity of material depends on H<sub>2</sub>O/Na<sub>2</sub>O molar ratio and ranges from 21,5% to 31,8%. Ekaputri et al. [101] reports that closed, open and total porosity of metakaolin-based geopolymer (no aggregate) cured at ambient temperature is equal to respectively ~8,7%, 14,7% and 23,7%. The total porosity is higher than the one in this Thesis (13,69%). In turn, the open porosity of geopolymer reported by Ekaputri et al. is much lower and states much smaller ratio of total porosity than open porosity determined within this Thesis (13,64%). According to Ekaputri et al., the curing temperature is not influencing density of geopolymer which is equal to about 1800 kg/m<sup>3</sup> which is value convergent with the one described in this Thesis.

---

## 6.9 Physicochemical characteristics – discussion

Results achieved within this Thesis show that the number of particular elements leached from pure CRT glass is higher than from hardened geopolymer incorporating CRT glass. Comparatively substantial difference between the content of lead present in leachate from not-stabilized soils (raw material and milled CRT glass) and from geopolymer with CRT glass was previously reported by Ogundiran et al. [105]. According to [105], the amount of leached Pb is limited by over 91% when CRT glass is incorporated in geopolymer matrix (for maximal CRT glass content equal to 20% by mass). The very similar result is reported by Carrillo et al. [310] who reports the decrease of Pb leaching at level of about 92% comparing the pure CRT glass and metakaolin-based geopolymer containing 20% of CRT glass. The examined material fulfills the limits for toxic metals leaching. However, [310] observed that the immobilization ability is strongly dependent on the composition of a mixture and promoted by the low alkaline conditions. Gao et al. [302] reports that Pb leaching was limited by almost 90% after immobilization inside fly ash-based geopolymer matrix. An excellent immobilization capability of Pb coming from CRT glass inside the ground granulated blast furnace slag-based alkali activated matrix was derived also by Long et al. [307]. The amount of Pb present in leachate from not-stabilized materials was much higher than in leachate from hardened geopolymer. In sample containing 50% of CRT glass by mass, the leaching of CRT was reduced by over 94% in comparison to unreacted material. According to [307], the replacement of raw material with CRT glass up to 50% is not harmful for environment considering the Pb leaching. Results presented in this Thesis, where the amount of leached Pb was decreased by over 92% (for 50% of CRT glass content by mass) are convergent with previously reported studies. Moncea et al. [335] reports that slag-based and fly ash-based geopolymer containing 22,6% of powdered CRT glass fulfills the regulations for maximal lead emission and can be used as a building material without any restrictions. According to Long et al. [308], slag and fly ash-based geopolymer containing sand to CRT glass in mass ratio 1:1 fulfills the regulatory limits for Pb leaching but only when fly ash replaces slag in 0, 30 and 50%. Geopolymer with higher fly ash content does not fulfill Pb leaching limits. The amount of leached Pb was reduced by 96,1-99,1% in comparison to non-stable CRT glass. Garcia-Ten et al. [361] registered a great improvement in immobilization of CRT glass after incorporation inside fly ash-based geopolymer matrix. Moreover, scientists emphasize that the efficiency of immobilization ratio increase along with the increase of CRT glass particle size.

By contrast, Opletal in his Master Thesis [314] found out that Pb and Zn are leached more easily from metakaolin-based geopolymer than from not-stabilized crushed CRT glass. The increased leachability of Zn is explained by author of the cited Master Thesis by the fact that that Zn element form oxyanions which are more easily released and soluble at high pH. Although, the explanation is not convergent with results presented in Table 5.2.1 where the content of Zn in extract from CRT glass is much higher than in extract from geopolymer which has much higher pH. The increased leachability of Pb is explained in [314] by possibly not equal proportion of conical glass in compared samples. In the same work [314] slag-based geopolymer is reported to decrease leachability of Pb. Thomas Opletal [314] reports that the

pH was ranging from 10,7 to 11,3 in dependence on the exact composition of metakaolin-based geopolymer. Catauro et al. [303] reports that after 28 days, metakaolin-based geopolymer containing 40% of powdered CRT glass shows pH at the level of about 10,5. This results is close to the result obtained within Thesis (28<sup>th</sup> day geopolymer had pH equal to 11,0). According to [303], pH is falling down along with the age of geopolymer. In contrary to results from this Thesis, the Pb leaching from geopolymer containing CRT glass was increased by over 115% in comparison to the pure CRT glass.

## CHAPTER 7 (SUMMARY AND CONCLUSIONS)

The main goal of this Thesis was to evaluate if discarded crushed CRT glass can be applied as an aggregate in metakaolin-based geopolymer and to assess if metakaolin-based geopolymer with CRT glass can be potentially used as a building material considering chosen aspects (mostly the mechanical behavior). Additionally, the aim of this Thesis was to describe properties of metakaolin-based geopolymer with CRT glass and to determine the influence of chosen factors on its characteristics.

The last subsection of Chapter 2 “2.6 State-of-the-art critical analysis and summary”, has been concluded with the following main deficiencies in the existing works devoted to geopolymer incorporating CRT glass: limited amount of works devoted to application of CRT glass in geopolymer in form of an aggregate, lack of in-depth investigation of one chosen type of geopolymer including determination of both compressive and flexural strength, density, porosity and toxic metals leaching as well as factors influencing mechanical strength (concentration of activator, size of aggregate particles, curing regime etc.). In the light of observed deficiencies, an Author made an extensive investigation on metakaolin-based geopolymer incorporating crushed CRT glass from the local waste disposal. The working process was divided into three main stages: preliminary research, main research and complementary research.

The main part of preliminary research was proceeded by the determination of CRT glass properties, determination of the influence of the CRT glass batch on the mechanical behavior of the geopolymer and comparison between geopolymer containing CRT glass with geopolymer containing sand. Then, Author was searching for an optimal mixture where the main variable was metakaolin to CRT glass mass ratio. In the next part, the influence of the curing temperature on the mechanical behavior was determined. The further investigation described the change of the strength over time and changes of temperature inside the geopolymer during curing process and was conducted on the optimal mixtures cured at the optimal curing conditions (both variables were chosen in the previous steps). The preliminary research was concluded with determination of one optimal mixture containing metakaolin to CRT glass in ratio 1:1.

The main research contained determination of the influence of curing time and curing temperature as well as activator concentration and CRT glass size on the mechanical characteristics. The flexural and compressive strength changes over time were determined as well.

The complementary tests have been conducted on the mixture containing CRT to metakolin in mass ratio 1:1 and cured at the ambient temperature. The tests included determination of porosity, density and physicochemical analysis of aqueous extracts from the hardened material and non-stable CRT glass.

The following conclusions were drawn during the research process:

- The CRT glass content does not influence significantly the mechanical behavior of geopolymer. However, in this Thesis only the mixture containing metakaolin to CRT glass in ratio 1:1 was subjected to the extended analysis while the maximal preliminary

tested CRT glass content was equal to 75% (by mass). Moreover, one should be aware that the mechanical behavior of mixtures containing different amount of CRT glass should be investigated carefully since the characteristics of geopolymer made of various mixtures can change in time. For instance, the mechanical strength of geopolymer containing metakaolin to CRT glass in ratio 1:1 increased in time while geopolymer containing metakaolin to CRT glass in ratio 1:3 had tendency to lose the strength in time. Moreover, one should be aware that the increase of CRT glass content decreases workability of the mixture and increases density of the material.

- Elevated curing temperature (during the research samples were cured at 40°C and 60°C) provides high early strength and ability of quick demolding (after 1 day of curing). Geopolymer cured at the ambient temperature has lower early strength and has to be kept longer in moulds to avoid cracking. However, long-term strength of geopolymer cured at ambient temperature surpass strength of geopolymer cured at elevated temperature. Besides, curing in ambient temperature is more economic and environmentally friendly solution.
- Sodium hydroxide activator of low concentration is cheaper and more environmentally friendly solution although, it results in lower flexural and compressive strength. High concentration increases strength but decreases workability of the mixture. During the research only concentrations in range 6-12 mol/L were investigated.
- Tested geopolymer shows the similar mechanical behavior (flexural and compressive strength) independently on the aggregate size. Maximal particle size used during the research was equal to 4 mm.
- The temperature inside material during curing increases along with the increase of metakaolin content. Temperature inside the material surpasses the external temperature (temperature in climatic chamber) by 24% and 15% respectively to the metakaolin content. Tests were done on samples of dimensions 40x40x160 mm.
- The number of toxic metals (lead, cadmium and chromium) leached from hardened material is reduced in comparison to amount of the same elements leached from unbounded CRT glass. The number of listed elements leached from hardened geopolymer fulfills the limit values.

Conclusions drawn in reference to hypothesis presented in Chapter “1.3 Hypotheses and limitations”:

1. Conducted tests have shown that CRT glass can be used as an aggregate without any special pretreatments in metakaolin-based geopolymer. During the research, tests has been done with the use of CRT glass from several batches. Flexural and compressive strength results achieved on geopolymer of the same composition and subjected to the same curing regime were similar independently on the batch of CRT glass. The size of used CRT glass particles did not show any significant impact on the strength as well. The toxic metals leaching test made with the use of atomic absorption spectrometry method has shown that geopolymer containing CRT glass which was not subjected to any pretreatment before application into the mixture, does not pose an environmental threat.

2. Metakaolin-based geopolymer with CRT glass is characterized by good mechanical characteristics. In dependence on various factors, it can achieve flexural strength equal to about 5-6 MPa and compressive strength equal to 50-60 MPa (long term compressive strength can reach over 70 MPa). The average density after demolding is equal to about 2100 kg/m<sup>3</sup> (about 2000 kg/m<sup>3</sup> when cured at elevated temperatures) and decreases with time to about 1850 kg/m<sup>3</sup>. The characteristics listed above are good enough to consider tested geopolymer as a building material (regarding only to the investigated features of the material). Flexural and compressive strength can be compared with high quality concrete. Material is relatively brittle what should be taken into account during designing. The issue of application of tested material as a structural building element requires the essential further future analysis including the description of rheology, durability, an impact of material on living organisms and on reinforcement.
3. Metakaolin-based geopolymer with CRT glass has been cured both at ambient temperature and at elevated temperatures (40°C or 60°C for the first 24 hours). Independently on the curing regime, geopolymer achieved acceptable values of both flexural and compressive strength although, curing temperature had more visible impact on flexural than on compressive strength. Geopolymer cured at ambient temperature has to be kept in moulds longer than geopolymer cured at elevated temperature to avoid cracks. According to the observations, demolding of geopolymer cured at ambient temperature after 7 days is enough to avoid extent shrinkage and cracking of the material.
4. According to the toxic metals leaching test made with the use of atomic absorption spectrometry, the number of heavy metals leached from the broken, hardened metakaolin-based geopolymer containing CRT glass fulfills required regulations. Moreover, the amount of chosen heavy metals leached from the hardened material is considerably smaller than from non-stabilized CRT glass what means that incorporation of CRT glass into the geopolymer matrix limits leaching of toxic elements. The only investigated characteristic which did not fulfill regulatory limits was pH which was slightly below the lowest allowed value. That issue should be taken into account during the future researches together with the following essential problems such as the behavior of material in different humidity or the accordance with the exposure classes.

## CHAPTER 8 (DIRECTIONS FOR FURTHER RESEARCH)

The investigation presented in this Thesis is an important contribution to the topic of the possibility of application of metakaolin-based geopolymer with CRT glass as a building material in the civil engineering branch of science. However, the performed tests state only the first part of the whole investigation process which should be done before acceptance of new material and its application on construction sites. Therefore, the author is planning to continue investigation on metakaolin-based geopolymer with aggregate in form of CRT glass. One of the first future steps will be the determination of durability of geopolymer of new composition developed within this Thesis. The changes of the strength through the years, the influence of wet conditions and influence of freeze and thaw cycles on mechanical behavior, the rheology as well as an impact of material on living organisms and on reinforcement are obligatory directions of further investigation if new material is to be applied in civil engineering. Obviously, the author is planning also big-scale tests. The consideration of big size construction units implies consideration of aggregate of bigger fractions than used so far. The author is weighing up prospects of application of bigger CRT glass particles or conjunction of CRT glass as a fine aggregate with one of commonly used coarse aggregates.

The next important direction is the determination of the mechanical behavior in the multiaxial stress state and determination of the boundary surface of the geopolymer. Determination of the boundary surface of geopolymer allows for the establishment of its material model which could be introduced to appropriate software for numerical analyses. It enables designing construction elements made of geopolymer using the computer software. The main idea, procedure and first attempts of determination of the boundary surface of geopolymer basing on another precursor (tungsten mine waste mud) is described by the author of this Thesis and coauthors in [332].

An extension of scientific research in the area of possible negative impact of tested geopolymer on the human health and the environment is also the important path of further investigation. The leaching tests presented in section "5.2 Physicochemical characteristics" indicates that heavy metals are effectively neutralized within the matrix, nevertheless, tests should be extended especially, if discussed geopolymer is to be considered for the external applications. Tests should cover among the others the influence of the material fatigue and any possible external impacts on the heavy metal's encapsulation capabilities.

## Abstract

Nowadays, the world is facing serious environmental problems. The huge emission of CO<sub>2</sub>, the enlarging consumption of water and the quantity of discarded waste are one of the existing threats. Scientists are looking for new, environmental friendly solutions in many branches. The concrete manufacture is responsible for significant amount of released CO<sub>2</sub> and consumed water. The part or total replacement of concrete by other materials in some investments is one of the possible ways to help the environment. The geopolymer, material created by mixing of an aluminosilicate powder (precursor) and liquid activator, is considered as an excellent alternative for a concrete. Geopolymer has similar mechanical properties and can be casted, but its manufacture requires less water and emits less CO<sub>2</sub>. Moreover, the production of geopolymer enable to reuse the various types of waste. This, recently extensively explored material, has a long history and numerous potential applications such as in the role of a building material, in restoration of monuments, in stabilization of hazardous waste, in reparation of existing structures, in 3D printing, in self-repairing materials and in protection of concrete or steel structures.

Geopolymers states the subject of the numerous researches all over the world but its characteristics are still not fully known. The majority of existing works focuses on the composition with some kind of waste in the role of a precursor and the natural aggregate (mainly sand). The following Thesis presents the new type of geopolymer which consists of metakaolin and crushed, discarded CRT glass in the role of an aggregate. The described geopolymer can help the environment by being the alternative for a concrete. Moreover, it proposes the new kind of waste aggregate for geopolymers production and states the method of recycling of CRT glass which disposal is considered as a serious environmental threat because of the Pb content. The works on geopolymer with CRT glass aggregate states the completion of existing researches which present mainly the use of CRT glass in powdered form. Additionally, this Thesis presents a deep study on one type of geopolymer containing CRT glass, as an answer to the defined deficiencies in the existing publications.

This Thesis presents three stages of research on the novel, metakaolin-based geopolymer with CRT glass aggregate. The initial research contains description of all used materials and research methods, the determination of optimal CRT glass content, determination of the optimal curing temperature, the measurement of temperature changes inside the cured geopolymer and change of the strength over time. In all tests, both the flexural and compressive strength have been examined. As the result of the initial tests, the one optimal mixture has been chosen for the next part of the research. The main part focuses on the influence of different factors on geopolymer's mechanical behavior. The change of the strength over time of samples cured at different temperatures has been compared. Then, the influence of the activator concentration and the CRT glass particle size have been determined. The last part presents the complementary tests and contains the determination of porosity of geopolymer and its physicochemical characteristics, including the ability to stabilize the chosen heavy metals present in the CRT glass.

This Thesis is concluded with the summarization of all results with respect to the determined deficiencies in the existing works and with initially assumed goals. At the very end, the directions for the further research have been introduced.

## List of symbols

Al – aluminum  
AlO<sub>4</sub><sup>-</sup> - aluminate oxyanion  
Al<sub>2</sub>O<sub>3</sub> – aluminum oxide  
As – arsenic  
*b* – width of sample  
Ba – barium  
BaO – barium oxide  
Ca – calcium  
CaCO<sub>3</sub> – calcium carbonate  
CaO – calcium oxide  
Cd – cadmium  
Cl – chlorine  
Co – cobalt  
CO<sub>2</sub> – carbon dioxide  
Cr – chromium  
Cu – copper  
°C – Celsius degrees  
g/cm<sup>3</sup> – gram per cubic centimeter  
g/mol – gram per mole  
h – hour  
*h* – height of sample  
Hg - mercury  
H<sub>2</sub>O – dihydrogen monoxide (water)  
Fe – iron  
Fe<sub>2</sub>O<sub>3</sub> – ferric oxide  
*f<sub>c</sub>* – compressive strength  
*f'<sub>c</sub>* – specified compressive strength  
*f<sub>cm</sub>* – mean cylinder strength  
*f<sub>ct,f</sub>* – mean characteristic flexural  
*f<sub>r</sub>* – modulus of rupture  
*f<sub>x</sub>* – flexural strength  
K – potassium  
K<sub>2</sub>O – potassium oxide  
KOH – Potassium hydroxide  
l – liter  
*l<sub>1</sub>* – distance between supports  
M - molar  
MgO – magnesium oxide  
M/G – metakaolin/ CRT glass  
mm – millimetre  
Mn - manganese  
kg/m<sup>3</sup> – kilogram per cubic meter  
mg/m<sup>2</sup> – milligrams per square meter  
mg/l – milligrams per litre  
Mn – manganese

MPa – megapascal  
 $m_1$  - mass of dry sample, measured in air  
 $m_2$  - mass of saturated sample, measured in water  
 $m_3$  - mass of saturated sample, measured in air  
Na – sodium  
Na<sup>+</sup> - sodium ion  
Na<sub>2</sub>O – sodium oxide  
NaOH – sodium hydroxide  
Ni – nickel  
N/s – Newton per second  
O – oxygen  
OH<sup>-</sup> - hydroxide  
 $P$  - maximal compressive force in the moment of sample failure  
pH – potential of hydrogen  
Pb – lead  
PbO – lead monoxide  
Po – open porosity  
Pt – total porosity  
SO<sub>2</sub> – sulphur dioxide  
Si – silicon  
SiO<sub>2</sub> – silicon dioxide  
Sn – tin  
V<sub>p</sub> – apparent volume  
WA – water absorption  
X-ray – roentgen radiation  
Zn – zinc  
μm – micrometer  
 $\rho_a$  – 0,001205 g/cm<sup>3</sup> - density of air in temperature 20 ± 1°C  
 $\rho_p$  – apparent density of sample  
 $\rho_s$  – density of sample  
 $\rho_w$  – 0,998203 g/cm<sup>3</sup> - density of deionized water in temperature 20 ± 1°C

## List of abbreviations

AAS – atomic absorption spectrometry  
ACI – American Concrete Institute  
AGH – Akademia Górniczo-Hutnicza  
3D – three dimensional  
CFC - Cold Fusion Concrete  
CoV – coefficient of variation  
CRT – cathode ray tube  
CT – computerized tomography  
DSC - differential scanning calorimetry  
EDX – energy dispersive X-ray analysis  
EDXRD – energy dispersive X-ray diffractometry  
EN – European Norm (European Standards)  
ESEM - environmental scanning electron microscopy  
Et al. – et alia (and others)  
GGBFS - ground granulated blast furnace slag  
i.e. – id est (that is)  
LCD - liquid crystal display  
LED - light-emitting diode  
NMR - nuclear magnetic resonance  
OPC – ordinary Portland cement  
PCM – phase change materials  
PDP - plasma display panels  
PN – Polska Norma  
RTC – real time clock  
S.A. – societe anonyme (public limited company)  
SD – secure digital  
SEM – scanning electron microscope  
TCLP – toxicity characteristic leaching procedure  
U.S. – United States  
WEEE – waste electrical and electronic equipment  
Wi-fi – wireless fidelity  
wt% - percentage by weight  
XRD – X-ray diffraction  
XRF – X-ray fluorescence

## References

- [1] United Nations Environment Programme, *Emissions Gap Report 2020*. Nairobi: United Nations Environment Programme, 2020. Accessed: Apr. 12, 2021. [Online]. Available: <https://www.unep.org/emissions-gap-report-2020>
- [2] United Nations Environment Programme, 'Emission Gap Report 2022', in *The Closing Window: Climate crisis calls for rapid transformation of societies : Emissions Gap Report 2022*, Nairobi, 2022, p. 132. Accessed: Mar. 11, 2023. [Online]. Available: <https://www.unep.org/resources/emissions-gap-report-2022>
- [3] 'Paris Agreement'. United Nations, 2015. Accessed: Mar. 11, 2023. [Online]. Available: [https://unfccc.int/sites/default/files/english\\_paris\\_agreement.pdf](https://unfccc.int/sites/default/files/english_paris_agreement.pdf)
- [4] 'United Nations Climate Change', *The Paris Agreement*. <https://unfccc.int/process-and-meetings/the-paris-agreement> (accessed Mar. 11, 2023).
- [5] Garside, M., 'Statista', *Cement production worldwide from 1995 to 2020*, Mar. 19, 2021. <https://www.statista.com/statistics/1087115/global-cement-production-volume/#statisticContainer> (accessed Apr. 12, 2021).
- [6] Levi, Peter, Vass, Tiffany, Mandová, Hana, and Gouy, Alexander, 'Cement', IEA, Paris, Tracking report, Jun. 2020. Accessed: Apr. 12, 2021. [Online]. Available: <https://www.iea.org/reports/cement>
- [7] Andrew, Robbie, M., 'Global CO<sub>2</sub> emissions from cement production, 1928–2018', *Earth System Science Data*, no. 11, pp. 1675–1710, 2019.
- [8] A. M. Neville, *Properties of concrete*, 5th ed. Harlow, England ; New York: Pearson, 2011.
- [9] A. Arrigoni *et al.*, 'Life cycle greenhouse gas emissions of concrete containing supplementary cementitious materials: cut-off vs. substitution', *Journal of Cleaner Production*, vol. 263, p. 121465, Aug. 2020, doi: 10.1016/j.jclepro.2020.121465.
- [10] S. A. Miller, 'Supplementary cementitious materials to mitigate greenhouse gas emissions from concrete: can there be too much of a good thing?', *Journal of Cleaner Production*, vol. 178, pp. 587–598, Mar. 2018, doi: 10.1016/j.jclepro.2018.01.008.
- [11] de Brito, Jorge and Agrela, Francisco, 'New Trends in Eco-efficient and Recycled Concrete', in *New Trends in Eco-efficient and Recycled Concrete*, Elsevier, 2019, pp. i–iii. doi: 10.1016/B978-0-08-102480-5.00022-1.
- [12] A. Król, Z. Giergiczny, and J. Kuterasińska-Warwas, 'Properties of Concrete Made with Low-Emission Cements CEM II/C-M and CEM VI', *Materials*, vol. 13, no. 10, p. 2257, May 2020, doi: 10.3390/ma13102257.
- [13] Giergiczny, Zbigniew and Synowiec Katarzyna, 'Popiół lotny i granulowany żużel wielopieczowy składnikami cementu o niskiej emisji CO<sub>2</sub>.', presented at the Dni betonu. Tradycja i nowoczesność., Wisła: Stowarzyszenie Producentów Cementu, 14.10 2014, pp. 529–538.
- [14] L. Czarnecki and H. Justnes, 'Sustainable and Durable Concrete (Zrównoważony, trwały beton)', *Cement, Wapno, Beton*, vol. 17/79, no. 6, pp. 341–362, 2012.
- [15] Nazari, Ali and Sanjayan, Jay G., 'Handbook of Low Carbon Concrete', in *Handbook of Low Carbon Concrete*, Elsevier, 2017, pp. i–iii. doi: 10.1016/B978-0-12-804524-4.00016-6.
- [16] L. K. Turner and F. G. Collins, 'Carbon dioxide equivalent (CO<sub>2</sub>-e) emissions: A comparison between geopolymer and OPC cement concrete', *Construction and Building Materials*, vol. 43, pp. 125–130, Jun. 2013, doi: 10.1016/j.conbuildmat.2013.01.023.
- [17] P. Duxson, J. L. Provis, G. C. Lukey, and J. S. J. van Deventer, 'The role of inorganic polymer technology in the development of "green concrete"', *Cement and Concrete Research*, vol. 37, no. 12, pp. 1590–1597, Dec. 2007, doi: 10.1016/j.cemconres.2007.08.018.

- [18] S. A. Miller, Horvath, Arpad, and Monteiro, Paulo J. M., 'Impacts of booming concrete production on water resources worldwide', *Nature Sustainability*, vol. 1, pp. 69–76, 2018, doi: 10.1038/s41893-017-0009-5.
- [19] 'Water policy', *Cementirholding*, Apr. 21, 2023. <https://www.cementirholding.com/en/sustainability/our-commitment-environment/water-policy> (accessed May 26, 2023).
- [20] 'DECARBONIZING BUILDING SUSTAINABILITY PERFORMANCE REPORT 2022', *Holcim Sustainability Performance Report 2022*. [https://annual-report.holcim.com/fileadmin/user\\_upload/2022/pdf/24022023-sustainability-holcim-fy-2022-report-en-3114693266.pdf](https://annual-report.holcim.com/fileadmin/user_upload/2022/pdf/24022023-sustainability-holcim-fy-2022-report-en-3114693266.pdf) (accessed May 26, 2023).
- [21] K. Neupane, "'Fly ash and GGBFS based powder-activated geopolymer binders: A viable sustainable alternative of portland cement in concrete industry'", *Mechanics of Materials*, vol. 103, pp. 110–122, Dec. 2016, doi: 10.1016/j.mechmat.2016.09.012.
- [22] D. B. Istuque *et al.*, 'Effect of sewage sludge ash on mechanical and microstructural properties of geopolymers based on metakaolin', *Construction and Building Materials*, vol. 203, pp. 95–103, Apr. 2019, doi: 10.1016/j.conbuildmat.2019.01.093.
- [23] Sitarz, Mateusz, Zdeb, Tomasz, Castro Gomes, João, Grünhäuser Soare, Eric, and Hager, Izabela, 'The immobilisation of heavy metals from sewage sludge ash in geopolymer mortars', in *MATEC Web of Conferences*, Kraków, Poland: EDP Sciences, 21.10 2020, pp. 1–8. doi: 10.1051/mateconf/202032201026.
- [24] B. Ren, Y. Zhao, H. Bai, S. Kang, T. Zhang, and S. Song, 'Eco-friendly geopolymer prepared from solid wastes: A critical review', *Chemosphere*, vol. 267, p. 128900, Mar. 2021, doi: 10.1016/j.chemosphere.2020.128900.
- [25] P. Zhang, K. Wang, Q. Li, J. Wang, and Y. Ling, 'Fabrication and engineering properties of concretes based on geopolymers/alkali-activated binders - A review', *Journal of Cleaner Production*, vol. 258, p. 120896, Jun. 2020, doi: 10.1016/j.jclepro.2020.120896.
- [26] S. Mabroum, S. Moukannaa, A. El Machi, Y. Taha, M. Benzaazoua, and R. Hakkou, 'Mine wastes based geopolymers: A critical review', *Cleaner Engineering and Technology*, vol. 1, p. 100014, Dec. 2020, doi: 10.1016/j.clet.2020.100014.
- [27] S. Luhar, T.-W. Cheng, D. Nicolaidis, I. Luhar, D. Panias, and K. Sakkas, 'Valorisation of glass wastes for the development of geopolymer composites – Durability, thermal and microstructural properties: A review', *Construction and Building Materials*, vol. 222, pp. 673–687, Oct. 2019, doi: 10.1016/j.conbuildmat.2019.06.169.
- [28] Hardjito, D. and Rangan, B.V., 'Development and Properties of Low-Calcium Fly Ash-Based Geopolymer Concrete', Faculty of Engineering, Curtin University of Technology, Perth, Australia, GC 1, 2005.
- [29] M. Sitarz, M. Urban, and I. Hager, 'Rheology and Mechanical Properties of Fly Ash-Based Geopolymer Mortars with Ground Granulated Blast Furnace Slag Addition', *Energies*, vol. 13, no. 10, p. 2639, May 2020, doi: 10.3390/en13102639.
- [30] F. Pacheco-Torgal, J. Castro-Gomes, and S. Jalali, 'Properties of tungsten mine waste geopolymeric binder', *Construction and Building Materials*, vol. 22, no. 6, pp. 1201–1211, Jun. 2008, doi: 10.1016/j.conbuildmat.2007.01.022.
- [31] S. Top and H. Vapur, 'Effect of basaltic pumice aggregate addition on the material properties of fly ash based lightweight geopolymer concrete', *Journal of Molecular Structure*, vol. 1163, pp. 10–17, Jul. 2018, doi: 10.1016/j.molstruc.2018.02.114.
- [32] S. Akçaözöğlü and C. Ulu, 'Recycling of waste PET granules as aggregate in alkali-activated blast furnace slag/metakaolin blends', *Construction and Building Materials*, vol. 58, pp. 31–37, May 2014, doi: 10.1016/j.conbuildmat.2014.02.011.
- [33] L. Y. Loon, 'BIOMASS AGGREGATE GEOPOLYMER CONCRETE – MALAYSIA EXPERIENCE', *International Journal of Civil Engineering and Technology*, vol. 5, no. 3, pp. 340–356, 2014.

- [34] M. S. H. Khan, A. Castel, A. Akbarnezhad, S. J. Foster, and M. Smith, 'Utilisation of steel furnace slag coarse aggregate in a low calcium fly ash geopolymer concrete', *Cement and Concrete Research*, vol. 89, pp. 220–229, Nov. 2016, doi: 10.1016/j.cemconres.2016.09.001.
- [35] M. Panizza, M. Natali, E. Garbin, S. Tamburini, and M. Secco, 'Assessment of geopolymers with Construction and Demolition Waste (CDW) aggregates as a building material', *Construction and Building Materials*, vol. 181, pp. 119–133, Aug. 2018, doi: 10.1016/j.conbuildmat.2018.06.018.
- [36] X. Yao, Z. Zhang, H. Zhu, and Y. Chen, 'Geopolymerization process of alkali–metakaolinite characterized by isothermal calorimetry', *Thermochimica Acta*, vol. 493, no. 1–2, pp. 49–54, Sep. 2009, doi: 10.1016/j.tca.2009.04.002.
- [37] K. J. D. MacKenzie, 'What are These Things Called Geopolymers? A Physicochemical Perspective', in *Ceramic Transactions Series*, N. P. Bansal, J. P. Singh, W. M. Kriven, and H. Schneider, Eds., Hoboken, NJ, USA: John Wiley & Sons, Inc., 2012, pp. 173–186. doi: 10.1002/9781118406892.ch12.
- [38] P. D. Silva, K. Sagoe-Crenstil, and V. Sirivivatnanon, 'Kinetics of geopolymerization: Role of Al<sub>2</sub>O<sub>3</sub> and SiO<sub>2</sub>', *Cement and Concrete Research*, vol. 37, no. 4, pp. 512–518, Apr. 2007, doi: 10.1016/j.cemconres.2007.01.003.
- [39] L. Hou, J. Li, and Z. Lu, 'Effect of Na/Al on formation, structures and properties of metakaolin based Na-geopolymer', *Construction and Building Materials*, vol. 226, pp. 250–258, Nov. 2019, doi: 10.1016/j.conbuildmat.2019.07.171.
- [40] H. Rahier, J. Wastiels, M. Biesemans, R. Willem, G. Van Assche, and B. Van Mele, 'Reaction mechanism, kinetics and high temperature transformations of geopolymers', *J Mater Sci*, vol. 42, no. 9, pp. 2982–2996, May 2007, doi: 10.1007/s10853-006-0568-8.
- [41] J. Davidovits, 'Geopolymers: Inorganic polymeric new materials', *Journal of Thermal Analysis*, vol. 37, pp. 1633–1656, 1991.
- [42] R. A. Fletcher, K. J. D. MacKenzie, C. L. Nicholson, and S. Shimada, 'The composition range of aluminosilicate geopolymers', *Journal of the European Ceramic Society*, vol. 25, no. 9, pp. 1471–1477, Jun. 2005, doi: 10.1016/j.jeurceramsoc.2004.06.001.
- [43] J. Mikuła and M. Łach, 'Wytwarzanie i właściwości geopolimerów na bazie tufu wulkanicznego', *INŻYNIERIA MATERIAŁOWA*, no. 3, pp. 270–276, 2014.
- [44] G. Ascensão, M. P. Seabra, J. B. Aguiar, and J. A. Labrincha, 'Red mud-based geopolymers with tailored alkali diffusion properties and pH buffering ability', *Journal of Cleaner Production*, vol. 148, pp. 23–30, Apr. 2017, doi: 10.1016/j.jclepro.2017.01.150.
- [45] Z. Pan, L. Cheng, Y. Lu, and N. Yang, 'Hydration products of alkali-activated slag–red mud cementitious material', *Cement and Concrete Research*, vol. 32, no. 3, pp. 357–362, Mar. 2002, doi: 10.1016/S0008-8846(01)00683-4.
- [46] N. Toniolo, A. Rincón, Y. S. Avadhut, M. Hartmann, E. Bernardo, and A. R. Boccaccini, 'Novel geopolymers incorporating red mud and waste glass cullet', *Materials Letters*, vol. 219, pp. 152–154, May 2018, doi: 10.1016/j.matlet.2018.02.061.
- [47] M. Zhang *et al.*, 'Reaction kinetics of red mud-fly ash based geopolymers: Effects of curing temperature on chemical bonding, porosity, and mechanical strength', *Cement and Concrete Composites*, vol. 93, pp. 175–185, Oct. 2018, doi: 10.1016/j.cemconcomp.2018.07.008.
- [48] A. B. Pascual, M. T. Tognonvi, and A. Tagnit-Hamou, 'WASTE GLASS POWDER-BASED ALKALI-ACTIVATED MORTAR', p. 5.
- [49] H. Rashidian-Dezfouli and P. R. Rangaraju, 'A comparative study on the durability of geopolymers produced with ground glass fiber, fly ash, and glass-powder in sodium sulfate solution', *Construction and Building Materials*, vol. 153, pp. 996–1009, Oct. 2017, doi: 10.1016/j.conbuildmat.2017.07.139.
- [50] M. R. El-Naggar and M. I. El-Dessouky, 'Re-use of waste glass in improving properties of metakaolin-based geopolymers: Mechanical and microstructure examinations', *Construction and Building Materials*, vol. 132, pp. 543–555, Feb. 2017, doi: 10.1016/j.conbuildmat.2016.12.023.

- [51] Z. Emdadi *et al.*, 'Development of Green Geopolymer Using Agricultural and Industrial Waste Materials with High Water Absorbency', *Applied Sciences*, vol. 7, no. 5, p. 514, May 2017, doi: 10.3390/app7050514.
- [52] A. Pereira *et al.*, 'Mechanical and durability properties of alkali-activated mortar based on sugarcane bagasse ash and blast furnace slag', *Ceramics International*, vol. 41, no. 10, pp. 13012–13024, Dec. 2015, doi: 10.1016/j.ceramint.2015.07.001.
- [53] P. Shekhawat, G. Sharma, and R. M. Singh, 'Strength behavior of alkaline activated eggshell powder and flyash geopolymer cured at ambient temperature', *Construction and Building Materials*, vol. 223, pp. 1112–1122, Oct. 2019, doi: 10.1016/j.conbuildmat.2019.07.325.
- [54] F. Matalkah, P. Soroushian, S. Ul Abideen, and A. Peyvandi, 'Use of non-wood biomass combustion ash in development of alkali-activated concrete', *Construction and Building Materials*, vol. 121, pp. 491–500, Sep. 2016, doi: 10.1016/j.conbuildmat.2016.06.023.
- [55] F. A. Kuranchie, S. K. Shukla, and D. Habibi, 'Utilisation of iron ore mine tailings for the production of geopolymer bricks', *International Journal of Mining, Reclamation and Environment*, vol. 30, no. 2, pp. 92–114, Mar. 2016, doi: 10.1080/17480930.2014.993834.
- [56] B. Wei, Y. Zhang, and S. Bao, 'Preparation of geopolymers from vanadium tailings by mechanical activation', *Construction and Building Materials*, vol. 145, pp. 236–242, Aug. 2017, doi: 10.1016/j.conbuildmat.2017.03.234.
- [57] S. Moukannaa, M. Loutou, M. Benzaazoua, L. Vitola, J. Alami, and R. Hakkou, 'Recycling of phosphate mine tailings for the production of geopolymers', *Journal of Cleaner Production*, vol. 185, pp. 891–903, Jun. 2018, doi: 10.1016/j.jclepro.2018.03.094.
- [58] I. Fatimah, P. W. Citradewi, R. M. Iqbal, S. A. I. S. M. Ghazali, A. Yahya, and G. Purwiandono, 'Geopolymer from Tin Mining tailings Waste using Salacca Leaves Ash as Activator for Dyes and Peat Water Adsorption', *South African Journal of Chemical Engineering*, p. 27, Nov. 2022, doi: 10.1016/j.sajce.2022.11.008.
- [59] S. Horpibulsuk, C. Suksiripattanapong, W. Samingthong, R. Rachan, and A. Arulrajah, 'Durability against Wetting–Drying Cycles of Water Treatment Sludge–Fly Ash Geopolymer and Water Treatment Sludge–Cement and Silty Clay–Cement Systems', *J. Mater. Civ. Eng.*, vol. 28, no. 1, p. 04015078, Jan. 2016, doi: 10.1061/(ASCE)MT.1943-5533.0001351.
- [60] M. Merabtene, L. Kacimi, and P. Clastres, 'Elaboration of geopolymer binders from poor kaolin and dam sludge waste', *Heliyon*, vol. 5, no. 6, p. e01938, Jun. 2019, doi: 10.1016/j.heliyon.2019.e01938.
- [61] K.-L. Lin, K.-W. Lo, T.-W. Cheng, W.-T. Lin, and Y.-W. Lin, 'Utilization of Silicon Carbide Sludge as Metakaolin-Based Geopolymer Materials', *Sustainability*, vol. 12, no. 18, p. 7333, Sep. 2020, doi: 10.3390/su12187333.
- [62] J. Provis, *Alkali activated materials: state-of-the-art report*, RILEM TC 224-AAM. New York: Springer, 2013.
- [63] J. L. Provis, S. L. Yong, and P. Duxson, 'Nanostructure/microstructure of metakaolin geopolymers', in *Geopolymers*, Elsevier, 2009, pp. 72–88. doi: 10.1533/9781845696382.1.72.
- [64] X. Y. Zhuang *et al.*, 'Fly ash-based geopolymer: clean production, properties and applications', *Journal of Cleaner Production*, vol. 125, pp. 253–267, Jul. 2016, doi: 10.1016/j.jclepro.2016.03.019.
- [65] P. Chindaprasirt, S. Jenjirapanya, and U. Rattanasak, 'Characterizations of FBC/PCC fly ash geopolymeric composites', *Construction and Building Materials*, vol. 66, pp. 72–78, Sep. 2014, doi: 10.1016/j.conbuildmat.2014.05.067.
- [66] Z. Giergiczny, 'Fly ash and slag', *Cement and Concrete Research*, vol. 124, p. 105826, Oct. 2019, doi: 10.1016/j.cemconres.2019.105826.
- [67] A. Fernández-Jiménez, J. G. Palomo, and F. Puertas, 'Alkali-activated slag mortars Mechanical strength behaviour', *Cement and Concrete Research*, p. 9, 1999.
- [68] K.-H. Yang, A.-R. Cho, and J.-K. Song, 'Effect of water–binder ratio on the mechanical properties of calcium hydroxide-based alkali-activated slag concrete', *Construction and Building Materials*, vol. 29, pp. 504–511, Apr. 2012, doi: 10.1016/j.conbuildmat.2011.10.062.

- [69] T. W. Cheng and J. P. Chiu, 'Fire-resistant geopolymer produced by granulated blast furnace slag', *Minerals Engineering*, vol. 16, no. 3, pp. 205–210, Mar. 2003, doi: 10.1016/S0892-6875(03)00008-6.
- [70] A. Kallamalayil Nassar and P. Kathirvel, 'Effective utilization of agricultural waste in synthesizing activator for sustainable geopolymer technology', *Construction and Building Materials*, vol. 362, p. 129681, Jan. 2023, doi: 10.1016/j.conbuildmat.2022.129681.
- [71] A. Sathonsaowaphak, P. Chindaprasirt, and K. Pimraksa, 'Workability and strength of lignite bottom ash geopolymer mortar', *Journal of Hazardous Materials*, vol. 168, no. 1, pp. 44–50, Aug. 2009, doi: 10.1016/j.jhazmat.2009.01.120.
- [72] P. Duxson, S. W. Mallicoat, G. C. Lukey, W. M. Kriven, and J. S. J. van Deventer, 'The effect of alkali and Si/Al ratio on the development of mechanical properties of metakaolin-based geopolymers', *Colloids and Surfaces A: Physicochemical and Engineering Aspects*, vol. 292, no. 1, pp. 8–20, Jan. 2007, doi: 10.1016/j.colsurfa.2006.05.044.
- [73] A. A. Arslan *et al.*, 'Influence of wetting-drying curing system on the performance of fiber reinforced metakaolin-based geopolymer composites', *Construction and Building Materials*, vol. 225, pp. 909–926, Nov. 2019, doi: 10.1016/j.conbuildmat.2019.07.235.
- [74] N. Belmokhtar, M. Ammari, J. Brigui, and L. Ben allal, 'Comparison of the microstructure and the compressive strength of two geopolymers derived from Metakaolin and an industrial sludge', *Construction and Building Materials*, vol. 146, pp. 621–629, Aug. 2017, doi: 10.1016/j.conbuildmat.2017.04.127.
- [75] S. Chen, C. Wu, and D. Yan, 'Binder-scale creep behavior of metakaolin-based geopolymer', *Cement and Concrete Research*, vol. 124, p. 105810, Oct. 2019, doi: 10.1016/j.cemconres.2019.105810.
- [76] M. A. Longhi, B. Walkley, E. D. Rodríguez, A. P. Kirchheim, Z. Zhang, and H. Wang, 'New selective dissolution process to quantify reaction extent and product stability in metakaolin-based geopolymers', *Composites Part B: Engineering*, vol. 176, p. 107172, Nov. 2019, doi: 10.1016/j.compositesb.2019.107172.
- [77] M. Sarkar, K. Dana, and S. Das, 'Microstructural and phase evolution in metakaolin geopolymers with different activators and added aluminosilicate fillers', *Journal of Molecular Structure*, vol. 1098, pp. 110–118, Oct. 2015, doi: 10.1016/j.molstruc.2015.05.046.
- [78] C. Dupuy, J. Havette, A. Gharzouni, N. Texier-Mandoki, X. Bourbon, and S. Rossignol, 'Metakaolin-based geopolymer: Formation of new phases influencing the setting time with the use of additives', *Construction and Building Materials*, vol. 200, pp. 272–281, Mar. 2019, doi: 10.1016/j.conbuildmat.2018.12.114.
- [79] Q. Wan *et al.*, 'Geopolymerization reaction, microstructure and simulation of metakaolin-based geopolymers at extended Si/Al ratios', *Cement and Concrete Composites*, vol. 79, pp. 45–52, May 2017, doi: 10.1016/j.cemconcomp.2017.01.014.
- [80] M. Lizcano, A. Gonzalez, S. Basu, K. Lozano, and M. Radovic, 'Effects of Water Content and Chemical Composition on Structural Properties of Alkaline Activated Metakaolin-Based Geopolymers', *J. Am. Ceram. Soc.*, vol. 95, no. 7, pp. 2169–2177, Jul. 2012, doi: 10.1111/j.1551-2916.2012.05184.x.
- [81] C. Kuenzel, L. J. Vandeperre, S. Donatello, A. R. Boccaccini, and C. Cheeseman, 'Ambient Temperature Drying Shrinkage and Cracking in Metakaolin-Based Geopolymers', *J. Am. Ceram. Soc.*, vol. 95, no. 10, pp. 3270–3277, Oct. 2012, doi: 10.1111/j.1551-2916.2012.05380.x.
- [82] I. Perná, M. Šupová, T. Hanzlíček, and A. Špaldoňová, 'The synthesis and characterization of geopolymers based on metakaolin and high LOI straw ash', *Construction and Building Materials*, vol. 228, p. 116765, Dec. 2019, doi: 10.1016/j.conbuildmat.2019.116765.
- [83] Z. Sun and A. Vollpracht, 'One year geopolymerisation of sodium silicate activated fly ash and metakaolin geopolymers', *Cement and Concrete Composites*, vol. 95, pp. 98–110, Jan. 2019, doi: 10.1016/j.cemconcomp.2018.10.014.

- [84] P. He *et al.*, 'Effects of Si/Al ratio on the structure and properties of metakaolin based geopolymer', *Ceramics International*, vol. 42, no. 13, pp. 14416–14422, Oct. 2016, doi: 10.1016/j.ceramint.2016.06.033.
- [85] M. Lahoti, P. Narang, K. H. Tan, and E.-H. Yang, 'Mix design factors and strength prediction of metakaolin-based geopolymer', *Ceramics International*, vol. 43, no. 14, pp. 11433–11441, Oct. 2017, doi: 10.1016/j.ceramint.2017.06.006.
- [86] S. Riahi, A. Nemati, A. R. Khodabandeh, and S. Baghshahi, 'The effect of mixing molar ratios and sand particles on microstructure and mechanical properties of metakaolin-based geopolymers', *Materials Chemistry and Physics*, vol. 240, p. 122223, Jan. 2020, doi: 10.1016/j.matchemphys.2019.122223.
- [87] M. Rowles and B. O'Connor, 'Chemical optimisation of the compressive strength of aluminosilicate geopolymers synthesised by sodium silicate activation of metakaolinite', *J. Mater. Chem.*, vol. 13, no. 5, pp. 1161–1165, Apr. 2003, doi: 10.1039/b212629j.
- [88] A. Kamaloo, Y. Ganjkanlou, S. H. Aboutaleb, and H. Nouranian, 'Modeling of compressive strength of metakaolin based geopolymers by the use of artificial neural network', *IJE Transactions A: Basics*, vol. 23, no. 2, pp. 145–152, Apr. 2010.
- [89] K. Juengsuwattananon, F. Winnefeld, P. Chindaprasirt, and K. Pimraksa, 'Correlation between initial SiO<sub>2</sub>/Al<sub>2</sub>O<sub>3</sub>, Na<sub>2</sub>O/Al<sub>2</sub>O<sub>3</sub>, Na<sub>2</sub>O/SiO<sub>2</sub> and H<sub>2</sub>O/Na<sub>2</sub>O ratios on phase and microstructure of reaction products of metakaolin-rice husk ash geopolymer', *Construction and Building Materials*, vol. 226, pp. 406–417, Nov. 2019, doi: 10.1016/j.conbuildmat.2019.07.146.
- [90] D. Yan, S. Chen, Q. Zeng, S. Xu, and H. Li, 'Correlating the elastic properties of metakaolin-based geopolymer with its composition', *Materials & Design*, vol. 95, pp. 306–318, Apr. 2016, doi: 10.1016/j.matdes.2016.01.107.
- [91] V. F. F. Barbosa, K. J. D. MacKenzie, and C. Thaumaturgo, 'Synthesis and characterisation of materials based on inorganic polymers of alumina and silica: sodium polysialate polymers', *International Journal of Inorganic Materials*, vol. 2, no. 4, pp. 309–317, Sep. 2000, doi: 10.1016/S1466-6049(00)00041-6.
- [92] M. Lahoti, K. K. Wong, E.-H. Yang, and K. H. Tan, 'Effects of Si/Al molar ratio on strength endurance and volume stability of metakaolin geopolymers subject to elevated temperature', *Ceramics International*, vol. 44, no. 5, pp. 5726–5734, Apr. 2018, doi: 10.1016/j.ceramint.2017.12.226.
- [93] I. Ozer and S. Soyer-Uzun, 'Relations between the structural characteristics and compressive strength in metakaolin based geopolymers with different molar Si/Al ratios', *Ceramics International*, vol. 41, no. 8, pp. 10192–10198, Sep. 2015, doi: 10.1016/j.ceramint.2015.04.125.
- [94] M. Clausi, S. C. Tarantino, L. L. Magnani, M. P. Riccardi, C. Tedeschi, and M. Zema, 'Metakaolin as a precursor of materials for applications in Cultural Heritage: Geopolymer-based mortars with ornamental stone aggregates', *Applied Clay Science*, vol. 132–133, pp. 589–599, Nov. 2016, doi: 10.1016/j.clay.2016.08.009.
- [95] R. Pouhet, M. Cyr, and R. Bucher, 'Influence of the initial water content in flash calcined metakaolin-based geopolymer', *Construction and Building Materials*, vol. 201, pp. 421–429, Mar. 2019, doi: 10.1016/j.conbuildmat.2018.12.201.
- [96] G. da Luz, P. J. P. Gleize, E. R. Batiston, and F. Pelisser, 'Effect of pristine and functionalized carbon nanotubes on microstructural, rheological, and mechanical behaviors of metakaolin-based geopolymer', *Cement and Concrete Composites*, vol. 104, p. 103332, Nov. 2019, doi: 10.1016/j.cemconcomp.2019.05.015.
- [97] R. Si, Q. Dai, S. Guo, and J. Wang, 'Mechanical property, nanopore structure and drying shrinkage of metakaolin-based geopolymer with waste glass powder', *Journal of Cleaner Production*, vol. 242, p. 118502, Jan. 2020, doi: 10.1016/j.jclepro.2019.118502.
- [98] B. Singh, M. R. Rahman, R. Paswan, and S. K. Bhattacharyya, 'Effect of activator concentration on the strength, ITZ and drying shrinkage of fly ash/slag geopolymer concrete', *Construction and Building Materials*, vol. 118, pp. 171–179, Aug. 2016, doi: 10.1016/j.conbuildmat.2016.05.008.
- [99] J. Xiang, L. Liu, X. Cui, Y. He, G. Zheng, and C. Shi, 'Effect of Fuller-fine sand on rheological, drying shrinkage, and microstructural properties of metakaolin-based geopolymer grouting materials',

- Cement and Concrete Composites*, vol. 104, p. 103381, Nov. 2019, doi: 10.1016/j.cemconcomp.2019.103381.
- [100] T. Luukkonen, M. Sarkkinen, K. Kempainen, J. Rämö, and U. Lassi, 'Metakaolin geopolymer characterization and application for ammonium removal from model solutions and landfill leachate', *Applied Clay Science*, vol. 119, pp. 266–276, Jan. 2016, doi: 10.1016/j.clay.2015.10.027.
- [101] J. J. Ekaputri, S. Junaedi, and Wijaya, 'Effect of Curing Temperature and Fiber on Metakaolin-based Geopolymer', *Procedia Engineering*, vol. 171, pp. 572–583, 2017, doi: 10.1016/j.proeng.2017.01.376.
- [102] G. Görhan, R. Aslaner, and O. Şinik, 'The effect of curing on the properties of metakaolin and fly ash-based geopolymer paste', *Composites Part B: Engineering*, vol. 97, pp. 329–335, Jul. 2016, doi: 10.1016/j.compositesb.2016.05.019.
- [103] N. Billong, J. Kinuthia, J. Oti, and U. C. Melo, 'Performance of sodium silicate free geopolymers from metakaolin (MK) and Rice Husk Ash (RHA): Effect on tensile strength and microstructure', *Construction and Building Materials*, vol. 189, pp. 307–313, Nov. 2018, doi: 10.1016/j.conbuildmat.2018.09.001.
- [104] J. Tan *et al.*, 'Preliminary study on compatibility of metakaolin-based geopolymer paste with plant fibers', *Construction and Building Materials*, vol. 225, pp. 772–775, Nov. 2019, doi: 10.1016/j.conbuildmat.2019.07.142.
- [105] M. Ogundiran B. and I. Enakerakpo S., 'Metakaolin clay-derived geopolymer for recycling of waste cathode ray tube glass', *Afr. J. Pure Appl. Chem.*, vol. 12, no. 6, pp. 42–49, Jun. 2018, doi: 10.5897/AJPAC2018.0759.
- [106] A. Fernández-Jiménez and A. Palomo, 'Factors affecting early compressive strength of alkali activated fly ash (OPC-free) concrete', *Mater. construcc.*, vol. 57, no. 287, pp. 7–22, Aug. 2007, doi: 10.3989/mc.2007.v57.i287.53.
- [107] F. Pelisser, E. L. Guerrino, M. Menger, M. D. Michel, and J. A. Labrincha, 'Micromechanical characterization of metakaolin-based geopolymers', *Construction and Building Materials*, vol. 49, pp. 547–553, Dec. 2013, doi: 10.1016/j.conbuildmat.2013.08.081.
- [108] H. Wang, H. Li, and F. Yan, 'Synthesis and mechanical properties of metakaolinite-based geopolymer', *Colloids and Surfaces A: Physicochemical and Engineering Aspects*, vol. 268, no. 1–3, pp. 1–6, Oct. 2005, doi: 10.1016/j.colsurfa.2005.01.016.
- [109] S. Alonso and A. Palomo, 'Alkaline activation of metakaolin and calcium hydroxide mixtures: influence of temperature, activator concentration and solids ratio', *Materials Letters*, vol. 47, no. 1–2, pp. 55–62, Jan. 2001, doi: 10.1016/S0167-577X(00)00212-3.
- [110] E. Álvarez-Ayuso *et al.*, 'Environmental, physical and structural characterisation of geopolymer matrixes synthesised from coal (co-)combustion fly ashes', *Journal of Hazardous Materials*, vol. 154, no. 1–3, pp. 175–183, Jun. 2008, doi: 10.1016/j.jhazmat.2007.10.008.
- [111] J. Davidovits and C. James, *Why the pharaohs built the pyramids with fake stones*. Saint-Quentin, France: Institut Géopolymère, 2009.
- [112] K. J. D. MacKenzie, A. Wong, and M. Barsoum, 'Were the casing stones of Senefru's Bent Pyramid in Dahshour cast or carved? Multinuclear NMR evidence', *Materials Letters*, vol. 65, pp. 350–352, 2011.
- [113] 'FAQ for artificial stone supporters', *Geopolymer Institute*, Aug. 03, 2016. <https://www.geopolymer.org/faq/faq-for-artificial-stone-supporters/> (accessed Apr. 14, 2021).
- [114] 'Are Pyramids Made Out of Concrete? (1)', *Geopolymer Institute*, Apr. 10, 2006. <https://www.geopolymer.org/archaeology/pyramids/are-pyramids-made-out-of-concrete-1/> (accessed Apr. 14, 2021).
- [115] J. Davidovits, 'Ancient and modern concretes: what is the real difference?', *Concrete International*, vol. 9, pp. 23–29, 1987.
- [116] R. Malinowski, A. Slatkine, and M. Ben Yair, 'Durability of Roman Mortars and Concretes', presented at the RILEM, International Symposium on durability of Concrete, Prague, 1961.

- [117] J. Davidovits, L. Huaman, and R. Davidovits, 'Ancient geopolymer in south-American monument. SEM and petrographic evidence', *Materials Letters*, vol. 235, pp. 120–124, Jan. 2019, doi: 10.1016/j.matlet.2018.10.033.
- [118] 'India's "Geopolymer Casting" disguised as Stone Sculpture', <https://sciencetheory.wordpress.com/>, Aug. 02, 2019. <https://sciencetheory.wordpress.com/2019/08/02/indias-geopolymer-casting-disguised-as-stone-sculpture/> (accessed Apr. 06, 2020).
- [119] H. Kuhl, 'Slag cement and process of making the same', 900,939, 1908
- [120] J. L. Provis and S. A. Bernal, 'Milestones in the analysis of alkali-activated binders', *Journal of Sustainable Cement-Based Materials*, vol. 4, no. 2, pp. 74–84, Apr. 2015, doi: 10.1080/21650373.2014.958599.
- [121] C. Shi, P. V. Krivenko, and D. Roy, *Alkali-Activated Cements and Concretes*. Abingdon: Taylor & Francis, 2006.
- [122] A. O. Purdon, 'The action of alkalis on blast-furnace slag', *Journal of the Society of Chemical Industry - Trans. Commun.*, vol. 59, pp. 191–202, 1940.
- [123] A. Buchwald, M. Vanooteghem, E. Gruyaert, H. Hilbig, and N. De Belie, 'Purdocement: application of alkali-activated slag cement in Belgium in the 1950s', *Mater Struct*, vol. 48, no. 1–2, pp. 501–511, Jan. 2015, doi: 10.1617/s11527-013-0200-8.
- [124] V. S. Ramachandran, *Concrete Admixtures Handbook. Properties, Science and Technology*, Second edition. New Jersey, United States of America: Noyes Publications, 1995.
- [125] V. Glukhovskiy D., *Gruntosilikaty (Soil Silicates)*. Gosstroyizdat, Kiev, 1959.
- [126] D. M. Roy, 'Alkali-activated cements Opportunities and challenges', *Cement and Concrete Research*, p. 6, 1999.
- [127] D. J. Davidovits, '30 Years of Successes and Failures in Geopolymer Applications. Market Trends and Potential Breakthroughs.', presented at the Geopolymer 2002 Conference, Meulborn, Australia, 2002, pp. 1–16.
- [128] J. Davidovits, 'Mineral polymers and methods of making them', 4,349,386, 1982
- [129] J. Davidovits, *Geopolymer chemistry and applications*, 4th edition. Saint-Quentin, France: Institut Géopolymère, 2015.
- [130] J. Davidovits and J. L. Sawyer, 'Early high-strength mineral polymer', 4,509,985, 1985
- [131] R. F. Heitzmann, B. B. Gravitt, and J. L. Sawyer, 'Cement composition curable at low temperatures', 4,842,649, 1989
- [132] R. E. Lyon, P. N. Balaguru, A. Foden, U. Sorathia, J. Davidovits, and M. Davidovics, 'FIRE RESISTANT ALUMINOSILICATE COMPOSITES', *Fire and Materials*, vol. 21, pp. 67–73, 1997.
- [133] J. Davidovits, 'Environmentally Driven Geopolymer Cement Applications', presented at the Geopolymer 2002 Conference, Melbourne, Australia, 2002.
- [134] J. Małolepszy and M. Petri, 'High strength slag alkaline binders', presented at the 8 th International Congress on the Chemistry of Cement, Rio de Janeiro, Brazilia, 1986, pp. 108–112.
- [135] J. Małolepszy, 'Activation of synthetic melilite slags by alkalies', presented at the 8 th International Congress on the Chemistry of Cement, Rio de Janeiro, Brazilia, 1986, pp. 104–107.
- [136] J. Małolepszy and W. Nocuń-Wczelik, 'Microcalorimetric Studies of Slags Alkaline Binders', *Journal of Thermal Analysis*, vol. 33, pp. 431–434, 1988.
- [137] J. Deja and J. Małolepszy, 'Resistance of Alkali-Activated Slag Mortars to Chloride Solution', *American Concrete Insitute*, vol. 114, pp. 1547–1564, 1989.
- [138] J. Małolepszy and J. Deja, 'Immobilization of heavy metal ions by the alkali activated slag cementitious materials', presented at the WASCON'94 – Environmental Implications of Construction Materials and Technology Developments, Studies in Environmental Science 60, Maastricht: ELSEVIER, 1994, pp. 519–524.
- [139] J. Małolepszy and J. Deja, 'Effect of Heavy Metals Immobilization on the Properties of Alkali Activated Slag Mortars', presented at the Fifth International Conference „Fly Ash, Silica Fume, Slag and Pozzolans in Concrete,, CANMET/ACI, Milwaukee, USA, 1995, pp. 1087–1095.

- [140] J. Deja, W. Brylicki, and J. Matolepszy, 'Anti-filtration screens based on alkali-activated slag bindres', presented at the 2007-International conference „Alkali Activated Materials – Research, Production and Utilization”, Praga, Czechy, Jun. 2007, pp. 123–136.
- [141] J. L. Provis and J. S. J. van Deventer, 'Geopolymerisation kinetics. 1. In situ energy-dispersive X-ray diffractometry', *Chemical Engineering Science*, vol. 62, pp. 2309–2317, 2007.
- [142] J. L. Provis, P. Duxson, J. S. J. van Deventer, and G. C. Lukey, 'The role of mathematical modeling and gel chemistry in advancing geopolymer technology', *Chemical Engineering Research and Design*, vol. 83, pp. 853–860, 2005.
- [143] J. L. Provis, A. L. Munoz Gomez, O. H. Hussein, G. Koma, E. Manolova, and V. Petrov, 'Production of alkali-activated binders from iron silicate fines', presented at the International Conference on Sustainable Materials, Systems and Structures (SMSS2019) New Generation of Construction Materials, Rovinj, Croatia: RILEM Publications S.A.R.L, 2019, pp. 353–360.
- [144] A. Runci, J. Provis, and M. Serdar, 'Microstructure as a key parameter for understanding chloride ingress in alkali-activated mortars', *Cement and Concrete Composites*, vol. 134, p. 104818, Nov. 2022, doi: 10.1016/j.cemconcomp.2022.104818.
- [145] T. Suwan and M. Fan, 'Influence of OPC replacement and manufacturing procedures on the properties of self-cured geopolymer', *Construction and Building Materials*, vol. 73, pp. 551–561, 2014.
- [146] G. Kastiukas, X. Zhou, and J. Castro-Gomes, 'Development and optimisation of phase change material-impregnated lightweight aggregates for geopolymer composites made from aluminosilicate rich mud and milled glass powder', *Construction and Building Materials*, vol. 110, pp. 201–210, 2016.
- [147] F. Pacheco-Torgal, J. P. Castro-Gomes, and S. Jalali, 'Bond Strength Between Concrete Substrate And Repair Materials. Comparisons Between Tungsten Mine Waste Geopolymeric Binder Versus Current Commercial Repair Products.', presented at the Seventh International Congress on Advances in Civil Engineering, Yildiz Technical University, Istanbul, Turkey, Oct. 2006, pp. 1–10.
- [148] A. Benhamouda and J. Castro-Gomes, 'Preliminary Study of the Rheological and Mechanical Properties of Alkali-activated Concrete Based on Tungsten Mining Waste Mud', *KEG*, Apr. 2020, doi: 10.18502/keg.v5i4.6801.
- [149] N. Sedira and J. Castro-Gomes, 'Microstructure Features of Ternary Alkali-activated Binder Based on Tungsten Mining Waste, Slag and Metakaolin', *KEG*, Apr. 2020, doi: 10.18502/keg.v5i4.6810.
- [150] I. Beghoura and J. Castro-Gomes, 'Development of Porous Tungsten Mud Waste-based Alkali-activated Foams with Low Thermal Conductivity', *KEG*, May 2020, doi: 10.18502/keg.v5i5.6927.
- [151] I. Beghoura and J. Castro-Gomes, 'Design of alkali-activated aluminium powder foamed materials for precursors with different particle sizes', *Construction and Building Materials*, vol. 224, pp. 682–690, Nov. 2019, doi: 10.1016/j.conbuildmat.2019.07.018.
- [152] P. S. Humbert, J. P. Castro-Gomes, and H. Savastano, 'Clinker-free CO<sub>2</sub> cured steel slag based binder: Optimal conditions and potential applications', *Construction and Building Materials*, vol. 210, pp. 413–421, Jun. 2019, doi: 10.1016/j.conbuildmat.2019.03.169.
- [153] J. Duran-Suarez, M.-A. Villegas, R. Peralbo-Cano, and J. Castro Gomes, 'New casting glass technique through the use of geopolymers', *MATEC Web Conf.*, vol. 274, p. 03004, 2019, doi: 10.1051/mateconf/201927403004.
- [154] Sáez-Pérez, Paz M., Brümmer, Monika, and Durán-Suárez, Jorge A., 'Effect of the state of conservation of the hemp used in geopolymer and hydraulic lime concretes', *Construction and Building Materials*, vol. 285, no. 24, p. 122853, May 2021, doi: /10.1016/j.conbuildmat.2021.122853.
- [155] M. A. Gómez-Casero, F. J. Moral-Moral, L. Pérez-Villarejo, P. J. Sánchez-Soto, and D. Eliche-Quesada, 'Synthesis of clay geopolymers using olive pomace fly ash as an alternative activator. Influence of the additional commercial alkaline activator used', *Journal of Materials Research and Technology*, Apr. 2021, doi: 10.1016/j.jmrt.2021.03.102.

- [156] J. G. S. van Jaarsveld, J. S. J. van Deventer, and G. C. Lukey, 'The effect of composition and temperature on the properties of fly ash- and kaolinite-based geopolymers', *Chemical Engineering Journal*, vol. 89, no. 1–3, pp. 63–73, Oct. 2002, doi: 10.1016/S1385-8947(02)00025-6.
- [157] J. S. J. van Deventer, J. L. Provis, P. Duxson, and G. C. Lukey, 'Reaction mechanisms in the geopolymeric conversion of inorganic waste to useful products', *Journal of Hazardous Materials*, vol. 139, no. 3, pp. 506–513, 2007.
- [158] J. Zhang, J. L. Provis, D. Feng, and J. S. J. van Deventer, 'Geopolymers for immobilization of Cr<sup>6+</sup>, Cd<sup>2+</sup>, and Pb<sup>2+</sup>', *Journal of Hazardous Materials*, vol. 177, no. Issues 2-3, pp. 587–598, 2008.
- [159] J. S. J. Van Deventer, J. L. Provis, and P. Duxson, 'Technical and commercial progress in the adoption of geopolymer cement', *Minerals Engineering*, vol. 29, pp. 89–104, Mar. 2012, doi: 10.1016/j.mineng.2011.09.009.
- [160] G. Liang, H. Zhu, Z. Zhang, and Q. Wu, 'Effect of rice husk ash addition on the compressive strength and thermal stability of metakaolin based geopolymer', *Construction and Building Materials*, vol. 222, pp. 872–881, Oct. 2019, doi: 10.1016/j.conbuildmat.2019.06.200.
- [161] X. Lv, K. Wang, Y. He, and X. Cui, 'A green drying powder inorganic coating based on geopolymer technology', *Construction and Building Materials*, vol. 214, pp. 441–448, 2019.
- [162] D.-W. Zhang, D. Wang, X.-Q. Lin, and T. Zhang, 'The study of the structure rebuilding and yield stress of 3D printing geopolymer pastes', *Construction and Building Materials*, vol. 184, pp. 575–580, Sep. 2018, doi: 10.1016/j.conbuildmat.2018.06.233.
- [163] J. Zhong, G.-X. Zhou, P.-G. He, Z.-H. Yang, and D.-C. Jia, '3D printing strong and conductive geopolymer nanocomposite structures modified by graphene oxide', *Carbon*, vol. 117, pp. 421–426, Jun. 2017, doi: 10.1016/j.carbon.2017.02.102.
- [164] G.-X. Zhou *et al.*, '3D printing geopolymer nanocomposites: Graphene oxide size effects on a reactive matrix', *Carbon*, vol. 164, pp. 215–223, Aug. 2020, doi: 10.1016/j.carbon.2020.02.021.
- [165] Z. Li, L. Wang, and G. Ma, 'Mechanical improvement of continuous steel microcable reinforced geopolymer composites for 3D printing subjected to different loading conditions', *Composites Part B: Engineering*, vol. 187, p. 107796, Apr. 2020, doi: 10.1016/j.compositesb.2020.107796.
- [166] R. Davidovits, C. Pelegris, and J. Davidovits, 'Standardized Method in Testing Commercial Metakaolins for Geopolymer Formulations.', p. 9, 2019.
- [167] J. Davidovits and R. Davidovits, 'Ferro-sialate Geopolymers (-Fe-O-Si-O-Al-O-)', *Technical papers # 27, Geopolymer Institute Library*, Jan. 2020, doi: DOI:10.13140/RG.2.2.25792.89608/2.
- [168] N. Thakur, M. F. Wahab, D. D. Khanal, and D. W. Armstrong, 'Synthetic aluminosilicate based geopolymers – Second generation geopolymer HPLC stationary phases', *Analytica Chimica Acta*, vol. 1081, pp. 209–217, Nov. 2019, doi: 10.1016/j.aca.2019.07.017.
- [169] A. T. Akono, S. Koric, and W. M. Kriven, 'Influence of pore structure on the strength behavior of particle- and fiber-reinforced metakaolin-based geopolymer composites', *Cement and Concrete Composites*, vol. 104, p. 103361, Nov. 2019, doi: 10.1016/j.cemconcomp.2019.103361.
- [170] Mikuła, Janusz, Łach, Michał, and Grela, Agnieszka, 'Sposób wytwarzania zeolitów na bazie filipowickiego tufu wulkanicznego (Method for producing zeolites on the basis of Filipowice volcanic tuff)', Pat.232899, Apr. 16, 2019
- [171] Mikuła, Janusz and Łach, Michał, 'Tworzywo geopolimerowe oraz sposób wytwarzania tworzywa geopolimerowego (Geopolymer material and method for manufacturing geopolymer material)', Pat.226104, Dec. 20, 2016
- [172] P. Mazur, J. Mikuła, and J. S. Kowalski, 'The corrosion resistance of the base geopolymer fly ash', *Advances in Science and Technology*, vol. 7, no. 19, pp. 88–92, 2013, doi: 10.5604/20804075.1062704.
- [173] J. S. Mikuła, *Rozwiązania proekologiczne w zakresie produkcji: praca zbiorowa. T. 1*, vol. 1. Kraków: Wydawnictwo Politechniki Krakowskiej, 2014.
- [174] K. Korniejenko, E. Frączek, E. Pytlak, and M. Adamski, 'Mechanical Properties of Geopolymer Composites Reinforced with Natural Fibers', *Procedia Engineering*, vol. 151, pp. 388–393, 2016, doi: 10.1016/j.proeng.2016.07.395.

- [175] K. Korniejenko *et al.*, 'Mechanical Properties of Short Fiber-Reinforced Geopolymers Made by Casted and 3D Printing Methods: A Comparative Study', *Materials*, vol. 13, no. 3, p. 579, Jan. 2020, doi: 10.3390/ma13030579.
- [176] J. Jaglarz, D. Wyszynski, M. Lach, J. Mikuła, and R. Duraj, 'The effect of molding conditions on the quality of geopolymer surfaces', *Optica Applicata*, vol. 50, no. 1, pp. 135–146, 2020, doi: 10.37190/oa200111.
- [177] M. Sitarz, I. Hager, and M. Choiniska, 'Evolution of Mechanical Properties with Time of Fly-Ash-Based Geopolymer Mortars under the Effect of Granulated Ground Blast Furnace Slag Addition', *Energies*, vol. 13, no. 5, p. 1135, Mar. 2020, doi: 10.3390/en13051135.
- [178] I. Hager and M. Sitarz, 'Influence of the activator nature on mechanical properties of fly ash-based geopolymer', *International Journal of Advanced Science and Technology*, vol. 29, no. 02, pp. 631–637, 2020.
- [179] P. Duży, M. Choiniska, I. Hager, O. Amiri, and J. Claverie, 'Mechanical Strength and Chloride Ions' Penetration of Alkali-Activated Concretes (AAC) with Blended Precursor', *Materials*, vol. 15, no. 13, p. 4475, Jun. 2022, doi: 10.3390/ma15134475.
- [180] J. Marczyk *et al.*, 'Optimizing the L/S Ratio in Geopolymers for the Production of Large-Size Elements with 3D Printing Technology', *Materials*, vol. 15, no. 9, p. 3362, May 2022, doi: 10.3390/ma15093362.
- [181] W. Brylicki, Stryczek, Stanisław, and Gonet, Andrzej, 'Zaczyny geopolimerowe do prac iniekcyjnych', *Wiertnictwo Nafta Gaz*, vol. 23, no. 1, pp. 121–129, 2006.
- [182] Stryczek, Stanisław, Wiśniowski, Rafał, and Gonet, Andrzej, 'Zaczyny geopolimerowe do uszczelniania górotworu metodami iniekcji otworowej', *Wiertnictwo Nafta Gaz*, vol. 24, no. 2, pp. 895–900, 2007.
- [183] A. Koleżyński, M. Król, and M. Żychowicz, 'The structure of geopolymers – Theoretical studies', *Journal of Molecular Structure*, vol. 1163, pp. 465–471, Jul. 2018, doi: 10.1016/j.molstruc.2018.03.033.
- [184] Zarebska, Katarzyna, Klima, Kinga, Złotkowski, Albert, Kamienowska, Marta, Czuma, Natalia, and Baran, Paweł, 'Synteza geopolimerów z wykorzystaniem żużla wielkopieczowego', *Przemysł Chemiczny*, vol. 98, no. 2, pp. 298–301, 2019.
- [185] L. Czarnecki, 'Use of Polymers to Enhance Concrete Performance', *AMR*, vol. 1129, pp. 49–58, Nov. 2015, doi: 10.4028/www.scientific.net/AMR.1129.49.
- [186] L. Czarnecki, 'Concrete-Polymer Composites C-PC – Reading with Understanding', *Restoration of Buildings and Monuments*, vol. 18, no. 3–4, pp. 135–142, Aug. 2012, doi: 10.1515/rbm-2012-6519.
- [187] L. Czarnecki, 'Polymer-Concrete Composites for the repair of concrete structures', *MATEC Web Conf.*, vol. 199, p. 01006, 2018, doi: 10.1051/mateconf/201819901006.
- [188] R. Wang, J. Li, T. Zhang, and L. Czarnecki, 'Chemical interaction between polymer and cement in polymer-cement concrete', *Bulletin of the Polish Academy of Sciences Technical Sciences*, vol. 64, no. 4, pp. 785–792, Dec. 2016, doi: 10.1515/bpasts-2016-0087.
- [189] Dariusz, 'Galeria zdjęć wyrobów z geopolimerów i technologii produkcji', *AlsiTech*, Jan. 28, 2016. <http://alsitech.pl/galeria-zdjec-wyrobow-z-geopolimerow-i-technologie-produkcji/> (accessed Apr. 15, 2021).
- [190] Tedeusz, Hop, *Betony modyfikowane polimerami*, 1st ed. Warszawa: Arkady, 1976.
- [191] Kwiecień, A, Kubica, Jan, and Zajac, B, 'Pilotażowe badania statyczne wielkogabarytowego modelu pękniętego muru ceglanego sklejonego polimerową masą trwale sprężysto-plastyczną', in *Inżynierskie problemy odnowy staromiejskich zespołów zabytkowych*, Kraków, Poland, 2006, pp. 83–95.
- [192] Flávio Daniel Martins Lacão, 'Monitorização da temperatura em ligantes geopoliméricos', UNIVERSIDADE DA BEIRA INTERIOR, Covilhã, 2015.
- [193] Paszek, Natalia, 'Mechanical properties of geopolymers', Silesian University of Technology, Gliwice, Poland, 2016.

- [194] Górski, Marcin, Krzywoń, Rafał, Safuta, Małgorzata, Paszek, Natalia, Dawczyński, Szymon, and Pizoń, Jan, 'Badania cech materiałowych geopolimerów z odpadowych kruszyw pokopalnianych i ich symulacje numeryczne', *Materiały Budowlane*, no. 8, pp. 89–91, 2016, doi: 10.15199/33.2016.08.25.
- [195] S. Dawczyński, M. Górski, and R. Krzywoń, 'Granulated cork as a component of geopolymer - preliminary studies', *Annals Warsaw University of Life Sciences; Forestry and Wood Technology*, vol. 94, pp. 124–128, 2016.
- [196] Dawczyński, Szymon, Górski, Marcin, and Krzywoń, Rafał, 'Geopolymer as an alternative ecological material for buildings', presented at the 14th International Conference on New Trends in Statics and Dynamics of Buildings, Bratislava, Slovakia: Slovak University of Technology, 2016, pp. 374–378.
- [197] N. Paszek, 'Wpływ warunków pielęgnacji na wytrzymałość geopolimeru na bazie suspencji popiołu ze spalania węgla kamiennego', in *Ujęcie Aktualnych Problemów Budownictwa*, Gliwice, Poland: Wydawnictwo Politechniki Śląskiej, 2018, pp. 91–98.
- [198] S. Dawczyński, M. Soczyński, and M. Górski, 'Feasibility and strength properties of the geopolymer binder made of fly ash suspension', *MATEC Web of Conferences*, vol. 262, no. 3, p. 06001, 2019.
- [199] N. Paszek and M. Górski, 'The basic mechanical properties of the fluidised bed combustion fly ash-based geopolymer', *CT*, vol. 9, pp. 107–118, 2019, doi: 10.4467/2353737XCT.19.100.10882.
- [200] N. Paszek and M. Górski, 'Influence of sodium hydroxide concentration on mechanical parameters of fly ash-based geopolymer', presented at the SynerCrete'18 International Conference on Interdisciplinary Approaches for Cement-based Materials and Structural Concrete, Funchal, Madeira Island, Portugal: RILEM Publications, Oct. 2018, pp. 461–466.
- [201] N. Wielgus, M. Górski, and J. Kubica, 'Discarded Cathode Ray Tube Glass as an Alternative for Aggregate in a Metakaolin-Based Geopolymer', *Sustainability*, vol. 13, no. 2, p. 479, Jan. 2021, doi: 10.3390/su13020479.
- [202] N. Wielgus, J. Kubica, and M. Górski, 'Influence of the Composition and Curing Time on Mechanical Properties of Fluidized Bed Combustion Fly Ash-Based Geopolymer', *Polymers*, vol. 13, no. 15, p. 2527, Jul. 2021, doi: 10.3390/polym13152527.
- [203] S. Dawczyński and A. Stokłosa, 'Modification of AA Binder Matrix with the Use of PP Fibres – Strength Investigations', *KEG*, pp. 111–123, Apr. 2020, doi: 10.18502/keg.v5i4.6802.
- [204] Patrycja Światała, 'Geopolimery z CFRP', Silesian University of Technology.
- [205] M. Krystek, S. Dawczyński, M. Górski, and M. Stępień, 'Experimental investigation on mechanical and electrical properties of GO-geopolymer composite', in *Technology Transfer in Action*, Hong Kong, Dec. 2018, pp. 1–8.
- [206] R. Krzywoń and S. Dawczyński, 'Strength Parameters of Foamed Geopolymer Reinforced with GFRP Mesh', *Materials*, vol. 14, no. 3, p. 689, Feb. 2021, doi: 10.3390/ma14030689.
- [207] Łażniewska-Piekarczyk, Beata *et al.*, 'Geopolimer jako innowacyjne zagospodarowanie wełny szklanej case study', in *Współczesne problemy ochrony środowiska i energetyki 2020*, Gliwice, Poland: Katedra Technologii i Urządzeń Zagospodarowania Odpadów, Politechnika Śląska, 2021, pp. 249–260.
- [208] T. Glasby, J. Day, R. Genrich, and D. J. Aldred, 'EFC Geopolymer Concrete Aircraft Pavements at Brisbane West Wellcamp Airport', p. 9, 2015.
- [209] 'MIDAR Technology', *Lucideon Materials Development and Commercialization*. <https://www.lucideon.com/materials-technologies/midar-technology> (accessed Apr. 15, 2021).
- [210] 'banah UK....A Concrete Study in R&D', *matrix*. <https://matrixni.org/banah-uk/> (accessed Apr. 15, 2021).
- [211] 'Nu-core A2FR Geopolymer Panels', *ArchiEXPO*. <https://pdf.archiexpo.com/pdf/nuccore-smartfix/nu-core-brochure/143213-248904.html> (accessed Apr. 15, 2021).
- [212] 'RENCA'. <https://www.renca.org/> (accessed Apr. 07, 2021).
- [213] 'GeoTree Products', *Clock Spring NRI*. <https://www.cs-nri.com/brands/geotree-solutions/products-services/geotree-products/> (accessed Apr. 15, 2021).

- [214] 'GEOPOLYMERSOLUTIONS', *Products* 100% *Eco-Friendly*.  
<https://www.geopolymertech.com/products/> (accessed Nov. 23, 2022).
- [215] 'Kiran Geopolymer Concrete', *Kiran Geopolymer Concrete*.  
<http://www.geopolymer.in/www.geopolymer.in/index.html> (accessed Apr. 15, 2021).
- [216] Dariusz, 'AlsiTech', *AlsiTech*, Jan. 28, 2018. <http://alsitech.pl/> (accessed Apr. 15, 2021).
- [217] M. Alshaaer, B. El-Eswed, R. I. Yousef, F. Khalili, and H. Rahier, 'Development of functional geopolymers for water purification, and construction purposes', *Journal of Saudi Chemical Society*, vol. 20, pp. S85–S92, Sep. 2016, doi: 10.1016/j.jscs.2012.09.012.
- [218] D. S. Cheema, N. A. Lloyd, and B. V. Rangan, 'Durability of geopolymer concrete box culverts – a green alternative', presented at the 34th Conference on OUR WORLD IN CONCRETE & STRUCTURES, Singapore, Aug. 2009, pp. 85–92.
- [219] Wimpenny, Don, P. Duxson, Cooper, Tony, Provis, John, L., and Zeuschener, Robert, 'Wimpenny D., Duxson P., Cooper T., Provis J.L., Zeuschener R.: Fibre reinforced geopolymer concrete products for underground infrastructure.', presented at the Concrete 2011, Perth, Australia: Concrete Institute of Australia, 2011.
- [220] C. Suksiripattanapong, S. Horpibulsuk, P. Chanprasert, P. Sukmak, and A. Arulrajah, 'Compressive strength development in fly ash geopolymer masonry units manufactured from water treatment sludge', *Construction and Building Materials*, vol. 82, pp. 20–30, May 2015, doi: 10.1016/j.conbuildmat.2015.02.040.
- [221] M. Hoy, S. Horpibulsuk, and A. Arulrajah, 'Strength development of Recycled Asphalt Pavement – Fly ash geopolymer as a road construction material', *Construction and Building Materials*, vol. 117, pp. 209–219, Aug. 2016, doi: 10.1016/j.conbuildmat.2016.04.136.
- [222] S. Rios, N. Cristelo, T. Miranda, N. Araujo, J. Oliveira, and E. Lucas, 'Increasing the reaction kinetics of alkali-activated fly ash binders for stabilization of a silty sand pavement sub-base', *Road Materials and Pavement Design*, vol. 19, no. 1, pp. 201–222, 2018.
- [223] A. R. G. Azevedo, C. M. F. Vieira, W. M. Ferreira, K. C. P. Faria, L. G. Pedroti, and B. C. Mendes, 'Potential use of ceramic waste as precursor in the geopolymerization reaction for the production of ceramic roof tiles', *Journal of Building Engineering*, vol. 29, p. 101156, May 2020, doi: 10.1016/j.jobbe.2019.101156.
- [224] T. E. McGrath *et al.*, 'LowCoPreCon – low carbon precast concrete products for an energy efficient built environment', presented at the International Conference on Sustainable Materials, Systems and Structures (SMSS2019) New Generation of Construction Materials, Rovinj, Croatia: RILEM Publications S.A.R.L., Mar. 2019, pp. 550–557.
- [225] G. Gu, T. Ma, F. Chen, H. Li, Y. Pei, and F. Xu, 'Soft magnetic geopolymer in airport pavement induction heating: Effect of Fe powder distribution on the electromagnetic loss', *Ceramics International*, Aug. 2022, doi: 10.1016/j.ceramint.2022.09.136.
- [226] Z. Zhang, X. Yao, and H. Zhu, 'Potential application of geopolymers as protection coatings for marine concrete. Basic properties', *Applied Clay Science*, vol. 49, no. 1–2, pp. 1–6, Jun. 2010, doi: 10.1016/j.clay.2010.01.014.
- [227] Z. Zhang, X. Yao, and H. Zhu, 'Potential application of geopolymers as protection coatings for marine concrete. Microstructure and anticorrosion mechanism', *Applied Clay Science*, vol. 49, no. 1–2, pp. 7–12, Jun. 2010, doi: 10.1016/j.clay.2010.04.024.
- [228] A. M. Aguirre-Guerrero, R. A. Robayo-Salazar, and R. M. de Gutiérrez, 'A novel geopolymer application: Coatings to protect reinforced concrete against corrosion', *Applied Clay Science*, vol. 135, pp. 437–446, Jan. 2017, doi: 10.1016/j.clay.2016.10.029.
- [229] Z. Zhang, X. Yao, and H. Wang, 'Potential application of geopolymers as protection coatings for marine concrete III. Field experiment', *Applied Clay Science*, vol. 67–68, pp. 57–60, Oct. 2012, doi: 10.1016/j.clay.2012.05.008.
- [230] F. Pacheco-Torgal, Z. Abdollahnejad, S. Miraldo, S. Baklouti, and Y. Ding, 'An overview on the potential of geopolymers for concrete infrastructure rehabilitation', *Construction and Building Materials*, vol. 36, pp. 1053–1058, Nov. 2012, doi: 10.1016/j.conbuildmat.2012.07.003.

- [231] P. Balaguru, 'Geopolymer for Protective Coating of Transportation Infrastructures', New Jersey Department of Transportation, New Jersey, United States of America, Final Report FHWA-NJ-1998-012, Sep. 1998.
- [232] K. Sakkas, D. Pantias, P. P. Nomikos, and A. I. Sofianos, 'Potassium based geopolymer for passive fire protection of concrete tunnels linings', *Tunnelling and Underground Space Technology*, vol. 43, pp. 148–156, Jul. 2014, doi: 10.1016/j.tust.2014.05.003.
- [233] J. Temuujin, W. Rickard, M. Lee, and A. van Riessen, 'Preparation and thermal properties of fire resistant metakaolin-based geopolymer-type coatings', *Journal of Non-Crystalline Solids*, vol. 357, no. 5, pp. 1399–1404, Mar. 2011, doi: 10.1016/j.jnoncrysol.2010.09.063.
- [234] Frantisek Martaus, 'Fiber Reinforced Geopolymer Composite in Aircraft Structure', presented at the Future Sky Safety Final Event, 2019, June 20–21, EUROCAE, Paris: Unpublished, Jun. 2019. doi: 10.13140/RG.2.2.25645.23522.
- [235] F. Rao and Q. Liu, 'Geopolymerization and Its Potential Application in Mine Tailings Consolidation: A Review', *Mineral Processing and Extractive Metallurgy Review*, vol. 36, no. 6, pp. 399–409, Nov. 2015, doi: 10.1080/08827508.2015.1055625.
- [236] R. A. A. Boca Santa, C. Soares, and H. G. Riella, 'Geopolymers with a high percentage of bottom ash for solidification/immobilization of different toxic metals', *Journal of Hazardous Materials*, vol. 318, pp. 145–153, Nov. 2016, doi: 10.1016/j.jhazmat.2016.06.059.
- [237] M. Xia and J. Sanjayan, 'Method of formulating geopolymer for 3D printing for construction applications', *Materials & Design*, vol. 110, pp. 382–390, Nov. 2016, doi: 10.1016/j.matdes.2016.07.136.
- [238] B. Panda, S. C. Paul, N. A. N. Mohamed, Y. W. D. Tay, and M. J. Tan, 'Measurement of tensile bond strength of 3D printed geopolymer mortar', *Measurement*, vol. 113, pp. 108–116, Jan. 2018, doi: 10.1016/j.measurement.2017.08.051.
- [239] S. A. L. de Koster, R. M. Mors, H. W. Nugteren, H. M. Jonkers, G. M. H. Meesters, and J. R. van Ommen, 'Geopolymer Coating of Bacteria-containing Granules for Use in Self-healing Concrete', *Procedia Engineering*, vol. 102, pp. 475–484, 2015, doi: 10.1016/j.proeng.2015.01.193.
- [240] K. J. D. MacKenzie, N. Rahner, M. E. Smith, and A. Wong, 'Calcium-containing inorganic polymers as potential bioactive materials', *J Mater Sci*, vol. 45, no. 4, pp. 999–1007, Feb. 2010, doi: 10.1007/s10853-009-4031-5.
- [241] M. Arnhof *et al.*, 'Basalt fibre reinforced geopolymer made from lunar regolith simulant', presented at the 8th European Conference for Aeronautics and Space Sciences (EUCASS), Madrid, Spain, Jul. 2019, p. 9. doi: 10.13009/EUCASS2019-725.
- [242] S. Pilehvar, M. Arnhof, R. Pamies, L. Valentini, and A.-L. Kjøniksen, 'Utilization of urea as an accessible superplasticizer on the moon for lunar geopolymer mixtures', *Journal of Cleaner Production*, vol. 247, p. 119177, Feb. 2020, doi: 10.1016/j.jclepro.2019.119177.
- [243] N. Singh, Wang, Jiecong, and Li, Jinhui, 'Waste Cathode Rays Tube: An Assessment of Global Demand for Processing', *Procedia Environmental Sciences*, no. 31, pp. 465–474, 2016, doi: 10.1016/j.proenv.2016.02.050.
- [244] F. Andreola, L. Barbieri, A. Corradi, I. Lancellotti, R. Falcone, and S. Hreglich, 'Glass-ceramics obtained by the recycling of end of life cathode ray tubes glasses', *Waste Management*, vol. 25, no. 2, pp. 183–189, Jan. 2005, doi: 10.1016/j.wasman.2004.12.007.
- [245] Y. Qi, X. Xiao, Y. Lu, J. Shu, J. Wang, and M. Chen, 'Cathode ray tubes glass recycling: A review', *Science of The Total Environment*, vol. 650, pp. 2842–2849, Feb. 2019, doi: 10.1016/j.scitotenv.2018.09.383.
- [246] Z. Yao *et al.*, 'Recycling difficult-to-treat e-waste cathode-ray-tube glass as construction and building materials: A critical review', *Renewable and Sustainable Energy Reviews*, vol. 81, pp. 595–604, Jan. 2018, doi: 10.1016/j.rser.2017.08.027.
- [247] W. Meng, X. Wang, W. Yuan, J. Wang, and G. Song, 'The Recycling of Leaded Glass in Cathode Ray Tube (CRT)', *Procedia Environmental Sciences*, vol. 31, pp. 954–960, 2016, doi: 10.1016/j.proenv.2016.02.120.

- [248] N. Menad, 'Cathode ray tube recycling', *Resources, Conservation and Recycling*, vol. 26, no. 3–4, pp. 143–154, Jun. 1999, doi: 10.1016/S0921-3449(98)00079-2.
- [249] I. C. Nnorom, O. Osibanjo, and M. O. C. Ogwuegbu, 'Global disposal strategies for waste cathode ray tubes', *Resources, Conservation and Recycling*, vol. 55, no. 3, pp. 275–290, Jan. 2011, doi: 10.1016/j.resconrec.2010.10.007.
- [250] Grzegorz Rosa, '120 lat technologii CRT - jak ewoluowały monitory?', *Gaming Society*, Jun. 07, 2017. <https://gamingsociety.pl/artykul/120-lat-technologiei-crt-jak-ewoluowaly-monitory-474/> (accessed Apr. 15, 2021).
- [251] jwo, 'Co zrobić ze szkłem ze starych telewizorów? Płytki podłogowe!', *Portal Komunalny*, Apr. 21, 2016. <https://portalkomunalny.pl/plytki-telewizory-kineskopowe-331048/> (accessed Apr. 15, 2021).
- [252] C. S. Poon, 'Management of CRT glass from discarded computer monitors and TV sets', *Waste Management*, vol. 28, no. 9, p. 1499, Jan. 2008, doi: 10.1016/j.wasman.2008.06.001.
- [253] K. Mrowiec and S. Kubica, 'Recykling odpadowego szkła kineskopowego', p. 3.
- [254] 'Directive 2002/96/EC of the European Parliament and of the Council of 27 January 2003 on waste electrical and electronic equipment (WEEE)'. Official Journal of the European Union L 37/24, Feb. 13, 2003.
- [255] F. Andreola, L. Barbieri, A. Corradi, A. M. Ferrari, I. Lancellotti, and P. Neri, 'Recycling of EOL CRT glass into ceramic glaze formulations and its environmental impact by LCA approach', *Int J Life Cycle Assess*, vol. 12, no. 6, pp. 448–454, Sep. 2007, doi: 10.1065/lca2006.12.289.
- [256] R. Gebel and B. Synowiec, 'Badanie możliwości zastosowania odpadowego szkła kineskopowego do produkcji szklów, topników i barwnych kształtek ceramicznych', *Materiały Ceramiczne*, vol. 62, no. 2, pp. 234–238, 2012.
- [257] A. S. Apkaryan and A. I. Kudyakov, 'Thermal insulation of pipelines by foamed glass-ceramic', *IOP Conf. Ser.: Mater. Sci. Eng.*, vol. 71, p. 012004, Jan. 2015, doi: 10.1088/1757-899X/71/1/012004.
- [258] J. König, R. R. Petersen, and Y. Yue, 'Fabrication of highly insulating foam glass made from CRT panel glass', *Ceramics International*, vol. 41, no. 8, pp. 9793–9800, Sep. 2015, doi: 10.1016/j.ceramint.2015.04.051.
- [259] A. R. Barbosa, A. A. S. Lopes, R. C. C. Monteiro, and F. Castro, 'Glass foams from cathode ray tubes', *Ciência & Tecnologia dos Materiais*, vol. 27, p. 6, 2015.
- [260] Fernandes, Hugo, R., Andreola, Fernanda, Barbieri, Luisa, Lancellotti, Isabella, Pascual, Maria, J., and Ferreira, Jose, M.F., 'The use of egg shells to produce Cathode Ray Tube (CRT) glass foams', *Ceramics International*, vol. 39, no. 8, pp. 9071–9078, 2013.
- [261] Revelo, Raul, J., Menegazzo, Ana, P., and Ferreira, Eduardo, B., 'Cathode-Ray Tube panel glass replaces frit in transparent glazes for ceramic tiles', *Ceramics International*, vol. 44, no. 12, pp. 13790–13796, 2018.
- [262] M. Dondi, G. Guarini, M. Raimondo, and C. Zanelli, 'Recycling PC and TV waste glass in clay bricks and roof tiles', *Waste Management*, vol. 29, no. 6, pp. 1945–1951, 2009.
- [263] Pozzi, P., Taurino, R., Zanasi, T., Andreola, Fernanda, Barbieri, Luisa, and Lancellotti, Isabella, 'New polypropylene/glass composites: Effect of glass fibers from cathode ray tubes on thermal and mechanical properties', *Composites Part A: Applied Science and Manufacturing*, vol. 41, no. 3, pp. 435–440, 2010.
- [264] Benzerga, Ratiba *et al.*, 'Waste-glass recycling: A step toward microwave applications', *Materials Research Bulletin*, vol. 67, pp. 261–265, 2015.
- [265] S. Mostaghel, Q. Yang, and C. Samuelsson, 'Recycling of cathode ray tube in metallurgical processes: influence on environmental properties of the slag', *Global Journal of Environmental Science and Technology*, vol. 1, no. 19, 2011.
- [266] D. Pant and Singh, Pooja, 'Chemical modification of waste glass from cathode ray tubes (CRTs) as low cost adsorbent', *Journal of Environmental Chemical Engineering*, vol. 1, no. 3, pp. 226–232, 2013.

- [267] M. Chen, F.-S. Zhang, and J. Zhu, 'Detoxification of cathode ray tube glass by self-propagating process', *Journal of Hazardous Materials*, vol. 165, no. 1–3, pp. 980–986, Jun. 2009, doi: 10.1016/j.jhazmat.2008.10.098.
- [268] H. Miyoshi, D. Chen, and T. Akai, 'A Novel Process Utilizing Subcritical Water to Remove Lead from Wasted Lead Silicate Glass', *Chem. Lett.*, vol. 33, no. 8, pp. 956–957, Aug. 2004, doi: 10.1246/cl.2004.956.
- [269] Yuan, Wenyi, Li, Jinhui, Zhang, Qiwu, and Saito, Fumio, 'Innovated Application of Mechanical Activation To Separate Lead from Scrap Cathode Ray Tube Funnel Glass', *Environmental Science & Technology*, vol. 46, no. 7, pp. 4109–4114, 2012.
- [270] G. Grause, N. Yamamoto, T. Kameda, and T. Yoshioka, 'Removal of lead from cathode ray tube funnel glass by chloride volatilization', *Int. J. Environ. Sci. Technol.*, vol. 11, no. 4, pp. 959–966, May 2014, doi: 10.1007/s13762-013-0286-0.
- [271] T. Liu, S. Qin, D. Zou, and W. Song, 'Experimental investigation on the durability performances of concrete using cathode ray tube glass as fine aggregate under chloride ion penetration or sulfate attack', *Construction and Building Materials*, vol. 163, pp. 634–642, Feb. 2018, doi: 10.1016/j.conbuildmat.2017.12.135.
- [272] T. Liu, H. Wei, D. Zou, A. Zhou, and H. Jian, 'Utilization of waste cathode ray tube funnel glass for ultra-high performance concrete', *Journal of Cleaner Production*, vol. 249, p. 119333, Mar. 2020, doi: 10.1016/j.jclepro.2019.119333.
- [273] D. Romero, J. James, R. Mora, and C. D. Hays, 'Study on the mechanical and environmental properties of concrete containing cathode ray tube glass aggregate', *Waste Management*, vol. 33, no. 7, pp. 1659–1666, Jul. 2013, doi: 10.1016/j.wasman.2013.03.018.
- [274] M. Najduchowska, K. Różycka, and G. Rolka, 'Ocena możliwości wykorzystania stłuczki szklanej w przemyśle budowlanym w aspekcie jej wpływu na środowisko naturalne', *PRACE Instytutu Ceramiki i Materiałów Budowlanych*, no. 17, p. 12, 2014.
- [275] Z. Hui and W. Sun, 'Study of properties of mortar containing cathode ray tubes (CRT) glass as replacement for river sand fine aggregate', *Construction and Building Materials*, vol. 25, no. 10, pp. 4059–4064, Oct. 2011, doi: 10.1016/j.conbuildmat.2011.04.043.
- [276] P. Walczak, J. Małolepszy, M. Reben, and K. Rzepa, 'Mechanical Properties of Concrete Mortar Based on Mixture of CRT Glass Cullet and Fluidized Fly Ash', *Procedia Engineering*, vol. 108, pp. 453–458, 2015, doi: 10.1016/j.proeng.2015.06.170.
- [277] P. Walczak, J. Małolepszy, M. Reben, P. Szymański, and K. Rzepa, 'Utilization of Waste Glass in Autoclaved Aerated Concrete', *Procedia Engineering*, vol. 122, pp. 302–309, 2015, doi: 10.1016/j.proeng.2015.10.040.
- [278] J. Jura and M. Ulewicz, 'Zastosowanie popiołu lotnego i szkła kineskopowego w zaprawach cementowych', *Przegląd Naukowy Inżynieria i Kształtowanie Środowiska*, vol. 27, no. 3, pp. 348–354, Sep. 2018, doi: 10.22630/PNIKS.2018.27.3.34.
- [279] A. Pietrzak and M. Ulewicz, 'Wpływ odpadów z kineskopowej stłuczki szklanej (CRT) na parametry wytrzymałościowe zapraw cementowych', *Materiały Budowlane*, no. 10, pp. 49–50, 2017.
- [280] Y. Ouldkaoua, B. Benabed, R. Abousnina, E.-H. Kadri, and J. Khatib, 'Effect of using metakaolin as supplementary cementitious material and recycled CRT funnel glass as fine aggregate on the durability of green self-compacting concrete', *Construction and Building Materials*, vol. 235, p. 117802, Feb. 2020, doi: 10.1016/j.conbuildmat.2019.117802.
- [281] D. Kim, M. Quinlan, and T. F. Yen, 'Encapsulation of lead from hazardous CRT glass wastes using biopolymer cross-linked concrete systems', *Waste Management*, vol. 29, no. 1, pp. 321–328, Jan. 2009, doi: 10.1016/j.wasman.2008.01.022.
- [282] T.-C. Ling and C.-S. Poon, 'Feasible use of recycled CRT funnel glass as heavyweight fine aggregate in barite concrete', *Journal of Cleaner Production*, vol. 33, pp. 42–49, Sep. 2012, doi: 10.1016/j.jclepro.2012.05.003.

- [283] T.-C. Ling, C.-S. Poon, W.-S. Lam, T.-P. Chan, and K. K.-L. Fung, 'Utilization of recycled cathode ray tubes glass in cement mortar for X-ray radiation-shielding applications', *Journal of Hazardous Materials*, vol. 199–200, pp. 321–327, Jan. 2012, doi: 10.1016/j.jhazmat.2011.11.019.
- [284] T.-C. Ling and C.-S. Poon, 'Use of recycled CRT funnel glass as fine aggregate in dry-mixed concrete paving blocks', *Journal of Cleaner Production*, vol. 68, pp. 209–215, Apr. 2014, doi: 10.1016/j.jclepro.2013.12.084.
- [285] T. Liu, W. Song, D. Zou, and L. Li, 'Dynamic mechanical analysis of cement mortar prepared with recycled cathode ray tube (CRT) glass as fine aggregate', *Journal of Cleaner Production*, vol. 174, pp. 1436–1443, Feb. 2018, doi: 10.1016/j.jclepro.2017.11.057.
- [286] W. Song, D. Zou, T. Liu, J. Teng, and L. Li, 'Effects of recycled CRT glass fine aggregate size and content on mechanical and damping properties of concrete', *Construction and Building Materials*, vol. 202, pp. 332–340, Mar. 2019, doi: 10.1016/j.conbuildmat.2019.01.033.
- [287] B. Witkowski and A. Pietrzak, 'Wpływ odpadowej stłuczki kineskopowej na wybrane właściwości zaprawy cementowej', *Zeszyty Naukowe Politechniki Częstochowskiej. Budownictwo*, vol. 174, no. 24, pp. 373–376, Jan. 2019, doi: 10.17512/znb.2018.1.57.
- [288] N. N. M. Pauzi, M. Jamil, R. Hamid, A. Z. Abdin, and M. F. M. Zain, 'Influence of spherical and crushed waste Cathode-Ray Tube (CRT) glass on lead (Pb) leaching and mechanical properties of concrete', *Journal of Building Engineering*, vol. 21, pp. 421–428, Jan. 2019, doi: 10.1016/j.jobee.2018.10.024.
- [289] A. M. Rashad, 'Recycled cathode ray tube and liquid crystal display glass as fine aggregate replacement in cementitious materials', *Construction and Building Materials*, vol. 93, pp. 1236–1248, Sep. 2015, doi: 10.1016/j.conbuildmat.2015.05.004.
- [290] S. Luhar and I. Luhar, 'Potential application of E-wastes in construction industry: A review', *Construction and Building Materials*, vol. 203, pp. 222–240, Apr. 2019, doi: 10.1016/j.conbuildmat.2019.01.080.
- [291] N. Singh, J. Li, and X. Zeng, 'Solutions and challenges in recycling waste cathode-ray tubes', *Journal of Cleaner Production*, vol. 133, pp. 188–200, Oct. 2016, doi: 10.1016/j.jclepro.2016.04.132.
- [292] Lancellotti, Isabella, Barbieri, Luisa, and Leonelli, C., 'Use of alkali-activated concrete binders for toxic waste immobilization', in *Handbook of Alkali-activated Cements, Mortars and Concretes.*, ELSEVIER, 2015, pp. 539–554.
- [293] J. G. S. Van Jaarsveld, J. S. J. Van Deventer, and L. Lorenzen, 'The potential use of geopolymeric materials to immobilise toxic metals: Part I. Theory and applications', *Minerals Engineering*, vol. 10, no. 7, pp. 659–669, Jul. 1997, doi: 10.1016/S0892-6875(97)00046-0.
- [294] J. W. Phair, J. S. J. van Deventer, and J. D. Smith, 'Effect of Al source and alkali activation on Pb and Cu immobilisation in fly-ash based "geopolymers"', *Applied Geochemistry*, vol. 19, no. 3, pp. 423–434, Mar. 2004, doi: 10.1016/S0883-2927(03)00151-3.
- [295] Somna, Kiatsuda, Jaturapitakkul, Chai, Kajitvichyanukul, Puangrat, and Chindapasirt, Prinya, 'Immobilization of Heavy Metals by Fly Ash-Based Geopolymer', presented at the 12th International 12th Conference on Integrated Diffuse Pollution Management (IWA DIPCON 2008), Research Center for Environmental and Hazardous Substance Management (EHSM), 2008, pp. 1191–1198.
- [296] A. Palomo and M. Palacios, 'Alkali-activated cementitious materials: Alternative matrices for the immobilisation of hazardous wastes Part II. Stabilisation of chromium and lead', *Cement and Concrete Research*, vol. 33, pp. 289–295, 2003, doi: 10.1016/S0008-8846(02)00964-X.
- [297] Z. Ji, L. Su, and Y. Pei, 'Synthesis and toxic metals (Cd, Pb, and Zn) immobilization properties of drinking water treatment residuals and metakaolin-based geopolymers', *Materials Chemistry and Physics*, vol. 242, p. 122535, Feb. 2020, doi: 10.1016/j.matchemphys.2019.122535.
- [298] A.-M. Moncea, M. Georgescu, A. Badanoiu, E. Matei, and S. Stoleriu, 'Alkali activated binders as matrices for the immobilization of glass waste with Pb content', in *Proceedings of the 18th International Conference on Building Materials (IBAUSIL 2012), 12. bis 15. September, Weimar, Germany*, Weimar, Germany: Bauhaus-Universität Weimar, Aug. 2012, p. 9.

- [299] 'NEN 7345: LEACHING CHARACTERISTICS OF SOLID EARTHY AND STONY BUILDING AND WASTE MATERIALS - LEACHING TESTS - DETERMINATION OF THE LEACHING OF INORGANIC COMPONENTS FROM BUILDINGS AND MONOLITIC WASTE MATERIALS WITH THE DIFFUSION TEST'. Netherlands Standards, 1994.
- [300] 'THE BUILDING MATERIALS DECREE, (an English translation of the decree and an English brochure on the Building Materials Decree (Bouwstoffenbesluit)'. The Netherlands Ministry of Housing, Spatial Planning and the Environment (VROM), 1995.
- [301] A. M. Moncea, M. Georgescu, A. Melinescu, T. Stoleriu, and A. Moncea, 'Hardening processes and hydrates in alkali-activated slag and geopolymer with Pb content', *Romanian Journal of Materials*, vol. 42, no. 4, pp. 356–363, 2012.
- [302] X. Gao, X. Yao, R. Xie, X. Li, J. Cheng, and T. Yang, 'Performance of fly ash-based geopolymer mortars with waste cathode ray tubes glass fine aggregate: A comparative study with cement mortars', *Construction and Building Materials*, vol. 344, p. 128243, Aug. 2022, doi: 10.1016/j.conbuildmat.2022.128243.
- [303] M. Catauro, I. Lancellotti, and C. Leonelli, 'Addition of WEEE Glass to Metakaolin-Based Geopolymeric Binder: A Cytotoxicity Study', *Environments*, vol. 4, no. 4, p. 89, Dec. 2017, doi: 10.3390/environments4040089.
- [304] 'EN 12457: CHARACTERIZATION OF WASTE - LEACHING - COMPLIANCE TEST FOR LEACHING OF GRANULAR WASTE MATERIALS AND SLUDGES'. Comite Europeen de Normalisation, 2002.
- [305] 'SW-846 Test Method 1311: Toxicity Characteristic Leaching Procedure (TCLP)'. National Environmental Laboratory Accreditation Committee (NELAC), 1992.
- [306] D. T. Ogundele, O. O. Owoyemi, I. J. Akinruli, and I. Toyin, 'Synthesis of a Geopolymer with the Blend of Clay from Share Deposit and Cullet of Cathode Ray Tube', *Technology Reports of Kansai University*, vol. 62, no. 02, p. 12, 2020.
- [307] W.-J. Long, H.-D. Li, H. Ma, Y. Fang, and F. Xing, 'Green alkali-activated mortar: Sustainable use of discarded cathode-ray tube glass powder as precursor', *Journal of Cleaner Production*, vol. 229, pp. 1082–1092, Aug. 2019, doi: 10.1016/j.jclepro.2019.05.066.
- [308] W.-J. Long, C. Lin, T.-H. Ye, B. Dong, and F. Xing, 'Stabilization/solidification of hazardous lead glass by geopolymers', *Construction and Building Materials*, vol. 294, p. 123574, Aug. 2021, doi: 10.1016/j.conbuildmat.2021.123574.
- [309] W.-J. Long *et al.*, 'Recycling of waste cathode ray tube glass through fly ash-slag geopolymer mortar', *Construction and Building Materials*, vol. 322, p. 126454, Mar. 2022, doi: 10.1016/j.conbuildmat.2022.126454.
- [310] H. R. Guzmán-Carrillo *et al.*, 'Encapsulation of toxic heavy metals from waste CRT using calcined kaolin base-geopolymer', *Materials Chemistry and Physics*, vol. 257, p. 123745, Jan. 2021, doi: 10.1016/j.matchemphys.2020.123745.
- [311] 'A new integrated process to valorise hazardous leaded glass from CRTs and transform it into high performance geopolymer blocks - VirtuCrete', *European Commission*, Jun. 24, 2019. <https://cordis.europa.eu/project/id/673527> (accessed Apr. 15, 2021).
- [312] 杨涛, 程俊华, 高璇, 吴浩, 诸华军, and 吴其胜, 'Radiation-proof geopolymer and preparation method thereof', CN108484014A
- [313] A. Badanoiu, E. Iordache, R. Ionescu, G. Voicu, and E. Matei, 'EFFECT OF COMPOSITION AND CURING REGIME ON SOME PROPERTIES OF GEOPOLYMERS BASED ON CATHODE RAY TUBES GLASS WASTE AND FLY ASH', *Romanian Journal of Materials*, vol. 45, no. 1, pp. 3–13, 2015.
- [314] T. Opletal, 'Možnosti zpracování odpadního obrazovkového skla (Possibilities of recycling waste screen glass)', Master's thesis, Univerzita Palackého v Olomouci, Přírodovědecká fakulta, Katedra Geologie (Palacký University in Olomouc, Faculty of Science, Department of Geology), Olomouc, 2013.
- [315] 'Vyhláška č. 294/2005 Sb. Vyhláška o podmínkách ukládání odpadů na skládky a jejich využívání na povrchu terénu'. Jun. 2005.

- [316] 'EN 196-1 Method of testing cement – Part 1: Determination of strength'. EUROPEAN COMMITTEE FOR STANDARDIZATION, Apr. 01, 2016.
- [317] Q. Wan, F. Rao, S. Song, D. F. Cholico-González, and N. L. Ortiz, 'Combination formation in the reinforcement of metakaolin geopolymers with quartz sand', *Cement and Concrete Composites*, vol. 80, pp. 115–122, Jul. 2017, doi: 10.1016/j.cemconcomp.2017.03.005.
- [318] Z. Sun, A. Vollpracht, and H. A. van der Sloot, 'pH dependent leaching characterization of major and trace elements from fly ash and metakaolin geopolymers', *Cement and Concrete Research*, vol. 125, p. 105889, Nov. 2019, doi: 10.1016/j.cemconres.2019.105889.
- [319] J.-X. Lu and C. S. Poon, 'Use of waste glass in alkali activated cement mortar', *Construction and Building Materials*, vol. 160, pp. 399–407, Jan. 2018, doi: 10.1016/j.conbuildmat.2017.11.080.
- [320] A. Hajimohammadi, T. Ngo, and A. Kashani, 'Glass waste versus sand as aggregates: The characteristics of the evolving geopolymer binders', *Journal of Cleaner Production*, vol. 193, pp. 593–603, Aug. 2018, doi: 10.1016/j.jclepro.2018.05.086.
- [321] A. Albidah, M. Alghannam, H. Abbas, T. Almusallam, and Y. Al-Salloum, 'Characteristics of metakaolin-based geopolymer concrete for different mix design parameters', *Journal of Materials Research and Technology*, vol. 10, pp. 84–98, Jan. 2021, doi: 10.1016/j.jmrt.2020.11.104.
- [322] Md. N. N. Khan and P. K. Sarker, 'Effect of waste glass fine aggregate on the strength, durability and high temperature resistance of alkali-activated fly ash and GGBFS blended mortar', *Construction and Building Materials*, vol. 263, p. 120177, Dec. 2020, doi: 10.1016/j.conbuildmat.2020.120177.
- [323] H. Zhao, C. S. Poon, and T. C. Ling, 'Utilizing recycled cathode ray tube funnel glass sand as river sand replacement in the high-density concrete', *Journal of Cleaner Production*, vol. 51, pp. 184–190, Jul. 2013, doi: 10.1016/j.jclepro.2013.01.025.
- [324] R. Mejía de Gutiérrez, M. A. Villaquirán-Caicedo, and L. A. Guzmán-Aponte, 'Alkali-activated metakaolin mortars using glass waste as fine aggregate: Mechanical and photocatalytic properties', *Construction and Building Materials*, vol. 235, p. 117510, Feb. 2020, doi: 10.1016/j.conbuildmat.2019.117510.
- [325] P. S. Humbert, J. P. D. C. Gomes, L. F. A. Bernardo, C. M. Pinto, and N. Paszek, 'Elastic modulus and stress-strain curve analysis of a tungsten mine waste alkali-activated concrete', *MATEC Web Conf.*, vol. 274, p. 02003, 2019, doi: 10.1051/matecconf/201927402003.
- [326] A. M. M. A. Bakri, H. Kamarudin, M. BinHussain, I. K. Nizar, Y. Zarina, and A. R. Rafiza, 'The Effect of Curing Temperature on Physical and Chemical Properties of Geopolymers', *Physics Procedia*, vol. 22, pp. 286–291, 2011, doi: 10.1016/j.phpro.2011.11.045.
- [327] B. Mo, H. Zhu, X. Cui, Y. He, and S. Gong, 'Effect of curing temperature on geopolymerization of metakaolin-based geopolymers', *Applied Clay Science*, vol. 99, pp. 144–148, Sep. 2014, doi: 10.1016/j.clay.2014.06.024.
- [328] J. Yuan *et al.*, 'Effect of curing temperature and SiO<sub>2</sub>/K<sub>2</sub>O molar ratio on the performance of metakaolin-based geopolymers', *Ceramics International*, vol. 42, no. 14, pp. 16184–16190, Nov. 2016, doi: 10.1016/j.ceramint.2016.07.139.
- [329] S. Kumaravel, 'Development of various curing effect of nominal strength Geopolymer concrete', *JESTR*, vol. 7, no. 1, pp. 116–119, Apr. 2014, doi: 10.25103/jestr.071.19.
- [330] L. Chen, Z. Wang, Y. Wang, and J. Feng, 'Preparation and Properties of Alkali Activated Metakaolin-Based Geopolymer', *Materials*, vol. 9, no. 9, p. 767, Sep. 2016, doi: 10.3390/ma9090767.
- [331] N. Paszek and M. Górski, 'Defining the optimal mixture composition of geopolymers based on the coal mine waste and the shale.', *MATEC Web Conf.*, vol. 274, p. 01002, 2019, doi: 10.1051/matecconf/201927401002.
- [332] N. Paszek, L. Szojda, and M. Górski, 'Preliminary determination of the boundary surface of the geopolymer on the basis of the multiaxial compression tests', presented at the CMM-2017-22nd Computer Methods in Mechanics, Lublin, Aug. 2017, p. 2.

- [333] N. Paszek and M. Krystek, 'Numerical simulation of mechanical properties tests of tungsten mud waste geopolymer', *Selected Scientific Papers - Journal of Civil Engineering*, vol. 13, no. s1, pp. 87–94, Mar. 2018, doi: 10.1515/sspjce-2018-0008.
- [334] P. Rovnaník, 'Effect of curing temperature on the development of hard structure of metakaolin-based geopolymer', *Construction and Building Materials*, vol. 24, no. 7, pp. 1176–1183, Jul. 2010, doi: 10.1016/j.conbuildmat.2009.12.023.
- [335] A. M. Moncea, A. Badanoiu, M. Georgescu, and S. Stoleriu, 'Cementitious composites with glass waste from recycling of cathode ray tubes', *Mater Struct*, vol. 46, no. 12, pp. 2135–2144, Dec. 2013, doi: 10.1617/s11527-013-0041-5.
- [336] J. C. Swanepoel and C. A. Strydom, 'Utilisation of fly ash in a geopolymeric material', *Applied Geochemistry*, vol. 17, no. 8, pp. 1143–1148, Aug. 2002, doi: 10.1016/S0883-2927(02)00005-7.
- [337] Z. Zuhua, Y. Xiao, Z. Huajun, and C. Yue, 'Role of water in the synthesis of calcined kaolin-based geopolymer', *Applied Clay Science*, vol. 43, no. 2, pp. 218–223, Feb. 2009, doi: 10.1016/j.clay.2008.09.003.
- [338] M. Nasir, Azmi Megat Johari, Megat, Maslehuddin, Mohammed, Olalekan Yusuf, Moruf, and A. Al-Harhi, Mamdouh, 'Influence of heat curing period and temperature on the strength of silico-manganese fume-blast furnace slag-based alkali-activated mortar', *Construction and Building Materials*, vol. 251, p. 118961, 2020, doi: 10.1016/j.conbuildmat.2020.118961.
- [339] M. L. Granizo, M. T. Blanco-Varela, and A. Palomo, 'Influence of the starting kaolin on alkali-activated materials based on metakaolin. Study of the reaction parameters by isothermal conduction calorimetry', *Journal of Materials Science*, vol. 35, no. 24, pp. 6309–6315, 2000, doi: 10.1023/A:1026790924882.
- [340] C. Kuenzel, T. P. Neville, S. Donatello, L. Vandeperre, A. R. Boccaccini, and C. R. Cheeseman, 'Influence of metakaolin characteristics on the mechanical properties of geopolymers', *Applied Clay Science*, vol. 83–84, pp. 308–314, Oct. 2013, doi: 10.1016/j.clay.2013.08.023.
- [341] Z. Zhang, J. L. Provis, H. Wang, F. Bullen, and A. Reid, 'Quantitative kinetic and structural analysis of geopolymers. Part 2. Thermodynamics of sodium silicate activation of metakaolin', *Thermochimica Acta*, vol. 565, pp. 163–171, Aug. 2013, doi: 10.1016/j.tca.2013.01.040.
- [342] A. Buchwald, R. Tatarin, and D. Stephan, 'Reaction progress of alkaline-activated metakaolin-ground granulated blast furnace slag blends', *J Mater Sci*, vol. 44, no. 20, pp. 5609–5617, Oct. 2009, doi: 10.1007/s10853-009-3790-3.
- [343] H. Rashidian-Dezfouli, P. R. Rangaraju, and V. S. K. Kothala, 'Influence of selected parameters on compressive strength of geopolymer produced from ground glass fiber', *Construction and Building Materials*, vol. 162, pp. 393–405, Feb. 2018, doi: 10.1016/j.conbuildmat.2017.09.166.
- [344] S. K. Adhikary and Z. Rudzionis, 'Influence of expanded glass aggregate size, aerogel and binding materials volume on the properties of lightweight concrete', *Materials Today: Proceedings*, vol. 32, pp. 712–718, 2020, doi: 10.1016/j.matpr.2020.03.323.
- [345] Z. Li, S. Zhang, Y. Zuo, W. Chen, and G. Ye, 'Chemical deformation of metakaolin based geopolymer', *Cement and Concrete Research*, vol. 120, pp. 108–118, Jun. 2019, doi: 10.1016/j.cemconres.2019.03.017.
- [346] *318-19 Building Code Requirements for Structural Concrete and Commentary*. American Concrete Institute, 2019. doi: 10.14359/51716937.
- [347] P. Nath and P. K. Sarker, 'Flexural strength and elastic modulus of ambient-cured blended low-calcium fly ash geopolymer concrete', *Construction and Building Materials*, vol. 130, pp. 22–31, Jan. 2017, doi: 10.1016/j.conbuildmat.2016.11.034.
- [348] X. Zhang *et al.*, 'Porous geopolymer composites: A review', *Composites Part A: Applied Science and Manufacturing*, vol. 150, p. 106629, Nov. 2021, doi: 10.1016/j.compositesa.2021.106629.
- [349] V. Medri *et al.*, 'Production and characterization of lightweight vermiculite/geopolymer-based panels', *Materials & Design*, vol. 85, pp. 266–274, Nov. 2015, doi: 10.1016/j.matdes.2015.06.145.
- [350] C. Bai and P. Colombo, 'Processing, properties and applications of highly porous geopolymers: A review', *Ceramics International*, vol. 44, no. 14, pp. 16103–16118, Oct. 2018, doi: 10.1016/j.ceramint.2018.05.219.

- [351] N. Narayanan and K. Ramamurthy, 'Structure and properties of aerated concrete: a review', *Cement and Concrete Composites*, vol. 22, no. 5, pp. 321–329, Oct. 2000, doi: 10.1016/S0958-9465(00)00016-0.
- [352] B. A. Latella, D. S. Perera, D. Durce, E. G. Mehrtens, and J. Davis, 'Mechanical properties of metakaolin-based geopolymers with molar ratios of Si/Al  $\approx$  2 and Na/Al  $\approx$  1', *J Mater Sci*, vol. 43, no. 8, pp. 2693–2699, Apr. 2008, doi: 10.1007/s10853-007-2412-1.
- [353] H. Hao *et al.*, 'Utilization of solar panel waste glass for metakaolinite-based geopolymer synthesis', *Environ. Prog. Sustainable Energy*, vol. 32, no. 3, pp. 797–803, Oct. 2013, doi: 10.1002/ep.11693.
- [354] 'Rozporządzenie Ministra Gospodarki Morskiej i Żeglugi Śródlądowej z dnia 12 lipca 2019 r. w sprawie substancji szczególnie szkodliwych dla środowiska wodnego oraz warunków, jakie należy spełnić przy wprowadzaniu do wód lub do ziemi ścieków, a także przy odprowadzaniu wód opadowych lub roztopowych do wód lub do urządzeń wodnych. (Regulation of the Ministry of Marine Economy and Inland Navigation of 12 July 2019 on substances particularly harmful to the aquatic environment and the conditions to be met when discharging sewage into waters or soil, as well as discharging rainwater or meltwater into waters or into water facilities)'. Jul. 15, 2019.
- [355] H. Liu, J. Shi, H. Qu, and D. Ding, 'Feasibility of using recycled CRT funnel glass as partial replacement of high density magnetite sand in radiation shielding concrete', *Transactions of Nonferrous Metals Society of China*, vol. 29, no. 4, pp. 831–839, Apr. 2019, doi: 10.1016/S1003-6326(19)64993-9.
- [356] B. S. Al-Shathr, T. S. Al-Attar, and Z. A. Hasan, 'Effect of Curing System on Metakaolin Based Geopolymer Concrete', *Engineering Sciences*, p. 8, 2016.
- [357] Y. Zhang, R. Xiao, X. Jiang, W. Li, X. Zhu, and B. Huang, 'Effect of particle size and curing temperature on mechanical and microstructural properties of waste glass-slag-based and waste glass-fly ash-based geopolymers', *Journal of Cleaner Production*, vol. 273, p. 122970, Nov. 2020, doi: 10.1016/j.jclepro.2020.122970.
- [358] M. Steveson and K. Sagoe-Crentsil, 'Relationships between composition, structure and strength of inorganic polymers. Part I Metakaolin-derived inorganic polymers', *Journal of Materials Science*, no. 40, pp. 2023–2036, doi: 10.1007/s10853-005-1226-2.
- [359] B. Zhang, P. He, and C. S. Poon, 'Improving the high temperature mechanical properties of alkali activated cement (AAC) mortars using recycled glass as aggregates', *Cement and Concrete Composites*, vol. 112, p. 103654, Sep. 2020, doi: 10.1016/j.cemconcomp.2020.103654.
- [360] S. Yang, T.-C. Ling, H. Cui, and C. S. Poon, 'Influence of particle size of glass aggregates on the high temperature properties of dry-mix concrete blocks', *Construction and Building Materials*, vol. 209, pp. 522–531, Jun. 2019, doi: 10.1016/j.conbuildmat.2019.03.131.
- [361] F. J. García-Ten and M. Vicent, 'Effect of CRT glass particle size on the lead leachability of alkali-activated materials', *Materials Letters*, vol. 320, p. 132163, Aug. 2022, doi: 10.1016/j.matlet.2022.132163.

## List of Figures

Fig. 2.1.1: The representation of possible tetrahedral silicate units [37], [41].	13
Fig. 2.1.2: Schematic structure of sodium poly-siloxo silicate geopolymer [37].	14
Fig.2.2.1: Josepha Davidovits during the exploration of pyramids in Egypt [111], [112].	18
Fig.2.2.2: Structures in Brussels made partly of Purdocement [121].	19
Fig.2.2.3: a) 24-storey building made of alkali activated slag-based material in Lipetsk (Russia, 1994), b) Residential building build with alkali hydroxide-activated slag-based precast elements in Mariupol (Ukraine, 1960) [60].	19
Fig.2.3.1: 3D printed, metakaolin-based geopolymer cellular structure [164].	22
Fig.2.3.2: Examples of products made of geopolymer based on tuff: a) cobblestones, b) decorative plate [189].	23
Fig.2.4.1: a) Prototype fibre reinforced geopolymer tunnel segments, b) cross-section of a segment [219].	25
Fig.2.4.2: Sewage pipeline during and after rehabilitation [230].	26
Fig.2.5.1: a) The old television set containing cathode ray tube (CRT) [250], b) schematic view of CRT components [245], c) CRT glass [251].	28
Fig.2.5.2: Possible ways of CRT glass recycling a) in open-loop, b) in closed-loop.	29
Fig.2.5.3: a) Natural sand grains versus, b) CRT glass particles [285].	32
Fig.2.5.4: SEM micrographs of metakaolin based geopolymer with CRT glass with the molar elements ratios: a) Na/Si=0,74, b) Na/Si=0,51 [310].	37
Fig.2.5.5: SEM micrographs of geopolymer containing a) CRT glass (G - glass particle) b) fly ash (FA – fly ash particle) [313].	38
Fig.2.5.6: a) reaction on the surface between CRT particle and metakaolin, b) microcracks caused probably by improper amount of liquid, c) microcracks caused probably by too much CRT glass inside matrix [314].	39
Fig.3.2.1: a) Metakaolin, b) CRT glass.	44
Fig.3.2.2: The particle size distribution of CRT glass (done by the Author in Laboratory of Civil Engineering, Silesian University of Technology).	45
Fig.3.2.3: The particle size distribution of metakaolin and fine particles of CRT glass (done by Professor Sara Rios at Faculty of Civil Engineering, University of Porto).	45
Fig.3.3.1: Schematic view of the prismatic sample (all dimensions in mm) a) overall dimensions, b) sample during the flexural strength test.	46
Fig.3.3.2: Strength tests machine Controls® Model 65-L27C12 Serial nr 12020060, during the compressive strength test.	47
Fig.3.3.3: Metal plates of dimensions 40x40 mm in compressive strength test machine, a) the bottom plate, b) geopolymer sample after compressive strength test, the bottom and upper plates are marked with the use of green circle.	48
Fig.3.5.1: Seventh day flexural and compressive strength of geopolymer containing CRT glass from three different batches, cured at 20°C or at 40°C.	50
Fig.3.6.1: a) Samples with CRT glass aggregate, b) samples with sand aggregate.	51
Fig.3.6.2: Cross section of sample containing a) CRT glass, b) sand.	52
Fig.3.6.3: Flexural and compressive strength of samples containing CRT glass or sand cured for 7 days.	52
Fig.3.7.1: a) Metakaolin-based geopolymer samples with CRT glass, b) weighing of sample, c) measuring of sample's cross-section dimensions.	55
Fig.3.7.2: Sample from series M/G 50/50, after a) flexural strength test b) compressive strength test.	56
Fig.3.7.3: a) Sample with high CRT glass content (from series M/G 40/60), b) sample with low CRT glass content (from series M/G 75/25).	57

Fig.3.7.4: Sample after compressive strength test a) sample without CRT glass (only metakaolin), b) sample from series M/G 50/50 (metakaolin to CRT glass mass ratio equal to 1:1), c) sample from series M/G 25/75 (metakaolin to CRT glass mass ratio equal to 1:3). .....	58
Fig.3.7.5: The surface of a broken sample a) without CRT glass (series M/G 100/0), b) with CRT glass (series M/G 40/60). .....	58
Fig.3.7.6: Seventh days compressive and flexural strength of geopolymer made of mixtures containing different metakaolin to CRT glass mass ratio.....	59
Fig.3.7.7: The $f_x/f_c$ ratio of geopolymer with different CRT glass content. ....	60
Fig.3.8.1: a) Climatic chamber, b) samples cured inside the climatic chamber. ....	62
Fig.3.8.2: Comparison of differences in color of the surface of the same sample a) only after unmolding, b) after 7 days of curing.....	63
Fig.3.8.3: Uncracked side surface of samples cured at a) 60°C (M/G 50/50) and b) 40°C (M/G 60/40). Photos made after 7 days of curing. There was no significant difference in color between samples. The difference visible in photos is caused by the difference in lighting. ....	64
Fig.3.8.4: a) Cracked side surface of samples cured at 20°C and demoulded after 24 hours (M/G 50/50) b) uncracked side surface of samples cured at 20°C and demoulded after 7 days (M/G 60/40). Photos made after 7 days of curing. ....	64
Fig.3.8.5: Samples cured at 20°C and demoulded after 24 hours (M/G 60/40): a) upper surface, b) side surface, c) bottom surface. Photos made after 7 days of curing.....	64
Fig.3.8.6: The beam after flexural strength test. Samples containing metakaolin to glass in mass ratio (M/G 50/50): a) series 20°C (2), b) series 60°C. There is visible the difference in color between picture a) and b). The color of samples cured at 20°C was darker than of samples cured at 60°C. ....	67
Fig.3.8.7: Seventh days flexural strength of geopolymer made of mixtures containing different metakaolin to CRT glass mass ratio and cured in different conditions. ....	67
Fig.3.8.8: Seventh days compressive strength of geopolymer made of mixtures containing different metakaolin to CRT glass mass ratio and cured in different conditions. ....	68
Fig.3.8.9: The $f_x/f_c$ ratio of geopolymer of different CRT glass content and cured in different temperatures. ....	69
Fig.3.9.1: Samples prepared for measurement with use of a caliper.....	72
Fig.3.9.2: Thermometers attached inside the forms.....	72
Fig.3.9.3: Broken surface of sample containing a) 75% of CRT glass b) 50% of CRT glass (photographs were taken by dr Fatima Pawelczyk in Institute of Physics, Centre for Science and Education, Silesian University of Technology).....	75
Fig.3.9.4: Cavities in geopolymer containing 75% of CRT glass. The biggest cavities were marked with the green circle.....	75
Fig.3.9.5: The temperature changes during the first 10 hours of curing.....	77
Fig.3.9.6: The temperature changes during the first 30 hours of curing.....	77
Fig.3.9.7: Flexural strength of geopolymer made of mixtures containing different metakaolin to CRT glass mass ratio and cured for different time.....	78
Fig.3.9.8: Compressive strength of geopolymer made of mixtures containing different metakaolin to CRT glass mass ratio and cured for different time.....	79
Fig.3.9.9: The change of $f_x/f_c$ ratio of geopolymer with different CRT glass content over time. ....	80
Fig.3.9.10: The loss of the mass of the samples during the following curing days. ....	81
Fig.4.1.1: Samples cured at different temperatures and cured for different time period: a) 20°C, 3 days, b) 20°C, 7 days, c) 20°C, 28 days, d) 40°C, 3 days, e) 40°C, 7 days, f) 40°C, 28 days. The color of samples cured at 20°C (a), b), and c)) was significantly darker than color of samples cured at 40°C (d), e) and f)). ....	84
Fig.4.1.2: Sample cured at 20°C and demoulded after 24 hours. Picture taken after 27 days of further curing at the room temperature in the laboratory. ....	85

Fig.4.1.3: The upper surface of sample cured at 20°C and demoulded after 24 hours a) picture taken after unmolding (after 24 hours of curing) b) picture taken after 27 days of further curing at the room temperature in the laboratory.....	85
Fig.4.1.4: Crack formed in the middle of the beam span (below the concentrated force) after flexural strength test. Sample cured for: a) 1 day, b) 3 days, c) 7 days, d) 14 days, e) 28 days. There was no significant difference in color between samples. The difference visible in pictures has been caused by the difference in lighting. ....	87
Fig.4.1.5: Change of the flexural strength of geopolymer made of mixture M/G 50/50 and cured at different temperatures over time. ....	88
Fig.4.1.6: Change of the compressive strength of geopolymer made of mixture M/G 50/50 and cured at different temperatures over time. ....	89
Fig.4.1.7: Change of the $f_x/f_c$ ratio of geopolymer made of mixture M/G 50/50 and cured at different temperatures over time. ....	90
Fig.4.2.1: Beams before strength tests. Series containing NaOH of concentration a) 6 mol/L, b) 8 mol/L, c) 10 mol/L, d) 12 mol/L. ....	92
Fig.4.2.2: Beams cracked after flexural strength test. Sample containing NaOH of concentration a) 6 mol/L, b) 8 mol/L, c) 10 mol/L.....	94
Fig.4.2.3: Seventh days compressive and flexural strength of geopolymer made of mixtures activated with NaOH of different concentration.....	94
Fig.4.2.4: The $f_x/f_c$ ratio of geopolymer of different NaOH concentration. ....	95
Fig.4.3.1: CRT glass of grain fraction a) < 0,5 mm, b) < 4 mm, c) 0,5 – 4 mm. ....	96
Fig.4.3.2: Samples containing CRT glass of grain fraction a) < 0,5 mm, b) < 4 mm, c) 0,5 – 4 mm. ....	97
Fig.4.3.3: Beams cracked after flexural strength test. Sample containing CRT glass of fraction a) < 0,5 mm, b) < 4 mm, c) 0,5 – 4 mm. ....	98
Fig.4.3.4: Cross-section of a broken sample containing CRT glass of size a) < 0,5 mm, b) < 4 mm, c) 0,5 – 4 mm. Picture taken 7 days after strength test.....	98
Fig.4.3.5: Cross-section of a broken sample containing CRT glass of size a) < 0,5 mm, b) < 4 mm, c) 0,5 – 4 mm. Picture taken immediately after flexural strength test. ....	99
Fig.4.3.6: Seventh days compressive and flexural strength of geopolymer made of mixtures containing CRT glass of different particle's size.....	100
Fig.4.3.7: The $f_x/f_c$ ratio of geopolymer made of mixtures containing CRT glass of different particle's size. ....	100
Fig.4.4.1: Crack appearing in the place of subjection of load after flexural strength test. Sample cured for: a) 1 day, b) 3 days, c) 7 days, d) 14 days, e) 28 days, f) 56 days, g) 112 days. There was no significant difference in color between samples presented in a), b), c), d) and e). The difference visible in photos is caused by the difference in lighting. Samples presented in f) and g) were visibly brighter. ....	104
Fig.4.4.2: Broken surface of four samples made of mixture M/G 50/50 (containing 50% of CRT glass). (Photographs were taken by dr Fatima Pawelczyk in Institute of Physics, Centre for Science and Education, Silesian University of Technology). ....	105
Fig.4.4.3: Broken surface of one chosen sample made of mixture M/G 50/50. (Photograph was taken by dr Fatima Pawelczyk in Institute of Physics, Centre for Science and Education, Silesian University of Technology). ....	106
Fig.4.4.4: Change of the compressive and flexural strength of geopolymer made of mixture M/G 50/50 and cured at ambient temperature, over time. ....	106
Fig.4.4.5: Change of the $f_x/f_c$ ratio of geopolymer made of mixture M/G 50/50 and cured at ambient temperature, over time. ....	107

## List of Tables

Table 3.2.1: Chemical composition of metakaolin <sup>1</sup> .....	44
Table 3.2.2: Chemical composition of CRT glass <sup>1</sup> , [%].....	45
Table 3.5.1: Flexural ( $f_x$ ) and compressive ( $f_c$ ) strength results. ....	49
Table 3.5.2: Standard deviation and coefficient of variation of flexural and compressive strength results. ....	49
Table 3.6.1: Mixture composition.....	50
Table 3.6.2: Flexural ( $f_x$ ) and compressive ( $f_c$ ) strength results. ....	51
Table 3.6.3: Average density of geopolymer containing CRT glass or sand.....	53
Table 3.7.1: Mixtures compositions.....	54
Table 3.7.2: Flexural ( $f_x$ ) and compressive ( $f_c$ ) strength results. ....	56
Table 3.7.3: Standard deviation and coefficient of variation (CoV) of flexural and compressive strength results. ....	57
Table 3.7.4: Average density and mass loss of geopolymer samples made of each mixture. ....	61
Table 3.8.1: Mixtures compositions.....	61
Table 3.8.2: Flexural ( $f_x$ ) and compressive ( $f_c$ ) strength results. ....	65
Table 3.8.3: Standard deviation and coefficient of variation of flexural and compressive strength results. ....	66
Table 3.8.4: Average density and mass loss of geopolymer samples made of different mixtures and cured at different conditions. ....	70
Table 3.9.1: Mixtures compositions.....	71
Table 3.9.2: Flexural ( $f_x$ ) and compressive ( $f_c$ ) strength results.....	74
Table 3.9.3: Standard deviation and coefficient of variation of flexural and compressive strength results. ....	74
Table 3.9.4: Mass of each sample tested after 7 days on each following day of curing. ....	76
Table 3.9.5: Average density and mass loss of geopolymer samples made of different mixtures and cured for different time periods. ....	80
Table 3.9.6: Average density of geopolymer in the following curing days.....	82
Table 4.1.1: Mixture composition.....	83
Table 4.1.2: Flexural ( $f_x$ ) and compressive ( $f_c$ ) strength results. ....	86
Table 4.1.3: Standard deviation and coefficient of variation of flexural and compressive strength results. ....	87
Table 4.1.4: Average density of geopolymer made of mixture M/G 50/50 in the following curing days.....	90
Table 4.2.1: Flexural and compressive strength results. ....	93
Table 4.2.2: Standard deviation and coefficient of variation of compressive strength results. ....	93
Table 4.2.3: Average density of geopolymer activated by NaOH of different concentrations. ....	95
Table 4.3.1: Flexural and compressive strength results.....	97
Table 4.3.2: Standard deviation and coefficient of variation of flexural and compressive strength results. ....	98
Table 4.3.3: Average density of geopolymer containing CRT glass of different size.....	101
Table 4.4.1: Flexural ( $f_x$ ) and compressive ( $f_c$ ) strength results.....	102
Table 4.4.2: Standard deviation [-] and coefficient of variation [%] of compressive and flexural strength results. ....	103
Table 4.4.3: Average density of geopolymer in the following curing days [kg/m <sup>3</sup> ]. ....	109
Table 5.1.1: Results.....	111
Table 5.1.2: Average values, standard deviations and coefficient of variation for each test result. ....	111
Table 5.2.1: Physicochemical analysis of aqueous extracts from CRT glass and geopolymer containing CRT glass. ....	113

## SUMMARY

### **CHAPTER 1 INTRODUCTION**

The chapter contains the description of background and motivation for the work together with the definition of the problem – the escalating environmental problems, mainly with CO<sub>2</sub> emission and water sources. Geopolymer (the mixture of aluminosilicate material called a precursor and liquid activator) is considered as an environmentally friendly alternative for ordinary Portland cement concrete which production consumes significant amounts of water and is responsible for significant CO<sub>2</sub> emission. Despite savings on CO<sub>2</sub> emission and extent water consumption, geopolymer allows to reuse many kinds of industrial waste (including the hazardous one) inside its matrix. The use of the various kinds of waste as the precursor is popular, but the aggregate role is still the most often played by natural materials such as sand. This Thesis responds for that issue offering solution in the form of discarded, crushed CRT glass aggregate. The reuse of CRT glass inside geopolymer in form of an aggregate offers simultaneously the solution of the problem of safe recycling of that hazardous waste.

The chapter presents as well four research hypotheses:

Hypothesis 1: Discarded CRT glass can be used in metakaolin-based geopolymer in the role of aggregate without special pre-treatment.

Hypothesis 2: Metakaolin-based geopolymer with CRT glass can be considered as a building material, regarding to the flexural and compressive strength.

Hypothesis 3: Metakaolin-based geopolymer with CRT glass can be cured in different temperatures without crucial impact on strength.

Hypothesis 4: The incorporation of CRT glass inside metakaolin-based geopolymer reduces the danger of environment pollution with heavy metals.

The chapter emphasizes also the main aim of this thesis – the presentation and description of the metakaolin-based geopolymer with CRT glass as potential building material together with proposition of the new way of CRT glass recycling – and the minor goals such as: the summary of existing knowledge about the raised topic, the description of the influence of various factors on mechanical behavior of geopolymer, the determination of porosity, density and leaching of heavy metals, the comparison of achieved results with results presented in scientific literature, the summary, conclusions and determination of future goals.

Finally, the chapter shows the organization of this Thesis and characterizes briefly each of eight main chapters.

### **CHAPTER 2 STATE-OF-THE-ART**

The chapter begins with the description of general characteristics of geopolymer with the special emphasis on the chemical characteristics. Geopolymerization is concluded as the process built of three main stages: deconstruction, polymerization and stabilization. Further, the most popular types of precursors are listed and described (metakaolin, fly ash and ground granulated blast furnace slag) but the rarely used are mentioned as well. As the most popular activators there are indicated sodium silicate and sodium hydroxide or potassium hydroxide. Then, the most popular methods of mixture designing are presented. Most of scientists adjust components of the mixture to obtain the desired Si/Al ratio and Na/Al ratio.

The chapter introduces as well the historical background, starting from the potential ancient beginnings (Joseph Davidovits should be mentioned here as the father of those ideas), through the first published researches (as the most notable scientists should be listed here Hans Kuhl, Arthur Oscar Purdon and years later – Victor Glukhovskiy) finishing on undeniable Polish input of

professor Jan Małolepszy, Jan Deja and Wiesława Nocuń-Wczelik. The next part focuses on the more current works carried on all-over the World: in Great Britain, Australia, China, Spain, Portugal, France and United States. The special emphasize has been put on researches done by Jannie van Deventer and John Provis. Finally, the works currently carried on in Poland have been described, focusing mainly on researches published by scientists from Cracow University of Technology and Silesian University of Technology: professor Janusz Mikula, professor Izabela Hager, professor Jan Kubica, professor Marcin Górski and works published by the Author of this Thesis.

Further, the various possible applications of geopolymers have been described. The civil engineering branch includes the masonry units, pavements, culverts, roof tiles and even the airport runways. Due to the high fire and chemical resistance as well as anti-corrosion properties, geopolymers found application as protective layers for reinforced concrete and steel. The less popular applications include: self-healing materials, 3D printing, restoration of monuments or even the possible material for lunar structures.

The next part is devoted to the CRT glass – the general characteristics, the parts of cathode ray tube, the heavy metals content, the recycling methods (in open loop and closed-loop) and methods of special treating to make it safer for environment. The application of CRT glass in concrete is described precisely, mainly in the role of an aggregate. According to the scientists, application of CRT glass into the concrete structures can be safe way of its utilization but it causes the decrease of strength.

The chapter includes as well the examples of successful immobilization of heavy metals inside geopolymer mixture. Then, the extended presentation of publications devoted to the utilization of CRT glass inside geopolymer mixture is given. The CRT glass has been utilized in geopolymers based on different type of precursors (metakaolin, fly ash, slag and combinations of listed ones) both in a form of a powder and in form of an aggregate.

The chapter is concluded with summary of all information and with the deficiencies both in existing knowledge and researches about geopolymers with CRT glass. As the main deficiency there is defined the lack of the extended research on one type of geopolymer. As an answer to the defined deficiencies, an Author decided to do the extended research on metakaolin-based geopolymer with CRT glass in form of an aggregate. The research includes among the others both flexural and compressive strength tests, the finding of an optimal mixture and study of an influence of various factors on its mechanical behavior.

### **CHAPTER 3 PRELIMINARY RESEARCH**

At the very beginning the graphical scheme of the research part is presented.

Then, the chapter continuous with the characteristics and origin of all materials used during the tests: metakaolin, CRT glass, sodium silicate and sodium hydroxide. Next, the research methods are presented including shape of the samples, description of equipment and used standards. Then, the Author presents the initial tests. The first test has been done on samples containing CRT glass coming from different batches to check the convergence of results. The next test contains comparison between strength of geopolymer containing sand and CRT glass to asses superficially how does the replacement of aggregate influence the mechanical behavior (it occurs that the strength of geopolymer containing CRT glass is smaller than strength of geopolymer with sand).

The next part describes precisely the influence of the CRT glass content on flexural and compressive strength of samples. The whole procedure of the test together with presentation of results and analysis is presented. The flexural to compressive strength ratio and the density has been calculated as well. According to results, there is no monotonic dependence between CRT glass content and mechanical behavior. The range of flexural strength values was equal to

3,6 - 6,2 MPa, while the range of compressive strength results was equal to 41,6 – 50,1 MPa. Four mixtures have been chosen for the further tests.

The next test has been devoted to the influence of curing temperature on the mechanical behavior of geopolymer. Samples were cured at 20°C, 40°C and 60°C. According to the results, the flexural strength increases along with the increase of the curing temperature while the compressive strength behaves in not monotonic way and is approximately similar for all curing temperatures. Two mixtures and one curing conditions were chosen for the further test.

The last from the initial tests has been focused on the temperature changes inside the geopolymer and the changes of strength over time. Samples were cured at 40°C for the first 24 hours and then at the room temperature. According to the results, the temperature inside geopolymer grows along with the increase of the metakaolin content. The strength of geopolymer samples containing more CRT glass showed the tendency to decrease in time. On the grounds of achieved results, one mixture containing metakaolin to CRT glass in mass ratio 1:1 has been chosen for the main research.

#### **CHAPTER 4 MAIN RESEARCH**

The whole main research has been performed on samples containing metakaolin to CRT glass in mass ratio 1:1. All tests are described precisely (samples preparation, curing regime, testing procedure, pictures of samples before and after tests, all results gathered and presented in form of charts, the description and analysis of results).

The first part of the main research describes comparison of the changes of strength over time of geopolymer cured in two conditions: all the time at the room temperature (~20°C), and for the first 24 hours in climatic chamber at 40°C and then at the room temperature. According to the results, curing at elevated temperature assures the rapid growth of strength while geopolymer cured at the room temperature gains the strength slowly. However, after 14 days, the compressive strength of samples cured at the room temperature overgrowth the strength of samples cured at elevated temperature. That difference increased in time. After the test, an Author decided to continue the research on samples cured all the time at the room temperature.

Then, the influence of sodium hydroxide concentration on mechanical behavior has been checked. According to the results, the strength of geopolymer increases along with the increase of NaOH concentration from 6 mol/L to 12 mol/L. It has been concluded that 10 mol/L is an optimal concentration for this type of geopolymer.

The next test describes the influence of CRT glass particle sizes on mechanical behavior. No evident dependence between CRT glass particles size and flexural nor compressive strength values was observed. In further tests, the CRT glass of particles size in range (0 mm: 4 mm) has been used.

At the end of the main research part, an Author investigated the behavior of the geopolymer made of the chosen mixture over long period of time (1 day – 112 days). Generally, both flexural and compressive strength increased in time. No monotonic dependence between flexural strength to compressive strength ratio ( $f_x/f_c$ ) has been noticed. That part of the chapter includes the comparison of dependence between flexural and compressive strength of metakaolin based geopolymer with CRT glass and flexural to compressive strength dependence presented by different codes and standards as well as by other scientists. Summarizing, the tested geopolymer should be considered as the brittle material so the proper reinforcement has to be applied.

#### **CHAPTER 5 COMPLEMENTARY RESEARCH**

The complementary research has been done on samples containing metakaolin to CRT glass in mass ratio 1:1 and cured all the time at the room temperature.

The first from the complementary tests describes the porosity of geopolymer. The average total porosity was equal to 13,7% while the average density of geopolymer was equal to 1,80 g/cm<sup>3</sup>.

The next test concerned physical and chemical characteristics and has been done with the use of atomic absorption spectrometry. The examination of leachate from geopolymer incorporating CRT glass has been compared with leachate from not-stabilized CRT glass. According to the results, the amount of leached heavy metals (especially Pb) is significantly limited when CRT glass is closed inside the geopolymer matrix. The achieved values were compared with binding standards. The only examined characteristics of leachate from the hardened geopolymer which did not fulfill standard limits was pH.

## CHAPTER 6 DISCUSSION

The chapter contains the comparison of results achieved during all tests with findings of other scientists.

Regarding to the influence of various CRT glass content on mechanical behavior, scientists are divergent. Some publications claim the increase of strength along with the increase of CRT glass content and some the opposite dependence. Due to the limited number of publications devoted to CRT glass added to the geopolymer in form of an aggregate, that subsection is presenting also the sources describing geopolymers with CRT glass in form of a powder and concrete with CRT glass aggregate. The majority of cited publications describing concrete with CRT glass aggregate reports the decrease of strength along with the increase of CRT glass content.

Scientists are more aggregable about the influence of curing temperature on geopolymer strength. Most of researchers noted the increase of strength along with the increase of curing temperature, although, some of them reports the optimal value of curing temperature above which, the strength starts falling down. However, there are also sources reporting that geopolymers cured at room temperatures (20°C or even lower) achieve higher (especially long-term) strength than geopolymers cured at elevated temperatures.

Many scientists determined the changes inside the geopolymer mixture with the use of isothermal calorimetry. As in this Thesis, scientists report appearance of exothermic peaks. The first peak occurs while metakaolin particles are dissolving (in dependence on accuracy of measurement, some scientists identify here two peaks) and the second one is caused by the polymerization process.

According to results described in the scientific literature, the strength of geopolymer increases in time. Geopolymers cured at elevated temperature gains the strength more rapid than geopolymer cured at the room temperature. Some sources report that long-term strength of geopolymer cured at the room temperature overgrows the strength of geopolymer cured at the elevated temperature. Those conclusions are convergent with findings withdrawn within this Thesis.

The most of scientists declare that geopolymer strength increases along with the increase of activator concentration, although, many of them do not indicate the highest tested value as an optimal one, mostly because of economic aspects and because of the rapid decrease of workability of a mixture. Despite, some publications report the decrease of strength above the given value of activator concentration.

The quantity of publications devoted to the CRT glass particle size on mechanical behavior is limited and the one found by the Author are presenting divergent conclusions.

The total porosity of metakaolin-based geopolymer with CRT glass is smaller than in most of cited publications. In case of the bulk density, some sources give smaller and some, higher values than the one found within this Thesis.

Most of the cited publications confirms that the concentration of heavy metals in leachate from geopolymer incorporating CRT glass is significantly smaller than in leachate from not-

stabilized CRT glass (what is convergent with the result obtained within this Thesis). Some sources declare that geopolymer with CRT glass fulfills regulatory limits and some declare that not or, that its dependent on CRT glass amount.

## **CHAPTER 7 SUMMARY AND CONCLUSIONS**

The chapter begins with the summary of the research part of this Thesis. Then, the chapter presents the following final conclusions drawn on the basis of the research part of this Thesis:

- The CRT glass content does not influence significantly the mechanical behavior of geopolymer.
- Elevated curing temperature provides higher early strength and ability of quicker demolding than curing at the ambient temperature. Although, long-term strength of geopolymer cured at ambient temperature surpass strength of geopolymer cured at elevated temperature.
- The increase of an activator concentration led to the increase of strength and decrease of the mixture workability.
- The change of CRT glass particles does not influence significantly the strength.
- The temperature inside the geopolymer during the curing process increases along with the increase of metakaolin content.
- The concentration of chosen heavy metals in the leachate from geopolymer fulfills the regulatory limits.

Conclusions drawn in the response to the initial hypotheses:

1. CRT glass can be used as an aggregate in metakaolin-based geopolymer without any additional treatment.
2. Metakaolin-based geopolymer with CRT glass has good mechanical characteristics (flexural strength 5-6 MPa, compressive strength 50-60 MPa, density 1850 kg/m<sup>3</sup>) and therefore can be potentially considered as building material although, one can be aware of its brittleness.
3. Both geopolymer cured at ambient as well as in elevated temperatures showed good mechanical behavior, although, geopolymer cured at ambient temperature should be demoulded later (7 days was found as enough) to avoid cracks.
4. Addition of CRT glass to metakaolin-based geopolymer helps in immobilization of heavy metals in comparison to not-stabilized CRT glass.

## **CHAPTER 8 DIRECTIONS FOR FURTHER RESEARCH**

The chapter contains the main research directions planned by the Author for the future. The list includes among the others: determination of changes of the geopolymer strength over years; the influence of humidity and freeze and thaw cycles on the mechanical behavior; determination of material's rheology; the influence on the living organisms, human's health and on the reinforcement; big-scale tests and determination of the boundary surface of the material.